Investigation of platinum drug mode of action and resistance using yeast and human neuroblastoma cells as model systems

2016

Lara Sanders

A thesis submitted to the University of Kent for the degree of Doctor of Cell Biology

University of Kent

Faculty of Sciences

Declaration

No part of this thesis has been submitted in support of an application for any degree or other qualification of the University of Kent, or any other University or Institution of learning.

Lara Sanders

Date: 28th March 2017

Acknowledgements

I would like to thank first and foremost my supervisor, Professor Martin Michaelis, whose knowledge of his field is so admirable, as is his scientific creativity. I have learnt so many things from Martin for which I am most grateful, and I am so grateful for his tireless guidance and patience. Thankyou to Martin's colleagues in Germany (Jindtich Cinatl and his group at the Institute of Medical Virology, Goethe University, Frankfurt/Main, Germany) for providing me with the valuable neuroblastoma parental and corresponding platinum drug resistant cell lines and the required information to start this project. I am also very thankful to Campbell Gourlay for the privilege of working in his laboratory as part of the Kent Fungal Group (KFG) with his precious yeast library. He has also been so tirelessly patient and I much appreciate all his advice, encouragement and his upbeat humour. Thankyou to both Martin and Campbell for taking the time to proof-read my thesis.

A big thank you to Cat Hogwood and Mark Smales for all of their time and help with the neuroblastoma proteomics studies, and I am so grateful to Kevin Howland for his time, knowledge and assistance with the spot processing and mass spectroscopy. I would also like thank Jacob Graham, who prepared the cell lysates and 2D gels for the proteomics studies of the UKF-NB-6 parental and UKF-NB-6^{r}CDDP^{2000} cell lines. I would also like to give special thanks to Joanna Bird, who performed the time kinetics responses to cisplatin for the UKF-NB-3 and UKF-NB-6 parental and their cisplatin resistant sub-lines by MTT assay.

Appreciation also goes out to my friends and colleagues in the Michaelis, Smales and Gourlay/KFG laboratories for all their emotional support and friendship, and also their scientific advice.

This work would not have been possible without the financial assistance from The University of Kent, for which I am very grateful.

Ultimately, I dedicate this thesis to my daughter, Brooke, who is my reason for everything, to show her that however tough things get, you can still make it. I am indebted to my parents Gill and Glenn, and to Samuel Powell, for all their love, patience and financial support; I literally could not have done this without them. I also want to deeply thank Sam's parents John and Teresa for their continuous love and support throughout my PhD. And finally, Tony and Chris; without you this would not have been possible...thank you so very, very much.

Table of contents

List of Figures

List of Tables

List of Abbreviations

2D	2-dimensional
Abs	absorbance
AFT1	Activator of Ferrous Transport
AKT	v-akt murine thymoma viral oncogene homologue
ANKRD1	ankyrin repeat domain 1
ANOVA	analysis of variance
ARE	AU-rich element
ATP	adenosine triphosphate
ATP	adenosine triphosphate
ATP7A or B	copper-transporting P-type adenosine triphosphatase A or B
ATR	ATM- and RAD3-related protein
AU	absorbance unit
BAK	Bcl2 Antagonist Killer-1
BAX	Bcl2 Associated X-protein
BCL2	B-Cell Leukaemia-2
BDF1	Bromodomain-containing factor 1
BER	base excision repair
BET	Bromodomain and Extra-Terminal domain
BRCA1	breast cancer 1
BRCA2	breast cancer 2
Brd	bromodomain
Brdt	bromodomain testis-specific protein
BSA	bovine serum abumin
BSO	buthionine sulfoximine
c-ABL	v-abl Abelson murine leukaemia viral oncogene homologue
CARBO	carboplatin
CDDP	cisplatin
CHAPS	3-((3-cholamidopropyl) dimethylammonio)-1-propanesulphonate
CHEK1	checkpoint kinase 1
CK2	casein kinase 2

COX	cytochrome c oxidase
CRISPR	clustered regularly interspaced short palindromic repeats
CWG424	wild type *S.cerevisae* strain, known generically as BY4741
DC	dendritic cells
DLB	Dunn lysis buffer
DMF	Dimethylformamide
DMSO	dimethyl sulphoxide
DNA	deoxyribonucleaic acid
DNMT	DNA methyltransferase
DSB	double-strand break
DTT	dithiothreitol
ECM	extracellular matrix
EDTA	ethylenediaminetetraacetic acid
EMT	epithelial to mesenchymal transition
ER	endoplasmic reticulum
ERAD	endoplasmic reticulum (ER)-associated degradation
ERCC1	excision repair complementation group 1 protein
ERK	extracellular signal-related kinase
GCR2	GlyColysis Regulation
GO	Gene Ontology
GRP	glucose related protein
GSH	glutathione
GST	glutathione-S-transferase
GSTP	glutathione-S-transferase P
GTP	guanine triphosphate
HAT	histone acetylase
HCCA	α-cyano-4-hydroxycinnamic acid
HCl	hydrochloric acid
HDAC	histone deacetylase
HDM	histone demethylase
HIP	haploinsufficiency profiling
HIR1	Histone Regulation

HMGB1	high-mobility group box 1
HOP	homozygous profiling
HR	homologous recombination
HSP	heat shock protein
HSP	heat shock protein
HU	hydroxyurea
IAA	iodoacetic acid
IC_{50}	half-inhibitory concentration
ICD	immunogenic cell death
IEF	isoelectric focussing
IMDM	Iscove's Modified Dulbecco's Medium
INNS	International Neuroblastoma Staging System
Jak	Janus kinase
JNK	c-Jun NH2-terminal kinase
MAC1	Metal binding ACtivator
MALDI	Matrix-Assisted Laser Desorption/Ionisation
MAPK	mitogen-activated protein kinase
MBF	transcriptional activator (Mbp1/Swi6 protein complex)
MDR	multi-drug resistance
MDR1	P-glycoprotein, also known as multi-drug resistance protein 1
miRNA	micro RNA
MMR	DNA mismatch repair
MMS	methyl methanesulfonate
MQ H_20	Milli-Q water
Mr *th*	theoretical molecular weight
Mr	molecular weight
MRGBP	MRG-binding protein
mRNA	messenger RNA
MRP1	multi-drug resistance-associated protein 1
MRP2	multi-drug resistance-associated protein 2
MS	mass spectroscopy
MT	metallothionein

mtDNA	mitochondrial DNA
MTT	3-(4,5-dimethylthiazol-2-yl)-2,5-diphenyltetrazolium bromide
MTT	3-(4,5-dimethylthiazol-2-yl)-2,5-diphenyltetrazolium bromide
NaCl	sodium chloride
NB	neuroblastoma
nDNA	nuclear DNA
NER	nuclear excision repair
NF-kB	nuclear factor kappa-light-chain-enhancer of activated B cells
NH_4HCO_3	sodium bicarbonate
NHE1	Na+/H+ membrane exchanger-1
nLC-MS^E	nanoflow liquid chromatography mass spectroscopy
NSCLC	non-small-cell lung carcinoma
OCT-1 or 2	organic cation transporter 1 or 2
OMM	outer mitochondrial membrane
OXALI	oxaliplatin
p53	tumour protein p53
PARP	poly(adenosine diphosphate [ADP]-ribose) polymerase protein
PBS	phosphate-buffered saline
PCG279	standard multi-copy expression vector PRS426, used as the negative control
PCG596	PRS426 plasmid but with the *S.cerevisiae* gene BDF1 and its own promotor cloned into ORF frame 3
PCR	polymerase chain reaction
PD-L	programmed cell death receptor ligand
PDR	pleiotropic drug resistance
PET	positron-emission tomography
PFF	peptide fragment fingerprint
pI	isoelectric point
pI *th*	theoretical isoelectric point
Pi3K	Phosphatidylinositol-4,5-bisphosphate 3-kinase
PKM	pyruvate kinase
PMF	protein mass fingerprint
PSA	prostate specific antigen
PTPC	mitochondrial permeability transition complex pore complex

PUMA	p53 upregulated modulator of apoptosis
RACK1	receptor of activated protein C kinase 1
RAD27	RADiation sensitive
RAD52	RADiation sensitive
RCCL	The Resistant Cancer Cell Line Collection
RIP	receptor-interacting protein kinases
RKIP	Raf kinase inhibitor protein/ phosphatidylethanolamine-binding protein 1
RNA	ribonucleic acid
RNAi	RNA intereference
ROS	reactive oxygen species
RTG	ReTrograde Regulation
SAGA	Spt-Ada-Gcn5 Acety-Transferase
SBF	transcriptional activator (Swi4/Swi6 protein complex)
SD	synthetic defined
SDS	sodium dodecyl sulphate
SDS-PAGE	sodium dodecyl sulphate-polyacrylamide gel electrophoresis
SD-URA	synthetic defined without uracil
SFP1	Split Finger Protein
SGD	Saccharomyces Gene Database
shRNA	short hairpin RNA
siRNA	silencing RNA
snRNA	small nuclear ribonucleic acid
SLA1	Synthetic Lethal with ABP1
SRBC kinase	serum deprivation response factor (sdr)-related gene product that binds to c-
STAT	Signal Transducer and Activator of Transcription
STDEV	standard deviation
SUM1	SUppresor of Mar1-1
SWI4 or SWI6	Switching deficient 4 or 6
TAFs	TBP-associated factors
tBID	truncated BID
TBP	TATA-binding protein
TFA	trifluoroacetic acid

TFIID	Transcription Factor IID
TGS	Tris-glycine SDS
TNBC	triple-negative breast cancer
TNF-α	tumour necrosis factor-α
TOF	time of flight
TOR	target of rapamycin
UME6	Unscheduled Meiotic gene Expression
UPR	unfolded protein response
VDAC	voltage-dependent anion selective channel protein
YFD	Yeast Fitness database
YKO	Yeast Knock-out
YPD	yeast, peptone, dextrose
ZAP1	Zinc-response Activator Protein
γ-GCS	γ-glutamylcysteine synthetase

1 Abstract

The platinum-based cytotoxic chemotherapeutics cisplatin, carboplatin, and oxaliplatin are widely used as anti-cancer drugs, but their efficacy is limited by the occurrence of resistance. The mechanisms of actions of these drugs as well as the mechanisms underlying resistance (formation) to platinum drugs remain incompletely understood. More knowledge is required to develop more effective therapies.

In this study, we used yeast cells and neuroblastoma cell lines to investigate the mode of action and resistance to platinum drugs. First, we screened a *Saccharomyces cerevisiae* transcription factor heterozygous gene deletion library to identify genes that when deleted result in enhanced sensitivity to cisplatin, carboplatin and/or oxaliplatin. In addition, data on platinum drug sensitivity in yeast, derived from screening a yeast whole-genome homozygous deletion library, was extracted from the Yeast Fitness Database (http://fitdb.stanford.edu/). There was a substantial overlap in the genes (and related pathways) that determine sensitivity to the individual platinum drugs, but also considerable differences. Notably, cisplatin and carboplatin are anticipated to be more similar in their mode of action compared to oxaliplatin, but the yeast data did not entirely support this notion. Amoung the genes involved in response to platinum drugs, BDF1 (Bromodomain-containing factor 1) was identified as a novel gene which, when deleted, resulted in increased sensitivity to all three platinum drugs. Its re-expression reversed platinum drug sensitivity, confirming its role in determining the yeast cell response to platinum drugs. Notably, BET proteins (the human equivalents of Bdf1) are increasingly recognised as potential anti-cancer drug targets. Our data suggest that they may have a role in sensitising cancer cells to platinum drugs.

Next, we investigated a unique panel of cell lines consisting of neuroblastoma cell lines UKF-NB-3 and UKF-NB-6 and their sub-lines with acquired resistance to cisplatin (UKF-NB-3^{r}CDDP^{1000}, UKF-NB-6^{r}CDDP^{2000}), oxaliplatin (UKF-NB-3^{r}OXALI^{2000}, UKF-NB6^{r}OXALI^{4000}), or carboplatin (UKF-NB3^{r}CARBO^{2000}, UKF-NB-6^{r}CARBO^{2000}). Adaption to platinum drugs was associated with changes in doubling times and cell morphology but there were no consistent patterns. This suggests that resistance mechanisms are complex and heterogeneous. The resistance phenotype was stable after cultivation of the resistant sub-lines for three months in the absence of drugs, indicating that resistance was not a consequence of the reversible enrichment of a pre-existing sub-population of cells, but due to a permanent, irreversible genomic change. This notion was supported by the determination of sensitivity profiles to cisplatin, carboplatin and oxaliplatin in the cell line panel. Both UKF-NB-3 and UKF-NB-6 parental lines exhibited sensitivity to all three platinum drugs, and the platinum drug-adapted parental cells displayed generally increased resistance, not just to the drug to which they were adapted, but to all three platinum drugs. However cisplatin- and carboplatin- resistant UKF-NB-3 cells displayed no cross-resistance to oxaliplatin, and oxaliplatin-resistant UKF-NB-3 cells displayed none to cisplatin and carboplatin. In contrast to the yeast data, this supports the notion that cisplatin and carboplatin are more similar in their mode of action than oxaliplatin.

Finally, in a proteomics study, we compared the UKF-NB-3 and UKF-NB-6 cells with their cisplatin-resistant sub-lines to study acquired cisplatin resistance, and also investigated their responses to acute cisplatin treatment. The resulting data, together with previous proteomics studies that investigated acquired resistance in cisplatin-adapted neuroblastoma cell lines, suggested that, despite overlaps, the resistance mechanisms are heterogeneic and cell line-specific. This was also the case, comparing our cell lines only, for the acute cisplatin responses.

In conclusion our data demonstrate that resistance formation to cisplatin is a complex and individual/cell line specific process. Further research will be required to enable a systems-level understanding of cisplatin resistance that can be translated into improved therapeutic approaches.

2 Introduction

2.1 Overview of cancer, chemotherapies and chemoresistance

2.1.1 Cancer statistics and anti-cancer agents

Cancer is one of the leading causes of death in economically developed countries, with 352,197 cases diagnosed in the UK in 2013, and breast, prostate, lung and bowel cancers together accounted for over half (53 %) of these cases; in 2011 it was reported that 1 in 4 deaths in the UK were from cancer. Worldwide, an estimated, 14.1 million people were diagnosed and 8.2 million died from cancer in 2012, most commonly from cancer of the lung, liver, stomach or bowel. Numbers are constantly increasing due to ageing and growth of the population. Even though overall patient prognosis has significantly improved due to earlier diagnosis and better treatment, survival rates are still poor for some common cancers such as lung and pancreatic cancer, and there is a continuous pressing need for new therapeutic strategies (Quaresma, Coleman et al. 2015) (Cancer Research UK at http://www.cancerresearchuk.org/).

Cytotoxic chemotherapeutics such as the platinum drugs cisplatin, carboplatin and oxaliplatin, which we have focussed on in this project, remain the most commonly used anti-cancer drugs to date. However, they come with a host of severe side effects and the problem of chemoresistance, the latter of which shall be discussed later in more detail. Lately, efforts have been made to develop better tolerated and more effective metallodrugs (Wang, Wang et al. 2015). Overall, in recent years, an effort to develop new treatments promising fewer adverse events and superior response rates compared to these non-specific drugs has shifted the emphasis to more rationally designed, targeted therapeutics. Such molecularly targeted and 'targeted therapies' can be biopharmaceuticals (eg. antibodies) or small molecules (for example, kinase inhibitors) which selectively target cancer specific events such as receptors for overexpressed growth factors, for example cetuximab and gefitinib respectively, which both block epidermal growth factor receptor (EGFR) (Dancey 2004, Tonini, Calvieri et al. 2009, Workman, Clarke 2011). However the development of resistance is still an issue with these targeted therapies. One of the more modern movements in cancer treatment has been the development of drugs that target immune cells rather than tumour cells to induce a long lasting immune response in the patient against their own cancer cells, for example anti-CTLA4 and anti-PD-1 to treat recurring cancers like metastatic

melanomas, renal cell carcinoma or non-small-cell lung carcinoma (NSCLC) (Shekarian, Valsesia-Wittmann et al. 2015).

2.1.2 Neuroblastoma

For the majority of our experiments we have used neuroblastoma cell lines, both parental drug-sensitive lines and also corresponding sub-lines resistant to each of the platinum drugs cisplatin, carboplatin and oxaliplatin, which are clinically used to treatment neuroblastoma (Ruggiero, Trombatore et al. 2013). Neuroblastoma is a rare and clinically challenging childhood cancer that is diagnosed in around 100 children every year in the UK, who are mainly under the age of 5 and often diagnosed in the first year of life (http://www.cancerresearchuk.org/). Most children diagnosed over 1 year old already have extensive metastasis and poor prognosis (Brodeur 2003). It is a very complicated and heterogeneous cancer (Brodeur 2003), interestingly being able to regress spontaneously in most infants with little therapy, but in older children more likely, despite intense therapy using drug combinations, to mature into a tumour which is liable to metastasis and the development of chemoresistance (Brodeur 2003, Cheung, Dyer 2013). This cancer originally develops from neuroblasts (nerve cells) of the neural crest during development, and often initially presents in adrenal glands or nerve tissue of the abdomen. In about half of patients it commonly metastases to the bones, liver and skin via the blood and lymphatic system (http://www.cancerresearchuk.org/). Survival is dictated by, not just the stage and age at diagnosis, but also by the MYCN status of the tumour. The transcription factor MYCN regulates the proliferation, growth, differentiation and survival of nerve cells in the developing neural crest. Amplification of MYCN genomic copy number occurs in approximately 22 % of cases of neuroblastoma, and this is a biomarker for a poor prognosis (Brodeur 2003, Cheung, Dyer 2013). Another biomarker for poor treatment outcome, which is mutually exclusive to the amplification of MYCN, is the presence of deletions on the long arm of chromosome 11 (Caren, Kryh et al. 2010).

2.1.3 Chemoresistance

Unfortunately, drug resistance severely limits the successful treatment of cancer patients. Accounting for half of all drug resistant cancer cases is intrinsic resistance, which is when a patient has pre-existing molecular mechanisms that enable tumour cells to survive and proliferate in the presence of a drug before treatment starts. Acquired resistance is the main cause of relapse of disease after initial response to chemotherapy, developing due to tumour cell resistance mechanisms occurring as a result of chronic drug exposure (Lippert, Ruoff et al. 2011, Holohan, Van Schaeybroeck et al. 2013, Hu, Zhang 2016, Gottesman, Lavi et al. 2016). For example, colorectal, renal, lung and prostate cancer can be intrinsically resistant to the cytotoxic platinum

drug cisplatin, whereas ovarian cancer commonly becomes resistant after initially effective cisplatin treatment (Stewart 2007, Koeberle, Tomicic et al. 2010, Dmitriev 2011).

Overcoming drug resistance is a constant challenge because of the complex multi-factorial nature of the underlying molecular events. Many resistance mechanisms have been identified, such as reduced entry into the cell, accelerated drug efflux, enhanced detoxification inside the cell, interference with cell cycle dynamics, increased DNA repair and defective apoptosis (Ambudkar, Dey et al. 1999, Koeberle, Tomicic et al. 2010, Dmitriev 2011, Holohan, Van Schaeybroeck et al. 2013) as well as epigenetic modifications that effect gene expression (Brown, Curry et al. 2014, Easwaran, Tsai et al. 2014) and the tumour microenvironment (Holohan, Van Schaeybroeck et al. 2013), which together form a complex network mediating an individual resistance phenotype (Lage 2008). Contributing to this problem is the broad heterogenic variation of cancer cells both within tumours and between cancer types and patients (Sharma, Haber et al. 2010, Shekhar 2011). Multidrug resistance (MDR) often describes a phenotype when cancers treated with anti-cancer drugs develop cross-resistance to many other anti-cancer agents to which they have never been exposed, which is a severe issue when it comes to successful chemotherapeutic treatment of cancer patients (Ambudkar, Dey et al. 1999, Leslie, Deeley et al. 2005, Gottesman, Lavi et al. 2016, Wu, Yang et al. 2014). Interestingly, in neuroblastoma, MYCN (2.1.2) directly contributes to MDR by regulating specific ABC transporters including the multidrug resistance-associated MRP1 protein (Manohar, Bray et al. 2004, Porro, Haber et al. 2010, Harvey, Piskareva et al. 2015).

2.1.4 Monitoring and predicting chemoresistance

Historically, attempts have been made to profile patients' tumour cells pre-treatment for intrinsic drug resistance using fresh tumour cell culture assays that measure, for example, cell activity (such as thymidine incorporation into cell DNA (KERN, WEISENTHAL 1990) or the loss of cell ATP (ANDREOTTI, CREE et al. 1995)), against a range of drug concentrations, though results from such tests can be unreliable (Lippert, Ruoff et al. 2011). During chemotherapy treatment, positron-emission tomography (PET) can be used to determine the metabolic activity of tumour tissue and, though it cannot distinguish between intrinsic and acquired resistance, can be used to assess multi-drug resistance (Kurdziel, Kiesewetter 2010). Radiotracers may be used for measuring cellular activity in more detail and to detect the presence of cancer biomarkers (Dunphy, Lewis 2009, Lippert, Ruoff et al. 2011, Sharma, Aboagye 2011). Other examples of laboratory approaches to determine resistance are the measurement of half inhibitory concentration (IC_{50}), and resistance index (RI)/fold resistance using the MTT assay, rate of drug pump efflux using the drug efflux assay, growth curves and drug susceptibility using MTT or HDRA technology (histoculture drug-response assay), and the apoptosis index using high-content screening and analysis (Wu, Yang et al. 2014). The status of multidrug resistant genes (such as MRP, MDR-1 and MDR-2) and signalling pathways can be assessed using Western blotting and

immunohistochemistry methods, and drug resistance phenotypes can be assessed using high-throughput screening systems by means of RNA interference or array based chips (Wu, Yang et al. 2014).

Biomarkers may be cancer-derived molecules found in the blood (eg. prostate specific antigen (PSA) for prostate cancer), or in tumour tissue (eg. overexpression of HER2 in breast cancer (Harries, Smith 2002)). Biomarkers, which may include pathways, may be used to monitor drug resistance mechanisms and to guide therapies (Bild, Yao et al. 2006, Coughlin, Johnston et al. 2010). It is a constant challenge to identify cancer biomarkers that enable reliable monitoring of drug resistance during therapy or that can be used confidently to predict clinical outcome for individual patients.

Over the last decade, a greater knowledge of drug-resistance mechanisms combined with the introduction of 'targeted therapeutics' has initiated the concept of personalised or precision medicine. The aim is to develop specific cancer therapies to treat the individual patient and ultimately to enable better treatment and extend survival for more patients, including those who had previously failed platinum chemotherapy, whilst avoiding drug therapies which are ineffective, costly and harmful (de Bono, Ashworth 2010, Murphy, Stordal 2011, Lippert, Ruoff et al. 2011). This has culminated in a new generation of clinical trials requiring pre-selection of relevant patients based on appropriate predictive biomarker identification from the biological characterisation of tumour biopsies (de Bono, Ashworth 2010, Wistuba, Gelovani et al. 2011, Tursz, Andre et al. 2011, Biankin, Piantadosi et al. 2015, Renfro, Mallick et al. 2016). Examples are The Biomarker-integrated Approaches of Targeted Therapy for Lung Cancer Elimination (BATTLE) trial (Kim, Herbst et al. 2011) reviewed in (Wistuba, Gelovani et al. 2011, Renfro, Mallick et al. 2016) and the Alliance Trial, both for NSCLC (Hayden 2011), and also the I-SPY 2 trial for locally advanced breast cancer (Barker, Sigman et al. 2009), reviewed in (Renfro, Mallick et al. 2016).

2.2 The platinum drugs and resistance

2.2.1 The platinum drugs: clinical utility and mode of action

Platinum-based drugs are among the most active anti-cancer agents and are used as single agent, or in combination with, other cytotoxic or targeted drugs and/or radiotherapy to treat a wide variety of human malignancies (Stordal, Davey 2007, Kelland 2007, Wheate, Walker et al. 2010). Cisplatin is the most widely used platinum-based chemotherapeutic and was the first to be approved in 1979. Since then, over twenty other platinum drugs have entered clinical trials in an attempt to better cisplatin in terms of toxicity and acquired resistance, with only carboplatin and oxaliplatin gaining international marketing approval. No new platinum drug has entered clinical

trials since 1999, explained by the shift in focus to drug delivery systems and more targeted therapeutics (Wheate, Walker et al. 2010, Johnstone, Suntharalingam et al. 2016).

The main way that they are assumed to work is to enter cells by passive diffusion or through organic or metal transporters and, upon entrance, aquation occurs and the drug becomes positively charged, enabling it to bind to DNA and cause DNA lesions. Such lesions distort the DNA helix and block RNA polymerases, thus preventing replication and DNA repair, and ultimately cause cellular apoptosis and tumour damage (Wang, Lippard 2005, Stewart 2007, Klein, Hambley 2009, Koeberle, Tomicic et al. 2010, Wheate, Walker et al. 2010, Johnstone, Suntharalingam et al. 2016). Unfortunately, continued use of platinum drugs is restricted because of their severe dose-limiting side effects caused by the random drug uptake into all rapidly-dividing cells, not just cancer cells (Wheate, Walker et al. 2010).

The chemical structures of cisplatin, carboplatin and oxaliplatin are shown in Figure 1. Cisplatin and carboplatin are very similar structurally, and they are generally used to treat the same types of cancer such as testicular, cervical, head and neck cancers, and small-cell lung cancer, although cisplatin is the drug of choice for testicular cancer, and carboplatin is now the drug of choice for ovarian cancer. Carboplatin forms similar DNA adducts as cisplatin, most frequently intra-strand adducts between adjacent guanines or between guanine and adenine, but has a lower reactivity, so subsequently has fewer side effects and can be administered in higher doses (Rixe, Ortuzar et al. 1996, Heffeter, Jungwirth et al. 2008, Negoro, Yamano et al. 2009, Ahmad 2010, Wheate, Walker et al. 2010, Johnstone, Suntharalingam et al. 2016).

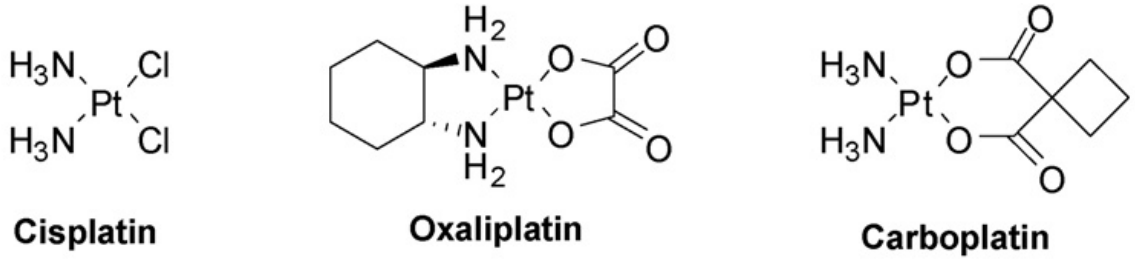

Figure 1. Chemical structures of platinum anti-cancer drugs (Heffeter, Jungwirth et al. 2008).

Oxaliplatin is currently the drug of choice, used in combination with 5-FU and folinic acid, to treat colorectal cancer (Wang, Lippard 2005, Heffeter, Jungwirth et al. 2008, Wheate, Walker et al. 2010). Oxaliplatin has structural differences which enable the formation of different intra-strand DNA adducts that prevent the binding of some DNA repair proteins, therefore it has fewer side effects than cisplatin and carboplatin. For example, DNA mismatch repair (MMR) machinery does not recognise DNA adducts formed by oxaliplatin, but does recognise cisplatin and carboplatin adducts resulting in mediation of apoptosis (Rabik, Dolan 2007, Ahmad 2010, Martinez-Balibrea,

Martinez-Cardus et al. 2015). It is also of larger structure than the other two drugs, therefore cause greater DNA deformation (Mehmood 2014), and produces fewer DNA adducts than the other two drugs at equi-molar concentrations, but a higher toxicity (Woynarowski, Faivre et al. 2000, Martinez-Balibrea, Martinez-Cardus et al. 2015). Copper transporter 1 (CTR1) has shown to be involved in the uptake of platinum drugs, but mainly of cisplatin and carboplatin (Holzer, Manorek et al. 2006), whereas oxaliplatin enters cells primarily via a different mechanism, for example by organic cation transporters such as OCT-1 and OCT-2 (Zhang, Lovejoy et al. 2006). It is interesting that colorectal cancer cells are often lacking MMR machinery, and also organic cation transporters are expressed at a high level in many colorectal cancer patients, thus oxaliplatin is the more active drug compared to cisplatin and carboplatin to treat this cancer type (Zhang, Lovejoy et al. 2006, Rabik, Dolan 2007, Martinez-Balibrea, Martinez-Cardus et al. 2015, Johnstone, Suntharalingam et al. 2016). Oxaliplatin is commonly believed to be capable of overcoming cisplatin resistance, for example in cisplatin-resistant ovarian cancers (Rabik, Dolan 2007, Wheate, Walker et al. 2010, Ahmad 2010, Johnstone, Suntharalingam et al. 2016), and interestingly, cisplatin may have activity in oxaliplatin-resistant colon cancer (Rixe, Ortuzar et al. 1996, Mohammed, Retsas 2000). As already mentioned, all three platinum drugs are clinically used to treat neuroblastoma (Ruggiero, Trombatore et al. 2013). Regarding their side effect profiles, cisplatin commonly causes ototoxicity, peripheral neuropathy, myelosuppression, and nephrotoxicity, carboplatin generally causes myelosuppression and occasionally neurotoxicity and nephrotoxicity, and oxaliplatin cause neurotoxicity (Rabik, Dolan 2007).

As mentioned, the platinum drugs enter the cell by passive diffusion or via organic or metal transporters such as CTR1, OCT-1 and OCT-2. In terms of active platinum drug efflux, copper-transporting P-type adenosine triphosphatases ATP7A (Samimi, Safaei et al. 2004) and ATP7B (Leonhardt, Gebhardt et al. 2009, Dmitriev 2011) have been implicated, which contribute to drug accumulation. There is a link between the uptake and efflux of cisplatin and copper metabolism (Wang, Lippard 2005). Platinum also binds to sulphur and therefore binds sulphur-containing cytoplasmic glutathione and metallothionein molecules (catalysed by glutathione-S-transferase), which ultimately causes platinum drug deactivation and detoxification, then inactive drug is exported from the cell via ATP-dependent efflux pumps such as the multi-drug resistance associated proteins MRP1 and MRP2 (Kelland 2007, Klein, Hambley 2009). However this detoxification process also depletes the cell of the antioxidants glutathione and metallothionein, which can cause oxidative stress and, in turn, damage to DNA.

Cisplatin is the most studied of the platinum drugs and a summary of its mode of action, post cellular entry, is illustrated in Figure 2. More research is required to elucidate the modes of action of the individual platinum drugs in more detail (Gatti, Cassinelli et al. 2015), though it can be presumed that there are similarites, in particularly between cisplatin and carboplatin (Rabik,

Dolan 2007). The key differences, compared to the other two drugs, regarding recognition and processing of oxaliplatin have already been highlighted, and also there are differences between cell death pathways, which shall be discussed later.

Focussing on Figure 2, cisplatin-induced post-translational modification of histones alters chromatin structure, enabling nuclear factors to bind that control DNA repair, transcription, and other processes (Wang, Lippard 2004). Nuclear DNA damage is recognised by proteins such as high-mobility group box protein (HMGB1) (a chromatin protein) (Siddik 2003, Wang, Lippard 2005, Lange, Vasquez 2009), and a DNA damage response is elicited to promote cell survival which, if the adducts are in low numbers, DNA repair machinery (mainly nuclear excision repair (NER)) can resolve with a temporary cell cycle arrest (Galluzzi, Vitale et al. 2014). However, if it is irrepairable, cell cycle arrest becomes permanent and the cell enters senescence (Gewirtz, Holt et al. 2008, Galluzzi, Vitale et al. 2014) which can ultimately lead to cell death. DNA damage modulates many signal transduction pathways that are an attempt to mediate or which contribute to platinum drug cytotoxicity, for example the AKT (v-akt murine thymoma viral oncogene homologue), c-ABL (v-abl Abelson murine leukaemia viral oncogene homologue), p53, MAPK (mitogen-activated protein kinase)/JNK (c-Jun NH2-terminal kinase)/ERK (extracellular signal-related kinase) pathways (Wang, Lippard 2005). The tumour suppressor protein p53 is a transcription factor that plays an important role in DNA repair, the cell cycle, senescence, the apoptotic pathway and overall genetic stability, and platinum resistance is often associated with p53 abnormalities (Reles, Wen et al. 2001, Vaseva, Moll 2009, Liu, Xu 2011). Over 50 % of cancers have mutations in p53, because with no or altered p53 function cellular control over growth and death is lost which results in a cancerous phenotype; mutant p53 is therefore a cancer drug target (Parrales, Iwakuma 2015). Normally, p53 is expressed at low levels, but when cells are stressed by, for example, DNA damage by cisplatin, p53 is stabilised and activated and can induce cell cycle arrest so that repair can take place and/or apoptosis (Parrales, Iwakuma 2015) (Figure 2) by upregulating genes such as NOXA and PUMA (p53 upregulated modulator of apoptosis) that encode pro-apoptotic proteins of the Bcl-2 family (Liu, Xu 2011). The stabilisation/activation of p53 results from the activation of ATR (ATM- and RAD3-related protein) followed downstream by activation of CHEK1 (checkpoint kinase 1) (Siddik 2003, Galluzzi, Vitale et al. 2014), as well as by pathways of MAPK signalling (Siddik 2003, Wang, Lippard 2005). These events can lead to cell senescene or to apoptosis via widespread mitochondrial membrane permeabilisation (Galluzzi, Vitale et al. 2014).

As previously mentioned, detoxification of platinum drugs causes redox stress. As depicted in Figure 2, this redox stress can also directly cause nuclear DNA damage by peroxides and free radicals (Kryston, Georgiev et al. 2011). It can also cause p53 activation; at low redox stress levels, p53 acts as an antioxidant and protects the cells, wherease if the stress levels increase, p53 acts in

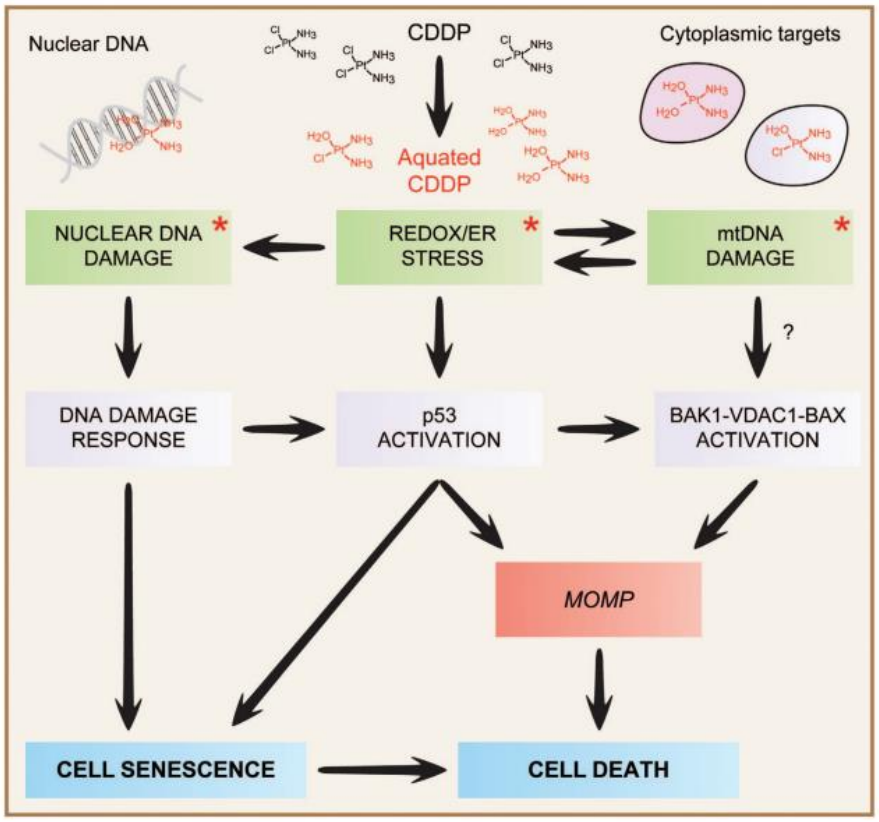

Figure 2. Cisplatin (CDDP) mode of action. On entering the cell by passive diffusion, cisplatin becomes aquated and positively charged, enabling it to bind nuclear DNA with high affinity, thus promoting the DNA damage response. It also binds to mitochondrial DNA (mtDNA) as well as various mitochondrial and extramitochondrial proteins, causing i) favouring the establishment of oxidative and reticular stress; ii) activating signaling pathways that involve pro-apoptotic BCL-2 family members BAK1 and BAX, as well as voltage-dependent anion channel 1 (VDAC1) and iii) activation of cytoplasmic p53. The relative contribution of these modules, and crosstalk between them, to the cytotoxicity of cisplatin remains to be precisely elucidated. Asterisks = primary reactivity effects, ER = endoplasmic reticulum, MOMP = mitochondrial outer membrane permeabilisation (Galluzzi, Vitale et al. 2014).

a pro-oxidative manner which increases stress levels further, leading to cell death (Liu, Xu 2011).

Cisplatin-induced DNA damage can cause ER (endoplasmic reticulum) stress too via calpain (Yadav, Chae et al. 2014), and cisplatin has also been proven to have the ability to induce a nucleus independent apoptotic signalling pathway which involves ER stress (Mandic, Hansson et al. 2003), as depicted in Figure 2. ER stress results in the accumulation of unfolded proteins in the ER, which, if not resolved by activation of the unfolded protein response (UPR), leads to cell death. ER stress-induced cell death is caused by an increase in transcription of pro-apoptotic protein genes such as NOXA and PUMA (Yadav, Chae et al. 2014) which are modulated by p53 stabilisation (Li, Lee et al. 2006).

Platinum drugs like cisplatin also bind to cytoplasmic targets to intitate cytotoxic effects (Figure 2) due to their low binding specificity and high activity. There are discrepancies between literature reports on the percentage of cisplatin that forms adducts with DNA compared to with cellular proteins; some say that the amount of intracellular cisplatin DNA and protein adducts formed are

10 % and 75-85 % respectively (Mehmood 2014), or 10 % and 90 % respectively (Goodsell 2006), whereas many others report that only 1 % of cellular cisplatin binds to nuclear DNA by quoting Gonzalez et al (Gonzalez, Fuertes et al. 2001), which tracks back to Eastman (EASTMAN 1986). Cytoplasmic targets include RNA, proteins, lipids, lysosomes, cytoskeletal components and thiol-containing molecules (Jamieson, Lippard 1999, Gonzalez, Fuertes et al. 2001, Fuertes, Castilla et al. 2003, Wang, Lippard 2005, Cullen, Yang et al. 2007, Heffeter, Jungwirth et al. 2008, Zhao, Wang et al. 2015, Gatti, Cassinelli et al. 2015). Important non-DNA targets, as already mentioned, are the thiol containing molecules cytoplasmic glutathione and metallothionein which are involved in drug detoxification (Fuertes, Castilla et al. 2003). As mentioned above is that in enucleated cells, the ER has been shown to be a target for cisplatin (Mandic, Hansson et al. 2003), likely via cytoplasmic cdk2 (Yu, Megyesi et al. 2008, Galluzzi, Vitale et al. 2014).

A central cytoplasmic target for cisplatin is the mitochondria along with mitochondrial DNA, which induces mitochondrial-mediated apoptosis; this is partly responsible for the cytotoxicity of the drug (Gonzalez, Fuertes et al. 2001, Cullen, Yang et al. 2007), and this is also the case for the other platinum compounds (Gatti, Cassinelli et al. 2015). Mitochondrial DNA can also be damaged directly by raised levels of peroxides and free radicals from cisplatin-induced redox stress and damaged mitochondria release (Figure 2) (Gatti, Cassinelli et al. 2015). It is interesting that the mitochondria have their own stores of glutathione, but as they cannot make it themselves, it is derived from active transport across the mitochondrial membrane against an electrochemical gradient (GRIFFITH, MEISTER 1985). It has been demonstrated that mitochondrial DNA (mtDNA) is more susceptible to damage and with the damage lasting longer than nuclear DNA (nDNA) (Yakes, VanHouten 1997), which is expected to be the case post-exposure of cells to the platinum drugs. The reason for this is mainly because the mitochondria lack their own DNA repair system, and mitochondrial DNA lacks protective histones and a lack of introns renders it susceptible to detrimental mutations (Preston, Abadi et al. 2001).

Activated p53 can initiate activation of BAK1, VDAC1 and BAX (Perfettini, Kroemer et al. 2004), but they can also be activated by mitochondrial DNA damage (Figure 2) (Galluzzi, Vitale et al. 2014). BAX (Bcl2 Associated X-protein) and BAK (Bcl2 Antagonist Killer-1) are pro-apoptotic proteins of the BCL2 (B-Cell Leukaemia-2) family that control OMM (outer mitochondrial membrane) permeabilisation, which is essential for mitochondrial mediated apoptosis (Wei, Zong et al. 2001, Roy, Ehrlich et al. 2009). VDAC (voltage-dependent anion selective channel protein) is a major component of the mitochondrial permeability transition pore complex (PTPC) that permeabilises the OMM, resulting in the release of cytochrome C (an apoptosis intermediate) (Shoshan-Barmatz, Ben-Hail 2012). Interestingly, in head and neck cancer it has been evidenced that high levels of cisplatin bind directly to VDAC more than 200-fold higher than the amount bound by other cellular components (Yang, Schumaker et al. 2006). This binding of VDAC by

cisplatin can directly assist the release of cytochrome c by disrupting the PTPC and in turn induce apoptosis in cancer cells, irrespective of mitochondrial DNA damage by cisplatin (Gonzalez, Fuertes et al. 2001, Yang, Schumaker et al. 2006, Cullen, Yang et al. 2007).

As mentioned, mitochondrial DNA can be damaged by raised levels of peroxides and free radicals (reactive oxygen species (ROS)) from cisplatin-induced redox stress. Conversely, however, damaged mitochondrial DNA leads to mitochondrial dysfunction which can also cause increased levels of ROS which in turn can damage its own DNA (Cline 2012) (Figure 2); this is because ROS are mainly produced in the mitochondria as by-products of respiratory chain reactions, the components of which are encoded by mitochondrial DNA. An increase in ROS levels, besides intensifying the cytotoxicity of platinum drugs, can also favour the opening of the PTPC (Shoshan-Barmatz, De Pinto et al. 2010, Galluzzi, Vitale et al. 2014).

Cisplatin induces two different modes of cell death in a concentration dependent manner; necrosis at high drug levels and apoptosis a lower drug levels (Gonzalez, Fuertes et al. 2001, Wang, Lippard 2005). Necrosis could be considered to be a random and uncontrolled process, its key mediators being RIP kinases (receptor-interacting protein kinases) and PARP (poly(ADP-ribose) polymerase). When cells undergo necrosis, plasma membrane integrity is disrupted and intracellular contents are released, ultimately causing an inflammatory response (Wang, Lippard 2005, Ouyang, Shi et al. 2012). Apoptosis is a more controlled type of cell death, and is the primary route of cell death for platinum drugs. It is characterised by cell shrinkage, chromatin condensation, DNA fragmentation, membrane budding, externalisation of phosphatidylserine, and activation of initiator and executioner caspases (Dasari, Tchounwou 2014). Examples of initiator caspases are caspases 8 and 9, which when activated subsequently activate executioner caspases, such caspases 3 and 7, which cleave many other proteins leading to apoptosis (Wang, Lippard 2005, Dasari, Tchounwou 2014). There are two major pathways, the extrinsic and intrinsic, the latter of which is favoured by platinum drugs. The extrinsic pathway is initiated by extracellular ligands binding to the tumour necrosis factor-α (TNF-α) receptors which then oligomerise, recruit caspase 8 and form a death-signalling complex (DISC) to ultimately cause apoptosis (Dasari, Tchounwou 2014). This pathway can be stimulated by sphingolipid ceramide, which is produced via the inhibition of the Na+/H+ membrane exchanger-1 (NHE1), which is initiated by exposure to cisplatin (Rebillard, Tekpli et al. 2007). Ceramide also interacts with lipids of the membrane causing changes in its composition and fluidity, which can influence the exposure of death receptors at the cell surface and ultimately affect drug sensitivity and resistance to apoptosis (Gatti, Cassinelli et al. 2015). The intrinsic pathway (mitochondrial mediated) is initiated by cellular stress such as cisplatin-induced DNA damage (Figure 2), and it relies on the release of mitochondrial cytochrome c via the PTPC (already discussed), which activates caspase 9 to ultimately cause apoptosis (Dasari, Tchounwou 2014). Interestingly,

oxaliplatin has been documented as an inhibitor of survivin, which is highly expressed in cancers and plays a key role in apoptosis and mitotic catastrophe (Fujie, Yamamoto et al. 2005, Rabik, Dolan 2007).

There is another mode of cell death initiated by cancer treatment termed immunogenic cell death (ICD), which is a cell death process that stimulates a host immune response against the tumour that has been reported to be activated by oxaliplatin (Apetoh, Ghiringhelli et al. 2007, Ghiringhelli, Apetoh et al. 2009, Gatti, Cassinelli et al. 2015), but not cisplatin (Martins, Kepp et al. 2011, Gatti, Cassinelli et al. 2015). This is mainly because cisplatin is not capable of inducing the translocation of calreticulin, which plays a main role in ICD, working together with ATP and HMGB1 (high-mobility group box 1) to activate dendritic cells (Martins, Kepp et al. 2011, Gatti, Cassinelli et al. 2015). Interestingly, it has also been reported that platinum drugs have immunomodulating effects, being able to decrease the immunosuppressive capabilities of tumour cells; Lesterhuis et al report that programmed cell death receptor ligand (PD-L) inhibitory molecules are downregulated by platinum drug treatment (mediated by STAT6 (signal transducer and activator of transcription)), particularly carboplatin, which results in both enhanced T cell stimulation by dendritic cells (DCs) and enhanced sensitivity of the tumour for lysis by cytotoxic T cells (Lesterhuis, Punt et al. 2011, Gatti, Cassinelli et al. 2015).

2.2.2 Platinum drug resistance

Mechanisms underlying the complex and multifactorial phenomenon of platinum drug resistance are poorly understood (Shahzad, Lopez-Berestein et al. 2009) with a need for more detailed knowledge around the specific differences between individual platinum drug class members. Cisplatin resistance has been studied to a greater extent than carboplatin and oxaliplatin resistance and, even though cisplatin and carboplatin resistance mechanisms are very similar, there does not appear to exist a common “cancer metal-drug resistance” phenotype. Consequently, resistance mechanisms cannot easily be predicted (Heffeter, Jungwirth et al. 2008). Many resistance mechanisms have been proposed (too many to cover in this section), mostly discovered using drug-resistant cancer cell lines, and they can result from modifications directly related to drug-induced damage to cellular components, as well as to the systems and pathways that regulate them (Gatti, Cassinelli et al. 2015). Various strategies to overcome platinum resistance and enhance therapeutic response are at the preclinical and clinical level, many utilising combinations of existing therapies and also newer approaches such as RNAi and small molecule inhibitors. This approach can lead to improvements in clinical responses due to differing modes of action. There are also continuous attempts to develop newer platinum drugs with differences in modes of action compared to cisplatin, carboplatin and oxaliplatin, for example the cisplatin analogues sarcoplatin and picoplatin, which show signs of overcoming resistance to other

platinum drugs (Koeberle, Tomicic et al. 2010). Johnstone et al have recently thoroughly reviewed the next generation of platinum drugs (Johnstone, Suntharalingam et al. 2016).

Regarding the tumour and its environment, tissue pressure and tumour blood flow can play a role in resistance, affecting drug delivery and hence intracellular accumulation and toxicity, and so may affect platinum drug efficacy in the clinic (Stewart 2007). Efforts have been made to increase platinum drug delivery to tumour cells specifically using a variety of drug targeting and delivery approaches, for example the use of liposomal or co-polymer products, or administering drug directly into the tumour (for ovarian cancer) (Kelland 2007, Wang, Guo 2013). An example is a recently successful attempt to deliver cisplatin directly to the mitochondria, which do not have NER capabilities, by engineering a pro-drug using a biocompatible nanoparticle (Marrache, Pathak et al. 2014). The role of the tumour microenvironment has also been explored with respect to platinum resistance (Tsai, Chang et al. 2014), in particularly the extracellular matrix (ECM); the production of collagen VI has been reported to cause such resistance (Sherman-Baust, Weeraratna et al. 2003, Shahzad, Lopez-Berestein et al. 2009).

Regarding cellular resistance mechanisms, they can be broadly grouped into five main categories; i) decreased cellular drug uptake and/or increased efflux, ii) increased enzymatic or chemical detoxification inside the cell, iii) enhanced repair or tolerance of platinum drug induced DNA adducts, iv) changes in molecular pathways involved in regulation of cell survival and/or cell death, and v) epigenetic changes (summarised in Figure 3) (Kuo, Chen et al. 2007, Rabik, Dolan 2007, Stewart 2007, Stordal, Davey 2007, Heffeter, Jungwirth et al. 2008, Shahzad, Lopez-Berestein et al. 2009, Koeberle, Tomicic et al. 2010, Galluzzi, Vitale et al. 2014).

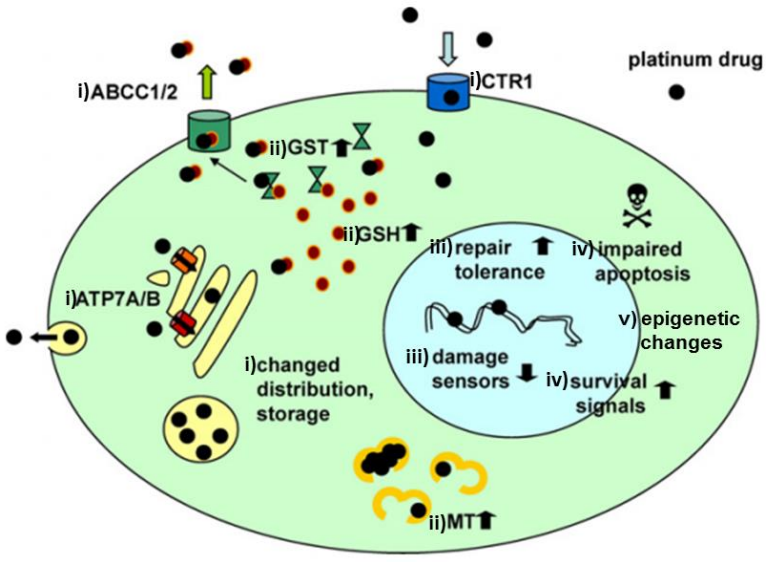

Figure 3. Key molecular mechanisms of tumour cells involved in platinum drug resistance. i) Decreased cellular drug uptake and/or increased efflux leading to reduced intracellular accumulation, ii) increased enzymatic or chemical detoxification inside the cell such as conjugation with intracellular thiols, iii) enhanced repair or tolerance of platinum drug induced DNA adduct, iv) changes in molecular pathways involved in regulation of cell survival and/or cell death, and v) epigenetic changes. See text for more details. (Heffeter, Jungwirth et al. 2008).

2.2.2.1 i) Decreased cellular drug uptake and/or increased efflux.

Platinum drugs enter cells by both passive diffusion and via transporters. Membrane rigidity can affect both of these processes, and resistant cells with reduced uptake have been shown to have rigid cell membranes associated with high sphingomyelin and cholesterol content (Popovic, Wong et al. 1994, Stewart 2007). Plasma membrane transporters play a role in resistance, ultimately impairing cellular accumulation, distribution and storage of platinum drugs in organelles and vesicular compartments such as lysosomes, mitochondria and the ER. For example, the copper transporter CTR1 (Song, Savaraj et al. 2004, Holzer, Manorek et al. 2006) and organic cation transporters such as OCT-1 and OCT-2 (Zhang, Lovejoy et al. 2006), as previously discussed (2.2.1) are involved in platinum drug uptake, and the copper-transporting P-type adenosine triphosphatases ATP7A (Samimi, Safaei et al. 2004) and ATP7B (Leonhardt, Gebhardt et al. 2009, Dmitriev 2011), which shuttle copper between the Golgi and the plasma membrane, have been implicated in platinum efflux. Certain ATP-binding cassette (ABC) efflux pumps also play a role in drug resistance, for example P-glycoprotein, also known as multi-drug resistance protein 1 (MDR1, encoded by ABCB1) and multi-drug resistance associated proteins (MRP1 and MRP2, encoded by ABCC1 and ABCC2 respectively) (Rabik, Dolan 2007, Heffeter, Jungwirth et al. 2008, Galluzzi, Vitale et al. 2014). Alterations in the expression levels, functionality and location of all of these receptors can be associated with resistance (Galluzzi, Vitale et al. 2014). For example, cells lacking CTR1 are resistant to cisplatin, and CTR1 receptors are rapidly internalised into the cytoplasm upon exposure to the drug which subsequently limits further drug uptake (Ishida, Lee et al. 2002, Stewart 2007). In an effort to circumvent such a resistance mechanism copper-lowering agents such as trientine have been trialled, for example, to enhance the efficacy carboplatin (which is also transported by CTR1) to overcome platinum resistance in ovarian cancer patients, with results that merit further investigation (Fu, Naing et al. 2012, Chen, Kuo 2013). Attempts have been made to overcome ABC-transporter-mediated drug resistance by developing effective ABC inhibitors, modulators or MDR-reversal agents, which has led to some success in pre-clinical studies (Falasca, Linton 2012). Utilisation of RNAi or other approaches to silence genes encoding drug transporters such as ATP7B have been shown to reverse drug resistance (Mangala, Zuzel et al. 2009). It is interesting that dysfunctional lysosomal and increased exosomal export of cisplatin has been reported in platinum drug resistant ovarian cancer cells (Safaei, Larson et al. 2005).

2.2.2.2 ii) Increased enzymatic or chemical detoxification inside the cell.

Platinum drugs can be inactivated by conjugation with intracellular thiols like metallothionein (MT), or to glutathione (GSH) catalysed by glutathione-S-transferase (GST). Increased levels of GSH may also enhance DNA repair and reduce drug-induced oxidative stress, leading to resistance to platinum drugs. Other GST-related enzymes as well as antioxidants have also been linked with

resistance. Picoplatin, a platinum compound that exerts a reduced reactivity with thiols, was suggested to be effective in cells expressing enhanced GSH levels (Heffeter, Jungwirth et al. 2008, Tang, Parham et al. 2011). Further agents that deplete GSH or inhibit GST have been described (Byun, Kim et al. 2005, Koeberle, Tomicic et al. 2010), for example 6-(7-nitro-2,1,3-benzoxadiazol-4-ylthio)hexanol (NBDHEX) is a GST inhibitor that strongly reversed cisplatin resistance in human osteosarcoma cell lines and so is a potential co-therapy with cisplatin (Pasello, Michelacci et al. 2008, Koeberle, Tomicic et al. 2010).

2.2.2.3 iii) Enhanced repair or tolerance of platinum drug induced DNA adducts

This mainly occurs via the nuclear excision repair (NER) pathway mediated by the proteins such as the excision repair complementation group 1 (ERCC1) protein, the homologous recombination (HR) pathways and the poly(adenosine diphosphate [ADP]-ribose) polymerase (PARP) proteins of base excision repair (BER), and the mismatch repair (MMR) system (Shahzad, Lopez-Berestein et al. 2009).

Regarding the NER pathway and ERCC1, there are many pre-clinical studies that have demonstrated that ERCC1 mRNA or protein expression levels are associated with cisplatin resistance (Gossage, Madhusudan 2007). For instance, upregulated expression of ERCC1 has been shown to correlate with enhanced NER and cisplatin resistance in a human ovarian cancer model system (Ferry, Hamilton et al. 2000, Shahzad, Lopez-Berestein et al. 2009). Also, inducible ERCC1 expression in colorectal cancer cells has been demonstrated to correlate with oxaliplatin resistance, which is reversible upon RNA silencing of ERCC1 (Seetharam, Sood et al. 2010). Methods like RNAi could be used to target ERCC1 to enhance platinum treatment outcome in patients with platinum resistant cancers (Shahzad, Lopez-Berestein et al. 2009), and due to its lack of enzyme activity, targeting protein interactions with ERCC1 has been explored (Gossage, Madhusudan 2007, Koeberle, Tomicic et al. 2010) . Intrinsically low levels of ERCC1 are associated with cisplatin and oxaliplatin sensitivity so ERCC1 has been investigated as a predictive biomarker of platinum treatment outcome in cancer (Gossage, Madhusudan 2007), though the value of this has lately been re-evaluated (Galluzzi, Vitale et al. 2014).

Homologous recombination (HR) pathways repair double strand breaks illicited by cisplatin at the same time as DNA synthesis, and cancers deficient in HR are more sensitive to cisplatin treatment. BRCA1 and BRCA2 (breast cancer 1 and 2 genes) are key components of HR and mutations in these genes can predispose to breast and other cancers (Farmer, McCabe et al. 2005), and cause sensitivity to drugs like cisplatin and to inhibitors of poly(adenosine diphosphate [ADP]-ribose) polymerase (PARP) proteins. PARP proteins are key players in the base excision repair (BER) system, which repairs single-strand breaks, and this dual sensitivity can be explained by the HR and BER pathways working together to repair DNA. When PARP proteins are inhibited, the

resulting persistent DNA lesions accumulate, leading to soluble strand breaks that are repaired by HR (Farmer, McCabe et al. 2005, Shahzad, Lopez-Berestein et al. 2009). Co-administration of cisplatin or carboplatin with PARP inhibitors appears to potentiate anti-cancer effects (Rottenberg, Jaspers et al. 2008, Michels, Vitale et al. 2013, Galluzzi, Vitale et al. 2014). It is interesting that in breast cancer cells it has been discovered that compensatory mutations can appear in these genes which contribute to cisplatin resistance (Sakai, Swisher et al. 2008, Galluzzi, Vitale et al. 2014).

The MMR system repairs DNA mismatch lesions, so does not repair platinum adducts, but it can detect them. In the case of cisplatin, the MMR repair proteins recognise the DNA adducts, but after several unsuccessful attempts of repair cycles, apoptotic signalling is finally initiated (Fink, Nebel et al. 1996, Siddik 2003, Kelland 2007, Heffeter, Jungwirth et al. 2008). As previously mentioned (2.2.1), DNA adducts formed by oxaliplatin DNA are not recognised by MMR machinery, but cisplatin and carboplatin adducts are (Rabik, Dolan 2007, Ahmad 2010, Martinez-Balibrea, Martinez-Cardus et al. 2015). This is why the loss of MMR has been correlated with increased tolerance of DNA damage and hence low-level resistance to cisplatin and carboplatin but not oxaliplatin (Fink, Nebel et al. 1996). Downregulation or mutations in MMR genes are frequently observed in cisplatin resistance (Siddik 2003, Galluzzi, Vitale et al. 2014). Therefore high expression levels of MMR proteins could be a biomarker indicative of more successful cisplatin treatment outcome, and low levels indicative of a higher risk of cisplatin resistance (Galluzzi, Vitale et al. 2014). In contrast to this MMR deficiency in resistance, another major recognition protein, HMGB1 (Lange, Vasquez 2009), is upregulated in cisplatin resistant cells (Nagatani, Nomoto et al. 2001) and RNA interference of HMBG1 increases apoptosis in cisplatin resistant NSCLC, which could be useful in clinical therapy (Zhang, Li et al. 2015).

Mitochondrial DNA is a central target for the platinum drugs (previously discussed in 2.2.1), and it can also be damaged directly by raised levels of peroxides and free radicals from cisplatin-induced redox stress and damaged mitochondria release, but mitochondria have no DNA repair system. Studies of mutations in mitochondrial DNA have been carried out in cisplatin resistant cancer cell lines, and mutations resulting in partial defects of the repiratory chain have been identified. However, retrograde nuclear signalling and peroxisome-dependent signalling resulting in compensatory mitochondrial activity has been proposed as a cellular mechanism for circumventing this. These mitochondrial mutations are potential anti-cancer drug targets (Mizutani, Miyato et al. 2009).

2.2.2.4 iv) Changes in molecular pathways involved in regulation of cell survival and/or cell death.

Overexpression of a number of anti-apoptotic proteins have been associated with platinum drug resistance, for example Bcl-2 (Beale, Rogers et al. 2000) and Bcl-XL (Williams, Lucas et al. 2005), XIAP (X-linked inhibitor of apoptosis) and survivin (Nomura, Yamasaki et al. 2005); these proteins promote cellular survival by counteracting the caspase activation caused by platinum drug-activated apoptotic pathways, and so they are promising drug targets to overcome resistance.

As previously described (2.2.1), cisplatin can induce a nucleus independent apoptotic signalling pathway via calpain and caspase 12, which involves endoplasmic reticulum (ER) stress (Mandic, Hansson et al. 2003). Associated with cisplatin resistance is the upregulation of proteins like the ankyrin repeat domain 1 (ANKRD1), which protects against ER-stress mediated apoptosis (Scurr, Guminski et al. 2008), and the ER resident chaperone GRP78, which is a key player in the UPR (Jiang, Mao et al. 2009, Lee 2014, Gatti, Cassinelli et al. 2015). It has also been discussed how cisplatin preferentially binds to VDAC compared to other cellular components, disrupting the PTPC to release cytochrome C and initiate apoptosis (Yang, Schumaker et al. 2006) (2.2.1). VDAC is a major component of the mitochondrial permeability transition complex pore complex (PTPC) involved in outer mitochondrial membrane (OMM) permeabilisation (Shoshan-Barmatz, Ben-Hail 2012) and is a candidate for cisplatin resistance. Downregulation or inhibition of the VDAC1 isoform reduces cisplatin-induced apoptosis-associated modifications of both mitochondrial and plasma membranes in NSCLC cells (Tajeddine, Galluzzi et al. 2008). Also, the protein adseverin (SCIN) binds to VDACs in the mitochondria and it has been suggested that that this interaction may inhibit the mitochondrial apoptosis pathway in cancer cells that are resistant to cisplatin (Miura, Takemori et al. 2012). Adseverin could be a promising therapeutic target to overcome platinum resistance mediated via VDACs.

The tumour suppressor protein p53, as already discussed (2.2.1), besides DNA repair it also plays an important role in cell cycle and the apoptotic pathway, and platinum resistance is often associated with p53 abnormalities (Reles, Wen et al. 2001, Parrales, Iwakuma 2015). This is also the case for aurora kinases (Landen, Lin et al. 2007), which are essential for mitotic integrity and the cell cycle; inhibiting these enzymes has proven to reverse platinum resistance in ovarian cancer models (Lin, Immaneni et al. 2008, Shahzad, Lopez-Berestein et al. 2009), as well as in neuroblastoma cells (the same cisplatin resistant cell lines in our testing panel used in this thesis) (Michaelis, Selt et al. 2014). It is relevant that the expression and amplification of aurora kinase A has been demonstrated as predictive of poor prognosis in neuroblastoma (Shang, Burlingame et al. 2009, Michaelis, Selt et al. 2014).

Similarly, activation of numerous transcription factors such as NF-kB (nuclear factor kappa-light-chain-enhancer of activated B cells) (Kim, Kim et al. 2004) and members of the Jak-Stat (Heffeter, Jungwirth et al. 2008) and Pi3K-Akt survival pathways (Stewart 2007), can confer platinum drug resistance. Targeting such key proteins with RNAi approaches and small molecule inhibitors, for example Pi3k inhibition (Ohta, Ohmichi et al. 2006), also holds promise for circumventing related resistance mechanisms and improve platinum drug therapeutic outcome.

The Wnt/β-catenin signalling is also a survival pathway that plays a key role in gene regulation, cell proliferation and apoptosis; its activation has been associated with poor chemotherapeutic outcome, and targeting this pathway by inhibition has been shown to improve efficacy of anti-cancer agents (Shen, Pouliot et al. 2012, Nagaraj, Joseph et al. 2015). Inhibition of Wnt/β-catenin signalling has also been shown to overcome platinum resistance; for example, the Wnt-specific inhibitor iCG-001 was shown to reverse cisplatin resistance in primary high-grade serous ovarian cancer (HGSOC) cells (Nagaraj, Joseph et al. 2015). Activation of Wnt/β-catenin signalling has been shown to increase cisplatin resistance; for example inhibition of cytoplasmic GSK-3 beta was shown to increase resistance to cisplatin via activation of Wnt/β-catenin signalling in cisplatin resistant human lung adenocarcinoma cells (Gao, Liu et al. 2013).

Heat shock proteins (HSPs) are copiously expressed, stress-inducible molecular chaperones that have been linked to platinum drug resistance (Mandic, Hansson et al. 2003, Shen, Pouliot et al. 2012, Ciocca, Cappello et al. 2015). HSPs are involved in the correct folding and unfolding of proteins, and degradation pathways such as the endoplasmic reticulum (ER)-associated degradation (ERAD) pathway and the regulation of apoptosis (Ciocca, Cappello et al. 2015). Even though targeting heat shock proteins to avoid resistance would be sensible, many have been evaluated as targets for anticancer therapy but none have successfully completed a phase III trial (Ciocca, Cappello et al. 2015).

Disruption of the extrinsic death pathway is a cellular mechanism for circumventing the action of platinum drugs, which is supported by many studies (Gatti, Cassinelli et al. 2015). As discussed previously (2.2.1), cisplatin treatment can cause an intracellular increase in sphingolipid ceramide levels which affect the composition and fluidity of the plasma membrane, detrimentally affecting the exposure of death receptors at the cell surface and, in NSCLC cells, despite having functional death receptor machinery, a dysfunctional asMASE enzyme hampers increases in ceramide levels and hence caspase cleavage, preventing apoptosis (Paul, Chacko et al. 2011, Gatti, Cassinelli et al. 2015). Activation of the extrinsic death pathway is a potential therapeutic strategy to enhance the efficacy of platinum agents.

2.2.2.5 iv) Epigenetic changes

Epigenetics is defined as mitotically and meiotically heritable changes in gene expression that do not involved alterations in DNA sequences. Such changes, examples of which are DNA methylation and histone modification, affect cell signalling, proliferation and apoptosis, and are thought to favour malignant phenotypes of cancer. DNA methylation and histone modification require epigenetic modifying enzymes such as DNA methyltransferases (DNMTs), histone deacetylases (HDACs), histone acetylases (HAT) and histone demethylases (HDMs) (Kala, Peek et al. 2013, Wu, Yang et al. 2014, Martinez-Balibrea, Martinez-Cardus et al. 2015).

DNA methylation is the most common covalent modification of human DNA. It involves the addition of a methyl groups at cytosine residues which are adjacent to guanine residues to ultimately inactivate gene transcription, especially upon hypermethylation of 5'CpG island regulatory regions; this may play a role in platinum drug resistance by silencing of genes that are required for drug sensitivity. It has been evidenced that overexpression of DNA methyltransferase is associated with cisplatin resistance in murine neuroblastoma cells (Wang, Mirkin et al. 2001). Also, in the same cell type, induced overexpression of DNA methyltransferase is linked to resistance to cisplatin and inhibition of DNA methylation can reverse cisplatin resistance (Qiu, Mirkin et al. 2005, Ibrahim, Srivenugopal et al. 2013). Furthermore, Chang et al demonstrated, using cancer cell lines, that DNA methylation of promoter regions is associated with chronic cisplatin treatment which leads to cisplatin resistance (Chang, Monitto et al. 2010). Several studies have identified genes that are regulated by DNA methylation and associated with platinum resistance. For example, SRBC (serum deprivation response factor (sdr)-related gene product that binds to c-kinase) interacts with BRCA1 which, as previously discussed (2.2.2.3), is involved in DNA repair; the epigenetic inactivation of the SRBC gene by promoter CpG island hypermethylation has been proven to be associated with acquired oxaliplatin resistance and poor outcome to oxaliplatin therapy (Shen, Pouliot et al. 2012, Moutinho, Martinez-Cardus et al. 2014, Martinez-Balibrea, Martinez-Cardus et al. 2015). Also, DNA methylation profiling of twenty gastric cancer cells lines revealed bone morphogenetic protein 4 (BMP4) to be a gene that is epigenetically regulated and expressed at high levels in cisplatin resistant gastric cancer cells (Ivanova, Zouridis et al. 2013, Wu, Yang et al. 2014). Investigation of genes that are DNA methylated may identify biomarkers predictive of platinum resistance and treatment outcome (Ibrahim, Srivenugopal et al. 2013). Epigenetic drugs that inhibit DNA methylation may have future application in platinum therapy, with the aim of increasing platinum efficacy and avoiding platinum resistance. For example, an increase in death receptor 4 expression (DR4) was demonstrated in a carboplatin resistant ovarian cancer cell line post exposure to azacitidine (DNA hypomethylating agent); this also increased the sensitivity of these cells to carboplatin (Li, Hu et al. 2009).

Modification of histones is important for maintaining chromatin structure and function (Shen, Pouliot et al. 2012) and aberrations of histone modifications are typical of cancer (Martinez-Balibrea, Martinez-Cardus et al. 2015). Histone deacetylases (HDACs) remove acetyl groups from prominent amino-terminal lysine residues of chromatin, promoting condensation of chromatin which leads to repression of gene transcription and DNA repair. This process has been implicated to silence growth regulatory and apoptotic pathways and linked to drug resistance (Falchook, Fu et al. 2013, Zuco, Cassinelli et al. 2015). Cisplatin-induced post-translational modification of histones alters chromatin structure, enabling nuclear factors to bind that control DNA repair, transcription, and other processes (Wang, Lippard 2004). Correlation of overexpression of HDACs with cisplatin resistance has been demonstrated in epithelial ovarian cancer cell lines (Kim, Pak et al. 2012). Inhibitors of HDACs have a variety of targets, including histones, transcription factors and chaperone proteins, (Scott, Mattie et al. 2006, Galluzzi, Vitale et al. 2014). Treatment with the HDAC inhibitor SAHA (suberanilohydroxamic acid) has been shown to enhance CDDP-induced apoptosis in oral squamous cell carcinoma cells (Rikiishi, Shinohara et al. 2007), and exposure to HDAC inhibitors MS275 and SBHA potentiates the cytotoxicity of oxaliplatin in colorectal cancer cells, probably due to an increase in apoptotic signalling (Flis, Gnyszka et al. 2009). A phase I trial treating patients with advanced solid malignancies (refractory to standard therapy) sequentially with azacitidine (DNA hypomethylating agent) and valproic acid (HDAC inhibitor) in combination with carboplatin was carried out for the first time recently. The outcome was stable disease or modest cytotoxic effects in 6 of 32 patients, 3 of which had platinum refractory ovarian cancer, but the therapy was poorly tolerated (Falchook, Fu et al. 2013). Such drug combinations need to be explored further.

Micro RNAs (miRNA) are small (~20 nucleotides long) non-coding RNA molecules which are post-transcriptional gene regulators that target mRNA for degradation. They play key roles in many processes, including the stress response, apoptosis and proliferation. Several miRNAs have been demonstrated to reverse cisplatin resistance in cancer cells by regulating apoptosis and cell survival pathways. Further research is required to understand miRNA dysregulation in cisplatin resistant cells (Shen, Pouliot et al. 2012). It is interesting that miRNAs can control the expression of a diverse range of epigenetic-modifying enzymes that are involved in carcinogenesis (Kala, Peek et al. 2013), and that some miRNAS that contribute to cisplatin resistance are under epigenetic control by DNA methylation and histone acetylation (Galluzzi, Vitale et al. 2014). Inhibitors of these epigenetic processes may reduce cisplatin resistance by modulating cellular levels of miRNAs. For example, histone deacetylase inhibition (LAQ824) in breast cancer cells has been shown to rapidly alter the levels of many miRNA species (Scott, Mattie et al. 2006, Galluzzi, Vitale et al. 2014).

2.3 Cancer cell lines and *Saccharomyces cerevisae* as models to investigate cancer

2.3.1 Cancer cell lines

2.3.1.1 The use and validity of cancer cell lines as pre-clinical cancer models

Human tumour-derived cell lines (grown in monolayer, 3D scaffold or in xenograft) have been, and can be assumed to remain, a mainstay model for the investigation of cancer cell biology. Such models, in combination with 'omics' technologies such as genomics and proteomics, hold potential for the investigation of novel drugs and the identification of biomarkers to allow the personalisation of cancer treatment (Neve, Chin et al. 2006, Sharma, Settleman 2007, Sos, Michel et al. 2009, Chao, Chiang et al. 2011, Goodspeed, Heiser et al. 2016). Intra-tumour heterogeneity is a limitation for the use of cancer biopsies as models, through tumour sampling bias (Burrell, McGranahan et al. 2013). Interestingly, cell lines can exhibit heterogeneity, representing tumours, which is discussed later in this section. Cell lines as pre-clinical models enable the systematic performance of functional studies that can only be performed to a very limited extent by the use of clinical samples. Also, cancer cell lines as pre-clinical models enable detailed systems level investigations in cancer cell populations that cannot be determined in patients suffering from multiple metastases, when not all cancer cells are accessible.

In the last few decades, biotechnology and pharmaceutical industries have more routinely utilised cancer cell lines to discover and study genetic determinants of drug response. Implementation of high throughput screening strategies, using much larger (>1000) cancer cell line platforms (for example, CMT1000 (McDermott, Sharma et al. 2007, McDermott, Sharma et al. 2008)) comprising more varied tumour types than historical smaller cell line platforms (for example, NCI60 (Shoemaker 2006) and JFCR39 (Yamori 2003)), has been an industrial attempt to capture the genomic variation of human cancer. Drug sensitivity and genomic data from experiments using large cell line panels has been collated into databases such as the Genomics of Drug Sensitivity in Cancer (GDSC) (Yang, Soares et al. 2013), the cancer cell line encyclopedia (CCLE) (Barretina, Caponigro et al. 2012) and the cancer therapeutics response portal (CTRP) (Basu, Bodycombe et al. 2013) which, along with NCI60 (Shoemaker 2006), contribute to large, international cancer projects, such as The Cancer Genome Atlas (TCGA) and the International Cancer Genome Consortium (ICGC) in an effort to characterise patient tumours. Such pan-cancer analysis has found both tissue-specific and recurrent patterns across many cancers (Goodspeed, Heiser et al. 2016).

Many drug resistant human tumour-derived cell lines have been established by exposing drug-sensitive (parental) cells to a chemotherapeutic over a period of time. The resulting sub-lines can be studied alongside the parental cells to elucidate specific drug resistance mechanisms and to investigate ways to overcome them (for example, new therapeutics or drug combinations), beside to discover biomarkers predictive of resistance (Sharma, Haber et al. 2010). Studies using such methods have been mentioned throughout the previous section discussing platinum drug resistance (2.2.2).

Despite cancer cell lines continuously growing and being easy to handle, a major criticism is that it is not possible to create cell lines from every type of cancer (Sharma, Haber et al. 2010, Borrell 2010), and that there may also be some bias in cell line representation if cells are sampled from different stages of disease and cancer subtypes which may not behave similarly in culture (Sharma, Haber et al. 2010). When culture is possible, the most worrying caveat is that the cancer cells can become genomically disarrayed and unstable as they adapt to their artificial environment, (Sos, Michel et al. 2009, Borrell 2010, Gillet, Calcagno et al. 2011), making it difficult to capture the frequency and histological distribution of genetic lesions within the primary tumour (Sos, Michel et al. 2009). Also, cell lines cannot be used to investigate anti-cancer agents that potentially function to affect the interaction of tumour cells with their environment, for example angiogenesis inhibitors (Sharma, Haber et al. 2010).

Conversely though, the large data resources mentioned above have enabled thorough assessment of how well cell lines can recapitulate the genomic irregularities of tumours. Studies have shown how cell lines actually do represent the genomic characteristics of tumours, tumour molecular subtypes and their patterns within tumours and also intra-tumour heterogeneic patterns (Goodspeed, Heiser et al. 2016). However, DNA methylation in cell lines has been shown to exhibit both similarities and differences to tumours (Goodspeed, Heiser et al. 2016). Two examples of studies in Nature emphasised the continued relevance of cancer cell lines (Borrell 2010). Firstly, Bignell et al analysed deletion mutations in 746 cell lines, including the NCL-60 collection, and consequently highlighted that cell lines are perfect for detecting genomic deletions because they do not contain any non-cancerous cells which can be found in primary tumours (Bignell, Greenman et al. 2010). Secondly, Beroukhim et al searched for DNA additions and deletions in 3,131 cancer entities, including 541 cell lines which mirrored those found in the primary tumour (Beroukhim, Mermel et al. 2010, Borrell 2010). Further evidence to support the use of cell lines as pre-clinical models (Neve, Chin et al. 2006, McDermott, Sharma et al. 2007, McDermott, Sharma et al. 2008, Lin, Baker et al. 2008, Sos, Michel et al. 2009) includes that from Sos et al (Sos, Michel et al. 2009), who studied the genomes of 84 NSCLC cell lines to show that they are highly representative of those of primary NSCLC tumours, and identified molecular and genomic predictors of drug sensitivity which they validated using lung cancer mouse models. Also,

Neve et al (Neve, Chin et al. 2006) catalogued the recurrent genomic, transcriptional and biological characteristics of 51 breast cancer cell lines and showed that they represented those of 145 primary breast tumours, although some significant differences were documented. They concluded from this, together with results from predictive studies using Trastuzamab (Herceptin), that the cell lines were appropriate pre-clinical tools to investigate and to identify biomarkers to predict sensitivity and resistance to anti-cancer agents. Resistance mechanisms in drug-adapted cancer cell line models have been shown to reflect drug resistance mechanisms in patients (Sharma, Haber et al. 2010, Domingo-Domenech, Vidal et al. 2012, Korpal, Korn et al. 2013, Joseph, Lu et al. 2013, Bucheit, Davies 2014, Crystal, Shaw et al. 2014).

2.3.1.2 The Resistant Cancer Cell Line Collection (RCCL)

Over the last 25 years, the first resistant cancer cell line collection (RCCL) has been created by Jindrich Cinatl (Institute of Medical Virology, Goethe University, Frankfurt/Main, Germany) and his co-workers including his former group member Martin Michaelis (University of Kent). It currently consists of nearly 1000 cancer cell lines, sourced from a broad range of entities, and adapted to growth in the presence of therapeutic concentrations of clinically relevant anti-cancer agents. This tool is constantly growing due to the addition of novel drugs and cancer cell lines, and has the potential to be used for high throughput screening in the future. From the RCCL, we have used platinum resistant neuroblastoma cell lines and their corresponding drug sensitive parental cell lines for our studies.

Initial studies using cell lines from the RCCL were carried out by Jindrich Cinatl et al, and they were mainly to evaluate chemotherapeutic agents belonging to the nucleoside analogue family, which are used to treat both cancer and viral diseases such as HIV-1. Michaelis along with Cinatl et al have continued to extensively use both sensitive and drug-resistant neuroblastoma cell lines from the RCCL collection to study cancer, in particularly to understand molecular chemotherapy drug resistance mechanisms (Michaelis, Klassert et al. 2009). Furthermore, they have used RCCL cell lines, in particularly neuroblastoma, to evaluate other new potential anti-cancer agents to overcome drug resistance, for example the murine double minute 2 (MDM2) antagonist Nutlin-3 (Michaelis, Rothweiler et al. 2009, Van Maerken, Ferdinande et al. 2009) and to study biomarkers and prospective drug targets, for example the overexpression of EGFR in cisplatin-resistant neuroblastoma cells (Michaelis, Bliss et al. 2008).

2.3.2 Saccharomyces cerevisiae

2.3.2.1 The use of S. cerevisiae as a pharmacogenomic tool in cancer research

The budding yeast *S.cerevisiae* is extensively used as a model organism to study eukaryotic cell biology and advantages to using *S.cerevisiae* is that it has simple growth requirements, has a rapid

doubling time, has a small genome which is easy to genetically manipulate, can exist in both haploid and diploid states, which means recessive mutations can be studied, and is inexpensive (Simon, Bedalov 2004, Matuo, Sousa et al. 2012). There is evidence for high levels of similarities between cellular processes of human and yeast that partake in carcinogenesis, such as DNA repair, cell cycle checkpoints, and epigenetic control systems. However, yeast is unicellular and cannot completely substitute for mammalian models because they cannot be used to study the tumour microenvironment and aspects such as angiogenesis and tissue invasion. Also, there may be a decrease in permeability to some anticancer agents, such as DNA topoisomerase toxins, and yeast are deficient in some drug metabolising, tumour suppression and apoptotic enzymes (Matuo, Sousa et al. 2012). *S. cerevisiae* can be used as an efficient tool to study modes of drug action as well as drug screening. Pharmacogenomics is the study of the genes that affect response to drugs, and large systemic studies have been carried out in the yeast *S. cerevisiae* compared to very few in humans (Silberberg, Kupiec et al. 2016).

For anti-cancer drug screening, single target genes can be overexpressed in yeast to lead to a specific phenotype to screen for chemical-induced inhibition of this protein. An example of this is screening for poly (ADP-ribose) polymerases 1 (PARP1) inhibitors which ultimately improve the efficacy of DNA damaging agents like the platinum drugs (Perkins, Sun et al. 2001, Gao, Chen et al. 2014) (see 2.2.2.3). Also anti-cancer drug screening can take advantage of cellular processes that are conserved between yeast and humans. For example, target of rapamycin (TOR) signalling mediates cell growth and is exacerbated in cancer cells, so *S.cerevisiae* is a suitable model to screen for TOR pathway inhibitors (Bjornsti, Houghton 2004, Gao, Chen et al. 2014).

There are different ways to screen yeast for studying the mode of action of drugs and understand more about drug resistance mechanisms, one of which is drug-induced haploinsufficiency profiling (HIP). Haploinsufficiency is when a diploid cell with one copy of a gene grows in the same way as wild type, except in conditions for which full protein activity is necessary. The concept of HIP profiling is that if an essential gene encoding a drug target contains a heterozygous deletion then in the presence of that drug that strain will exhibit drug sensitivity and reduced fitness, which can be measured by gene tagging (see 2.3.2.2). From parallel screening all possible heterozygous deletion strains, this type of assay enables the identification of both direct drug targets and proteins that may act in the same pathway (Smith, Ammar et al. 2010, Cheung-Ong, Giaever et al. 2013). An example of such a study is by Lum et al, who assessed the cellular effects of 78 compounds in this way, including cisplatin, for which they identified the genes PSY2 (Platinum SensitivitY; Subunit of protein phosphatase PP4 complex which regulates recovery from the DNA damage checkpoint), VPS65 (Vacuolar Protein Sorting; though unlikely to encode a functional protein), and ATP4 (ATP synthase; Subunit b of the stator stalk of mitochondrial F1F0 ATP synthase) as possible cisplatin targets (Lum, Armour et al. 2004). Another method of yeast

screening is homozygous profiling (HOP), which is analogous to HIP profiling except that non-essential genes are completely deleted in diploid or haploid strains and strains sensitive to the drug, as for HIP, exhibit drug sensitivity and reduced fitness. However, direct targets are not identified in this way because the genes are absent, so HOP profiling more identifies genes that are necessary for growth in the presence of drug and buffer drug effects. These genes can be potentially responsible for drug resistance (Smith, Ammar et al. 2010, Cheung-Ong, Giaever et al. 2013). We have used a type of HOP profiling in our studies by stamping haploid gene deletion strains (see 2.3.2.2) onto solid agar containing drug to assess strain growth based on colony size.

2.3.2.2 The Yeast Knock-out collection (YKO) deletion collection and the Yeast Fitness Database

The Yeast Knock-out collection (YKO) was created by Giaver et al (Giaever, Chu et al. 2002), which is comprised of four mutant libraries (heterozygous and homozygous diploids, and haploids of both *MAT***a** and *MAT*α mating types) as part of the Saccharomyces Gene Deletion Project (Saccharomyces Gene Deletion Project (Stanford University, Stanford CA)). The *S.cerevisiae* strains CWG424 (wild-type) and all deletion strains used in our studies were derived from one of the four libraries, the MATa haploid gene deletion library. For each of the four YKO libraries, the deletion strains cover approximately 96 % of the yeast genome and were created using a PCR-based gene deletion strategy (Giaever, Chu et al. 2002). Each deletion was replaced with a KanMX module and uniquely tagged with one or two 20mer sequences to act like an identification bar code. For history of this Yeast Knock-out collection (YKO), refer to (Giaever, Nislow 2014).

The Yeast Fitness Database (Yeast Fitness Database (2008). Hillenmeyer,Maureen E., Fung et al.) is a collection of growth fitness results generated from screening libraries of yeast gene deletion strains in the presence of numerous chemical or environmental stress conditions. This database was constructed by a group led by Maureen Hillenmeyer (Stanford University) and Guri Giaever (University of Toronto) (Hillenmeyer, Fung et al. 2008), also see accompanying supplementary material for detailed methodology and analysis) and has been used extensively in yeast pharmacogenomic research. The libraries of yeast deletion strains that they used were the homozygous and heterozygous diploid deletion strain libraries, which, along with the MATa library (see 2.3.2.2 and 3.1.2.1) are part of the Yeast Knock-out collection (YKO), created by (Giaever, Chu et al. 2002), as part of the Saccharomyces Gene Deletion Project (Saccharomyces Gene Deletion Project (Stanford University, Stanford CA)) as described above. Screening involved growing pools of deletion strains competitively in liquid culture in the presence of different conditions, purifying the genomic DNA and amplifying the unique molecular tags on the gene deletion cassettes by PCR (as in (Pierce, Fung et al. 2006) - also see supplementary material). These amplified unique tags, which allow for parallel analysis, were then hybridised to a TAG3 DNA array chip, which is specifically for use with the yeast deletion collections, and fluorescently labelled, the array scanned and the resulting fluorescence intensities were used to determine any

changes in the amount of each strain present (method detailed in (Pierce, Davis et al. 2007), although note that this describes TAG4, not TAG3, arrays and analysis). To assess for significant sensitivity to the conditions tested, a fitness defect (FD) z-score was generated for every gene-experiment test, from which an accompanying fitness defect p-value was calculated ((Hillenmeyer, Fung et al. 2008), see accompanying supplementary material for detailed analysis). For our studies we have taken, from the Yeast Fitness Database, the entire set of homozygous knockouts inhibited data for the drugs cisplatin, carboplatin and oxaliplatin. We used these data from screening the whole yeast genome to investigate gene hits unique and common to each drug, and to explore the functions and processes in which they are involved in to understand more about how these drugs work and to compare them to one another.

2.4 The aim and study plan for our investigations

The aim of our studies was to investigate platinum drug modes of action and resistance mechanisms using *S.cerevisiae* as a pharmacogenomic tool and human neuroblastoma cell lines, both the drug sensitive parental cells and their corresponding sub-lines resistant to each drug, as models of cancer. We focussed on the drugs cisplatin, carboplatin, and oxaliplatin. These were tested in a library 209 homozygous Mata strains of *S.cerevisiae* in which single genes (non-essential) encoding key transcription factors and transcriptional regulators were deleted. The rationale for focussing on transcription factors and transcriptonal regulators was because they are involved in the expression of many genes encoding proteins involved in many processes and pathways, enabling a broader picture of drug action and resistance to be generated from our screening, and also the potential to further study the process and pathways in which they are involved. Strains were stamped onto solid media containing and not containing each platinum drug. Growth was monitored over time to assess drug sensitivity by scoring colony size on agar with drug as a percentage of growth on agar with drug; hits were strains that exhibited the least growth on agar containing drug compared to that on agar containing no drug. The hits for each drug were assessed for genes common and unique to each drug, in an attempt to understand the action of individual drugs and potential resistance mechanisms, besides looking for possible drug targets to enhance platinum cytoxicity, or even biomarkers to predict outcome of platinum therapy. We also analysed the distribution of our screen hits between the drugs and the cellular processes in which these genes are involved. Additionally, we investigated the Yeast Fitness Database results from screening the entire homozygous diploid deletion library of *S.cerevisiae* against the three platinum drugs (for their screening methods refer to 2.3.2.2); hits were deletion strains with poor fitness in the presence of drug compared to without drug. We studied this large data set in an attempt to gain a better understanding of the bigger picture of the genes involved in their mode of action and potentially resistance to these agents because their screen was

essentially of the entire genome. We did this, not by individual gene comparison, but solely in terms of the distribution of the number of gene hits between the drugs, and also of the functions and processes that the genes are involved in. Again, we looked for similarities and differences between the drugs, and then compared the results to those of our smaller library screen.

In addition, we have characterised a panel consisting of the neuroblastoma parental cell lines UKF-NB-3 and UKF-NB-6 and the sub-lines with acquired resistance to cisplatin, carboplatin or oxaliplatin for growth kinetics, morphology and sensitivity profiles to the three platinum drugs to see whether we could identify patterns. The drug-resistant cell lines were also cultured in the absence and presence of drug for three months to assess whether resistance was reversible or a permanent genomic change. Finally, we compared UKF-NB-3 and UKF-NB-6 parental cells and their cisplatin-resistant sub-lines in a proteomics approach, using 2-dimensional gel electrophoresis and mass spectroscopy methods, to investigate proteins that could be implicated as playing a role in acquired cisplatin resistance and in response to acute cisplatin treatment.

3 Saccharomyces cerevisiae

3.1 Materials and Methods - yeast

3.1.1 Platinum drugs

All stocks, described below, of platinum drugs were stored at room temperature in the dark/wrapped in foil.

3.1.1.1 Platinum drugs for screening yeast grown on solid agar for platinum drug sensitivity

For the initial plate-based screening on solid agar of a transcription factor deletion strain library (see section 3.1.3), the cisplatin 1 mg/mL solution used was prepared manually by diluting solid cisplatin (Sigma, Poole, Dorset, UK, Ref P4394) in 0.9 % sodium chloride. The 0.9 % sodium chloride solution (Fisons, Ipswich, Suffolk, UK, now part of Rhone-Poulenc, Inc., Ref S/3160/60) was prepared by dissolving 9 g sodium chloride with MQ H_20 up to to 1000 mL and filter-sterilised (0.2 micron). Cisplatin was left to dissolve stirring on a magnetic stirrer (Bibby B212, Bibby Scientific Ltd, Stone, Staffordshire, UK) in the dark at room temperature for 5 days, after which it was adjusted to the final volume with diluent, filter-sterilised (0.2 micron), and aliquoted into sterile tubes. All filtering was carried out in a Class II biological safety cabinet (Cellgard Energy Saver (ES) Model NU 480-400E, Nuaire, Plymouth, UK) because this cisplatin was also to be used in mammalian cell culture. Note for this pH was not adjusted.

In a second set of experiments to re-screen strains to confirm drug sensitivity (see section 3.1.5), the cisplatin 1 mg/mL Concentrate for Solution for Infusion used was from Accord Healthcare Limited (North Harrow, Middlesex, UK) and purchased from Shakespeare Pharma Ltd. (Hilton, Derbyshire, UK). This solution contains 0.9 % sodium chloride, so for control experiments, instead of drug, 0.9 % sodium chloride solution (Fisons, Ipswich, Suffolk, UK, now part of Rhone-Poulenc, Inc., Ref S/3160/60) was prepared with MQ H_20 as diluent, and the pH was adjusted to 3.6-3.8 (to be of equivalent pH to the product) using hydrochloric acid (Fisons, Ipswich, Suffolk, UK, now part of Rhone-Poulenc, Inc., Ref H/1150/PB17) and filter-sterilised (0.2 micron).

For both plate-based screens (see sections 3.1.3 and 3.1.5), carboplatin 10 mg/mL concentrate for solution for Infusion was from Sun Pharmaceutical Industries (Leeds, Yorkshire, UK) and purchased from Shakespeare Pharma Ltd. (Hilton, Derbyshire, UK), the diluent being water for injections, with a pH between 4 and 7, so for control experiments, instead of drug, autoclaved MQ H_20 was used.

For both plate-based screens (see sections 3.1.3 and 3.1.5), oxaliplatin 5 mg/mL Concentrate for Solution for Infusion was from TEVA (Castleford, West Yorkshire, UK) and purchased from Shakespeare Pharma Ltd. (Hilton, Derbyshire, UK). This solution contains 4.5 % lactose monohydrate. Yeast cannot metabolise lactose monohydrate so for the initial plate-based screening of a transcription regulator based deletion strain library (section 3.1.3), for control experiments, instead of drug, MQ H_20 was used. However, for the hit re-screen (section 3.1.5), for control experiments, 4.5 % lactose monohydrate (Fisons, Ipswich, Suffolk, UK, now part of Rhone-Poulenc, Inc., Ref L/0200/60) was used – this was prepared by dissolving 45 g lactose monohydrate with MQ H_20 up to 1000 mL and filter-sterilised (0.2 micron), having a pH between 4 and 6, equivalent to the product.

3.1.1.2 Platinum drugs for use in liquid growth experiments

For liquid growth experiments see section 3.1.6.

All drugs were sourced by Shakespeare Pharma Ltd. (Hilton, Derbyshire, UK).

Cisplatin 1 mg/mL Concentrate for Solution for Infusion was from Accord Healthcare Limited (North Harrow, Middlesex, UK) – as described above for plate based re-screening in 3.1.1.1.

Carboplatin 10 mg/mL Intravenous Infusion was from Hospira (Leamington Spa, Warwickshire, UK) sourced by Shakespeare Pharma Ltd. (Hilton, Derbyshire, UK), the diluent being water for infusion with a pH between 4 and 7, so for control experiments, instead of drug, autoclaved MQ H_20 was used.

Oxaliplatin 5 mg/mL Concentrate for Solution for Infusion was from TEVA (Castleford, West Yorkshire, UK) – as described above for plate based screening in 3.1.1.1, except 4.5 % lactose monohydrate solution was used for all control experiments.

3.1.2 The MATa gene deletion library of yeast strains, media and growth conditions

3.1.2.1 Yeast strains

The *S. cerevisiae* strains CWG424 (also known in the CWG laboratory (UKC) as CGY424, and generically as BY4741) and all deletion strains were derived from the MATa haploid gene deletion library (2.3.2.2), which can be purchased from Open Biosystems, now (Dharmacon), GE Healthcare Life Sciences, Little Chalfont, Buckinghamshire, UK). These strains were routinely grown in YPD liquid medium at 30 °C in a shaking incubator (200rpm) or on YPD agar in a standing 30 °C incubator.

The following four transformants strains (for preparation and plasmid details see 3.1.6.1),

S. cerevisiae strain wild type CWG424 transformed with negative control plasmid PCG279
S. cerevisiae strain wild type CWG424 transformed with BDF1 plasmid PCG596
S. cerevisiae strain *ΔBdf1* transformed with negative control plasmid PCG279
S. cerevisiae strain *ΔBdf1* with BDF1 plasmid PCG596

can grow without uracil because the PCG279 and PCG596 plasmids have the URA3 gene. These transformant strains were routinely grown in synthetic defined (SD) medium lacking uracil, referred to as SD-URA medium at 30 °C in a shaking incubator (200 rpm), or on SD-URA agar in a 30 °C standing incubator.

3.1.2.2 YPD (Yeast, Peptone, Dextrose) medium and agar

YPD medium comprised of 1 % yeast extract (Oxoid, Fisher Scientific (part of Thermo Fisher Scientific), Loughborough, Leicestershire, UK, Ref LP0021) and 2 % peptone (BD biosciences, Oxford Science Park, Oxford UK, Ref BD 211677), was prepared with MQ H_20 as diluent in a glass Duran bottle, autoclaved and then 2 % dextrose (Fisons, Ipswich, Suffolk, UK, now part of Rhone-Poulenc, Inc., Ref G/0550/61) added once cooled to a temperature at which it can be held.

For YPD agar, 1.5 % granulated agar (Oxoid, Fisher Scientific (part of Thermo Fisher Scientific), Loughborough, Leicestershire, UK, Ref LP0013) was added to a YPD liquid medium mixture before autoclaving (just described) and, after autoclaving, the 2 % dextrose (Fisons, Ipswich, Suffolk, UK, now part of Rhone-Poulenc, Inc., Ref G/0550/61) was added once cooled to a temperature at which it can be held. The agar was then poured into standard 90 mm petri dish plates (about 20 mL per dish) and allowed to cool further at room temperature until set. Plates were the dried open and upturned for 20 mins in a drying cabinet set at 40 °C (Gallen Kamp, now Weiss Technik, Loughborough, Leicestershire, UK), and stored at 2-8° C until used.

3.1.2.3 Synthetic defined (SD) medium and agar lacking uracil (referred to as SD-URA medium or agar)

SD-URA medium comprised of 0.675 % Yeast Nitrogen base without amino acids (Formedium, Hunstanton, Norfolk, UK, Ref CYN0402), 0.192 % Synthetic complete mixture (Kaiser) drop-out medium supplement lacking uracil (Formedium, Hunstanton, Norfolk, UK, Ref DSCK1009), prepared using MQ H_20 as diluent in a glass Duran bottle and then 2 % dextrose (Fisons, Ipswich, Suffolk, UK, now part of Rhone-Poulenc, Inc., Ref G/0550/61) added once cooled to a temperature at which it can be held.

For Synthetic defined (SD) medium lacking uracil (SD-URA) agar, 1.5 % granulated agar (Oxoid, Fisher Scientific (part of Thermo Fisher Scientific), Loughborough, Leicestershire, UK, Ref LP0013)

was added to a SD-URA liquid medium mixture before autoclaving (just described) and, after autoclaving, the 2 % dextrose (Fisons, Ipswich, Suffolk, UK, now part of Rhone-Poulenc, Inc., Ref G/0550/61) was added once cooled to a temperature at which it can be held. Then the pouring and drying procedure was as for making YPD agar plates (3.1.2.2).

3.1.2.4 Making two-fold concentrated media or agar

When performing experiments involving the addition of drug to medium or agar (3.1.3.3 and 3.1.5.3) medium or agar was prepared by dissolving components in half the total volume of MQ H_20, resulting in a two-fold concentration. During experimental set up, the addition of MQ H_20 containing the drug and/or drug diluent (and, for medium only, yeast culture) at the required concentrations to this, resulted in the correct final concentration of medium/agar components.

3.1.2.5 Overnight cultures

Unless stated, an overnight culture of a yeast strain was prepared by transferring 3 mL of the required medium into sterile Universal tubes. The medium was inoculated with yeast cells from colonies on agar plates using a sterile pipette tip, and grown overnight, shaking at 200 rpm at 30 °C in an Innova 44 shaking incubator (New Brunswick, part of Eppendorf, Stevenage, Hertfordshire, UK).

3.1.2.6 Measuring the absorbance (Abs_{595}) of cultures

The Abs_{595} of cultures was routinely measured using an Eppendorf Biophotometer Plus (Eppendorf, Stevenage, Hertfordshire, UK), by diluting cultures 1 in 100 in 1 mL ddH_2O in a 1 mL cuvette (1 cm path length), and inverting several times to mix (with a cover of parafilm) before taking a reading. The resulting Abs_{600} was multiplied by 100 to get the true absorbance unit (AU) value.

3.1.3 Initial plate-based screening of a transcription regulator based deletion strain library

3.1.3.1 Creating the transcription regulator library of gene deletion yeast strains

The transcription regulator library of gene deletion yeast strains was provided as glycerol stocks stored at -80 °C in 96-well plates by the CWG laboratory, University of Kent. Members of this library were from the MATa haploid gene deletion library (Saccharomyces Gene Deletion Project (Stanford University, Stanford CA)) purchased from Open Biosystems, now (Dharmacon), GE Healthcare Life Sciences, Little Chalfont, Buckinghamshire, UK) (see 2.3.2.2 and methods 3.1.2.1 for MATa library details). The list of members of this library was originally generated by performing a search in SGD Gene Ontology (Saccharomyces Gene Database (SGD) (Stanford

University, Stanford CA)) using the term “transcription factor”. This search generated all *S. cerevisiae* transcription factor genes, and additionally pulled out some transcriptional regulators and a small percentage of non-transcriptional members. Some extra members were added manually and the resulting list comprised of 209 strains. All genes were non-essential genes.

A table of members of this transcription regulator library of gene deletion yeast strains, their names and role descriptions, and their positions in a total of three 96-well plates is shown in Appendix A; names and roles were taken from their locus overview in the SGD (Saccharomyces Gene Database (SGD) (Stanford University, Stanford CA)). Any non-transcriptional members have roles highlighted in purple. Each plate included wild type strain CWG424 (also known in the CWG laboratory (UKC) as CGY424, and generically as BY4741). Additional wells of CWG424 were added to each plate (highlighted bold, red type) along with the DNA repair mutants and *ΔRad52* and *ΔRad27* as control strains (highlighted bold, black type), making a total of 212 strains to be screened altogether.

3.1.3.2 Growth of the transcription regulator library in preparation for screening

Glycerol stock 96-well plates 1-3 of the transcription regulator based deletion strain library (described in 3.1.3.1) were, one at a time, placed on ice until just thawed. Then, using a 96-pronged metal replica plater (Sigma, Poole, Dorset, UK, Ref R-2508-IEA), they were gently mixed and stamped onto YPD agar (3.1.2.2) in large 150 mm petri dish plates (65 mL agar per plate). The replica plater was dipped in alcohol and flamed before stamping out each plate. These plates were left at room temperature until the stamped-out strains were dry, and then incubated upturned in a standing 30 °C incubator (Leec Classic Incubator, Leec, Nottingham, UK) for three days.

Next, the day before screening, strains on these plates were inoculated, in the same format, into each of three 96-well plates (Greiner Bio-One Cellstar 96-well plates, Greiner BioOne Ltd, Stonehouse, UK, Ref 655 180) containing 150 µL/well of YPD medium to make overnight cultures. This was carried out using autoclaved fine tipped plastic 96-pronged stampers (Singer Instruments, Watchet Somerset, UK Ref RP-MP-2L), a new one for each plate. These 96-well plates were subsequently sealed tightly with parafilm to prevent any evaporation, and then incubated with shaking overnight on a plate shaker (Grant Bio PMS-1000, Grant Instruments, Shepreth, Cambridge, UK) in a 30 °C static incubator (Stuart S160 incubator, Stuart, Stone, Staffordshire, UK).

3.1.3.3 Preparation of YPD agar plates with and without drug to screen the transcription regulator library

YPD agar containing 1000 µM cisplatin, 4000 µM carboplatin, or 4000 µM oxaliplatin, and corresponding control agar containing drug diluent only, was prepared on the same day of screening as follows. Drug solutions and drug diluents used are detailed in section 3.1.1.1.

Volumes of 75 mL of two-fold concentration YPD agar were prepared (3.1.2.4) in each of six 250 mL glass Duran bottles (three for the control agar, three for the agar containing drug). After autoclaving, the agar was cooled down for at least 30 mins in a water bath set at 55 °C (Grant SUB waterbath, Grant Instruments, Shepreth, Cambridge, UK). Bottles containing 0.9 % NaCl solution and MQ H_2O were also placed into a water bath set at 55°C. Each 75 mL two-fold concentration of YPD agar was to be adjusted to a final volume of 150 mL with drug and/or drug diluent, one at a time. For the agar containing drug, the volume of drug to give the required drug concentrations (1000 µM cisplatin, 4000 µM carboplatin, or 4000 µM oxaliplatin) at 150 mL final volume, and the volume of MQ H_2O required to make up to 150 mL, were added to the 75 mL two-fold concentration of YPD agar whilst swirling the bottle by hand to mix thoroughly. Next, the mixture was quickly transferred to each of seven standard 90 mm petri dish plates (21 mL per plate). It should be noted that drug was added last after the mixture had cooled to a temperature which could be held by hand. For control agar containing no drug, instead of drug, the equivalent volume of corresponding drug diluent was added. In this experiment the drug diluents were 0.9 % NaCl solution for cisplatin, and ddH_2O for carboplatin and oxaliplatin. It should also be noted that for both the cisplatin drug and control plates, an extra 33 % (compared to drug volume) of 0.9 % NaCl solution was added to the agar to maintain consistency with other cisplatin screening which had been carried out at 1500 µM. All agar plates were left to set for one hour at room temperature, and kept in the dark by covering them in a black cloth because the drugs are photosensitive. Plates were then dried open and upturned for 20 mins in a drying cabinet set at 40 °C (Gallen Kamp, now Weiss Technik, Loughborough, Leicestershire, UK).

3.1.3.4 Performing the yeast transcription regulator library screening

The overnight cultures of transcription regulator library plates 1-3 (prepared as described in 3.1.3.2), were removed from the shaker at 30°C, ready to stamp out on the YPD agar plates with and without drug (prepared as described in 3.1.3.3). These overnight library cultures were in 96-well plates, but were stamped as half plates (columns 1-6 (named a), and 7-12 (named b)), in singlicate, onto both the drug and no drug small agar plates using a using a 48-pronged metal replica plater (Sigma, Poole, Dorset, UK, Ref R-2383). To ensure strains were evenly in suspension before stamping out onto agar, a multi-channel pipette was used to by pipette them up and down

several times just before doing so. The replica plater was dipped in alcohol and flamed before stamping out each plate.

For stamping onto carboplatin and oxaliplatin onto drug and no drug control agar plates, the strains were diluted 1 in 10 with MQ H_2O (15 µL culture added to 135 µL ddH_2O per well in new 96-well plates (Greiner Bio-One Cellstar 96-well plates, Greiner BioOne Ltd, Stonehouse, UK, Ref 655 180), separate ones for each drug, prepared using multi-channel pipettes. The undiluted overnight library cultures strains were stamped onto cisplatin drug and no drug control agar plates. The reasoning behind diluting the yeast strains is explained in 3.2.1. All plates were transferred to and upturned in a standing 30 °C incubator (Leec Classic Incubator, Leec, Nottingham, UK), and growth was monitored by scanning images of the plates using a CanoScan 4400F scanner (Canon Europe Ltd, Uxbridge, London, UK) into Adobe photoshop software each day for four days.

It should be noted that for the cisplatin screening only, copies of strains YLR278C, UME6, ARR1, AFT1, AZF1 and SLA1 were inoculated into wells H7-H12 respectively of library plate 2. Also, library plate 2b (columns 7-12) was stamped out onto two cisplatin and two no cisplatin agar plates.

3.1.3.5 Analysis of the yeast transcription regulator library screening

Growth was assessed by measuring colony sizes on the daily scanned plate images (3.1.3.4) by eye. The size of the colony of a deletion strain on agar containing drug was expressed as a % of the size of the colony of the same deletion strain on agar containing no drug. Growth scores were assigned in increments as 0 % (no growth), ≤5 %, ≤10 %, ≤20 %, 30 %, ≤40 %, ≤50 % etc. and colour coded, and then also in 10 % increments post 50 %. These % growth values were recorded for each of the four days in 48-well formats in a Microsoft Excel 2010 spreadsheet, and an example of scoring of colony growth is shown in Figure 4. All % growth scores over all four days growth were then collated together for each individual yeast deletion strain, and tabulated as a time course of % growth values. Strains were broadly classed as hits if % growth was ≤50 % for each of the four days. Scoring of random colonies was validated by independent assessors to support accuracy of the method.

These hit strains were assembled as lists for each drug screen which were then organised into groups of unique and common genes to each drug in Venn diagrams using Venny 2.0 software (Oliveros 2007-2015), which excludes any duplicates, and Microsoft Powerpoint. These gene lists were also analysed using Gene Ontology (GO) Slim Mapper analysis via the Saccharomyces Gene Database (SGD) site (Saccharomyces Gene Database (SGD) (Stanford University, Stanford CA)), using the Yeast GO-slim terms ‘function’ and ‘process’ to group the genes into different functions and processes, which excludes duplicates, focussing on those with a fold enrichment value >1.0.

A. **1000 µM cisplatin** **Control/no drug**

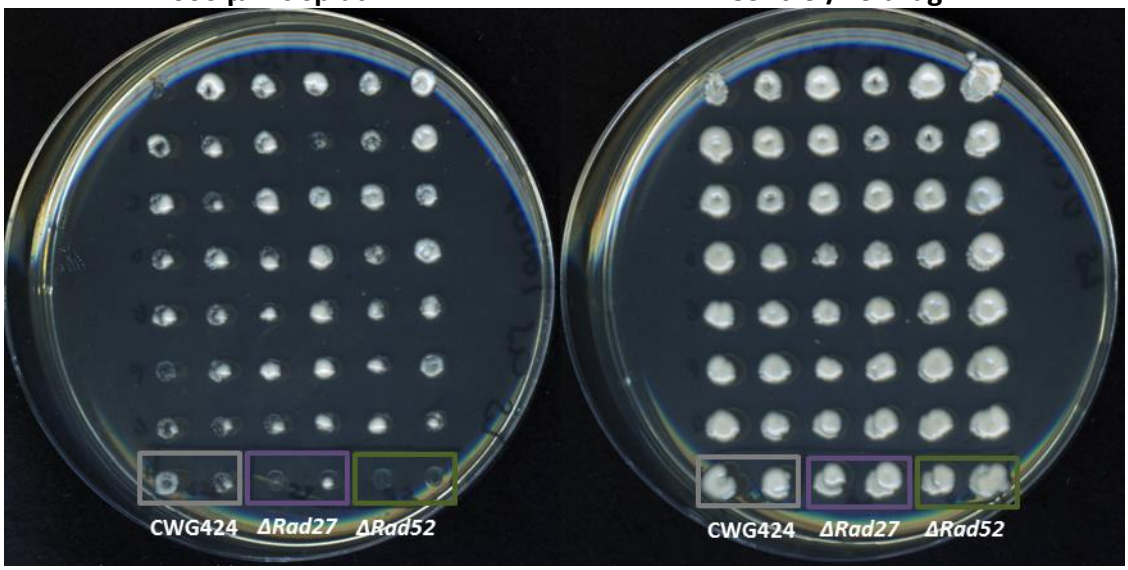

B. Scoring of strain growth in A.

	1	2	3	4	5	6
A	10	80	40	70	30	30
B	30	30	50	20	40	50
C	40	20	70	40	50	30
D	30	60	70	70	40	50
E	60	50	30	60	20	30
F	10	40	60	50	20	30
G	20	20	20	30	30	20
H	40	20	<5	10	<5	<5

Figure 4. A. An example of growth of members of the transcription regulator library of gene deletion yeast strains on agar with and without 1000 µM cisplatin. The results are from the cisplatin screen, day2, library plate 2a. Control strains are included – wild type CWG424 (grey), and DNA repair gene deletion strains **Δ**Rad27 (purple) and **Δ**Rad52 (green). B. Growth was assessed by colony size. The size of the colony of a deletion strain on agar containing drug was expressed as a % of the size of the colony of the same deletion strain on agar containing no drug. The table displays the scores for the results in A.

The stronger hit strains scoring ≤30 % for each of the four days were analysed in the same way but, because it was a smaller data set, we focussed on all of the gene hits, regardless of fold enrichment value.

3.1.4 The Yeast Fitness Database - analysis of platinum drug data

The entire homozygous knockouts inhibited data sets for sensitivity to cisplatin, carboplatin and oxaliplatin were downloaded from the Yeast Fitness Database (Yeast Fitness Database (2008). Hillenmeyer,Maureen E., Fung et al.) (refer to 2.3.2.2) into Microsoft Excel. For our analysis, we focussed on the genes generating a p-value cut off less than 0.01, which had a false discovery rate of 10 %, and hits from both generations -5 and 20 were included, as were hits from all

concentrations of drug tested (Hillenmeyer, Fung et al. 2008), see accompanying supplementary material for detailed analysis); cisplatin was tested at concentrations from 31.25 to 500 µM, carboplatin from 250 µM to 15000 µM, and oxaliplatin from 1000 µM to 4000 µM. The resulting gene hit lists were organised into groups of unique and common genes sensitive to each drug in Venn diagrams using Venny 2.0 software (Oliveros 2007-2015) and Microsoft Powerpoint, which excluded the duplicates gene hits. These gene lists were also analysed using Gene Ontology (GO) Slim Mapper analysis via the Saccharomyces Gene Database (SGD) site (Saccharomyces Gene Database (SGD) (Stanford University, Stanford CA)) using the Yeast GO-slim terms 'function' and 'process' to group the genes into different functions and processes, which excluded the duplicates gene hits. All resulting functions and processes with a fold enrichment value >1.0 were organised into those unique and common to each drug in Venn diagrams using Venny 2.0 software (Oliveros 2007-2015), which excluded duplicate gene hits, and Microsoft Powerpoint.

3.1.5 Confirmation screening of the 'hits' generated from the initial plate-based screening of the transcription regulator library

3.1.5.1 Creating master plates of hit deletion strains

A master plate was created of the 25 yeast gene deletion strains that were classed as hits (% growth was ≤30 % for each of the four days) in the initial plate-based screening of the transcriptional regulator library (see method 3.1.3 and results 3.2.1.3). Five extra strains were included - two extra transcriptional regulators, *ΔADR1* and *ΔHIR1*, and also *ΔHMS1*, *ΔKAR4* and *ΔAFT1* as additional controls. The hit strains were taken from the original MATa haploid gene deletion library (see sections 2.3.2.2 and 3.1.2.1) which was stored at -80°C. Using pipette tips the frozen strains were streaked onto YPD agar (3.1.2.2) and grown in a standing 30 °C incubator (Leec Classic Incubator, Leec, Nottingham, UK) for three days. Using pipette tips, each strain was individually inoculated into a well, one for each strain, of two 24-well cell culture plates (Greiner Bio-One Cellstar 24-well plates, Greiner BioOne Ltd, Stonehouse, UK, Ref 662 160) containing 1 mL /wellYPD liquid medium (3.1.2), and incubated shaking overnight at 200 rpm at 30 °C in an Innova 44 shaking incubator (New Brunswick, part of Eppendorf, Stevenage, Hertfordshire, UK). The next day, 75 µL of these overnight cultures were transferred into 75 µL 40 % glycerol (Fisher Scientific (part of Thermo Fisher Scientific), Loughborough, Leicestershire, UK, Ref G/0650/17) per well into one half of a 96-well cell culture plate (Greiner Bio-One Cellstar 96-well plates, Greiner BioOne Ltd, Stonehouse, UK, Ref 655 180), gently pipetted up and down to mix and then transferred to -80 °C to keep as glycerol stocks and to use for the hit conformation screening.

A table of the hit yeast gene deletion strains, their names and role descriptions, and their positions in the 96-well glycerol stock plate for screening is shown in Appendix B, created and labelled in the same way as described for Appendix A (3.1.3.1).

3.1.5.2 Growth of the hit yeast deletion strains in preparation for screening

The glycerol stock 96-well master plate of hit strains (3.1.5.1) was thawed, stamped out onto agar and grown in the same way as in 3.1.3.2, but using a 48 pronged metal replica plater (Sigma, Poole, Dorset, UK, Ref R-2383) and YPD agar in a standard 90 mm petri dish plate. The day before screening, these strains on the YPD plates were inoculated into 3 mL YPD medium in Universal tubes to make overnight cultures as described in section (3.1.2.5).

3.1.5.3 Preparation of YPD agar plates with and without drug to re-screen the twenty-five 'hits' from the transcription regulator library of gene deletion yeast strains

YPD agar containing 1000 µM cisplatin, YPD agar containing 4000 µM carboplatin, and YPD agar containing 4000 µM oxaliplatin, and corresponding control agar containing drug diluent only, was prepared on the same day of screening as follows. For the selection of these drug concentrations refer to section 3.2.1. Drug solutions and drug diluents used are detailed in section 3.1.1.1.

A volume of 300 mL of two-fold concentration YPD agar was prepared (3.1.2.4) in a 500 mL glass Duran bottle. After autoclaving, the agar was cooled down for at least 30 mins by transferring it into a water bath set at 55 °C (Grant SUB waterbath, Grant Instruments, Shepreth, Cambridge, UK) along with bottles containing 0.9 % NaCl solution, MQ H_2O and 4.5 % lactose monohydrate solution and six empty pre-autoclaved 250 mL Duran bottles. At this temperature the agar does not set.

A volume of 35 mL two-fold concentration of YPD agar was to be adjusted to a final volume of 70 mL with drug and/or drug diluent, one at a time. For the agar containing drug, the volume of drug to give the required drug concentrations (1000 µM cisplatin, 4000 µM carboplatin, or 4000 µM oxaliplatin) at 70 mL final volume, and the volume of MQ H_2O required to make up to 70 mL, were added to a warmed pre-autoclaved 250 mL Duran bottle, followed by the 35 mL two-fold concentration of YPD agar whilst swirling the bottle by hand to mix thoroughly. Next, the mixture was quickly transferred to each of three standard 90 mm petri dish plates (21 mL per plate). For control agar containing no drug, instead of drug, the equivalent volume of corresponding drug diluent (at 55°C) was added and three plates were again poured. In this experiment the drug diluents were 0.9 % NaCl solution for cisplatin, and MQ H_2O for carboplatin, and 4.5 % lactose monohydrate solution for oxaliplatin. It should also be noted that for both the cisplatin drug and control plates, an extra 33 % (compared to drug volume) of 0.9 % NaCl solution was added to the agar to maintain consistency with other cisplatin screening which had been carried out at 1500 µM. All agar plates were left to set and dry as in 3.1.3.3.

3.1.5.4 Performing the confirmation screen of the twenty-five 'hits' from the transcription regulator library

The overnight cultures of the hit deletion strains (prepared as in 3.1.5.2) were removed from the shaker at 30°C, ready to stamp out on the YPD agar plates with and without drug (prepared as described in 3.1.5.3). The A_{595} of each culture was measured as described in section 3.1.2.6 to check if they were in the same range of 13-15. If any culture measured as having an A_{595} above range it was adjusted diluting with MQ H_2O, and if an A_{595} was below range a culture sample was taken and centrifuged at 4000 rpm for 4 minutes using a Sigma 1-14 benchtop centrifuge (Sigma, Poole, Dorset, UK) and re-suspended in a reduced volume of MQ H_2O. A volume of 180 µL/well of each overnight culture was then transferred into a 96-well cell culture plate (Greiner Bio-One Cellstar 96-well plates, Greiner BioOne Ltd, Stonehouse, UK, Ref 655 180) in the same format as the 96-well glycerol plate as shown in Appendix B and as described in section 3.1.5.1.

From this culture plate, two further plates in the same format were prepared, but with the strains diluted 1 in 10 (15 µL culture in 13 5µL MQ H_2O per well), resulting in all a total volume of 150 µL/well. Strains were mixed into suspension by pipetting before stamping them out onto agar in triplicate, onto both drug and no drug agar plates using a 48-pronged metal replica plater (Sigma, Poole, Dorset, UK, Ref R-2383), dipping the plater in alcohol and flaming before stamping out each plate. The undiluted strains were used for the cisplatin drug and no drug plates, and the 1 in 10 diluted strains were used for the carboplatin and oxaliplatin drug and no drug plates. The reasoning behind diluting the yeast strains is explained in 3.2.1. Plates were grown and imaged as in 3.1.3.4.

3.1.5.5 Analysis of the conformation screen

Growth was assessed by measuring colony sizes on the daily scanned plate images (3.1.5.4) and scores recorded and tabulated as described in section 3.1.3.5. A score of 'ng' in these re-screens meant that there was no significant growth of the strain to score on either of the YPD containing drug or on the corresponding YPD agar containing no drug. Compared to the initial screen, growth inhibition in the presence of each drug was not as significant for this re-screen, so the method of classing strains as hits was re-designed as follows.

Strains were classed as strong hits if % growth for all three replicates was ≤30 % for two time points. Strains were classed as medium hits if % growth for two out of the three replicates was ≤30 % for two time points. Strains were classed as weaker hits if % growth for two out of the three replicates was ≤50 % for two time points. These hit strains were assembled as lists for each drug screen which were then organised into groups of unique and common genes to each drug in Venn diagrams using Venny 2.0 software (Oliveros 2007-2015) and Microsoft Powerpoint. As

before, scoring of random colonies was validated by independent assessors to support accuracy of the method.

3.1.6 Does the re-introduction of BDF1 into the *ΔBdf1* strains recover growth in the presence of the platinum drugs?

3.1.6.1 Transformations

Plasmid PCG279 (standard multi-copy expression vector PRS426, see Figure 5) was used as the negative control. PCG596 is the same PRS426 plasmid but with the *S.cerevisiae* gene BDF1 and its own promotor cloned into ORF frame 3. PCG279 and PCG596 were provided by Bianchi et al (Bianchi, Costanzo et al. 2004), and PRS426 was originally constructed by Christianson et al (CHRISTIANSON, SIKORSKI et al. 1992).

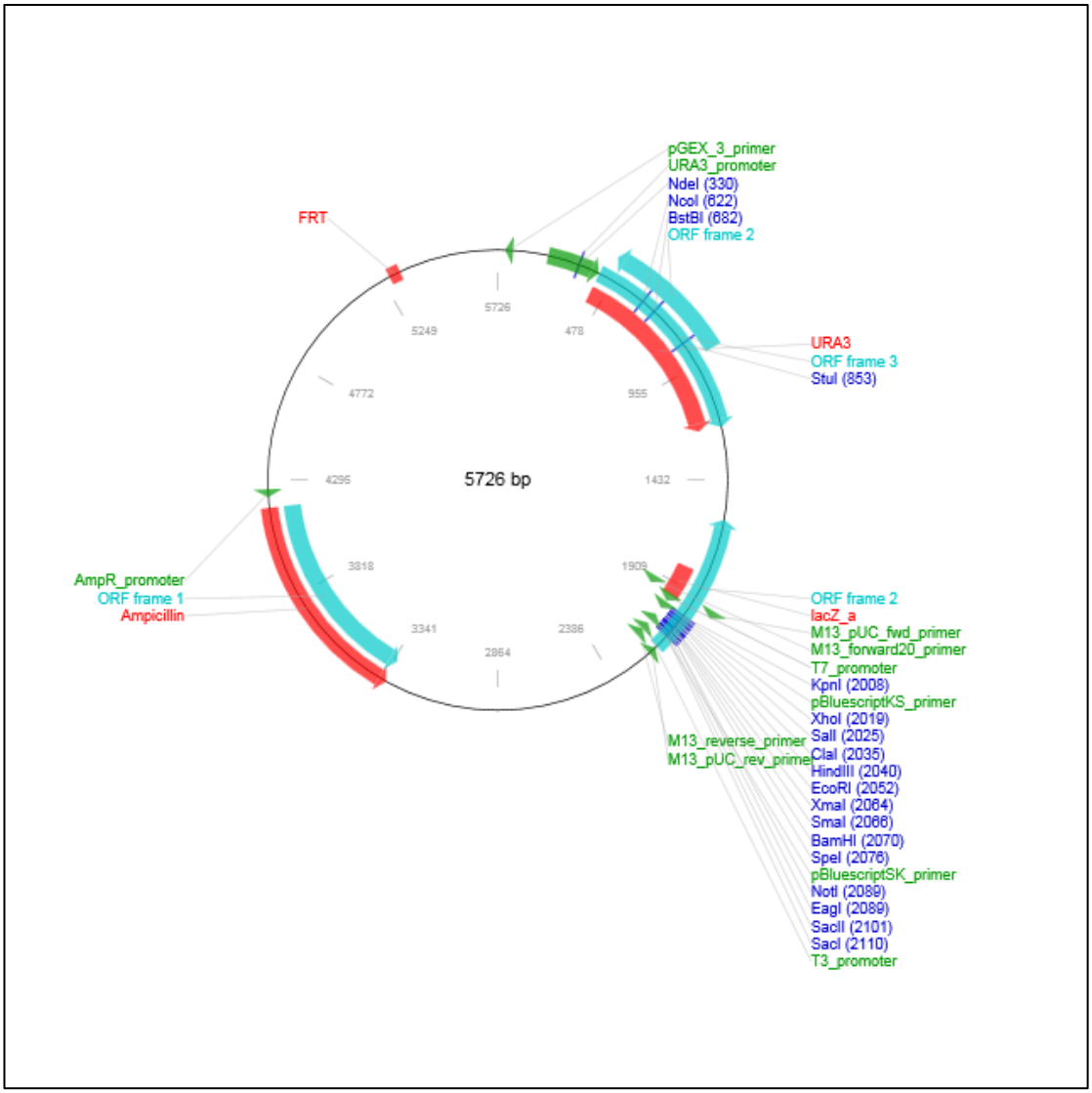

Figure 5. Plasmid PRS426 (https://www.addgene.org/vector-database/3989/).

Overnight cultures of *S. cerevisiae* strains CWG424 and *ΔBdf1* were prepared (3.1.2.5), and each strain was harvested by taking 1 mL overnight culture (A_{595} between 10-20 AU (absorbance units)) into each of two sterile Eppendorf tubes and centrifuging the total of four tubes at 4000 rpm for 4 mins in a Sigma 1-14 bench centrifuge. The supernatants were discarded, and then the cells were re-suspended with 1 mL TE (1 mM Tris (Fisons, Ipswich, Suffolk, UK, now part of Rhone-Poulenc, Inc.,Ref T/P630/60), 1 mM EDTA (Fisons, Ipswich, Suffolk, UK, now part of Rhone-Poulenc, Inc., Ref D/0700/53, pH8.0) and centrifuged at 4000 rpm for 4 mins in a Sigma 1-14 benchtop centrifuge (Sigma, Poole, Dorset, UK). The supernatants were then discarded and the cells were re-suspended with 1 mL 0.1 M LiOAc (Sigma Poole, Dorset, UK, Ref L4158) in TE and centrifuged again at 4000 rpm for 4 mins. This time the supernatants were discarded, the cells were re-suspended in 0.1 mL of 0.1 M LiOAc in TE, and then 15 µL (150 µg) carrier DNA (single stranded DNA from herring sperm (Sigma, Poole, Dorset, UK, Ref D7290), pre-boiled for 15 mins and then iced) was added to each cell mixture. Next, 1 µL (100 ng) PCG279 transforming DNA (see 3.1.6.1) was added to one tube of cell mixture originating from each of CWG424 or *ΔBdf1* strains, and 1 µL (100 ng) PCG596 transforming DNA (see 3.1.6.1) was added to the other tube of cell mixture originating from each of CWG424 or *ΔBdf1* strains, and all tubes were mixed gently by pipetting. Next, 700 µL of 40 % PEG4000 (Sigma, Poole, Dorset, UK, Ref 95904) in 0.1 M LiOAc in TE was added to each tube of cells and incubated with rotation (Stuart roller mixer SRT6, Stuart, Stone, Staffordshire, UK) for 90 mins at room temperature. The cells were then incubated for 15 mins at 42 °C in a Grant block heater (Grant Instruments, Shepreth, Cambridge, UK) and then centrifuged at 4000 rpm for 4 mins, the supernatant discarded and the cells re-suspended in 200 µL MQ H_20, which was dispensed and spread with a spreader across the surface of SD-URA agar plates (3.1.2.3), one for each transformant strain. These plates were subsequently incubated upturned at 30 °C for 3 days in a standing 30 °C incubator (Leec Classic Incubator, Leec, Nottingham, UK), and at that point ten colonies of each transformant strains were picked altogether onto one sterile pipette tip to mix and then streaked onto new SD-URA agar plates, incubated upturned at 30 °C for 3 days in a standing 30 °C incubator.

3.1.6.2 Drug titration growth curves using CWG424 transformed with negative control plasmid PCG279

At the outset, drug titration growth curves were generated alongside control growth curves, with no drug, using strain CWG424 transformed with negative control plasmid PCG279 only (for transformations see 3.1.6.1). This was to estimate the optimal concentration of each platinum drug to further study all four transformant strains. For this, cisplatin was tested at 250 µM, 500 µM and 1000 µM, carboplatin was tested at 400 0µM, 8000 µM and 12000 µM, and oxaliplatin was tested at 1000 µM, 2000 µM and 4000 µM.

These sets of growth curves were generated in a final volume of 1 mL SD-URA medium (3.1.2.3), each in a well of a 24-well plate (Greiner Bio-One 24 well cell culture plate, Greiner, Stonehouse, UK, Ref 662160). Each drug titration was carried out in singlicate (one well with one growth curve) from each of two separate overnight cultures (3.1.2.5) in SD-URA medium of strain CWG424 transformed with negative control plasmid PCG279, giving two biological repeats. The Abs_{595} of the two overnight cultures was measured (as described in 3.1.2.6) and the resulting AUs were used to calculate the volume of cells (which were added to the growth curve wells last) to add to 1mL to achieve a final Abs_{595} of 0.100, ready to start a growth curve at lag phase (Figure 12).

Initially, a volume of 500 µL of two-fold concentrated SD-URA medium was added to the required number of wells. The volume of drug to give the required dose concentration at 1 mL final volume was then added directly to the wells. Next, the volume of drug diluent (0.9 % NaCl solution for cisplatin, MQ H_2O only for carboplatin, and 4.5 % lactose monohydrate solution for oxaliplatin) required to equal the total drug volume used for the top concentration was calculated for each well and added - this was to keep drug/drug diluent volume consistent across the titration. The volume of MQ H_20 required to make each well volume up to a final volume of 1 mL (including the previously calculated required volume of cells) was then calculated and was added, followed lastly by the addition of the cells themselves.

3.1.6.3 Growth kinetics for drug titration growth curves

To assess growth, plates were transferred into a BMG Labtech SPECTROstar Nano plate reader (Aylesbury, Buckinghamshire, UK) to generate growth curves at 30°C. The protocol settings were as follows: Cycle time: 1800 secs, Flashes per well: 30, Excitation: 600, Shaking frequency: 400 rpm, Shaking mode: double orbital, Additional shaking time: 1750 secs after each cycle, Positioning delay: 0.5 secs. Experiments were stopped after 24 hours.

3.1.6.4 Data analysis for drug titration growth curves

Growth curve raw data was exported into Microsoft Excel 2010 using the BMG Labtech MARS data analysis software, where each growth curve was plotted as time in hours (x-axis) against Abs_{600} (y-axis). All data analysis was carried out in Microsoft Excel 2010.

The doubling time of a culture is the time it takes for the cell population to double during the log phase of growth (refer to Figure 12), and this can be measured from growth curves. Doubling times were determined by separately plotting sequential 2 hour data sets, overlapping by 30 mins, as time in hours (x-axis) against Abs_{600} (y-axis). For each 2 hour plot, an exponential trend line was fitted and an exponential line equation was generated, y = c *e^(b*x), which is equivalent to ln(y) = ln(c) + b*x, for which b represents the slope and In(c) represents the y-axis intercept. The 2 hour plot with the highest x value (which represents slope) in the exponential line equation

was selected, and that x-value was used to generate the doubling time (hours) using the formula LN(2)/x. The mean of doubling times for each biological repeat were plotted as bar charts.

3.1.6.5 Growth curves of all transformants with each platinum drugs

Assessment of viability by growth kinetics was carried out for all four transformant strains with and without one concentration of drug – 250 µM Cisplatin, 12000 µM carboplatin or 4000 µM oxaliplatin. These drug concentrations were chosen based on the results from the drug titration growth curves (see method 3.1.6.2 and results 3.2.3.1).

As for the drug titration experiments, these growth curves were generated in a final volume of 1 mL SD-URA medium (3.1.2.3), each tested as three technical repeats on the same 24-well plate (Greiner Bio-One Cellstar 24-well plates, Greiner BioOne Ltd, Stonehouse, UK, Ref 662 160) from one overnight culture (3.1.2.5) in SD-URA medium. This experiment was ultimately repeated on two more separate 24-well plates using two other different overnight cultures in SD-URA medium, giving three biological replicates in total. The Abs_{595} of overnight cultures of the four transformants was measured each time (3.1.2.6) and the resulting AUs were used to calculate the volume of cells (which were added to the growth curve wells last) to add to 1 mL to achieve a final Abs_{595} of 0.100, ready to start a growth curve at lag phase.

Initially, a volume of 500 µL of two-fold concentrated SD-URA medium was added to the required number of wells. The volume of drug to give the required dose concentration at 1mL final volume was then added directly to the wells. Next added was drug diluent (0.9 % NaCl solution for cisplatin, MQ H_2O only for carboplatin, and 4.5 % lactose monohydrate solution for oxaliplatin). The volume of drug diluent used per well was kept exactly the same as for equivalent drug concentration in the drug titration experiments, to maintain consistency. For the growth curves testing no drug, drug diluent only was used, at a volume equivalent to the total volume of drug/drug diluent used for the other growth curves. The volume of MQ H_20 required to make each well volume up to a final volume of 1 mL (including the previously calculated required volume of cells) was then calculated and was added, followed lastly by the addition of the cells themselves.

3.1.6.6 Growth kinetics for growth curves of all transformants with each platinum drug

Growth curve kinetics were then carried out using a BMG Labtech SPECTROstar Nano plate reader as previously described in 3.1.6.3.

3.1.6.7 Data analysis for growth curves of all transformants with each platinum drug

Data analysis was performed as detailed in section 3.1.6.4, except that the growth curves plotted for each biological repeat used the means of the three technical repeats, and the mean of doubling times of the total of three biological repeats were plotted as bar charts.

3.2 Results - yeast

3.2.1 Initial plate-based screening of the transcription regulator library

Initial plate-based screening was of the complete transcription regulator library of 209 gene deletion yeast strains plus control strains wild type (CWG424) and DNA repair mutants *ΔRad27* and *ΔRad52* (refer to section 3.1.3.), with the aim of identifying genes required for growth in the presence of drug to help better understand their mode of action and potentially their resistance mechanisms. Growth of the library strains on YPD agar containing cisplatin, carboplatin or oxaliplatin, was compared to growth on YPD agar containing no drug. Every day, for four days, growth was scored by expressing the size of a colony on agar containing drug as a % of the size of the colony of the same deletion strain on agar containing no drug. Images of the YPD agar screening plates themselves are not shown.

All deleted genes of the yeast deletion strains that grew ≤50 % over four days growth on YPD agar containing cisplatin, carboplatin and oxaliplatin compared to on YPD agar containing no drug, are displayed with their daily growth scores in Table 1, Table 2, and Table 3 respectively. All these '≤50 %' hit genes are presented as a Venn diagram in Figure 6, removing any duplicate genes, to illustrate which hits are exclusive to and common with the three drugs (described in 3.1.3.5). The gene hits that were common to all three drugs included the control strains *ΔRad27* and *ΔRad52,* but also wild type. Using this approach and scoring system we observed that wild type strains sometimes appeared sensitive to the drugs at the concentrations used. This was observed for cisplatin 3/45 times (6.7 %), for carboplatin 1/45 times (2.2 %), and for oxaliplatin 8/45 times (17.7 %) (refer to Table 1, Table 2, and Table 3).

It can be concluded that oxaliplatin was a stronger screen than the cisplatin screen and the carboplatin screen was the weakest of the three screens in terms of growth inhibition at the drug concentrations and strain dilutions tested. This was concluded from observing the overall strength of growth inhibition of the yeast strains and monitoring the control strains *ΔRad27* and *ΔRad52*. However, despite this, strong hits were detected for each drug screen, and we accepted that some middle to low strength hits may drop out. It should also be noted that a crude screening method like this comes with an acceptable variability due to factors such as the number of cells plated and differences in stamping out of strains; to avoid this would mean plating out exactly the same number of cells for each strain and repeating the assay many times.

The drug concentrations of 1000 µM cisplatin, 4000 µM carboplatin, and 4000 µM oxaliplatin were selected based on the results from testing the selected control yeast strains wild type (CWG424), *ΔRad52* and *ΔRad27* during the original optimisation of screening yeast strains on agar containing drug. All control strains grew well on YPD agar containing no drug after 2 days at 30°C,

though *ΔRad52* and *ΔRad27* grew less than CWG424. In comparison, after 2-3 days growing at 30 °C on 1000 µM cisplatin agar, 4000 µM carboplatin and 4000 µM oxaliplatin, we observed very slightly reduced growth of CWG424, but no growth of *ΔRad52,* and reduced growth of *ΔRad27*. Therefore, to achieve comparable results to 1000 µM cisplatin, for 4000 µM carboplatin and 4000 µM oxaliplatin the yeast strains were pre-diluted 1 in 10 with MQ H_2O before stamping them onto the agar. These control strains were included in all yeast screening.

Platinum drugs bind to DNA and form intra-strand adducts, therefore DNA repair mutants such as *ΔRad52* and *ΔRad27* are suitable control strains for screening the growth of yeast strains in the presence of such drugs. Rad52 (RADiation sensitive) is implicated in the repair of double-strand breaks (DSB) in DNA resulting from spontaneous damage, exposure to DNA damaging agents, and collapse of replication forks; mutations in RAD52 cause severe defects, especially in meiotic/mitotic recombination, because Rad52 is involved in multiple DSB repair pathways, reviewed in (Symington 2002) and (Paques, Haber 1999), used as a control in (CHUA, ROEDER 1995). Rad27 (RADiation sensitive) is a flap endonuclease involved in removing the 5'RNA end of Okazaki fragments during replication, and is also required for base excision repair (BER); mutations in RAD27 cause duplication between very short homologies which generates numerous lesions, and also DNA repair defects (Liu, Kao et al. 2004, Symington 2002).

3.2.1.1 Analysis of gene hit distribution and comparison with the Yeast Fitness Database

We investigated the Yeast Fitness Database (2.3.2.2) results, from screening the entire genomic homozygous diploid deletion library of *S.cerevisiae* against the three platinum drugs, in an attempt to get a whole genomic view of the genes involved in their mode of action and potentially resistance to these agents. We did this by comparing the distribution of individual genes hits between drugs and comparing this to the results of our screen. We also compared, for each drug, the functions and processes that the genes are involved in.

We downloaded from the Yeast Fitness Database (refer to 2.3.2.2) all hits from screening the entire yeast genome of homozygous gene knockouts with cisplatin, carboplatin and oxaliplatin, with a p value <0.01 (refer to 3.1.4), which totalled 2180 individual genes. We compared this gene hit distribution of the Yeast Fitness Database drug screens to the equivalent for our screens that grew less than 50 % over four days growth. Figure 7 shows our screen hits in Venn Diagram A and shows the collated Yeast Fitness Database gene hits in Venn diagram B, all expressed as percentage frequency values for ease of comparison.

For our screens, of the total of 212 yeast deletion strains tested (including control strains), 93 (43.9 %) were hits in one or more of the three platinum drug screens. The Venn diagram in Figure 7A shows that, when focussing on these 93 gene deletion hits, 51.5 % (48) had sensitivity to cisplatin, 26.9 % (25) to carboplatin and 61.3 % (57) oxaliplatin. Regarding the total of 2180 gene

deletion hits generated from the Yeast Fitness Database screens in Venn diagram Figure 7B, the vast majority, 76.0 % (1656), showed sensitivity to cisplatin, 26.7 % (582) to carboplatin and 30.1 % (657) to oxaliplatin.

Both datasets showed gene deletion hits exclusive to the individual drugs, but also hits common to two or all three of the drugs. Our screen of transcription regulators showed oxaliplatin sharing 6.5 % (6) of hits with cisplatin and 7.5 % (7) with carboplatin, whereas cisplatin and carboplatin shared fewer gene hits (4.3 % (4)) (Figure 7A). The Yeast Fitness Database data suggested that oxaliplatin is more similar to cisplatin (14.0 % (306) of gene hits shared) than cisplatin is to carboplatin (6.5 % (141) of gene hits shared), with oxaliplatin and carboplatin sharing just 1.6 % (34) gene hits Figure 7B. Regarding gene hits shared by all three drugs, 10.8 % (10) were shared in our screens (Figure 7A) and 5.4 % (117) in the Yeast Fitness database screens.

Cisplatin

Colour key for growth of stains over all 4 days

	All no growth (0)		All ≤30%
	All ≤5%		All ≤40%
	All ≤10%		All ≤50%
	All ≤20%		

	Plate	Position	Standard Name	Systematic Name	Name description	Size of colony on drug plate as a % of size of corresponding colony on control plate			
						1 day	2 days	3 days	4days
	3	G6	BDF1	YLR399C	BromoDomain Factor	0	0	0	0
*	2b rpt	D9	SLA1	YBL007C	Synthetic Lethal with ABP1	0	0	0	<5
*	2	H12	SLA1	YBL007C	Synthetic Lethal with ABP1	0	0	0	<5
	2	H5	**RAD52**	YML032C	RADiation sensitive	<5	<5	<5	<5
	2	H6	**RAD52**	YML032C	RADiation sensitive	<5	<5	<5	<5
	3	H11	**RAD52**	YML032C	RADiation sensitive	0	0	0	10
*	2	D9	SLA1	YBL007C	Synthetic Lethal with ABP1	<5	<5	<5	10
	1	E6	SWI5	YDR146C	SWItching deficient	0	0	<5	20
	1	F6	NDT80	YHR124W	Non-DiTyrosine	0	0	<5	20
	3	D2	MET18	YIL128W	METhionine requiring	<5	<5	<5	20
	3	F2	EMI1	YDR512C	Early Meiotic Induction	<5	<5	<5	20
	2b rpt	H10	AFT1	YGL071W	Activator of Ferrous Transport	<5	<5	<5	20
	1	E12	**RAD52**	YML032C	RADiation sensitive	<5	<5	<5	20
*	1	E5	SWF1	YDR126W	Spore Wall Formation	0	0	<5	30
	1	D1	HAP5	YOR358W	Heme Activator Protein	<5	<5	10	30
	1	G1	SWI6	YLR182W	SWItching deficient	<5	<5	<5	30
	3	G7	SFP1	YLR403W	Split Finger Protein	<5	<5	<5	30
	2b rpt	D11	TOD6	YBL054W	Twin Of Dot6p	0	0	<5	40
	1	F1	MOT2	YER068W	Modulator Of Transcription	<5	<5	10	40
*	2b rpt	H12	SLA1	YBL007C	Synthetic Lethal with ABP1	<5	10	10	40
	3	F4	URC2	YDR520C	URacil Catabolism	0	<5	20	40
	3	F5	SNT2	YGL131C	-	0	<5	20	40
	2	H3	**RAD27**	YKL113C	RADiation sensitive	<5	<5	20	40
	1	F4	RIM101	YHL027W	Regulator of IME2	<5	<5	20	40
	1	G10	HAP4	YKL109W	Heme Activator Protein	<5	<5	20	40
	2	H10	AFT1	YGL071W	Activator of Ferrous Transport	<5	<5	20	40
	3	F10	SWI4	YER111C	SWItching deficient	<5	<5	20	40
	1	H11	-	CWG424	Wild type BY4741	<5	<5	20	40
	3	D11	YOX1	YML027W	Yeast homeobOX	0	10	20	40
	3	G3	FKH1	YIL131C	ForK head Homolog	0	<5	30	40
	2	A11	-	CWG424	Wild type BY4741	0	<5	30	40
	1	A1	-	CWG424	Wild type BY4741	<5	<5	30	40
	3	B3	ZAP1	YJL056C	Zinc-responsive Activator Protein	<5	<5	30	40
	3	E6	-	YPR022C	-	<5	<5	30	40
	3	G4	SNF1	YDR477W	Sucrose NonFermenting	0	<5	40	40
	3	F1	PLM2	YDR501W	PLasmid Maintenance	<5	<5	40	40
*	1	B5	-	YLR046C	-	<5	<5	20	50
	3	F3	EMI2	YDR516C	Early Meiotic Induction	0	<5	30	50
	2	B11	ECM22	YLR228C	ExtraCellular Mutant	0	<5	30	50
	3	E2	DAL81	YIR023W	Degradation of Allantoin	<5	<5	30	50
	3	F6	SUT1	YGL162W	Sterol UpTake	<5	<5	30	50
	2	H8	UME6	YDR207C	Unscheduled Meiotic gene Expression	<5	<5	30	50
	3	C8	CRZ1	YNL027W	Calcineurin-Responsive Zinc finger	<5	<5	30	50
	2	C10	DIG1	YPL049C	Down-regulator of Invasive Growth	<5	<5	30	50
	3	H12	**RAD52**	YML032C	RADiation sensitive	<5	<5	30	50
	2	G12	SPT10	YJL127C	SuPpressor of Ty	<5	10	30	50
	3	D5	NNF2	YGR089W	-	<5	20	30	50
	1	G11	ASH1	YKL185W	Asymmetric Synthesis of HO	<5	20	30	50
	1	C6	STB1	YNL309W	Sin Three Binding protein	<5	<5	40	50
	2	H4	**RAD27**	YKL113C	RADiation sensitive	<5	10	40	50
	2b rpt	H8	UME6	YDR207C	Unscheduled Meiotic gene Expression	<5	10	40	50
	2	H9	ARR1	YPR199C	ARsenicals Resistance	<5	10	40	50
	2	C12	ECM23	YPL021W	ExtraCellular Mutant	<5	20	40	50
	3	B6	BAS1	YKR099W	BASal	10	20	40	50
	2	F5	OTU1	YFL044C	Ovarian TUmor	10	20	40	50
	2	B12	PDR8	YLR266C	Pleiotropic Drug Resistance	10	20	40	50
	2	E3	AFT1	YGL071W	Activator of Ferrous Transport	10	30	40	50
	3	B9	HIR3	YJR140C	HIstone Regulation	<5	10	50	50
	1	B6	CHA4	YLR098C	Catabolism of Hydroxy Amino acids	<5	20	50	50
	2	C2	UME6	YDR207C	Unscheduled Meiotic gene Expression	10	20	50	50
	3	C5	CBF1	YJR060W	Centromere Binding Factor	10	30	50	50
	2	C6	HAP2	YGL237C	Heme Activator Protein	20	30	50	50

Table 1. Yeast deletion strains that grew ≤50 % over 4 days growth on YPD agar containing 1000 µM cisplatin compared to growth on YPD containing no drug. *= non-transcriptional regulator.

Carboplatin

Colour key for growth of stains over all 4 days

	All no growth (0)		All ≤30%
	All ≤5%		All ≤40%
	All ≤10%		All ≤50%
	All ≤20%		

	Plate	Position	Standard Name	Systematic Name	Name description	Size of colony on drug plate as a % of size of corresponding colony on control plate			
						1 day	2 days	3 days	4days
	1	G1	SWI6	YLR182W	SWItching deficient	0	0	0	0
	2	E3	AFT1	YGL071W	Activator of Ferrous Transport	0	0	0	0
	2	C2	UME6	YDR207C	Unscheduled Meiotic gene Expression	0	0	<5	<5
	1	C1	MAC1	YMR021C	Metal binding ACtivator	0	0	0	10
	1	F4	RIM101	YHL027W	Regulator of IME2	0	0	<5	10
	3	F10	SWI4	YER111C	SWItching deficient	<5	<5	<5	10
	2	D9	SLA1	YBL007C	Synthetic Lethal with ABP1	0	0	20	20
	2	E5	GCR2	YNL199C	GlyColysis Regulation	0	<5	30	30
	2	D12	SEF1	YBL066C	Suppressor of Essential Function	0	<5	20	40
	2	E11	HEL2	YDR266C	Histone E3 Ligase	0	<5	30	40
	2	H5	**RAD52**	YML032C	RADiation sensitive	<5	10	30	40
	2	H3	**RAD27**	YKL113C	RADiation sensitive	<5	20	30	40
	1	F6	NDT80	YHR124W	Non-DiTyrosine	10	20	40	40
	2	F10	MSA2	YKR077W	Mbf and Sbf Associated	<5	30	40	40
	1	F1	MOT2	YER068W	Modulator Of Transcription	0	0	30	50
	1	D6	BUD29	YOL072W	Tho2/Hpr1 Phenotype	0	<5	40	50
	2	C3	UPC2	YDR213W	UPtake Control	<5	10	40	50
*	1	E5	SWF1	YDR126W	Spore Wall Formation	<5	10	40	50
	3	H12	**RAD52**	YML032C	RADiation sensitive	10	10	40	50
	2	F1	SUM1	YDR310C	SUppresor of Mar1-1	<5	20	40	50
	3	G6	BDF1	YLR399C	BromoDomain Factor	20	20	40	50
	3	E2	DAL81	YIR023W	Degradation of Allantoin	30	30	40	50
	2	F8	MET28	YIR017C	METhionine	<5	20	50	50
	2	F9	YAP5	YIR018W	Yeast AP-1	<5	20	50	50
	1	H4	-	CWG424	Wild type BY4741	10	20	50	50
	2	F7	MAL13	YGR288W	MALtose fermentation	10	30	50	50

Table 2. Yeast deletion strains, pre-diluted ten-fold, that grew ≤50 % over 4 days growth on YPD agar containing 4000 µM carboplatin compared to growth on YPD containing no drug. *= non-transcriptional regulator.

Oxaliplatin

Colour key for growth of stains over all 4 days

	All no growth (0)		All ≤30%
	All ≤5%		All ≤40%
	All ≤10%		All ≤50%
	All ≤20%		

	Plate	Position	Standard Name	Systematic Name	Name description	Size of colony on drug plate as a % of size of corresponding colony on control plate			
						1 day	2 days	3 days	4days
	1	C1	MAC1	YMR021C	Metal binding ACtivator	0	0	0	0
	2	H6	**RAD52**	YML032C	RADiation sensitive	0	0	0	0
	3	G6	BDF1	YLR399C	BromoDomain Factor	0	0	0	0
	1	G1	SWI6	YLR182W	SWItching deficient	0	0	0	<5
	2	H5	**RAD52**	YML032C	RADiation sensitive	0	0	0	<5
	3	H11	**RAD52**	YML032C	RADiation sensitive	0	0	0	<5
	1	E12	**RAD52**	YML032C	RADiation sensitive	0	0	0	<5
	3	H12	**RAD52**	YML032C	RADiation sensitive	0	0	0	<5
	1	C9	CIN5	YOR028C	Chromosome INstability	0	<5	10	10
	2	H4	**RAD27**	YKL113C	RADiation sensitive	<5	<5	10	20
	3	B3	ZAP1	YJL056C	Zinc-responsive Activator Protein	0	<5	20	20
	2	E3	AFT1	YGL071W	Activator of Ferrous Transport	0	<5	20	30
	2	H3	**RAD27**	YKL113C	RADiation sensitive	<5	10	20	30
	2	F1	SUM1	YDR310C	SUppresor of Mar1-1	<5	10	20	30
	1	F9	SKN7	YHR206W	Suppressor of Kre Null	<5	20	20	30
	2	C2	UME6	YDR207C	Unscheduled Meiotic gene Expression	0	10	30	30
	1	C11	**RAD27**	YKL113C	RADiation sensitive	0	10	30	30
	2	A4	-	CWG424	Wild type BY4741	<5	10	30	30
	1	D9	USV1	YPL230W	Up in StarVation	10	20	30	30
	1	A10	-	CWG424	Wild type BY4741	10	20	30	30
	1	B11	SOK2	YMR016C	Suppressor Of Kinase	10	30	30	30
	2	E2	MIG1	YGL035C	Multicopy Inhibitor of GAL gene expression	<5	20	30	40
	2	G12	SPT10	YJL127C	SuPpressor of Ty	<5	20	30	40
	1	B10	YAP1	YML007W	Yeast AP-1	10	30	30	40
	2	G1	HAL9	YOL089C	HALotolerance	20	30	30	40
	1	A8	-	CWG424	Wild type BY4741	20	30	30	40
	1	A9	-	CWG424	Wild type BY4741	20	30	30	40
	3	F10	SWI4	YER111C	SWItching deficient	0	20	40	40
	1	F7	STB5	YHR178W	Sin Three Binding protein	<5	20	40	40
	2	D1	-	YPR127W	-	20	20	40	40
*	3	G8	IME4	YGL192W	Inducer of MEiosis	20	20	40	40
*	2	D9	SLA1	YBL007C	Synthetic Lethal with ABP1	<5	30	40	40
	1	A11	-	CWG424	Wild type BY4741	<5	30	40	40
	1	D2	PIP2	YOR363C	Peroxisome Induction Pathway	10	30	40	40
	1	C7	SIP3	YNL257C	SNF1-Interacting Protein	20	30	40	40
	1	D7	GAL4	YPL248C	GALactose metabolism	20	30	40	40
	1	B8	GAL80	YML051W	GALactose metabolism	20	30	40	40
	1	C8	HMS1	YOR032C	High-copy Mep Suppressor	20	30	40	40
	2	G9	SUT2	YPR009W	Sterol UpTake	20	30	40	40
	2	G7	DAT1	YML113W	DATin	30	30	40	40
	1	H12	-	CWG424	Wild type BY4741	30	40	30	40
	1	D3	RDR1	YOR380W	Repressor of Drug Resistance	<5	40	40	40
	1	C3	MSS11	YMR164C	Multicopy Suppressor of STA genes	10	40	40	40
*	2	G10	SMK1	YPR054W	-	30	40	40	40
	1	F1	MOT2	YER068W	Modulator Of Transcription	0	0	40	50
	2	B1	RME1	YGR044C	Regulator of MEiosis	<5	20	40	50
	2	A3	-	CWG424	Wild type BY4741	10	30	40	50
	2	E1	PDR1	YGL013C	Pleiotropic Drug Resistance	20	30	40	50
	2	F7	MAL13	YGR288W	MALtose fermentation	30	30	40	50
	2	D3	ARR1	YPR199C	ARsenicals Resistance	20	40	40	50
	2	E12	MTH1	YDR277C	MSN Three Homolog	20	40	40	50
	1	C4	RGM1	YMR182C	-	10	40	50	50
	2	F9	YAP5	YIR018W	Yeast AP-1	20	40	50	50
	2	D11	TOD6	YBL054W	Twin Of Dot6p	20	40	50	50
	2	D12	SEF1	YBL066C	Suppressor of Essential Function	20	40	50	50
	1	D10	SMP1	YBR182C	Second MEF2-like Protein 1	20	40	50	40
	1	E9	SIP1	YDR422C	SNF1-Interacting Protein	20	40	50	40
	2	E5	GCR2	YNL199C	GlyColysis Regulation	20	50	40	40
*	2	G8	-	YMR102C	-	30	40	50	50
	2	F10	MSA2	YKR077W	Mbf and Sbf Associated	30	40	50	50
	2	F11	MOT3	YMR070W	Modifier of Transcription	30	40	50	50
	2	G11	ROX1	YPR065W	Regulation by OXygen	30	40	50	50
	1	C10	HIR2	YOR038C	HIstone Regulation	<5	50	50	50
	1	A4	-	CWG424	Wild type BY4741	20	50	50	50
	1	D8	AFT2	YPL202C	Activator of Fe (iron) Transcription	20	50	50	50
	1	B9	TDA9	YML081W	Topoisomerase I Damage Affected	20	50	50	50
	1	E8	GCN4	YEL009C	General Control Nonderepressible	20	50	50	40
	3	G7	SFP1	YLR403W	Split Finger Protein	40	40	40	50
	2	C12	ECM23	YPL021W	ExtraCellular Mutant	40	40	50	50
	3	D8	TEC1	YBR083W	Transposon Enhancement Control	40	50	50	50

Table 3. Yeast deletion strains, pre-diluted ten-fold, that grew ≤50 % over 4 days growth on YPD agar containing 4000 µM oxaliplatin compared to growth on YPD containing no drug. *= non-transcriptional regulator.

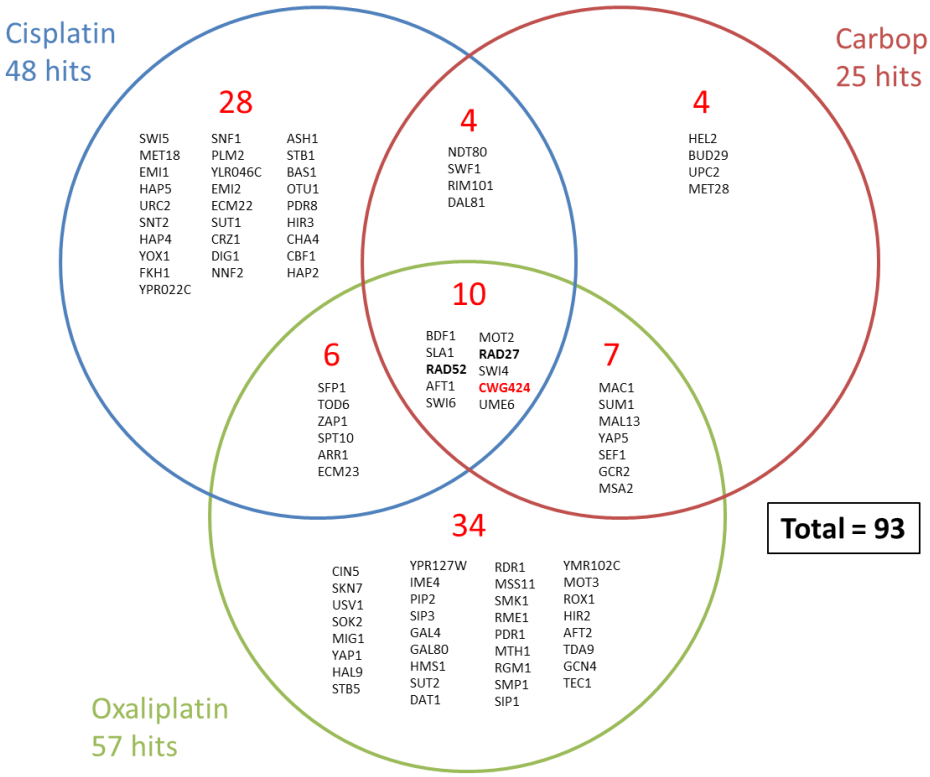

Figure 6. Venn diagram of cisplatin, carboplatin and oxaliplatin gene hits scoring ≤**50 %** growth on agar containing drug compared to growth on agar containing no drug from our screen of the transcription regulator library of gene deletion yeast strains.

A. Our screen – hits ≤50 % growth

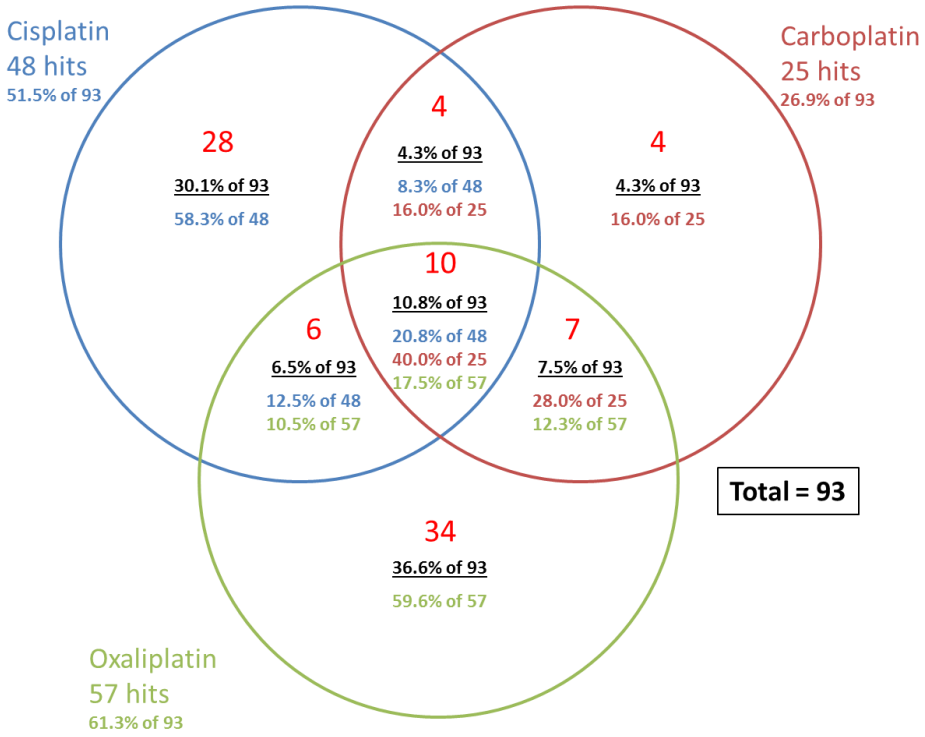

B. Yeast Fitness Database

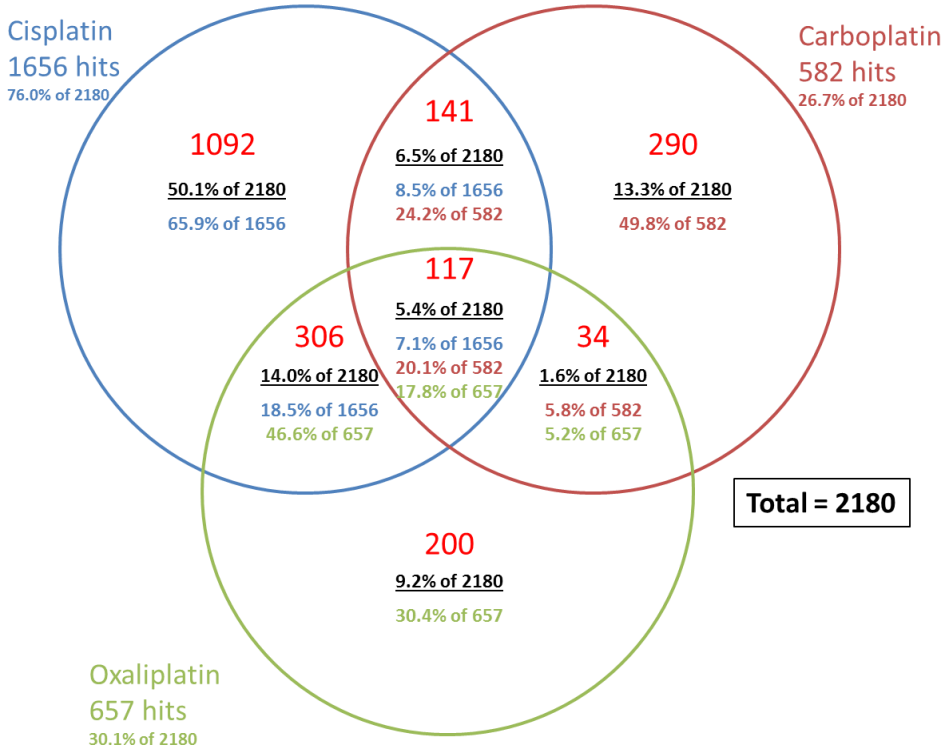

Figure 7. **A.** Venn diagram of cisplatin, carboplatin and oxaliplatin gene hits scoring ≤**50 %** growth on agar containing drug compared to growth on agar containing no drug from our screen of the transcription regulator library of gene deletion yeast strains. **B.** Venn diagram of cisplatin, carboplatin and oxaliplatin hits with p<0.01 from the Yeast Fitness Database. For **A**. and **B**., results are all in the form of percentage hits of the total number of hits (black type), of the total number of cisplatin hits (blue type), of the total number of carboplatin hits (dark red type), and of the total number of oxaliplatin hits (green type).

3.2.1.2 Analysis of gene hit functions and processes and comparison with the Yeast Fitness Database

All cisplatin, carboplatin and oxaliplatin gene hits from the Yeast Fitness database with a p value <0.01, were collated and then analysed using Gene Ontology (GO) Slim Mapper analysis via the Saccharomyces Gene Database (SGD) site (Saccharomyces Gene Database (SGD) (Stanford University, Stanford CA)) using the Yeast GO-slim terms 'function' and 'process' to group the genes (refer to 3.1.4). Gene Ontology (GO) Slim Mapper analysis has a total of 44 function terms and 101 process terms to group genes into. Functions and processes with fold enrichment values >1.0 were used to compile the Venn diagrams in Figure 8 and Figure 9. For more detailed data including the Frequency, Genome frequency and the Fold enrichment values for each function and process, refer to Appendix C and D respectively. These data from the Yeast Fitness database was generated by screening the entire yeast genome in the form of the homozygous diploid deletion library (2.3.2.2), and we collated it in this way to provide us with an interesting overview of all of the functions and processes that are exclusive to and shared by cisplatin, carboplatin and oxaliplatin.

The Venn diagram in Figure 8 focussed on functions, and demonstrated that there were functions both exclusive to the individual drugs and common to two or all three of the drugs. For these three platinum drugs as a group, they are generally centred around DNA, histone, and chromatin binding, protein and lipid binding, the activity of various enzyme groups, and protein and transmembrane transporter activity. Focussing on some of the these functions illustrated in Figure 8, DNA binding was common to all three drugs and enriched by 1.2-1.3 fold with a high frequency value, histone binding was enriched by two-fold for cisplatin and oxaliplatin, chromatin binding was a function for oxaliplatin and enriched by 1.6 fold, and nucleic acid binding transcription factor activity was a common function for cisplatin and carboplatin (1.1 and 1.3 fold enriched respectively) (see Appendix C for fold enrichment values). Regarding transport functions, protein transporter activity was enriched by 1.8 fold for the gene deletion hits of oxaliplatin and transmembrane transporter activity was enriched by 1.4 fold for hits of carboplatin (see Appendix C).

The Venn diagram in Figure 9 focussed on processes, and showed that there were functions both exclusive to the individual drugs and common to two or all three of the drugs. For cisplatin, carboplatin and oxaliplatin they mostly covered the repair, organisation, and transcription of DNA, histone and chromatin, along with vesicle and membrane trafficking, intracellular transport, protein modification and proteolysis, the cell cycle, metabolic processes and stress responses. The majority of processes were shared by all three drugs or by cisplatin with oxaliplatin, which was also the case for the gene hit distributions between the three drugs (3.2.1.1). However, compared to cisplatin and carboplatin, oxaliplatin had overall much higher process term fold enrichment

values (see Appendix D). Oxaliplatin had very high (1.8-3.7) fold enrichment values for processes more centred around vesicle and membrane trafficking such endosomal transport, membrane invagination, vesicle and vacuole organisation, endo- and exocytosis, Golgi vesicle transport, membrane fusion and organelle fusion, fission and inheritance (see Appendix D). Four of these highly enriched processes were exclusive to oxaliplatin (Figure 9). In contrast to oxaliplatin, the processes with the highest fold enrichment values for cisplatin and carboplatin were quite varied (see Appendix D).

Gene Ontology (GO) Slim Mapper analysis of our platinum drug screen hits using the Yeast GO-slim terms 'function' and 'process' was useful, but not as appropriate as it was for the Yeast Fitness database. This is because our transcription regulator library of gene deletion strains (3.1.3.1) was already enriched for transcription regulator gene deletions, and also this analysis is more powerful for larger data sets. For the results from analysing our screen (deletion strains that grew ≤50 % over four days with fold enrichment values >1.0 (3.1.3.5)), refer to Appendix E for functions and Appendix F for processes, including fold enrichment values. Due to this pre-enrichment, fold enrichment values (and frequency values) were very high for transcription factor and DNA/chromatin/histone binding function terms for all three drugs, and the majority of DNA process terms were shared by all three drugs. In terms of other processes, enriched terms generally covered the repair, organisation, and transcription of DNA, histone and chromatin, along with vesicle and membrane trafficking, intracellular transport, protein modification and proteolysis, the cell cycle, metabolic processes and stress responses; this was also the case, as already described, for the Yeast Fitness database (Figure 9 and Appendix D). However, due to our smaller dataset, it was very useful to focus on frequencies rather than enrichment. Regarding processes that were common to all three drugs, the higher frequencies were mainly for transcription from RNA polymerase II promoter, mitotic and meiotic cell cycles, response to chemical, and organelle fission. Compared to the Yeast Fitness Database Gene Ontology (GO), the majority of other processes were from smaller numbers of gene hits, many just one or two per process.

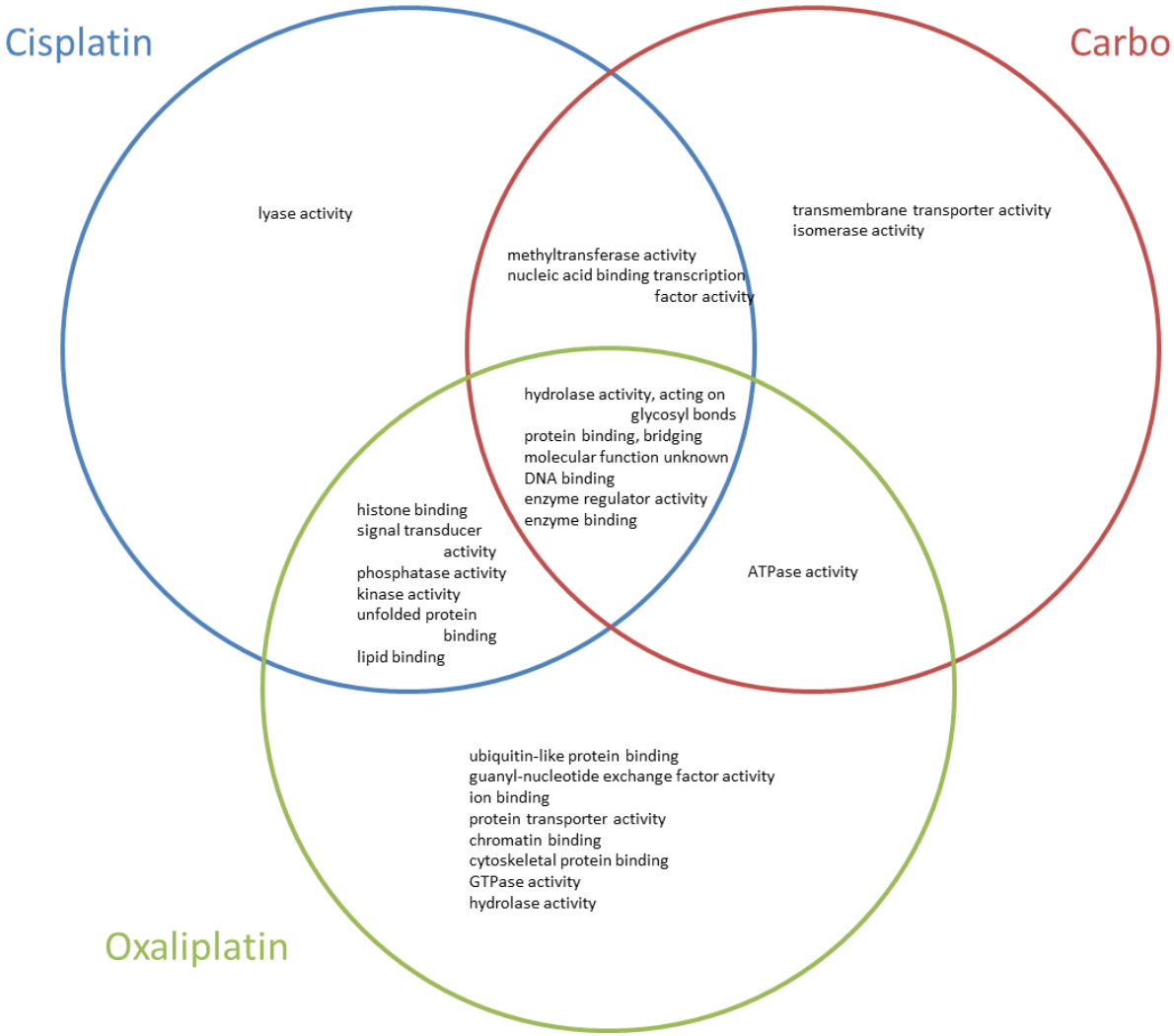

Figure 8. A Venn diagram of the functions of cisplatin, carboplatin and oxaliplatin gene hits with $p<0.01$ from screening the Yeast Fitness Database. These functions were collated using Gene Ontology (GO) Slim Mapper analysis via the Saccharomyces Gene Database (SGD), all having fold enrichment score of >1.0.

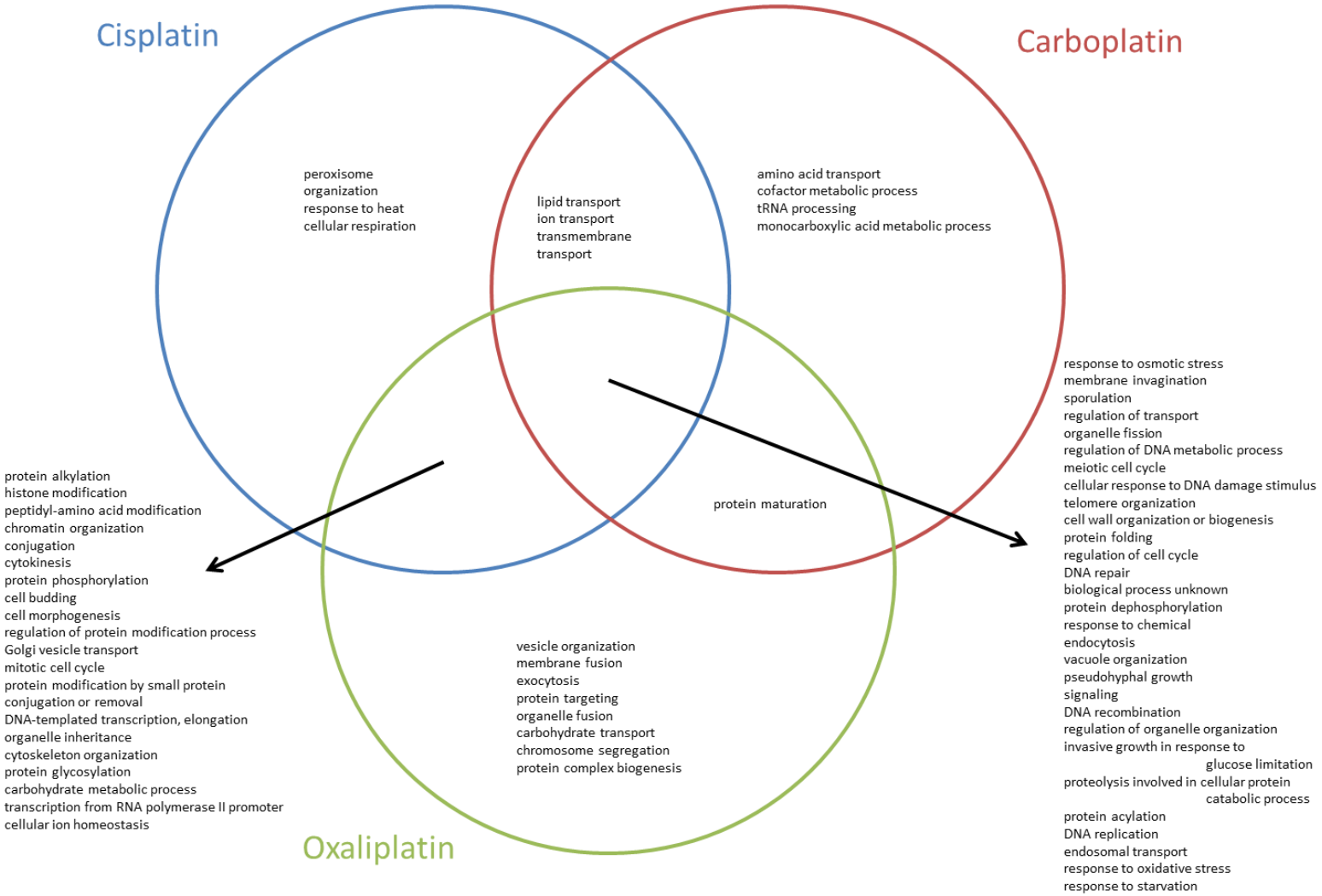

Figure 9. A Venn diagram of the processes of cisplatin, carboplatin and oxaliplatin gene hits with $p<0.01$ from screening the Yeast Fitness Database. These processes were collated using Gene Ontology (GO) Slim Mapper analysis via the Saccharomyces Gene Database (SGD), all having fold enrichment score of >1.0.

3.2.1.3 Gene deletion strains taken forward for confirmation screening

It was decided to take forward, for confirmation screening, the gene deletion strains that grew ≤30 % over four days growth on at least one of cisplatin, carboplatin or oxaliplatin in YPD agar, compared to on YPD agar containing no drug (refer to methods section 3.1.3.5). These totalled 25 strains and are highlighted in green for each drug screen in Table 1, Table 2 and Table 3 and are displayed in a Venn diagrams in Figure 10A (gene hits) and B (frequencies). Indeed, compared to using the ≤50 % cut off (compare Figure 10A with Figure 6), it can be seen that some gene hits shifted position in the Venn, however the overall frequencies (compare Figure 10B with Figure 7A) remained similar % values, apart from an increase of carboplatin exclusive hits. With this cut-off value of ≤30 %, wild type strain CWG424 did not class as a hit for cisplatin and carboplatin and was only a hit 2/45 times for oxaliplatin (refer to 3.2.1 to compare this to with a ≤50 % cut off).

For the results from analysing our ≤30 % cut-off screen results using Gene Ontology (GO) Slim Mapper refer to Appendix G for functions and Appendix H for processes. Compared to the 50 % cut off data, these results are presented as gene deletion hit names, with genes ordered in terms of frequency rather than fold enrichment, which was more useful for this smaller dataset. It can be seen how one gene hit can come under more than one function or process term. Compared to the ≤50 % cut off data (Appendix E and F), and common to the three drug screens, function frequencies remained highest for DNA binding and transcription factor terms, and process frequencies remained highest for transcription from RNA polymerase II promoter, mitotic and meiotic cell cycles and organelle fission. Overall, the process terms covered were the same as for the ≤50 % cut off hits.

A.

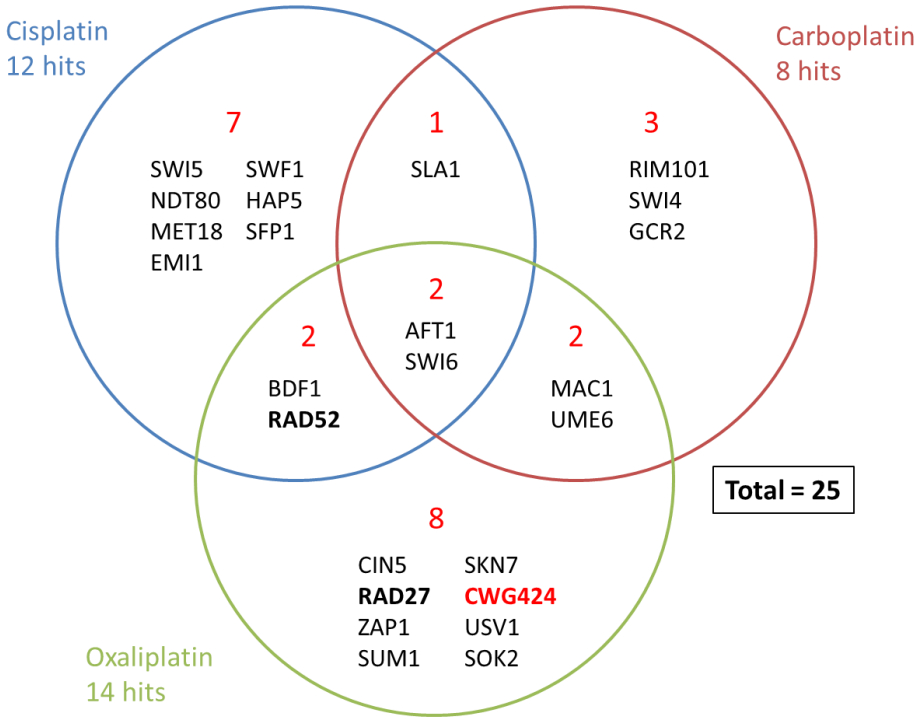

B.

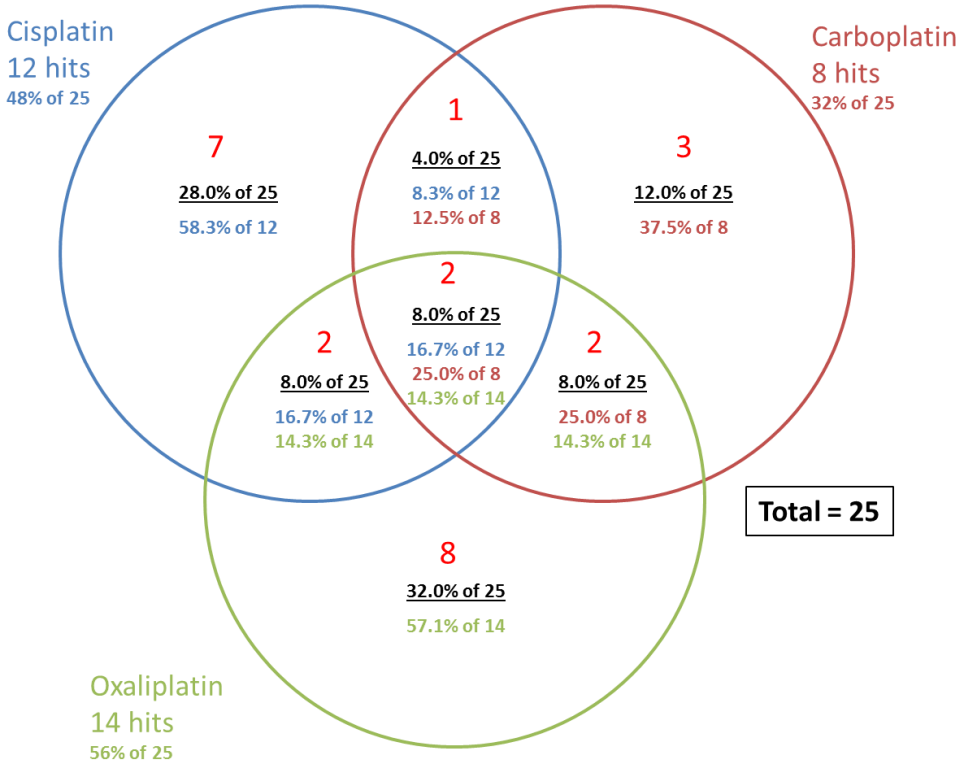

Figure 10. **A**. Venn diagram of cisplatin, carboplatin and oxaliplatin gene hits scoring ≤**30 %** growth on agar containing drug compared to growth on agar containing no drug from our screen of the transcription regulator library of gene deletion yeast strains. Note SLA1 and SWF1 are not transcriptional regulators. **B**. Venn diagram of the gene hits in A. in the form of percentage hits of the total number of hits (black type), of the total number of cisplatin hits (blue type), of the total number of carboplatin hits (dark red type), and of the total number of oxaliplatin hits (green type).

3.2.2 Confirmation screening of 'hits' generated from the initial transcription regulator library screen

A total of twenty-five hits, including control strains wild type CWG424 and DNA repair mutants *ΔRad27* and *ΔRad52*, were re-screened against cisplatin, carboplatin and oxaliplatin (3.1.5) with the aim of confirming them as hits. In the initial plate screening, these strains grew ≤30 % over four days growth on at least one of cisplatin, carboplatin or oxaliplatin in YPD agar compared to on YPD agar containing no drug (3.2.1.3). Comparing methodology to that of the initial screen (3.1.3), this time overnight cultures were prepared in 3mL YPD medium rather than in 96-well plates and strains were taken from the original Mata haploid gene deletion library (3.1.2.1), the A_{595} of each culture was measured and adjusted so that they were in the same range, and the strains were stamped out in triplicate (3.1.5.4.).

As for the initial screening, growth of these strains on YPD agar containing cisplatin, carboplatin or oxaliplatin, was compared to growth on YPD agar containing no drug. Every day, for four days, growth was scored by expressing the size of a colony on agar containing drug as a % of the size of the colony of the same deletion strain on agar containing no drug. However for the conformation screening, growth inhibition in the presence of each drug was not as significant, therefore the original scoring system (3.1.3.5) was re-designed to pick up the strongest of the hits (3.1.5.5). Also, as was the case for the initial plate screening, oxaliplatin was a stronger screen than the cisplatin screen and the carboplatin screen was the weakest of the three screens in terms of growth inhibition at the drug concentrations and strain dilutions tested. This was concluded from observing the overall strength of growth inhibition of the yeast strains and monitoring the control strains *ΔRad27* and *ΔRad52*. Importantly, strong gene deletion hits were still detected using this screening method.

Using the conformation screen scoring system (3.1.5.5), the yeast deletion strains were classed as strong hits if % growth for all three replicates tested was ≤30 % for two time points. Strains were classed as medium hits if growth for two out of the three replicates was ≤30 % for two time points. Strains were classed as weaker hits if growth for two out of the three replicates was ≤50 % for two time points. All hits meeting these criteria, with their scores over each of the four days growth, are represented in Table 4, Table 5, and Table 6. A Venn diagram of all the gene deletion hits for each drug is shown in Figure 11, and all these hits are shown again in Table 7 with their screen results and role descriptions.

Table 4, Table 5, and Table 6 along with Figure 11 show that there were 4 hits for cisplatin, 6 hits for carboplatin and 13 hits for oxaliplatin and in total, between all three drugs, there were 14 gene hits. Focussing on the Venn diagram for this conformation screening (Figure 11), comparing it with the initial screening (with a ≤30 % cut off) (Figure 10A) it can be seen that gene hits RAD52,

BDF1, MAC1, UME6, ZAP1, SUM1, and RAD27 were confirmed as hits for the same drugs again. AFT1 was confirmed as a hit for cisplatin and carboplatin and dropped out as a hit for oxaliplatin, and SWI6 was confirmed as a hit for oxaliplatin and dropped out as a hit for cisplatin and carboplatin. SLA1 was a hit for cisplatin and carboplatin in the initial screening using a ≤30 % cut off (Figure 10A), but confirmed here as a hit for cisplatin and also came up as a hit for oxaliplatin - this was not unexpected because it was a hit for all three drugs in the initial screen using a ≤50 % cut off (Figure 6). SWI4 and GCR2 were confirmed as hits for carboplatin but were also hits for oxaliplatin but again, and this was not unexpected either because both of these genes came up as hits for oxaliplatin in the initial screen using a ≤50 % cut off (Figure 6). SFP1, however, was a hit for cisplatin in the initial screening using a ≤30 % cut off but here in the conformation screen it was a borderline hit for cisplatin and also a hit for carboplatin and oxaliplatin; in the initial screen using a ≤50 % cut off though, SFP1 was a hit for only cisplatin and oxaliplatin, not carboplatin. HIR1 was added as a test strain at this confirmation stage only, however it did pass the cut off as a hit for oxaliplatin and so was included in the results figures and tables. For this screening there were no hits exclusive to cisplatin or carboplatin and there were no hits common to all three drugs.

Table 7 shows that this group of 14 genes, including controls RAD27 and RAD52, are involved in a vast range of cellular processes such as DNA synthesis and repair, glycolysis, metal ion utilisation, metal ion transport and homeostasis, mitotic and meiotic cell cycle, chromatin and histone regulation, cytoskeleton assembly, and response to stress. A breakdown of the functions and processes of these 14 hits can be found within Appendix tables G and H, where the 25 gene hits screened were matched to Yeast GO-slim function and process terms using Gene Ontology (GO) Slim Mapper analysis via the Saccharomyces Gene Database (SGD) site (Saccharomyces Gene Database (SGD) (Stanford University, Stanford CA)).

For this conformation screening, analysing Table 4, Table 5, and Table 6, it can be seen that the strongest gene deletion hits, with a % growth of ≤30 % for two time points for all three replicates, were the control RAD52 and BDF1 for both cisplatin and oxaliplatin (both genes had signs of growth inhibition by carboplatin for only one n number (data not shown) so did not pass as hits). As described in 3.2.1, Rad52 is implicated in the repair of double-strand breaks (DSB) in DNA, resulting from DNA damaging agents such as the platinum drugs. Bdf1 is a protein with two bromodomains that is involved in the initiation of gene transcription (Table 7) and was matched to the Yeast GO-slim process terms (using Gene Ontology (GO) Slim Mapper analysis) cellular response to DNA damage stimulus, DNA repair, regulation of DNA metabolic processes, and chromatin and organelle organisation (refer to Appendix tables G and H). The strongest gene deletion hits for carboplatin were AFT1 and MAC1 - AFT1 was also passed as a weaker hit for cisplatin, and MAC1 was also a medium hit for oxaliplatin. Aft1 is a transcription factor associated

with the utilisation and homeostasis of iron, and Mac1 is as transcription factor that senses copper and is involved in the regulation of genes required for high affinity copper transport (Table 7). AFT1 was matched to many Yeast GO-slim process terms (using Gene Ontology (GO) Slim Mapper analysis); transcription from RNA polymerase II promoter, organelle fission, mitotic and meiotic cell cycle, response to starvation, regulation of transport, chromosome segregation, and ion transport (refer to Appendix tables G and H). MAC1 was matched to the following process terms - transcription from RNA polymerase II promoter and cellular ion homeostasis (refer to Appendix tables G and H).

It was decided to take BDF1 forward for further studies. This was because in the conformation screening it was one of the strongest hits for cisplatin and oxaliplatin (Table 4, Table 5, Table 6). BDF1 also had signs of growth inhibition by carboplatin, though only for one n number (data not shown), so it did not pass as a hit. Also, it passed as a strong hit for cisplatin and oxaliplatin and a weaker hit for carboplatin in the initial screening (Table 1, Table 2, Table 3). BDF1 was also the only gene hit confirmed that has homology with human genes; Bdf1 is a member of the BET (Bromodomain and Extra-Terminal domain) family of transcriptional regulators (Florence, Faller 2001, Matangkasombut, Buratowski et al. 2000), along with human BET proteins including Brd2 (RING3), Brd3, Brd4 and Brdt (Brd6) (Garcia-Gutierrez, Mundi et al. 2012, Bunnage 2010). Additionally, in the homozygous knockouts inhibited data sets for sensitivity to cisplatin, carboplatin and oxaliplatin from the Yeast Fitness Database (Yeast Fitness Database (2008). Hillenmeyer,Maureen E., Fung et al.), there is no data for BDF1, making this hit, in comparison, unique to us.

CISPLATIN

Colour key for growth of stains over all 4 days

Three n# ≤30% for ≥two time points

Two n# ≤30% for ≥two time points

Two n# ≤50% for ≥two time points

Position	Standard Name	SystematicName	Name description	n #	Size of colony on drug plate as a % of size of corresponding colony on control plate			
					1 day	2 days	3 days	4days
E1	**RAD52**	YML032C	RADiation sensitive	1	20	10	20	20
				2	30	20	40	50
				3	30	10	20	40
D6	BDF1	YLR399C	BromoDomain Factor	1	20	20	40	60
				2	20	20	60	70
				3	10	20	50	60
E5	AFT1	YGL071W	Activator of Ferrous Transport	1	20	40	60	80
				2	30	70	80	90
				3	20	50	70	70
F1	SLA1	YBL007C	Synthetic Lethal with ABP1	1	30	40	60	80
				2	40	60	110	120
				3	30	40	50	60

Table 4. Cisplatin gene hits from the conformation screening of the 25 gene hits from the initial plate screens. For this conformation screening these genes scored, for at least two out of three n numbers, at least two time points with ≤50 % growth on YPD agar containing 1000 µM cisplatin compared to growth on YPD agar containing no drug – see colour key above table. Note: SLA1 is not a transcription factor. HIR1 was only tested in the re-screen. Rad52 control is in bold type.

CARBOPLATIN

Colour key for growth of stains over all 4 days

Three n# ≤30% for ≥two time points

Two n# ≤30% for ≥two time points

Two n# ≤50% for ≥two time points

Position	Standard Name	Systematic Name	Name description	n #	Size of colony on drug plate as a % of size of corresponding colony on control plate			
					1 day	2 days	3 days	4days
E5	AFT1	YGL071W	Activator of Ferrous Transport	1	30	<5	<5	<5
				2	20	<5	<5	<5
				3	20	<5	<5	>5
E2	MAC1	YMR021C	Metal binding ACtivator	1	20	20	30	40
				2	40	20	50	50
				3	60	20	30	50
E3	UME6	YDR207C	Unscheduled Meiotic gene Expression	1	60	40	40	50
				2	60	50	50	50
				3	60	40	40	40
D4	SWI4	YER111C	SWItching deficient	1	60	40	50	70
				2	60	40	50	40
				3	30	50	40	40
C1	SFP1	YLR403W	Split Finger Protein	1	ng	70	70	80
				2	ng	50	50	60
				3	40	30	40	50
D5	GCR2	YNL199C	GlyColysis Regulation	1	60	60	60	60
				2	ng	70	50	50
				3	30	50	40	50

Table 5. Carboplatin gene hits from the conformation screening of the 25 gene hits from the initial plate screens. For this conformation screening these genes scored, for at least two out of three n numbers, at least two time points with ≤50 % growth (yeast deletion strains, pre-diluted ten-fold) on YPD agar containing 4000 µM carboplatin compared to growth on YPD agar containing no drug – see colour key above table. A growth score of 'ng' means there was no significant growth of the strain to score on either of the YPD containing drug or on the corresponding YPD agar containing no drug.

OXALIPLATIN

Colour key for growth of stains over all 4 days

Three n# ≤30% for ≥two time points

Two n# ≤30% for ≥two time points

Two n# ≤50% for ≥two time points

Position	Standard Name	Systematic Name	Name description	n #	Size of colony on drug plate as a % of size of corresponding colony on control plate			
					1 day	2 days	3 days	4days
D6	BDF1	YLR399C	BromoDomain Factor	1	0	0	<5	10
				2	0	0	<5	10
				3	0	0	<5	<5
E1	**RAD52**	YML032C	RADiation sensitive	1	20	20	20	20
				2	30	<5	10	20
				3	20	<5	10	20
C4	ZAP1	YJL056C	Zinc-responsive Activator Protein	1	50	40	30	30
				2	30	20	30	30
				3	80	30	40	30
E2	MAC1	YMR021C	Metal binding ACtivator	1	30	40	40	50
				2	20	20	40	40
				3	20	30	40	40
E6	SWI6	YLR182W	SWItching deficient	1	50	70	60	50
				2	20	20	40	50
				3	30	20	40	50
C1	SFP1	YLR403W	Split Finger Protein	1	ng	50	50	70
				2	ng	30	50	60
				3	ng	30	30	50
D4	SWI4	YER111C	SWItching deficient	1	70	50	50	40
				2	30	50	50	40
				3	30	50	50	40
F1	SLA1	YBL007C	Synthetic Lethal with ABP1	1	40	70	60	60
				2	20	50	60	70
				3	40	30	50	50
D5	GCR2	YNL199C	GlyColysis Regulation	1	70	60	50	40
				2	20	40	40	50
				3	50	60	60	50
E3	UME6	YDR207C	Unscheduled Meiotic gene Expression	1	60	60	50	50
				2	20	60	50	40
				3	30	60	50	50
E4	HIR1	YBL008W	HIstone Regulation	1	60	60	50	40
				2	20	60	50	50
				3	40	60	60	50
C5	SUM1	YDR310C	SUppresor of Mar1-1	1	80	60	50	60
				2	20	60	50	50
				3	20	70	60	50
C3	**RAD27**	YKL113C	RADiation sensitive	1	60	70	60	60
				2	30	50	60	50
				3	50	80	60	50

Table 6. Oxaliplatin gene hits from the conformation screening of the 25 gene hits from the initial plate screens. For this conformation screening these genes scored, for at least two out of three n numbers, at least two time points with ≤50 % growth (yeast deletion strains, pre-diluted ten-fold) on YPD agar containing 4000 µM oxaliplatin compared to growth on YPD agar containing no drug – see colour key above table. A growth score of 'ng' means there was no significant growth of the strain to score on either of the YPD containing drug or on the corresponding YPD agar containing no drug. Note: SLA1 is not a transcription factor. HIR1 was only tested in the re-screen. Rad27 and Rad52 controls are in bold type.

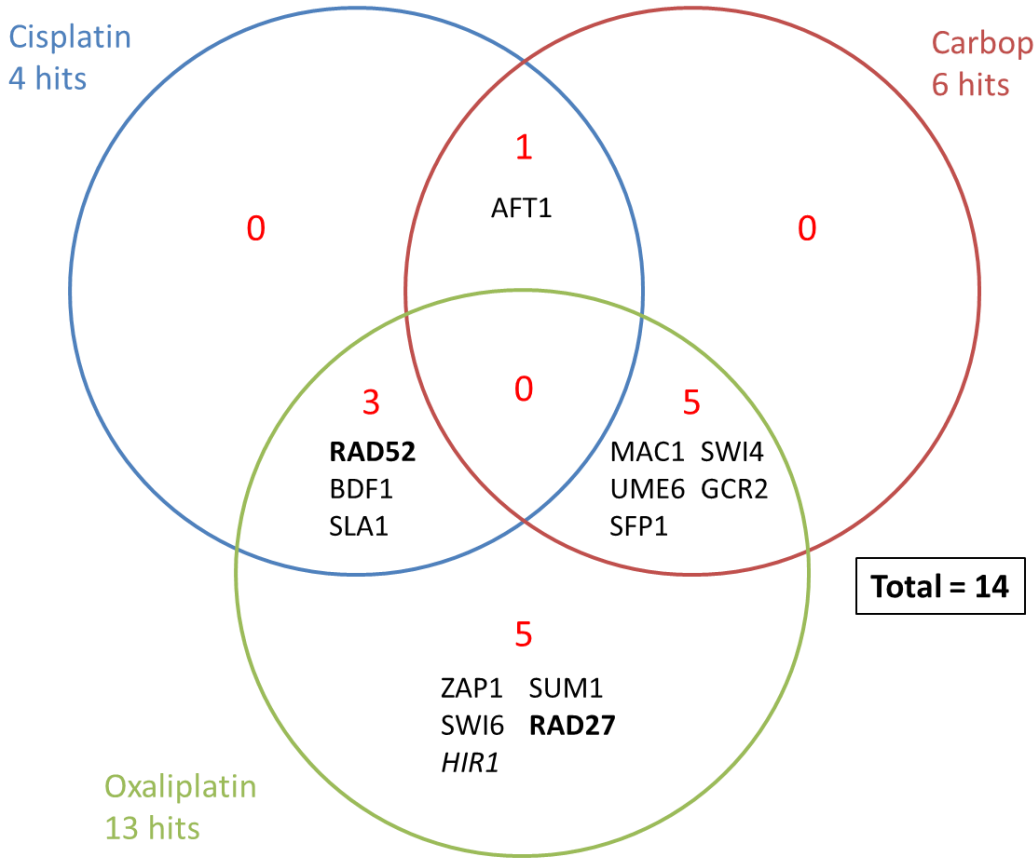

Figure 11. Venn diagram of cisplatin, carboplatin and oxaliplatin gene hits from the conformation screening of the 25 gene hits from the initial plate screens. For this conformation screening these genes scored, for at least two out of three n numbers, at least two time points with ≤50 % growth on YPD agar containing drug compared to growth on YPD agar containing no drug. Note: HIR1 (italics) was only tested in the conformation screen, not the intital screening.

Cisplatin	Carboplatin	Oxaliplatin	Standard Name	Systematic Name	Name description	Description
	Y	Y	SFP1	YLR403W	Split Finger Protein	Regulates transcription of ribosomal protein and biogenesis genes; regulates response to nutrients and stress, G2/M transitions during mitotic cell cycle and DNA-damage response, and modulates cell size; regulated by TORC1 and Mrs6p; sequence of zinc finger, ChIP localization data, and protein-binding microarray (PBM) data, and computational analyses suggest it binds DNA directly at highly active RP genes and indirectly through Rap1p at others; can form the [ISP+] prion
Y	Y		AFT1	YGL071W	Activator of Ferrous Transport	Transcription factor involved in iron utilization and homeostasis; binds consensus site PyPuCACCCPu and activates transcription in response to changes in iron availability; in iron-replete conditions localization is regulated by Grx3p, Grx4p, and Fra2p, and promoter binding is negatively regulated via Grx3p-Grx4p binding; AFT1 has a paralog, AFT2, that arose from the whole genome duplication; relative distribution to the nucleus increases upon DNA replication stress
	Y	Y	MAC1	YMR021C	Metal binding ACtivator	Copper-sensing transcription factor; involved in regulation of genes required for high affinity copper transport; required for regulation of yeast copper genes in response to DNA-damaging agents; undergoes changes in redox state in response to changing levels of copper or MMS
	Y	Y	UME6	YDR207C	Unscheduled Meiotic gene Expression	Rpd3L histone deacetylase complex subunit; key transcriptional regulator of early meiotic genes; involved in chromatin remodeling and transcriptional repression via DNA looping; binds URS1 upstream regulatory sequence, couples metabolic responses to nutritional cues with initiation and progression of meiosis, forms complex with Ime1p
	Y	Y	SWI4	YER111C	SWItching deficient	DNA binding component of the SBF complex (Swi4p-Swi6p); a transcriptional activator that in concert with MBF (Mbp1-Swi6p) regulates late G1-specific transcription of targets including cyclins and genes required for DNA synthesis and repair; Slt2p-independent regulator of cold growth; acetylation at two sites, K1016 and K1066, regulates interaction with Swi6p
	Y	Y	GCR2	YNL199C	GlyColysis Regulation	Transcriptional activator of genes involved in glycolysis; interacts and functions with the DNA-binding protein Gcr1p
Y		Y	**RAD52**	**YML032C**	RADiation sensitive	Protein that stimulates strand exchange; stimulates strand exchange by facilitating Rad51p binding to single-stranded DNA; anneals complementary single-stranded DNA; involved in the repair of double-strand breaks in DNA during vegetative growth and meiosis and UV induced sister chromatid recombination
Y		Y	**BDF1**	**YLR399C**	**BromoDomain Factor**	Protein involved in transcription initiation; functions at TATA-containing promoters; associates with the basal transcription factor TFIID; contains two bromodomains; corresponds to the C-terminal region of mammalian TAF1; redundant with Bdf2p; BDF1 has a paralog, BDF2, that arose from the whole genome duplication
Y		Y	SLA1	YBL007C	Synthetic Lethal with ABP1	Cytoskeletal protein binding protein; required for assembly of the cortical actin cytoskeleton; interacts with proteins regulating actin dynamics and proteins required for endocytosis; found in the nucleus and cell cortex; has 3 SH3 domains
		Y	ZAP1	YJL056C	Zinc-responsive Activator Protein	Zinc-regulated transcription factor; binds to zinc-responsive promoters to induce transcription of certain genes in presence of zinc, represses other genes in low zinc; regulates its own transcription; contains seven zinc-finger domains
		Y	SWI6	YLR182W	SWItching deficient	Transcription cofactor; forms complexes with Swi4p and Mbp1p to regulate transcription at the G1/S transition; involved in meiotic gene expression; also binds Stb1p to regulate transcription at START; cell wall stress induces phosphorylation by Mpk1p, which regulates Swi6p localization; required for the unfolded protein response, independently of its known transcriptional coactivators
		Y	HIR1	YBL008W	HIstone Regulation	Subunit of the HIR complex; HIR is a nucleosome assembly complex involved in regulation of histone gene transcription; contributes to nucleosome formation, heterochromatic gene silencing, and formation of functional kinetochores
		Y	SUM1	YDR310C	SUppresor of Mar1-1	Transcriptional repressor that regulates middle-sporulation genes; required for mitotic repression of middle sporulation-specific genes; also acts as general replication initiation factor; involved in telomere maintenance, chromatin silencing; regulated by pachytene checkpoint
		Y	**RAD27**	**YKL113C**	RADiation sensitive	5' to 3' exonuclease, 5' flap endonuclease; required for Okazaki fragment processing and maturation, for long-patch base-excision repair and large loop repair (LLR), ribonucleotide excision repair; member of the S. pombe RAD2/FEN1 family; relocalizes to the cytosol in response to hypoxia

Table 7. Cisplatin, carboplatin and oxaliplatin gene hits from the conformation screening of the 25 gene hits from the initial plate screens, along with their role descriptions, taken from the SGD (Saccharomyces Gene Database (SGD) (Stanford University, Stanford CA)). For this conformation screening these genes scored, for at least two out of three n numbers, at least two time points with ≤50 % growth on YPD agar containing drug compared to growth on YPD agar containing no drug. Highlighted grey are the screen results, with a Y meaning 'YES' - a hit for that drug. Note: SLA1 is not a transcription factor. HIR1 was only tested in the re-screen. Rad27 and Rad52 controls are in bold type. BDF1 was taken forward for further studies and is in red bold type.

3.2.3 Does the re-introduction of BDF1 into *ΔBdf1* strains recover viability in the presence of the platinum drugs?

Growth curves and doubling times were initially generated for wild type strain CWG424 transformed with negative control plasmid PCG279 with titrations of cisplatin, carboplatin and oxaliplatin. This enabled the selection of drug concentrations predicted to give the optimal assay window to capture growth curves and doubling times for each of the following four transformant strains;

S. cerevisiae strain CWG424 transformed with negative control plasmid PCG279
S. cerevisiae strain CWG424 transformed with BDF1 plasmid PCG596,
S. cerevisiae strain *ΔBdf1* transformed with negative control plasmid PCG279, and
S. cerevisiae strain *ΔBdf1* with BDF1 plasmid PCG596,

These experiments were carried out to overall assess whether the re-introduction of the BDF1 gene into the ΔBdf1 strain restored any resistance to the platinum drugs. The different phases of yeast growth are illustrated and described in Figure 12.

3.2.3.1 Drug titration growth curves using CWG424 transformed with negative control plasmid PCG279 to determine suitable drug concentrations

Wild type CWG424 transformed with negative control plasmid PCG279 was initially grown in the presence of serial dilutions of cisplatin, oxaliplatin, and carboplatin (Figure 13) in SD-URA liquid medium. The aim of this experiment was to select a concentration of each drug that clearly reduces the growth of CWG424 transformed with negative control plasmid PCG279, but not completely abolishes growth. The selected drug concentrations were hoped, for subsequent experiments testing all four transformants, to create a suitably sized assay window to capture minimal growth of the *S. cerevisiae* strain *ΔBdf1* transformed with negative control plasmid PCG279 grown in the presence of the drugs. Minimal growth of this strain in the presence of each drug in liquid medium was predicted due to the minimal or no growth observed when the *ΔBdf1* deletion strain was grown on YPD agar containing these platinum drugs - see results sections 3.2.1 and 3.2.2.

Growth in the presence of cisplatin was tested at 250 µM, 500 µM and 1000 µM, carboplatin was tested at 4000 µM, 8000 µM and 12000 µM, and oxaliplatin was tested at 1000 µM, 2000 µM and 4000 µM. These concentrations were selected based on the results from the agar plate-based drug screening of the *ΔBdf1* deletion strain in sections 3.2.1 and 3.2.2, the concentrations tested in liquid medium for the Yeast Fitness Database in (2.3.2.2 and 3.1.4), combined with the knowledge that cells are generally more sensitive to drugs in liquid culture compared to growth on agar. For oxaliplatin were used at 4000 µM and *ΔBdf1* was a strong hit for cisplatin and

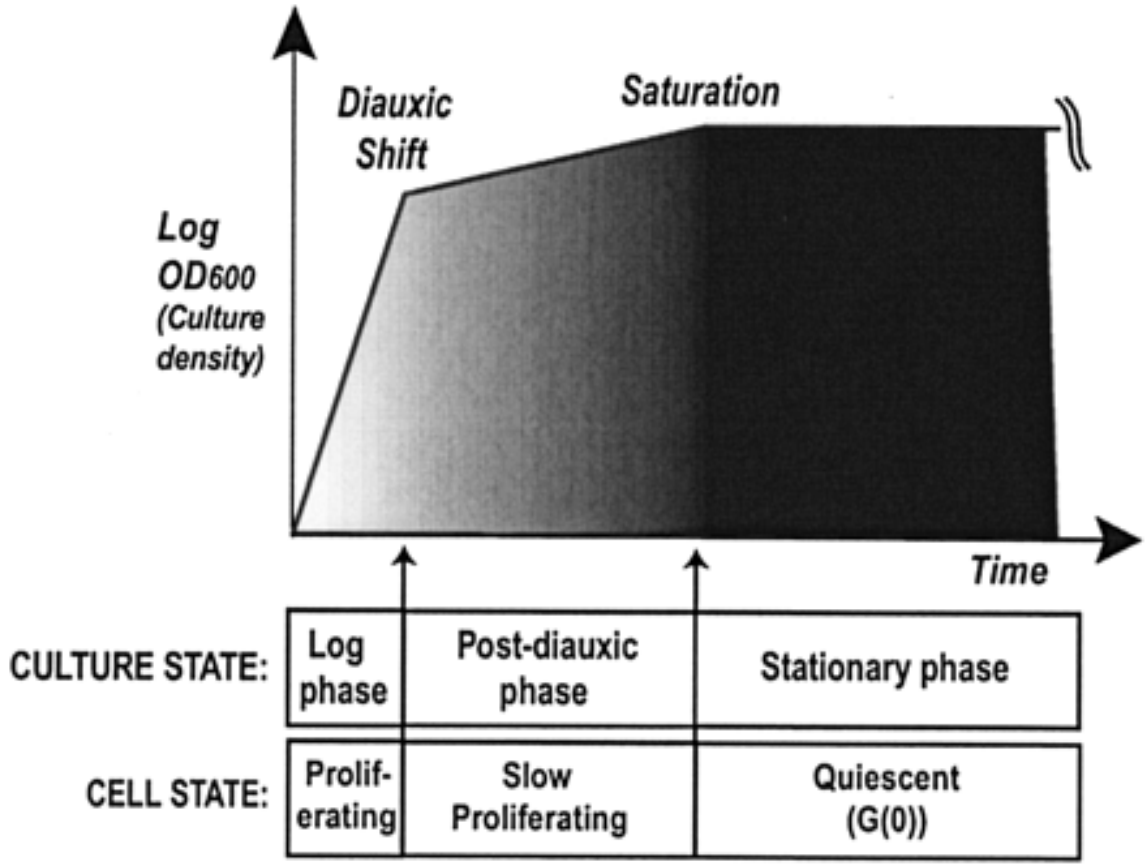

Figure 12. The different growth phases exhibited by *S. cerevisiae* exhibits when grown in medium containing glucose (Gray, Petsko et al. 2004). Yeast cells in a liquid culture will continuously proliferate if conditions are favourable and nutrients abundant. Growth of yeast cultures can be monitored by measuring the Abs_{600} of the cell suspension as a function of time. These data can then be used to construct a growth curve like the example depicted. At the outset there is a slight lag as the cells adjust themselves to their new environment and available nutrients. The initial log phase of growth is by glucose fermentation (glycolysis), during which the culture density increases exponentially as the cells rapidly divide. When glucose becomes limiting, the yeast cells adjust their metabolism from fermentation of glucose to respiration, and their growth rate slows (diauxic shift). This enables the cells, during the resulting post-diauxic phase, to aerobically utilise other carbon sources to produce energy, such as the ethanol that was produced from the glucose fermentation in the log phase. When these carbon sources are exhausted, the cells enter stationary phase, stop proliferating, and enter the quiescent state (Herman 2002, Gray, Petsko et al. 2004, Galdieri, Mehrotra et al. 2010)

oxaliplatin, but weaker in the presence of carboplatin. Therefore it was decided to titrate cisplatin down from 1000 µM, carboplatin up from 4000 µM, and oxaliplatin down from 4000 µM. From the cisplatin titration growth curves (Figure 13A), a concentration of 250 µM cisplatin was selected, for carboplatin (Figure 13B) a concentration of 12000 µM, and for oxaliplatin (Figure 13C) a concentration of 2000 µM.

During the log phase of growth, the doubling time with 4000 µM oxaliplatin was more comparable to the doubling times with 250 µM cisplatin and 12000 µM carboplatin (Figure 14). However, 4000 µM oxaliplatin (Figure 13C) significantly affected growth post 10hrs during the post-diauxic phase, remaining around half the maximum Abs_{600} of both the 250 µM cisplatin and 12000 µM carboplatin growth curves (Figure 13A and Figure 13B). This observation may be illustrative of a

mechanism of action of oxaliplatin not observed with the other two platinum drugs, for example perhaps the cells find the damage induced by exposure to oxaliplatin more difficult to repair than the damage from cisplatin and carboplatin. Therefore, even though it gave a slightly lower doubling time, 2000 μM oxaliplatin was selected because the maximum Abs_{600} was higher and therefore this concentration was predicted to have more chance of capturing all complete growth curves when later testing the four transformants (Figure 17).

Future experiments, generating growth curves for all four transformants in the presence of these selected drug concentrations resulted in suitable assay windows, successfully captured all growth curves for all transformants and conditions tested (Figure 15, Figure 16, and Figure 17).

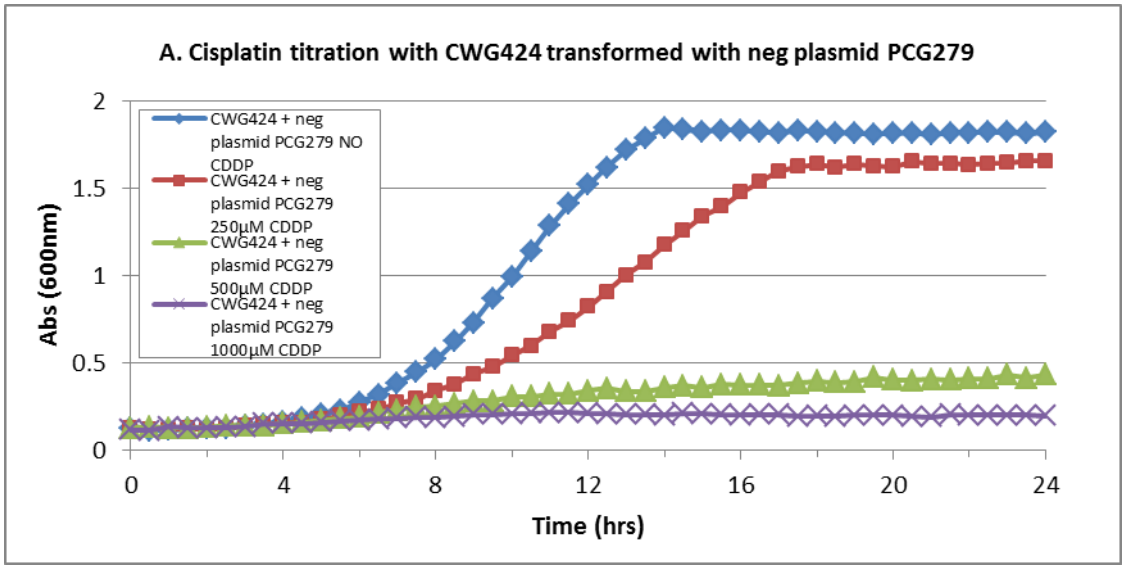

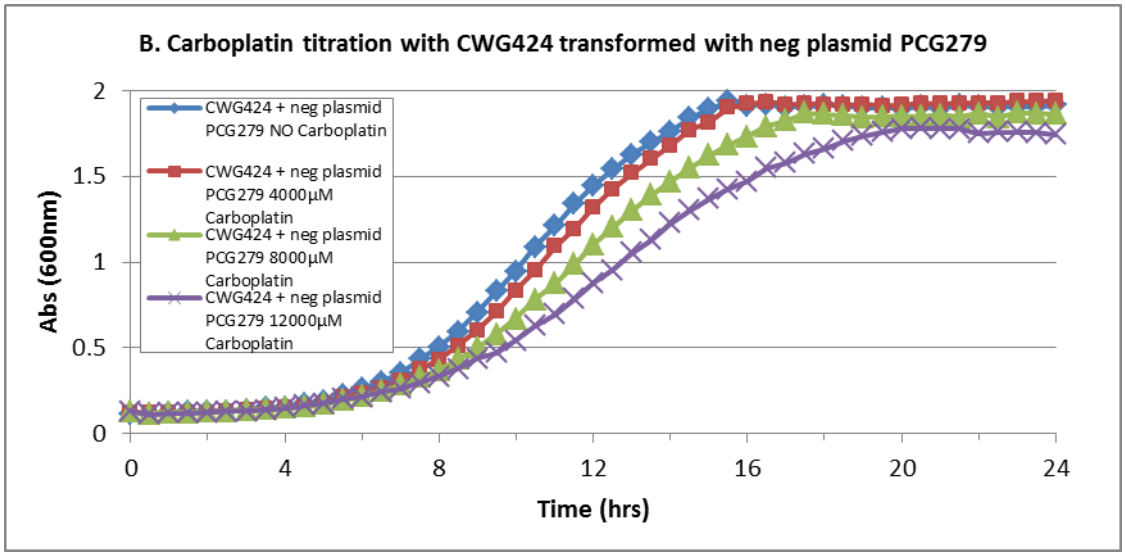

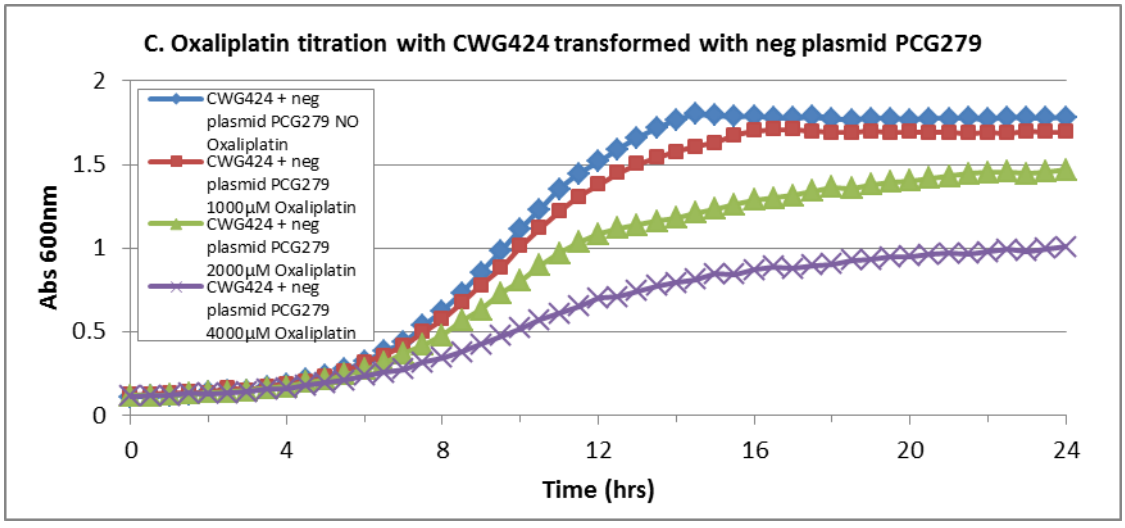

Figure 13**.** Growth curve examples of CWG424 transformed with negative control plasmid PCG279 tested with a titration of cisplatin (A), carboplatin (B) and oxaliplatin (C). This is single point testing – these titrations were also carried out with a second batch of overnight cultures to give a biological replicate, which gave identical results (data not shown), and doubling times for both are shown in Figure 14.

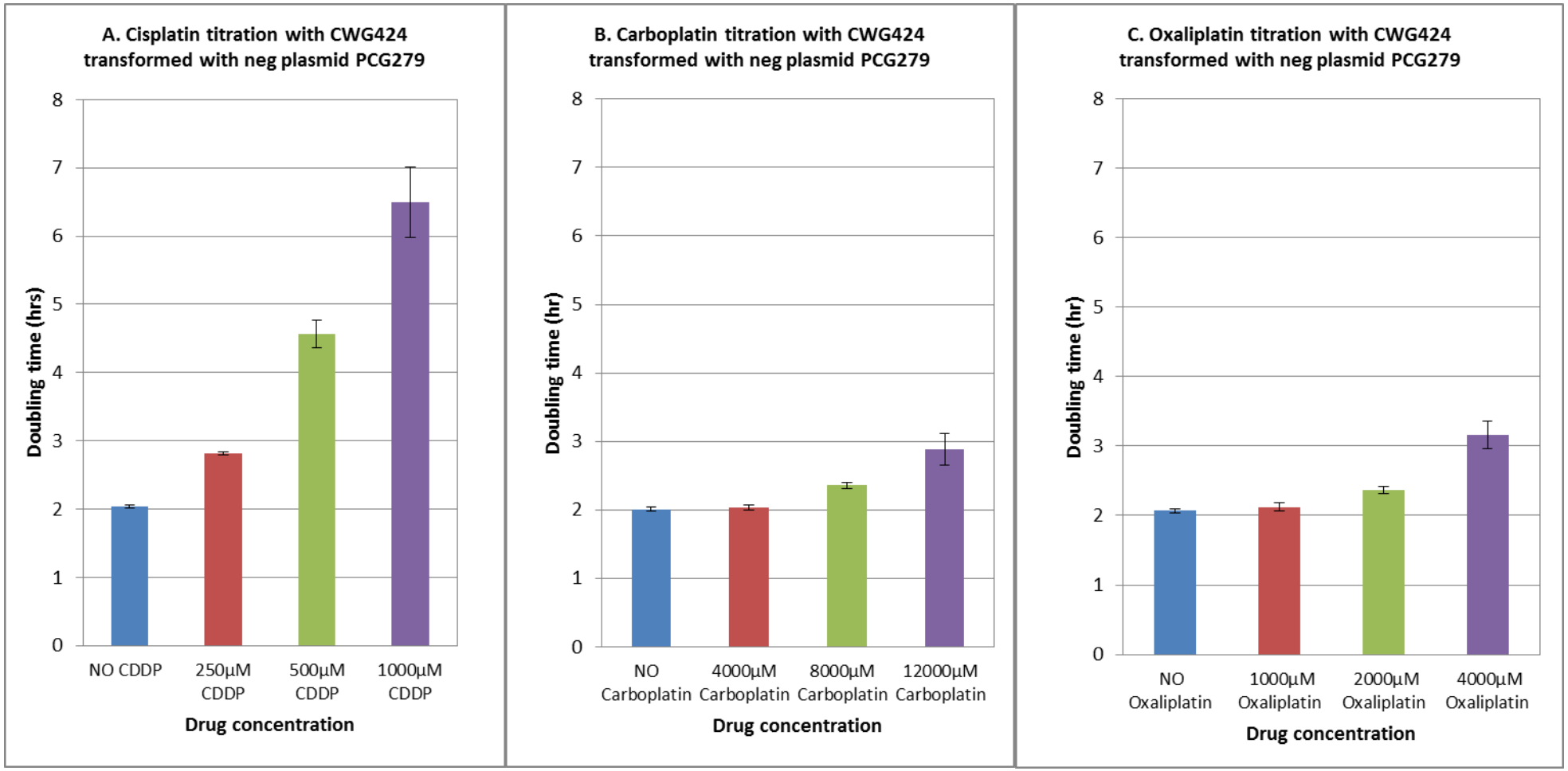

Figure 14. Mean doubling times for the growth curves for CWG424 transformed with negative control plasmid PCG279 grown with titrations of cisplatin (A), carboplatin (B) and oxaliplatin (C). Data are the mean of two biological repeats (of which examples of one are shown in Figure 13); error bars represent standard deviation.

3.2.3.2 Growth curves of all transformants with the platinum drugs

The following four transformant strains

S. cerevisiae strain wild type CWG424 transformed with negative control plasmid PCG279
S. cerevisiae strain wild type CWG424 transformed with BDF1 plasmid PCG596,
S. cerevisiae strain *ΔBdf1* transformed with negative control plasmid PCG279, and
S. cerevisiae strain *ΔBdf1* with BDF1 plasmid PCG596,

were all grown with and without each of the previously selected concentrations of the three platinum drugs: 250 µM cisplatin, 12000 µM carboplatin and 2000 µM oxaliplatin (Figure 15, Figure 16, and Figure 17).

In the absence of cisplatin, growth of wild type CWG424 transformed with BDF1 plasmid PCG596 was significantly slower than that of CWG424 transformed with negative control plasmid PCG279 (Figure 15A and Figure 18A). These plasmids can exist in cells anywhere between 2-200 copies per cell and so BDF1 is overexpressed when compared to wild type (which has a single copy of the gene). This result is in accordance with previous observations that high cellular levels of Bdf1 impair yeast growth (Matangkasombut, Buratowski et al. 2000). The presence of 250 µM cisplatin further reduced the growth of both CWG424 transformant strains.

In the absence of cisplatin, *ΔBdf1* yeast cells transformed with negative control plasmid PCG279 (Figure 15A and B, and Figure 18A) displayed the slowest growth. This is in concordance with the role of Bdf1 in the expression of numerous genes that are relevant for yeast cell proliferation (CHUA, ROEDER 1995, Ladurner, Inouye et al. 2003, Bandyopadhyay, Mehta et al. 2010). Reinstating the BDF1 gene into the *ΔBdf1* strain significantly recovered growth to a level comparable to that of CWG424 transformed with BDF1 plasmid PCG596, but not up to the level of the CWG424 strain transformed with negative control plasmid PCG279 (Figure 15A and B, and Figure 18A). This is because both the wild type and *ΔBdf1* strain have been transformed with a multi-copy plasmid containing BDF1 and, as mentioned above, elevated levels of Bdf1 impairs yeast growth; it can be assumed that these growth curves represent the maximum growth these cells can achieve when BDF1 is overexpressed in this way in the absence of cisplatin.

In the presence of 250µM cisplatin, cultivation of the *ΔBdf1* strain transformed with negative control plasmid PCG279 resulted in minimal growth, and the reintroduction of the BDF1 gene into the *ΔBdf1* strain via plasmid PCG596 resulted in a substantial recovery of yeast cell growth in the presence of cisplatin (Figure 15B and Figure 18A), to a level comparable to that of CWG424 transformed with BDF1 plasmid PCG596, but not up to the level of the CWG424 strain transformed with negative control plasmid PCG279. It can be assumed that this represents the

maximum growth these cells can achieve when BDF1 is overexpressed in the presence of cisplatin. Reintroduction of BDF1 into the *ΔBdf1* strain also recovered yeast cell growth in the presence of 12000 µM carboplatin (Figure 16 and Figure 18B) and 2000 µM oxaliplatin (Figure 17 and Figure 18C) in a similar fashion as in the presence of 250 µM cisplatin (Figure 15 and Figure 18A).

For the drug titration experiments (see section 3.2.3.1), it was discussed how, with the CWG424 strain transformed with negative control plasmid PCG279, the oxaliplatin growth curves displayed a slower growth during the post-diauxic phase and a lower maximum Abs_{600} compared to the curves with cisplatin and carboplatin (Figure 13). Here this is, as expected, again observed for each of the four transformant strains in the presence of oxaliplatin (Figure 17), compared to with the other two drugs (Figure 15 and Figure 16). A concentration of 2000 µM over 4000 µM oxaliplatin was selected to capture the complete growth curves of all strains (refer to section 3.2.3.1 and Figure 13), which here was successful (Figure 17), though, as expected, the toxic effect of 2000 µM oxaliplatin (Figure 17 and Figure 18C) was not quite as strong as 250 µM cisplatin (Figure 15 and Figure 18A) or 12000 µM carboplatin (Figure 16 and Figure 18B).

Taken together, these data indicate that the loss of BDF1 is associated with increased sensitivity of *S. cerevisiae* to cisplatin, carboplatin and oxaliplatin.

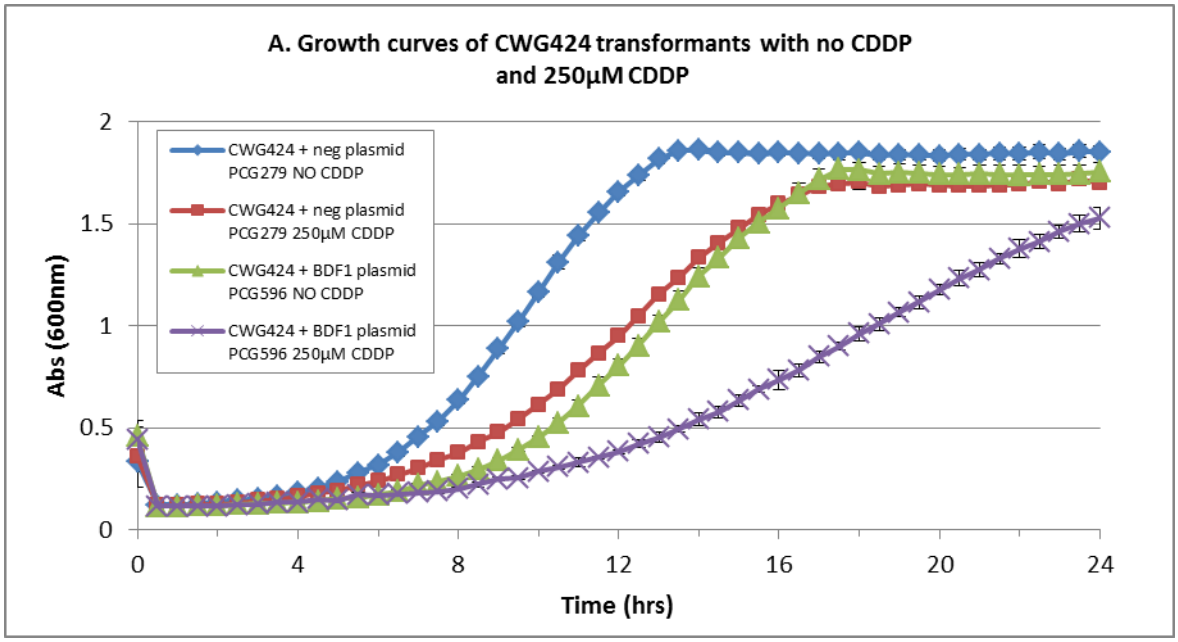

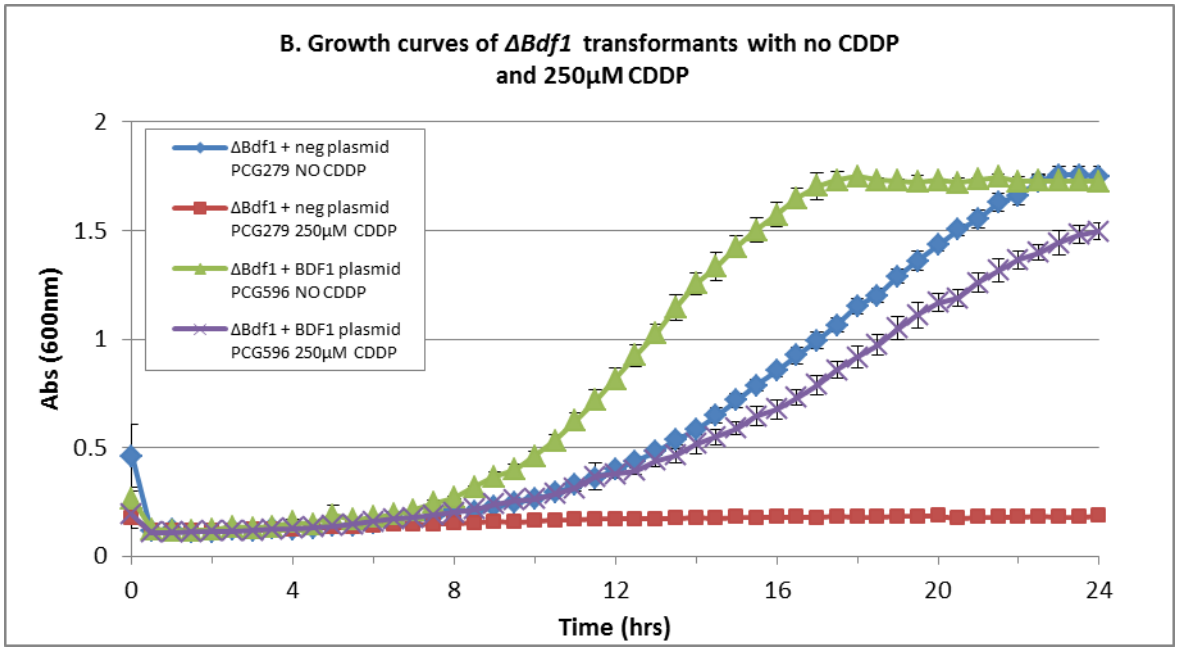

Figure 15. Growth curve examples of the CWG424 transformants (A) and the *ΔBdf1* transformants (B) grown with and without 250 µM cisplatin. Data are the mean of three technical replicates; error bars represent standard deviation. A further two biological replicates of this experiment were carried out with virtually identical results. Doubling times of all three biological replicates can be seen in Figure 18.

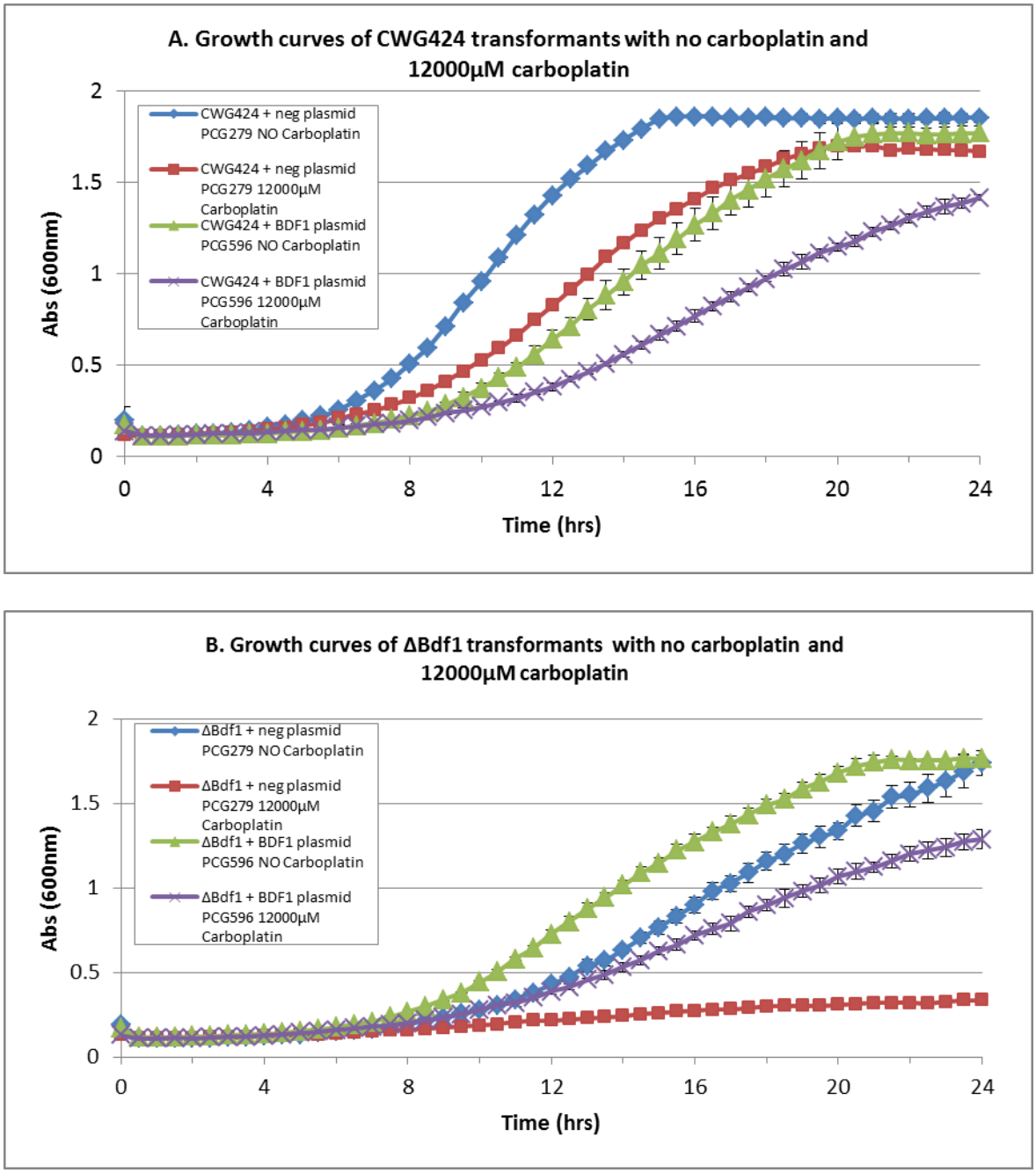

Figure 16. Growth curve examples of: the CWG424 transformants (A) and the *ΔBdf1* transformants (B) grown with and without 12000 µM carboplatin. Data are the mean of three technical replicates; error bars represent standard deviation. A further two biological replicates of this experiment were carried out with virtually identical results. Doubling times of all three biological replicates can be seen in Figure 18.

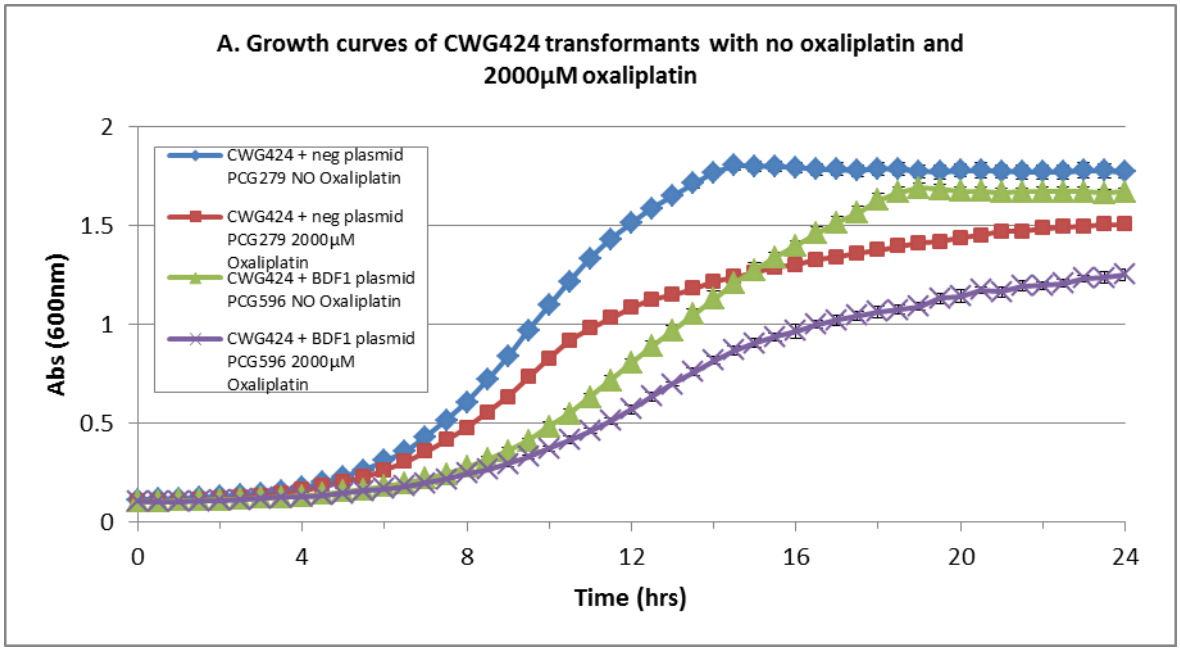

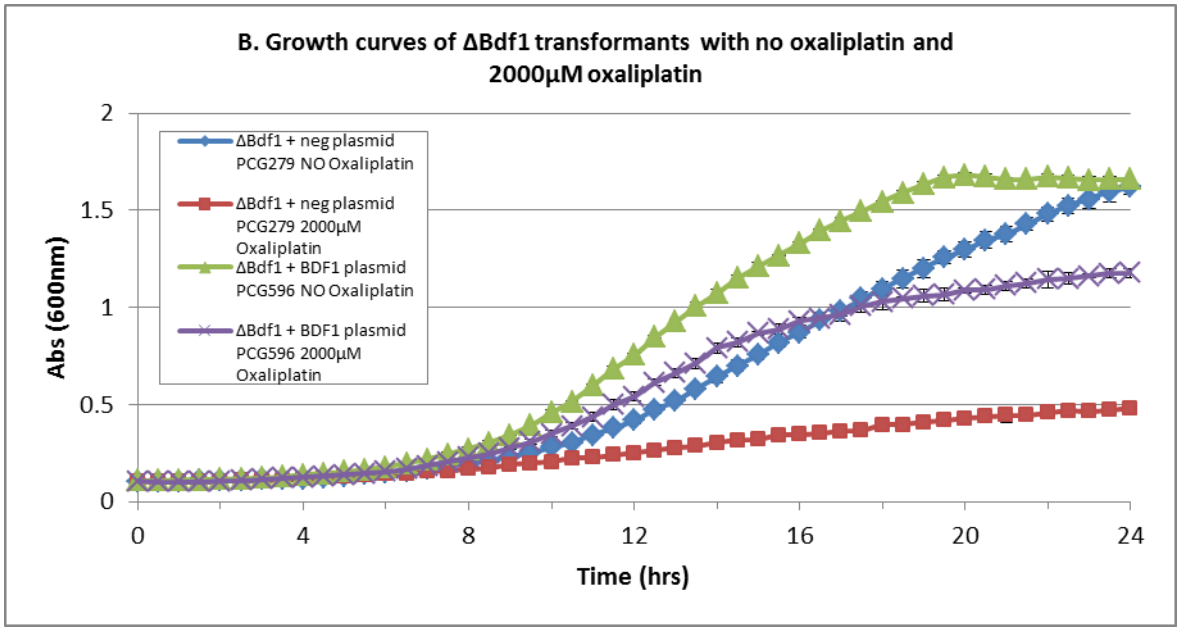

Figure 17. Growth curve examples of: the CWG424 transformants (A) and the *ΔBdf1* transformants (B) grown with and without 2000 µM oxaliplatin. Data are the mean of three technical replicates; error bars represent standard deviation. A further two biological replicates of this experiment were carried out with virtually identical results. Doubling times of all three biological replicates can be seen in Figure 18.

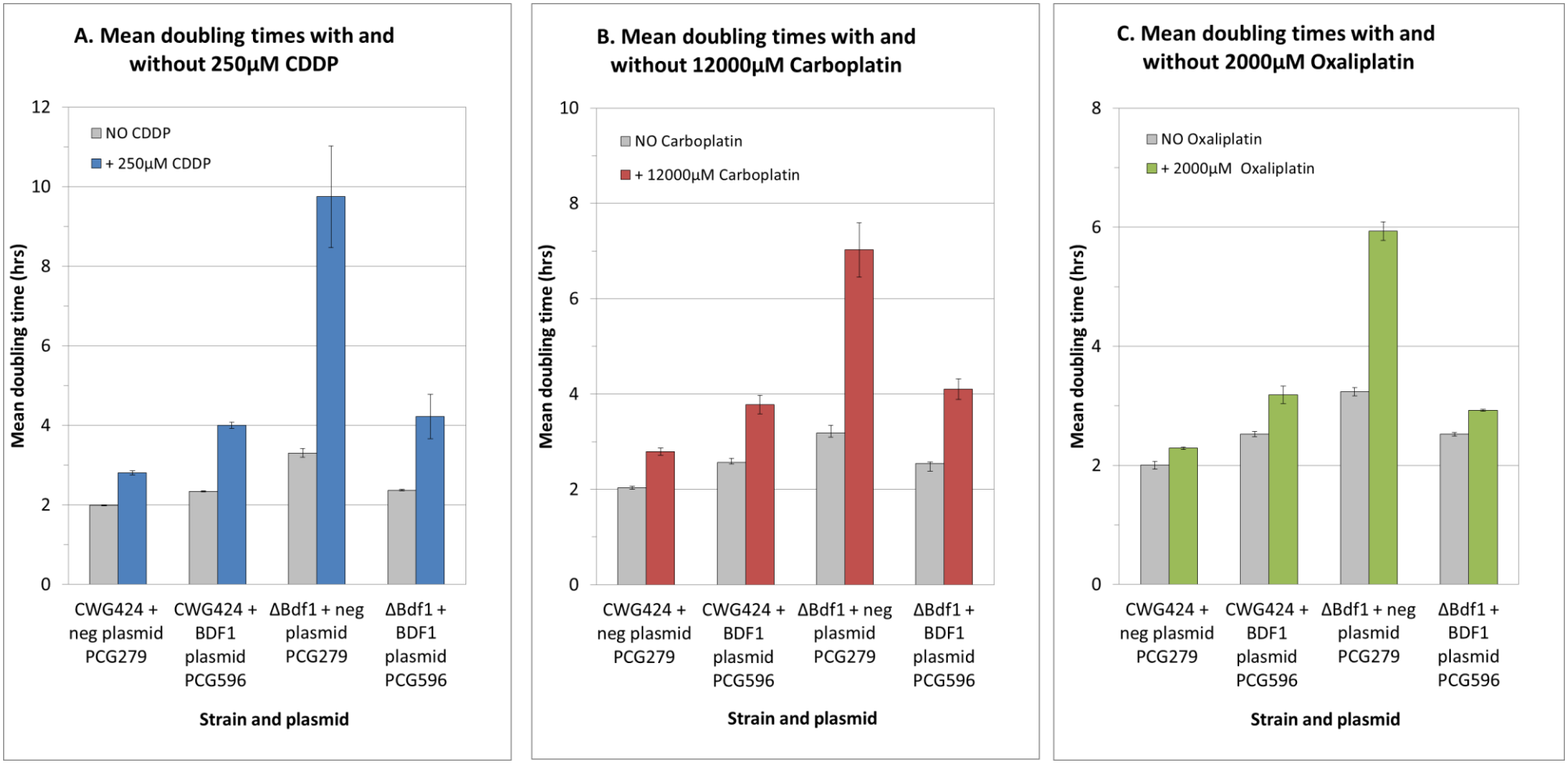

Figure 18. Mean doubling times for the growth curves of the S. cerevisiae strains CWG424 and *ΔBdf1* transformed with negative control plasmid PCG279 or plasmid PCG596 (which contains BDF1), and grown with and without 250 µM cisplatin (A), 12000 µM carboplatin (B) and 2000 µM oxaliplatin (C). Data are the mean of three biological repeats (of which examples of one are shown in Figure 15, Figure 16, and Figure 17); error bars represent standard deviation.

3.3 Discussion - yeast

The aim of our yeast (*Saccharomyces cerevisiae*) MATa haploid gene deletion library screens was to identify genes encoding transcription factors and regulators that were required for growth and potentially confer resistance in the presence of the platinum drugs cisplatin, carboplatin and oxaliplatin. This would possibly help to better understand the mode of action of and resistance to these medicines, and to compare these three drugs in parallel. Identified genes could help to identify potential resistance markers and pathways, drug targets or even biomarkers to help predict treatment outcome. Our screening was a type of homozygous profiling (HOP) – this type of assay uses complete homozygous deletion strains (Cheung-Ong, Giaever et al. 2013) to achieve the same goal.

3.3.1 Homozygous profiling (HOP) studies, including our screen

An example of a HOP screen, on an enormous scale, is the Yeast Fitness Database (Yeast Fitness Database (2008). Hillenmeyer,Maureen E., Fung et al.), for which the growth data generated was from screening both the homozygous and heterozygous diploid Yeast Knock-out (YKO) libraries under numerous chemical or environmental stress conditions (refer to 2.3.2). We used the resulting homozygous knockout data from the Yeast Fitness Database to look at the effects of three platinum drugs on the whole genome (3.2.1.1 and 3.2.1.2.). These YKO gene deletion libraries including the MATa haploid deletion library (see 2.3.2.2 and 3.1.2.1) used for our screening, have 'molecular barcodes' on the gene deletion cassettes that act as strain identifiers. These barcodes were exploited in the Fitness Database screening, enabling the simultaneous competitive growth of pools of gene deletion strains in the presence of, for example, drug. Growth was then assessed by quantitatively detecting PCR-amplified copies of these 'molecular barcodes' using tag micro-array technology, and comparing to growth in control conditions.

HOP has been used to determine genes that in particularly play a key role in the DNA damage response, an example of which is a study by Birrell et al in 2001 (Birrell, Giaever et al. 2001) (2.3.2.1). They used this method to screen the full yeast homozygous deletion library (Saccharomyces Gene Deletion Project (Stanford University, Stanford CA)) using competitive growth of pooled deletion strains and micro-array technology and identified three genes (THR1, LSM1, and YAF9) that are key players in the DNA damage response (here, damage was by UV radiation) for which this had not been demonstrated before, of which two have human orthologs involved in cancer predisposition. This research group subsequently used the same methodology again to reveal the genes required for growth in the presence four DNA damaging reagents - UV radiation, ionising radiation, hydrogen peroxide exposure and treatment with cisplatin (Birrell, Brown et al. 2002) and directly compared these data with the transcriptional response of wild

type strain to the same agents. Interestingly, they showed that there was no correlation, suggesting that the genes important for survival of yeast to DNA-damaging agents cannot be identified from the genes whose expression is elevated in response to these agents, which supports that HOP screening methodology similar to ours is appropriate for identifying drug resistance genes. Their findings contradict widespread assumption that the protection of cells from DNA damage comes from at least some of the genes induced after DNA damage (Birrell, Brown et al. 2002). Proposed explanations for this are that the DNA-damaging agents can also damage numerous other cell macromolecules, thus initiating the expression of protein chaperone and proteasome genes (as has been observed for MMS (methyl methanesulfonate) treatment) (Jelinsky, Estep et al. 2000), and also treatment of yeast by DNA damaging agents can induce an overall stress response that is independent of DNA damage (Gasch, Spellman et al. 2000); the stress response is now known to involve post-transcriptional events through translational reprogramming, which make it faster (Giaever, Nislow 2014). It should also be considered that wild-type levels of DNA repair enzymes can already be at sufficient levels to protect the cells from DNA damage, for example overexpressing RAD52 mRNA has no effect on yeast sensitivity to MMS (DORNFELD, LIVINGSTON 1991). Giaever et al also demonstrated a lack of correlation between the genes necessary for growth in a condition and genes whose transcription increases in the same condition when they announced the completion of the *S. cerevisiae* Deletion Project in 2002 (Giaever, Chu et al. 2002).

Another study using HOP was by Lee et al in 2005 (Lee, Onge et al. 2005). This group investigated the effects of 12 DNA damaging agents in parallel, including cisplatin, carboplatin and oxaliplatin, on the full yeast homozygous deletion library (Saccharomyces Gene Deletion Project (Stanford University, Stanford CA)) using competitive growth of pooled deletion strains and micro-array technology; here, microarray results were confirmed by performing independent individual growth analysis. They grouped the most sensitive 'hit' strains genes into several well-characterised DNA damage repair models, such as Nuclear Excision Repair (NER) and Homologous Recombination Repair (HRR), and were able to distinguish between drug mechanisms of action. In this way they demonstrated that carboplatin has a distinct profile, and less dependent on NER machinery, compared to cisplatin and oxaliplatin. They also showed that, along with mitomycin C, carboplatin had a larger number of gene deletion hits that were not previously associated with DNA metabolism. This challenges the assumption that because cisplatin and carboplatin are more structurally similar and form more closely related adducts than oxaliplatin, that they have more similar modes of action and spectrum of clinical activity (Lee, Onge et al. 2005, Rabik, Dolan 2007, Heffeter, Jungwirth et al. 2008, Wheate, Walker et al. 2010, Martinez-Balibrea, Martinez-Cardus et al. 2015). Clustering of the most sensitive gene deletion strains in the study correlated the platinum drugs together, and also revealed several genes to be linked to DNA-damage repair pathways which had not been linked previously. It would be of value to perform similar studies to

the one just described, (Lee, Onge et al. 2005), but focussing on other processes instead of DNA, for example the apoptotic response. Wu et al (Wu, Brown et al. 2004) also previously demonstrated that cisplatin and oxaliplatin have similar sensitivity profiles in their HOP screening of the same homozygous deletion library and competitive fitness profiling and microarray methodology, though they did not screen carboplatin.

In contrast to the Yeast Fitness Database micro-array screening, we used the MATa haploid gene deletion library (see 2.3.2.2 and 3.1.2.1) and screened a smaller subset of library strains for growth defects in the presence of cisplatin, carboplatin and oxaliplatin only. This smaller scale screening was more controlled and manageable than large-scale automated micro-array, more cost-effective, and by using different methodology we attempted to break new ground. The library subset was of 209 transcription factor/regulator gene deletion strains, plus three control strains, wild type CWG424, and the DNA repair mutants *ΔRad52* and *ΔRad27* (3.2.1). These transcription factor/regulator genes are master controllers of gene expression and regulation. We did not use liquid culture for our screening, we stamped this subset of yeast strains onto solid media (YPD agar) containing drug or no drug (control), and expressed growth on the agar containing drug to the growth on the control agar containing no drug (3.1.3). The strongest hits were then rescreened to confirm their drug sensitivity (3.1.5). Similar drug screening approaches to ours, on solid agar where sensitivity is measured by colony size, have been used previously (Smith, Ammar et al. 2010) but none comparing the three platinum compounds in parallel. For example, experiments by Parsons et al (Parsons, Brost et al. 2004) included using the same Mata library, but the whole of it, to screen 12 compounds (though unrelated to the platinum drugs), by robotically pinning all the strains onto solid agar containing drug, and then carrying out spot dilution assays to confirm hits. A study by Hartman et al (Hartman, Tippery 2004) included a genomic screen of deletion strains on solid media and the use of time-lapse image focussing to measure colony growth in the presence of the DNA synthesis, replication and repair inhibitor hydroxyurea (HU); sensitive hits were screened against other drugs including cisplatin, and the data suggested that cisplatin is similar to HU in terms of overlapping pathways required to grow when DNA is damaged. Baetz et al (Baetz, McHardy et al. 2004) and Carrol et al (Carroll, Stirling et al. 2009) also screened deletion strains on solid agar to study the action of the drug dihydromotuporamine C and yeast K28 (an A/B toxin) respectively.

For our screening on solid media (3.1.3 and 3.1.5) we stamped out many more cells per strain onto the agar than were initially inoculated into liquid culture for growth up to 20 generations for the Yeast Fitness Database micro-array screening (2.3.2.2), and we grew colonies over four days. For the Yeast Fitness Database screening they had measures in place to be sure that the same number of cells went into the original strain pools, and by starting growth from the same optical density in the test conditions during screening (2.3.2.2). We endeavoured to compensate for

growth rate differences between deletion strains by using overnight saturated cultures so there was the best possible chance of plating out similar numbers of cells for each strain, and for the conformation screening we actually adjusted the A_{595} of each culture to be in the same range. However, there would have been an unavoidable degree of variation in stamping out strains shown by, for example, the triplicate stamping out for our conformation screen (refer to Table 4, Table 5 and Table 6 for % growth values of colony size on agar containing drug over colony size on agar containing no drug for three parallel repeats). However, all our screens were qualitative not quantitative, and a level of variability was accepted. It was expected to possibly lose some low to middle strength hits but we were certain that the strong gene deletion hits would still be detected using this screening method, which they were.

Our screens were carried out using 1000 µM cisplatin, 4000 µM carboplatin and 4000 µM oxaliplatin, and for the oxaliplatin and carboplatin screens the yeast strains were pre-diluted 1 in 10 with MQ H_2O before stamping them onto the agar, in an attempt to obtain comparable results for the control strains to the cisplatin screen during optimisation (refer to 3.2.1). However, for both the initial screening and conformation screening, oxaliplatin was the strongest screen in terms of growth inhibition, followed by the cisplatin screen, and the carboplatin screen was the weakest. It is challenging to set an ideal concentration of drug because ideally we would have used a drug dilution series to screen a serial dilution of the yeast strains to get the most accurate idea of sensitivity. For our screening we were essentially generating a snapshot of drug inhibition which will not capture every single sensitive strain, but would capture the stronger sensitivities. If this screening method was to be repeated, a higher concentration of carboplatin would be used. The conformation screening was not as strong in terms of growth inhibition as for the initial screening; the yeast deletion strain colonies grew quicker in the presence of each of the three drugs, therefore the original scoring system (3.1.3.5) was re-designed to pick up the strongest of the hits (3.1.5.5). This highlights the variability of such a screening method. Explanations for this weaker screen could be that the yeast strains were grown overnight in 3mL YPD medium rather than in a small volume in 96-well plates as for the initial screen, and so they were healthier on stamping out on the agar so grew better in the presence of drug. Also, perhaps the strains were healthier because they were fresh from the MATa haploid deletion library, whereas the strains used for the initial screen had been freeze-thawed several times prior and they may have developed a degree of background mutation or maybe even contamination which could affect growth.

3.3.2 Initial plate-based screening of the transcription regulator library and comparison with the Yeast Fitness Database

From our initial screening (3.2.1.1) of our transcription factor/regulator gene deletion Mata haploid library subset in the presence of cisplatin, carboplatin and oxaliplatin, we discovered gene deletion hits that were exclusive to the individual platinum drugs, and hits that were common to two or all three drugs (focussing on hits growing ≤50 % for four days on YPD agar containing drug compared to on no drug) (Figure 6 and Figure 7A). This sharing of hits suggests that they may share mechanisms of action or potential resistance factors. The gene hit distribution also suggested that cisplatin and carboplatin are not necessarily the most similar of the three drugs. It is widely believed that because cisplatin and carboplatin are more structurally similar and form more closely related DNA adducts than oxaliplatin, that they have more similar modes of action and a similar spectrum of clinical activity, as reviewed in (Rabik, Dolan 2007, Heffeter, Jungwirth et al. 2008, Wheate, Walker et al. 2010, Martinez-Balibrea, Martinez-Cardus et al. 2015) (2.2.1) and, as previously mentioned, Lee et al demonstrated a unique profile for carboplatin in terms of DNA damage repair pathways (Lee, Onge et al. 2005). Refer to (2.2) for and overview of known platinum drug mode of action and resistance mechanisms.

Even though the Yeast Fitness Database platinum drug dataset was generated from screening the entire yeast genome in the form of the homozygous diploid deletion library (2.3.2.2) the gene hit distribution of this screening suggested similar conclusions to our screen (Figure 7B). Also, being a genomic screen, the Yeast Fitness Database platinum drug dataset gave us a more generic picture of the functions and processes of the gene hits required for fitness in the presence of the three platinum drugs compared to our dataset (3.2.1.2). We matched the gene hits from Yeast Fitness database to SGD Yeast GO-slim terms 'function' and 'process', and established, as for the gene hit distributions, terms that were unique to each drug and common to two or all three drugs (refer to Figure 8 and Appendix C for functions and Figure 9 and Appendix D for processes). For our initial screening dataset this was also true for 'process' terms, and for 'function' terms they were either were unique to each drug or common all three drugs (refer to Appendix E for functions and Appendix F for processes). This again suggested that these three drugs may have common mechanisms of action or potential resistance factors. It should be noted, though, that due to our subset library already being much smaller and also enriched for transcription factor/regulator gene deletion strains, this type of analysis was not as appropriate, and we had to focus on frequency values generated rather than fold enrichment values that we calculated using them.

As expected for our screen, fold enrichment values and frequency values were very high for transcription factor and DNA/chromatin/histone binding function terms for all three drugs as a group due to pre-enrichment for transcription factors and regulators (3.2.1.2.) (Appendix E). For the Yeast Fitness Database dataset, as a group of all three drugs, hits also centred around these

function terms (3.2.1.2) (Figure 8 and Appendix C); DNA binding was enriched for all three drugs (with high frequency values), which was expected because it is essential for platinum drug activity, as was protein binding, and other terms included, not necessarily present for all three drugs, were lipid binding, the activity of a variety of enzyme groups, and protein and transmembrane transporter activity. Examples of more specific functions were histone binding, which was very enriched by two-fold for cisplatin and oxaliplatin but not enriched for carboplatin, and chromatin binding was enriched for oxaliplatin but not enriched for the other two drugs, which may indicate differences in modes of action and resistance. Nucleic acid binding transcription factor activity was a common enriched function for cisplatin and carboplatin. It was interesting that there was not a fold enrichment value above 1.0 for these functions for all the three drugs considering that they are DNA binding agents. Platinum drugs enter cells by both passive diffusion and via plasma membrane transporters which likely explains the protein and transmembrane transporter activity functions being quite enriched for the gene deletion hits of oxaliplatin and carboplatin respectively. All these differences indicate dissimilarities in modes of action and resistance.

Regarding process terms, our initial screening gene deletion hits had the majority of DNA process terms were shared by all three drugs, due to pre-enrichment of our library subset (3.2.1.2.) (Appendix F). In terms of other processes, though, both our screen (Appendix F) and the Yeast Fitness database (Figure 9 and Appendix D) enrichment for matched terms generally covered the repair, organisation, and transcription of DNA, histone and chromatin, along with vesicle and membrane trafficking, intracellular transport, protein modification and proteolysis, the cell cycle, metabolic processes and stress responses, highlighting the complexity of the responses of cells to these drugs, and potentially their mechanism of action.

These enriched process made sense in terms of the published aspects of the better characterised platinum drug mechanism of action; they are taken into cells by passive diffusion or through metal transporters, in the cell they form adducts with DNA, the resulting DNA damage modulates several different signal transduction pathways leading to cell cycle check points and arrest, DNA repair, and apoptosis, reviewed in (Wang, Lippard 2005, Wheate, Walker et al. 2010) (2.2.1). However, it is also important to appreciate that, because of their low binding specificity and high activity, the platinum drugs also bind to numerous other cellular components besides DNA, such as RNA, proteins, lipids, cytoskeletal components and thiol-containing molecules (Jamieson, Lippard 1999, Gonzalez, Fuertes et al. 2001, Fuertes, Castilla et al. 2003, Wang, Lippard 2005, Cullen, Yang et al. 2007, Heffeter, Jungwirth et al. 2008, Zhao, Wang et al. 2015) (2.2.1). Studies have been carried out to show this in enucleated cancer cells; for example the endoplasmic reticulum as a target for cisplatin (Mandic, Hansson et al. 2003), and the mitochondrial apoptotic response for oxaliplatin (Gourdier, Crabbe et al. 2004). Mitochondria and mitochondrial DNA have

been shown to be targeted by cisplatin which can induce apoptosis, and this is partly responsible for the cytotoxicity of the drug (Gonzalez, Fuertes et al. 2001, Yang, Schumaker et al. 2006, Cullen, Yang et al. 2007), and is likely to be the case for the other two drugs. As mentioned, treatment with these drugs can also induce an overall stress response in the yeast cells that is independent of DNA damage (Gasch, Spellman et al. 2000). So the variety of process terms covered by both the Yeast Fitness database screen and our screens are unlikely to be entirely due to solely the DNA binding aspects of the drugs.

Due to the much smaller dataset from our screen, which meant many process terms were matched by just a few of the gene deletion hits, we focussed on frequencies rather than fold enrichment values, and the higher frequencies for processes that were common to all three drugs were mainly transcription from RNA polymerase II promoter, mitotic and meiotic cell cycles, response to chemical, and organelle fission (Appendix F). For the larger Yeast Fitness databases dataset, the majority of processes were shared by all three drugs or by cisplatin with oxaliplatin (Figure 9 and Appendix D). Referring back to the gene hit distributions (3.2.1.1), both our initial screen (Figure 7A) and the Yeast Fitness database dataset (Figure 7B) suggested that cisplatin and carboplatin and not necessarily the more similar of the three drugs (as is widely believed), with the Yeast Fitness database dataset suggesting that oxaliplatin is more similar to cisplatin. Here, in terms of enriched processes from screening the whole genome, the Yeast Fitness data suggests that oxaliplatin is more unique compared to the other two drugs (Figure 9 and Appendix D). This is because, interestingly, compared to cisplatin and carboplatin, oxaliplatin had overall much higher fold enrichment values, and these processes were more orchestrated around vesicle and membrane trafficking, whereas the processes with the highest fold enrichment values for cisplatin and carboplatin were quite varied (Appendix D). It is noteworthy that protein transporter activity and cytoskeletal protein binding were enriched 'function' terms for oxaliplatin (Appendix C). Oxaliplatin fold enrichment values in the Yeast Fitness database dataset were very high for endosomal transport, membrane invagination, vesicle and vacuole organisation, endo- and exocytosis, Golgi vesicle transport, membrane fusion and organelle fusion, fission and inheritance, and four of these process terms were exclusive to oxaliplatin hits (Figure 9 and Appendix D). Vesicular trafficking is important in the protection of yeast cells against DNA damage (Krol, Brozda et al. 2015) as is vacuolar trafficking (Hartman, Tippery 2004); the vacuole is involved in drug detoxification (Giaever, Nislow 2014). These processes could be more important for oxaliplatin due to this drug possibly binding more to lipid components of the cytoplasm compared to the other two drugs. Regarding carboplatin, as previously mentioned, focussing in on DNA damage repair pathways, Lee et al demonstrated a unique profile for carboplatin using the diploid deletion library (Lee, Onge et al. 2005).

3.3.3 Conformation screening

For the conformation screening we took forward the 25 gene deletion strains with the strongest phenotypes, growing ≤30 % over four days growth on at least one of cisplatin, carboplatin or oxaliplatin in YPD agar compared to on YPD agar containing no drug (3.2.1.3 and Figure 10). On reducing the cut off to ≤30 %, the overall frequencies for these 25 gene deletions in terms of gene deletion hits (Figure 10B) remained similar to the ≤50 % cut off dataset (Figure 6) (apart from an increase of carboplatin exclusive hits), along with some expected shifts in position between drugs in the gene hit Venn diagrams (compare Figure 10A with Figure 6). Compared to the ≤50 % cut off data (Appendix E and F), Gene Ontology (GO) Slim function frequencies (Appendix G) remained highest for DNA binding and transcription factor terms, and process frequencies (Appendix H) remained highest for transcription from RNA polymerase II promoter, mitotic and meiotic cell cycles and organelle fission for the three drugs. All process terms remained comparable to the ≤50 % cut off gene deletion hits.

Between all three drugs a total of 14 of the 25 gene deletion strains were hits in the conformation screening (Figure 11) - 4 hits for cisplatin (Table 4), 6 hits for carboplatin (Table 5) and 13 hits for oxaliplatin (Table 6), and there were no hits exclusive to cisplatin or carboplatin, and no hits common to all three drugs. Focussing on Figure 11 and comparing it to the ≤30 % cut off data of the initial screening (Figure 10A) illustrates how 7 yeast deletion strains were re-confirmed as hits for the same drugs; RAD52 (RADiation sensitive) and BDF1 (BromoDomain Factor) for cisplatin and oxaliplatin; MAC1 (Metal binding ACtivator) and UME6 (Unscheduled Meiotic gene Expression) for carboplatin and oxaliplatin; ZAP1 (Zinc-response Activator Protein), SUM1 (SUppresor of Mar1-1) and RAD27 (RADiation sensitive) for oxaliplatin. Some yeast deletion strains dropped out in the conformation screening for some drugs; for example, AFT1 (Activator of Ferrous Transport) was confirmed as a hit for cisplatin and carboplatin and dropped out as a hit for oxaliplatin, and SWI6 (Switching deficient) was confirmed as a hit for oxaliplatin and dropped out as a hit for cisplatin and carboplatin. Some yeast deletion strains also appeared as hits for a drug when the cut off of the initial screen was ≤50 % (Figure 6); examples were SLA1 (Synthetic Lethal with ABP1), which was confirmed here as a hit for cisplatin but not for carboplatin but also came up as a hit for oxaliplatin, however, it was a hit for all three drugs in the initial screen using a ≤50 % cut off. Also SWI4 (Switching deficient) and GCR2 (GlyColysis Regulation) which were confirmed as hits for carboplatin and came up as hits for oxaliplatin, however both of these genes were hits for oxaliplatin in the initial screen using a ≤50 % cut off (Figure 6). A discrepancy was SFP1 (Split Finger Protein), which was a hit for cisplatin in the initial screening using a ≤30 % cut off but here in the conformation screen it was a borderline hit for cisplatin (data not shown) and also a hit for carboplatin and oxaliplatin; however, in the initial screen using a ≤50 % cut off, SFP1 was a hit for only cisplatin and oxaliplatin, not carboplatin. This may be because SFP1 was

positioned on one of the weaker carboplatin drug plates (weak due to possible stamping issues) in the initial screen where the strains grew quicker on the drug plate compared to the control plate, so it was possibly lost as a hit. The test strain HIR1 (Histone Regulation) was a hit for oxaliplatin. This group of 14 genes, including controls RAD27 and RAD52, that are required for growth in the presence of platinum drugs together demonstrate varied roles, covering DNA synthesis and repair, glycolysis, metal ion utilisation, metal ion transport and homeostasis, mitotic and meiotic cell cycle, chromatin and histone regulation, cytoskeleton assembly, and response to stress (Figure 10 and refer to Appendix G and H). Many of these roles correlate with reported platinum drug mode of actions (2.2) and their roles/pathways in which they are involved could be potential platinum drug resistance mechanisms.

Of these 14 hit conformations, only 6 were hits in the Yeast Fitness Database; AFT1 was a hit for all three drugs, RAD52, MAC1 and SWI4 were hits for cisplatin only, SUM1 was a hit for cisplatin and oxaliplatin and HIR1 was a hit for cisplatin and oxaliplatin, some of which agreed with our results (see above). Some discrepancies between results using our screening methods and those used for the generation of data for the Yeast Fitness Database are not totally unexpected. Limitations of our screening methodology have already been discussed. Regarding the Yeast Fitness Database, as powerful a technique as tag micro-array analysis is, it also has its limitations. For example, if any small errors occur early on in the pool construction and cell cultivation steps they are likely to be amplified at the PCR stage of the process. Also, huge parts of the Yeast Fitness Database micro-array screening were automated, and there comes a risk of missing hits with the automation of such large-scale screens. Nevertheless, Costanzo et al have demonstrated that genetic interactions identified on solid media (using automated plating and computational analysis) have significant correlation with genetic interactions identified by assessing growth in liquid media (Costanzo, Baryshnikova et al. 2010). It should also be noted that the cells in the MATa library that we used were haploid whereas those screened for the Yeast Fitness database were diploid, which are generally larger in size and they may have different growth rates in comparison. However diploid strains, as used for the Fitness Database Screen, have two copies of every gene, some of which may be hetero-allelic that contribute to genetic variation; in contrast, in a haploid state there is less chance of such genetic variation because there is only one copy of each gene. It would be interesting to carry out our screen again but using the diploid strains as a comparison.

GCR2, along with the DNA binding protein GCR1 (which we did not screen), are both required for the transcriptional activation of glycolytic genes in yeast (UEMURA, FRAENKEL 1990, Uemura, Fraenkel 1999) with analogous function to the human gene hSGT1 (Sato, Jigami et al. 1999). Glucose metabolism is important for proliferation and survival and also recovery from damage, so it makes sense that such a gene deletion renders yeast cells more susceptible to the action of

platinum drugs. There are no publications directly linking GCR2 to platinum drug resistance. However, even though GCR2 was a hit for oxaliplatin and carboplatin, it is interesting that the Bromopyruvate (BP), a hexokinase (glycolytic enzyme) inhibitor, has been demonstrated to potentiate the anti-proliferative effects of cisplatin and oxaliplatin in human colon carcinoma cells (Ihrlund, Hernlund et al. 2008). Our data suggests that functional studies investigating inhibition of glycolytic activity, maybe via the human gene hSGT1, as a potential method to enhance platinum drug toxicity or reverse platinum drug resistance in cancer cells.

Our hits SUM1, UME6, SWI4 and SWI6, are all genes involved in proliferation, with SUM1 (Irlbacher, Franke et al. 2005) and UME6 (Lardenois, Becker et al. 2015) also playing roles in chromatin regulation (Table 7). Swi4 and Swi6 are both components of the SBF transcriptional activator (Swi4/Swi6 protein complex), with Swi4 being the DNA-binding protein; SBF regulates late G1-specific transcription of cyclins, cell wall biosynthesis genes and the HO gene. The related factor MBF (Mbp1/Swi6 protein complex) regulates late G1-specific transcription of genes required for DNA replication and repair (PRIMIG, SOCKANATHAN et al. 1992, Ho, Costanzo et al. 1999, Iyer, Horak et al. 2001, Coic, Sun et al. 2006). Swi6 also binds to Stb1 (Ho, Costanzo et al. 1999) - the STB1 gene deletion strain was a sensitive hit for cisplatin in the initial screening with a cut off of ≤50 % (Table 1). The DNA damage resulting from exposure of cells to platinum drugs regulates several various signal transduction pathways which lead to check points in the cell cycle and arrest (Wang, Lippard 2005, Wheate, Walker et al. 2010), so it follows that these genes are important for survival in the presence of platinum drugs. UME6 was a hit for carboplatin and oxaliplatin and is part of the Rpd3L histone deacetylase complex subunit (Carrozza, Florens et al. 2005), involved in chromatin remodelling. Supporting this, exposure to HDAC inhibitors MS275 and SBHA potentiates the cytotoxicity of oxaliplatin in human colorectal cancer cells, probably due to an increase in apoptotic signalling (Flis, Gnyszka et al. 2009) (2.2.2.5). Like UME6, the HIR1 gene is also involved in chromatin remodelling, and it is therefore not unexpected that the coresponding deletion mutant is sensitive to DNA damage by platinum drugs and is a hit for oxaliplatin in our conformation screen.

SLA1 does not encode a transcriptional regulator but a protein that is a central player in actin cytoskeleton assembly, and it has effects on proteins essential for endocytosis (Gardiner, Costa et al. 2007). In yeast, the actin cytoskeleton is important for maintenance of cell morphology, polarity, cell division, cell migration, vesicular trafficking and mechanosensation. It has also been mentioned that vesicular trafficking is important in the protection of yeast cells against DNA damage (Krol, Brozda et al. 2015). It has been demonstrated in human ovarian cancer cells that there is a direct role in actin remodelling and resistance to cisplatin, with resistant cells showing a dose-dependent increase in cell stiffness (Sharma, Santiskulvong et al. 2012). Also, actin plays a role in endocytosis, and this is a route of cellular entry of cisplatin and decreased endocytosis is

often a cisplatin resistance mechanism in cancer (Shen, Pouliot et al. 2012). Platinum drugs are also known to directly bind numerous other cellular components, including those of the cytoskeleton, which may contribute to their cytotoxicity (Jamieson, Lippard 1999, Gonzalez, Fuertes et al. 2001, Fuertes, Castilla et al. 2003, Cullen, Yang et al. 2007). Therefore it makes sense that a lack of SLA1 is detrimental to surviving exposure to platinum drugs.

RAD52 (one of the DNA repair deletion mutant control strains (Table 7)) and BDF1 (plays roles in growth, sporulation and DNA repair (Table 7)) were the strongest gene deletion hits (with a % growth of ≤30 % for two time points for all three replicates) for cisplatin and oxaliplatin, and both with weak sensitivity to carboplatin (data not shown); this again suggests more similarities between cisplatin and oxaliplatin in terms of how these drugs work and the resistance to them in yeast, though these strains would possibly have passed as carboplatin hits if our carboplatin screen was stronger. As described in (3.1.3), Rad52 is implicated in the repair of double-strand breaks (DSD) in DNA resulting from spontaneous damage, exposure to DNA damaging agents, and collapse of replication forks; mutations in RAD52 cause severe defects, especially in meiotic/mitotic recombination, because Rad52 is involved in multiple DSB repair pathways, reviewed in (Symington 2002) and (Paques, Haber 1999), used as a control in (CHUA, ROEDER 1995). BDF1 shall be discussed in more detail later.

AFT1 and MAC1 were the strongest hits for carboplatin, with AFT1 passing as a weaker hit for cisplatin, and MAC1 passing as a medium hit for oxaliplatin. AFT1 is a transcription factor that plays a key role in iron utilisation and homeostasis, which is an essential element that is important for redox reactions (YAMAGUCHIIWAI, DANCIS et al. 1995, Kimura, Ohashi et al. 2007). It is also involved in many other cellular processes, though it unclear if all these are regulated via iron homeostasis (Berthelet, Usher et al. 2010); AFT1 matched many Yeast GO-slim process terms (using Gene Ontology (GO) Slim Mapper analysis); transcription from RNA polymerase II promoter, organelle fission, mitotic and meiotic cell cycle, response to starvation, regulation of transport, chromosome segregation, and ion transport (refer to Appendix tables G and H). It has been reported that Aft1 affects the RIM101 pH pathway (Berthelet, Usher et al. 2010); the RIM101 gene deletion strain showed sensitivity to carboplatin in our initial screen using a ≤30 % cut off (Figure 10A), and to cisplatin and carboplatin using a ≤50 % cut off (Figure 6). Aft1 also plays an iron-mediated role in DNA repair, because iron has protective effects against DNA damage (Berthelet, Usher et al. 2010). Therefore it follows that AFT1 deletion strains can be sensitive to the DNA-damaging platinum drugs. Kimura et al (Kimura, Ohashi et al. 2007) used cDNA microarrays and PCR conformation experiments to demonstrate that the mRNA levels of a group of 14 proteins, including Fet3, are elevated in the presence of cisplatin, and that these genes are all controlled by Aft1, which is activated by low levels of iron. They showed that cisplatin inhibits cellular iron uptake, leading to an iron deficiency and thus activation of Aft1.

Kimura et al propose two theories for the how cisplatin inhibits the uptake of iron, the first being that the drug directly inhibits proteins involved in the process, and, interestingly the second is that cisplatin may do so indirectly via inhibition of copper uptake via the yeast and human cell copper transporter CTR1 (Ishida, Lee et al. 2002). This is because Fet3 is required (in a complex with Ftr1) for iron uptake but is only active in the presence of copper, so if cisplatin inhibits copper uptake, the Fet3-Ftr1 complex will not function and iron levels will decrease. However, another study revealed that copper levels in yeast are not affected by cisplatin (Ohashi, Kajiya et al. 2003). CTR1 has been shown in yeast and mammalian cells to be involved in the uptake of platinum drugs (Ishida, Lee et al. 2002, Song, Savaraj et al. 2004, Holzer, Manorek et al. 2006) (see 2.2.1), which evidences that oxaliplatin and carboplatin can also potentially inhibit copper transport via CTR1. It has been reported using murine cells, that at higher concentrations of each of the three drugs (superseding those typically established in patient plasma), oxaliplatin enters cells primarily via a different mechanism to CTR1 (Holzer, Manorek et al. 2006).

It is interesting that the other strong carboplatin hit gene, MAC1, is a copper-sensing transcription factor that contributes to copper level control by regulating the expression of the CTR1 and CTR3-encoded membrane-associated copper transport proteins (Labbe, Zhu et al. 1997, Ishida, Lee et al. 2002). Changes in copper levels induce a change in the redox state of Mac1, and this also happens on exposure to the DNA damaging agent MMS (methyl methanesulfonate) (Dong, Addinall et al. 2013). The expression of CTR1, along with other yeast copper genes, has been shown to be upregulated in response to DNA damage (by MMS (methyl methanesulfonate) treatment, and hydroxyurea) via mechanisms requiring Mac1 and Ace1. This, along with suppression of the gene encoding metallothionein, which collates copper, indicates that copper is required when DNA is damaged - this requires further investigations (Dong, Addinall et al. 2013). So we could propose that without MAC1, CTR1 cannot be upregulated in response to DNA damage by the platinum drugs, therefore there would be reduced copper uptake. This would also cause lack of Fet3 activation, so the Fet3-Ftr1 complex would not function and so iron levels and also AFT1 activation would decrease, and result in reduced protection against DNA damage. This could explain our results, which demonstrate sensitivity of the MAC1 deletion mutant strain in the presence of carboplatin and oxaliplatin. However, MAC1 was not a hit for cisplatin in our screen, just signs of sensitivity at early time points during the initial screen. Contradicting this result for cisplatin, Ishida et al (Ishida, Lee et al. 2002) used a transposon mutagenesis approach to create gene deletions in yeast, and then selected for stains that were able to grow in the presence of cisplatin; they found the strain lacking MAC1 showed the highest degree of cisplatin resistance. They then deleted each of the known MAC1 target genes and found that only the strain lacking CTR1 showed comparable resistance to the MAC1 mutant, suggesting that CTR1 is the major MAC1 target for resistance to cisplatin. This can be explained by the lack of MAC1 causing reduction in CTR1 expression, causing a decrease in the uptake of platinum drug via CTR1 and so a

reduction of intracellular drug accumulation and improved survival, resulting in drug resistance. Supporting this, cells lacking CTR1 are resistant to cisplatin, and CTR1 receptors are rapidly internalised into the cytoplasm upon exposure to the drug which subsequently limits further drug uptake (Ishida, Lee et al. 2002, Stewart 2007) (2.2.2.1). As already mentioned, at high concentrations, oxaliplatin enters cells primarily via a different mechanism to CTR1 (Holzer, Manorek et al. 2006), so this may not explain the case for oxaliplatin, but it suggests that an expected result in our screen would be for the MAC1 deletion strain to be resistant to cisplatin as well as carboplatin.

ZAP1 was a confirmed hit for oxaliplatin, and is a transcription factor that is a central player in controlling levels of zinc, which it does by increasing expression levels of zinc uptake genes in response to low levels of zinc (Table 7) (Zhao, Eide 1997) . This important because low levels of zinc lead to increased oxidative stress and DNA damage (Wu, Bird et al. 2007), which would cause a cell to be more susceptible to the DNA damaging effects of platinum drugs, as seen in our screen for the ZAP1 deletion mutant in the presence of oxaliplatin.

AFT1, MAC1 and ZAP1 (responsive to iron, copper and zinc respectively) all share many similarities, each responsible for upregulating the expression of their metal ion uptake system when environmental ion levels are low, each having DNA-binding domains, and all being able to constitutively express target genes due to having dominant alleles (Zhao, Eide 1997, Rutherford, Bird 2004). Figure 19 illustrates the protein products of these metalloregulated genes together. Note that ACE1 is also involved in copper homeostasis – it is a copper binding transcription factor that activates transcription of the metallothionein genes CUP1-1 and CUP1-2 in response to elevated copper concentrations, but was not included in our screen.

BDF1 was selected for further investigation (3.1.5.5); we wanted to explore whether the re-introduction of BDF1 into the *ΔBdf1* strain recovers viability in the presence of cisplatin, carboplatin and oxaliplatin to confirm these screening results, which we did (3.2.3.2). BDF1 was chosen because it was a strong hit for cisplatin and oxaliplatin with signs of sensitivity to carboplatin too, and it was the only confirmed hit with human homology - Bdf1 shares homology with human BET proteins (Florence, Faller 2001). Also, BDF1 has no data in the homozygous knockouts inhibited data sets for sensitivity to cisplatin, carboplatin and oxaliplatin from the Yeast Fitness Database (Yeast Fitness Database (2008). Hillenmeyer,Maureen E., Fung et al.), which we used as a comparison to our screening, making BDF1 an exclusive hit to us. We created four transformant strains; wild type *S. cerevisiae* strain CWG424 transformed with negative control plasmid PCG279, CWG424 transformed with BDF1 plasmid PCG596, *ΔBdf1* deletion strain transformed with negative control plasmid PCG279, and *ΔBdf1* deletion strain transformed with BDF1 plasmid PCG596. These strains were each grown with and without previously selected concentrations (3.2.3.1) of the three platinum drugs: 250 μM cisplatin, 12000 μM carboplatin and

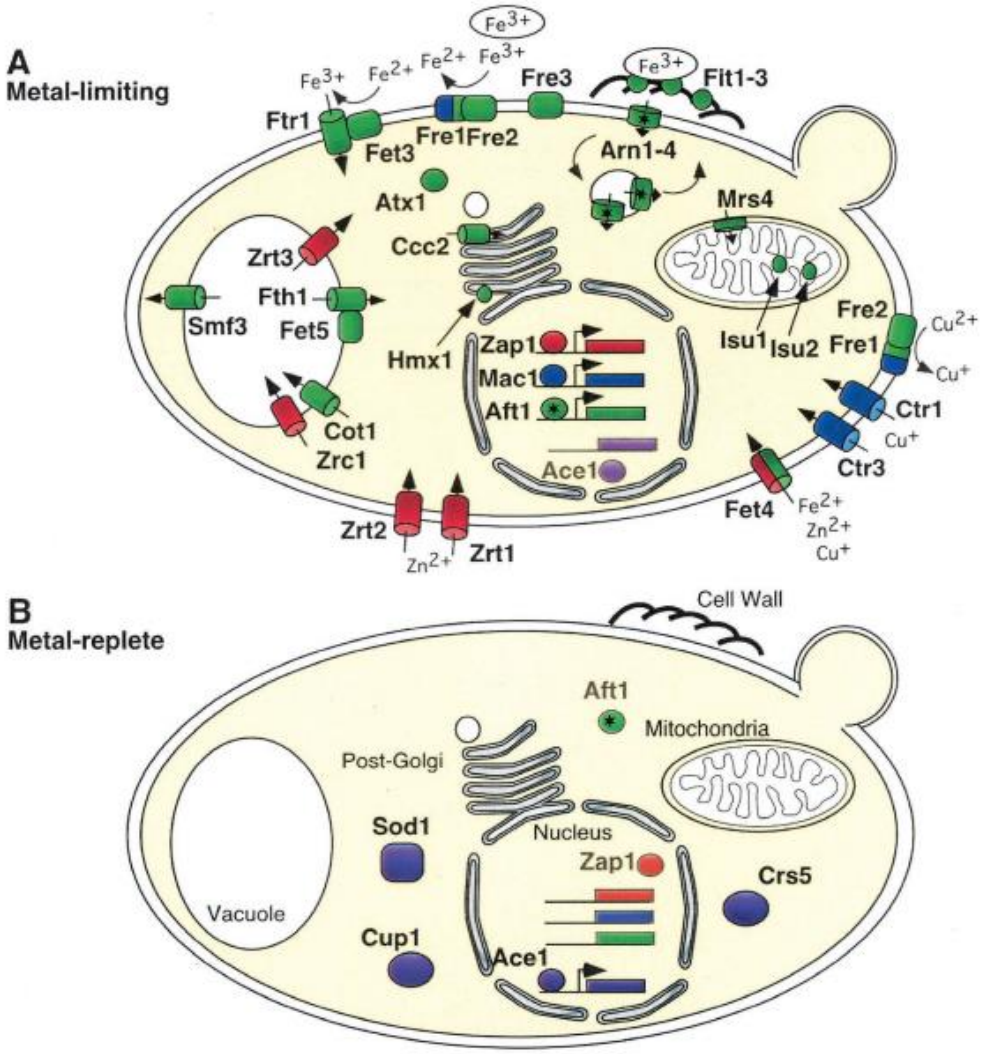

Figure 19. Protein products of metalloregulated genes involved in metal homeostasis in *S. cerevisiae*. Products of genes that are activated under metal-limiting conditions (A) and metal-replete conditions (B) by Aft1 (green), Mac1 (blue), Zap1 (red), and Ace1 (purple) are shown. Iron that is bound to siderophores has been circled, and stars indicate proteins that undergo iron-dependent cellular trafficking. The metal ion specificities of proteins required for metal uptake are indicated (Rutherford, Bird 2004).

2000 µM oxaliplatin (3.2.3.2), and the data generated proved, for the first time in yeast, that the absence of BDF1 is associated with increased sensitivity of *S. cerevisiae* to cisplatin, carboplatin and oxaliplatin, which confirmed our screening results.

The last to mention of our other conformation screen hits, SFP1, which nearly passed as a hit for for cisplatin, and was a hit for carboplatin and oxaliplatin, regulates transcription of ribosomal protein and biogenesis genes and the response to nutrients and stress, plays a role in the mitotic cell cycle, response to DNA damage and modulates cell size. It is interesting that it is also a putative regulator of BDF1, evidenced by microarray RNA expression levels (Table 7) (Cipollina, van den Brink et al. 2008). Regulators of BDF1 expression were pulled from the BDF1 regulation tab in the SGD (Saccharomyces Gene Database (SGD) (Stanford University, Stanford CA)), based

primarily on experiments showing that a regulator binds to the gene's promoter or affects the gene's transcription when the regulator is mutated. Other proposed regulators (with corresponding references evidencing their interaction with BDF1) are FKH1 (ForK head Homolog 1) and its paralog FKH2 (ForK head Homolog 2) (MacIsaac, Wang et al. 2006), LEU3 (LEUcine biosynthesis) (Venters, Wachi et al. 2011), RAP1 (Repressor/Activator site binding Protein) (MacIsaac, Wang et al. 2006) and SPT3 (SuPpressor of Ty's) (Venters, Wachi et al. 2011) which is a subunit of the SAGA and SAGA-like transcriptional regulatory complexes. RAP1 and SPT3 deletion strains were not included in our screen and LEU3 deletion strain was screened but was not a hit. Interestingly, FKH1, which plays a role in the cell cycle and chromatin silencing (Hollenhorst, Bose et al. 2000), did come up as a hit for cisplatin in the initial screening with a cut off of ≤50 % (Table 1), and the FKH2 deletion strain showed signs of cisplatin and oxaliplatin sensitivity but did not pass as a hit.

Together our findings show how important these conformation screen hit genes are for survival of yeast in the presence of platinum drugs, and supports these genes (and the systems that they regulate or are components of) as being potential drug resistance factors, and hence also as potential targets to treat platinum drug resistant cells, but additionally as targets for combination therapy to enhance platinum drug cytoxicity. The variety of processes that they are involved in also shows how complex the mode of platinum drug action is, and how it is also not solely focussed on DNA damage; this is mainly because the drugs bind to many other cellular components. It would be of value to investigate all of these genes further, starting with experiments introducing the genes back individually into the equivalent gene deletion strains using growth kinetics in liquid culture to further confirm the screening results, as we did for BDF1. It would subsequently be useful to test parallel treatment of cells with platinum drugs and inhibitors of these genes, if available, in an attempt to increase sensitivity to platinum drugs. The hits other than BDF1 have no direct human homology but the inhibition of equivalent mammalian systems could be explored further in our platinum drug resistant neuroblastoma cell lines in an attempt to recover resistance and to maybe identify biomarkers predictive of treatment outcome.

3.3.4 Bromodomain factor 1 (BDF1) and the Bromodomain and Extra-Terminal domain (BET) family

The BDF1 (BromoDomain factor) gene was originally discovered to encode a transcription factor, Bdf1, in a screen for genes that affect the synthesis of yeast snRNPs (LYGEROU, CONESA et al. 1994). Bdf1 contains two bromodomains and an extra-terminal domain and binds, via the bromodomains, to acetylated amino-terminal tails of histones, and is found in the nucleus throughout the cell cycle (LYGEROU, CONESA et al. 1994, CHUA, ROEDER 1995, Matangkasombut, Buratowski et al. 2000). Bdf1 is important for normal vegetative growth, but not essential for

viability (LYGEROU, CONESA et al. 1994, CHUA, ROEDER 1995). Our growth kinetics data has provided further evidence to show that BDF1 is not essential for viability in the growth kinetics experiments (3.2.3.2), where the *S. cerevisiae* strain *ΔBdf1* transformed with negative control plasmid PCG279 grew satisfactorily. However the growth rate was slightly lower than that of the wild type strain CWG424 transformed with negative control plasmid PCG279 (see Figure 15, Figure 16, Figure 17, and Figure 18), so there was a minimal effect on viability in the absence of BDF1, which is not unexpected considering the many transcriptional process in which Bdf1 is involved, including the expression of cell cycle genes (Dey, Chitsaz et al. 2003, Garcia-Gutierrez, Mundi et al. 2012). The *ΔBdf1* strain also grew satisfactorily on the control YPD agar plates compared to the wild type strain CWG424 in our preliminary plate based screening experiments (3.2.1 and 3.2.2, plate pictures no shown). The BDF1 gene has a paralogue, BDF2, and BDF2 mutants appear to be normal (Matangkasombut, Buratowski et al. 2000). If BDF1 or BDF2 is deleted there is no effect on viability, however a double deletion is lethal (Matangkasombut, Buratowski et al. 2000, Fu, Hou et al. 2013). In our initial screening, BDF2 showed signs of sensitivity to cisplatin, but none to carboplatin and oxaliplatin (data not shown). Together, BDF1 and BDF2 have been shown to interplay with each other, for example in the regulation of the yeast salt stress response (Fu, Hou et al. 2013).

Bdf1 is also necessary for meiosis and consequently sporulation, playing a role in chromatin structure (CHUA, ROEDER 1995, Ladurner, Inouye et al. 2003, Zhang, Roberts et al. 2005), and is required for DNA damage repair (CHUA, ROEDER 1995, Garabedian, Noguchi et al. 2012), hence represses sensitivity to DNA damaging agents (CHUA, ROEDER 1995, Garabedian, Noguchi et al. 2012). For the first time in yeast, we have demonstrated that BDF1 is required for viability of yeast cells in the presence of the DNA-damaging platinum drugs cisplatin, carboplatin and oxaliplatin (3.2.3.2) by reintroducing a BDF1 plasmid into a *ΔBdf1* deletion yeast strain. Our preliminary plate based screening of the yeast deletion library also validated the limited growth of the *ΔBdf1* strain in the presence of these platinum drugs in YPD agar (3.2.1.1 and 3.2.1.3). Cisplatin was the most potent of the drugs in terms of affecting viability of the *ΔBdf1* strain, followed by oxaliplatin and carboplatin. Sensitivity to these three platinum drugs is likely due to the *ΔBdf1* strain being weaker than wild type in terms of transcription, which can affect the ability to detect and repair DNA lesions (CHUA, ROEDER 1995, Garabedian, Noguchi et al. 2012). Alternatively, any irregular chromatin structure in the *ΔBdf1* strain could possibly limit access to damaged DNA by the DNA repair machinery (CHUA, ROEDER 1995). Another explanation could be that the mechanism of action of these drugs could be enhanced by a likely weaker and disrupted chromatin integrity in the BDF deletion strain; although the mechanism is not clear, cisplatin treatment, for example, besides initially inhibiting DNA synthesis, has been shown to reduce chromatin remodelling and thus transcription, which could contribute to its toxic effects (Mymryk, Zaniewski et al. 1995, Wu, Davey 2008). Interestingly, for oxaliplatin, we observed a slightly

different shape of yeast growth curve compared to those of cisplatin and carboplatin, which may be due to a mechanism of action that differs to the other two platinum drug - this may be due to the cells being less able to overcome damage induced by oxaliplatin than damage from cisplatin and carboplatin, or maybe oxaliplatin signals the cells to prematurely exit G0 of the cell cycle. As discussed, oxaliplatin differs from cisplatin and carboplatin in terms of structure, thus can form different types of DNA adducts (Wheate, Walker et al. 2010) – maybe this contributes to explaining this different response of the cells in terms of growth curves.

Both Bdf1 and Bdf2 are important transcriptional regulators that interact with components of the promoter binding initiation factor complexes TFIID (Transcription Factor IID) and SAGA (Spt-Ada-Gen5 Acety-Transferase); these complexes both have equivalent complexes in higher eukaryotes. The TFIID complex, comprising of a TATA-binding protein (TBP), encoded by the gene SPT15, (which binds to TATA elements) and 10-12 TBP-associated factors (TAFs) (whose role in transcription is poorly understood), is a key component of the RNA Pol II transcription machinery (Matangkasombut, Buratowski et al. 2000). Bdf1 interacts with Taf67p (also known as TAF7) in the context of the TFIID complex (TFIID has its own histone acetyltransferase activity (Mizzen, Yang et al. 1996, Dikstein, Ruppert et al. 1996)), and Bdf1 facilitates the recruitment of TFIID to promoters to TATA-containing promoters (via the TBP) or TATA-less promoters (via Sp1) located at acetylated nucleosomes, where the chromatin structure is less compact and more accessible (PUGH, TJIAN 1991, Matangkasombut, Buratowski et al. 2000, Huisinga, Pugh 2004). TBP is essential for transcription even at a TATA-less promoter (PUGH, TJIAN 1991, Basehoar, Zanton et al. 2004). The acidic carboxy-terminal region of Bdf1 has been shown to have associated kinase activity as observed for human $TAF_{II}250$ and BRD2 (RING3) (Denis, Green 1996, Dikstein, Ruppert et al. 1996), and both the structure and functions of Bdf1 suggest that it might correspond to the carboxy-terminal half of $TAF_{II}250$ (Matangkasombut, Buratowski et al. 2000). Bdf1 is also involved in the regulation of the SAGA (Spt-Ada-Gcn5 Acety-Transferase) complex in yeast, which is a significant transcriptional regulator, but is not essential for gene expression. SAGA functions in the stress-induced expression of ~10 % of the genome, the expression of the remaining 90 % involves the TFIID pathway (Matangkasombut, Buratowski et al. 2000, Huisinga, Pugh 2004, Basehoar, Zanton et al. 2004, Fu, Hou et al. 2013). SAGA, like TFIID, also has TBP binding and histone acetyltransferase activities (Grant, Duggan et al. 1997, Huisinga, Pugh 2004, Fu, Hou et al. 2013). Figure 20 illustrates the bipolar transcriptional regulation of stress- induced genes by SAGA (via TATA promoters) and housekeeping genes by TFIID (mainly via TATA-less promoters) (Huisinga, Pugh 2004, Lopez-Maury, Marguerat et al. 2008).

Bdf1 also forms part of the SWR1 chromatin remodelling complex, which directs Htz1 (H2A variant) deposition at the promoters of Pol II genes, removing H2A-H2B dimers and replacing them with Htz1-H2B dimers (Mizuguchi, Shen et al. 2004). Htz1 has an anti-silencing function that

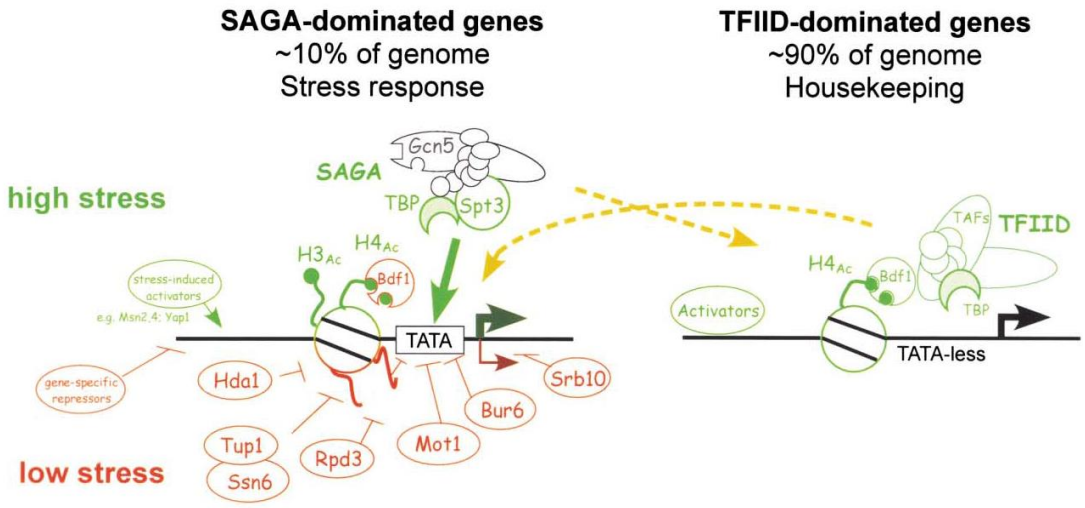

Figure 20. The bipolar transcriptional regulation of stress- induced genes by SAGA (via TATA promoters) and housekeeping genes by TFIID (mainly via TATA-less promoters). In budding yeast, stress-related genes tend to be extensively regulated, their control is dominated by the co-activator complex SAGA and their promoters often contain TATA boxes, whereas growth-related and housekeeping genes tend to have TATA-less promoters and their control is dominated by the co-activator complex TFIID. Factors depicted in red are negative regulators, whereas those in green are positive regulators. Stress-related genes tend to be positively regulated by the SAGA complex and by acetylation (Ac) of histones H3 and H4, and negatively regulated by histone de-acetylases (Hda1 and Rpd3), repressors and repressor complexes (Ssn6-Tup1 complex, Mot1, Bur6 and Bdf1), and a member of the mediator complex (Srb10). Growth-related genes, on the other hand, are positively regulated by histone H4 acetylation and Bdf1. The dashed arrows show that SAGA also contributes to the expression of genes targeted by TFIID, and vice versa. Gcn5, general control nonderepressible 5; TAF, TBP-associated factor; TBP, TATA-binding protein (Huisinga, Pugh 2004, Lopez-Maury, Marguerat et al. 2008).

can have effects on both transcriptional regulation and chromosome metabolism, and even genomic stability and DNA repair (Krogan, Keogh et al. 2003, Mizuguchi, Shen et al. 2004, Kobor, Venkatasubrahmanyam et al. 2004, Zhang, Roberts et al. 2005). It is suggested that Bdf1, via its bromodomains, assists recruitment of SWR1 to acetylated chromatin by binding acetylated H3 and H4 (Ladurner, Inouye et al. 2003, Zhang, Roberts et al. 2005), and also by physically interacting with promoter binding initiation factors TFIID and SAGA (Zhang, Roberts et al. 2005), thereby connecting chromatin remodelling together with transcription initiation (Zhang, Roberts et al. 2005, Albulescu, Sabet et al. 2012). Bdf1 may also be important in linking pre-mRNA splicing with chromatin remodelling with transcription initiation (Albulescu, Sabet et al. 2012). A schematic representation of the yeast SWR1 complex can be seen at the top right in Figure 21, which interestingly illustrates a model for the evolution of the yeast chromatin remodelling complexes SWR1 and also NuA4 HAT (responsible for histone H4 and H2A acetylation) to the human SRCAP (acetylation-independent exchange of H2A for H2AZ) and human NuA4/ Tip60 HAT (acetylation-linked exchange of H2A variants) complexes (Auger, Galarneau et al. 2008). Here it can be seen that in humans Brd8 is utilised as an equivalent to Bdf1, and the potential of Brd8 as a drug target is discussed later. It would be interesting to focus on screening the gene deletions of all the individual components of the SWR1, as well as SAGA and TFIID, complexes together in the

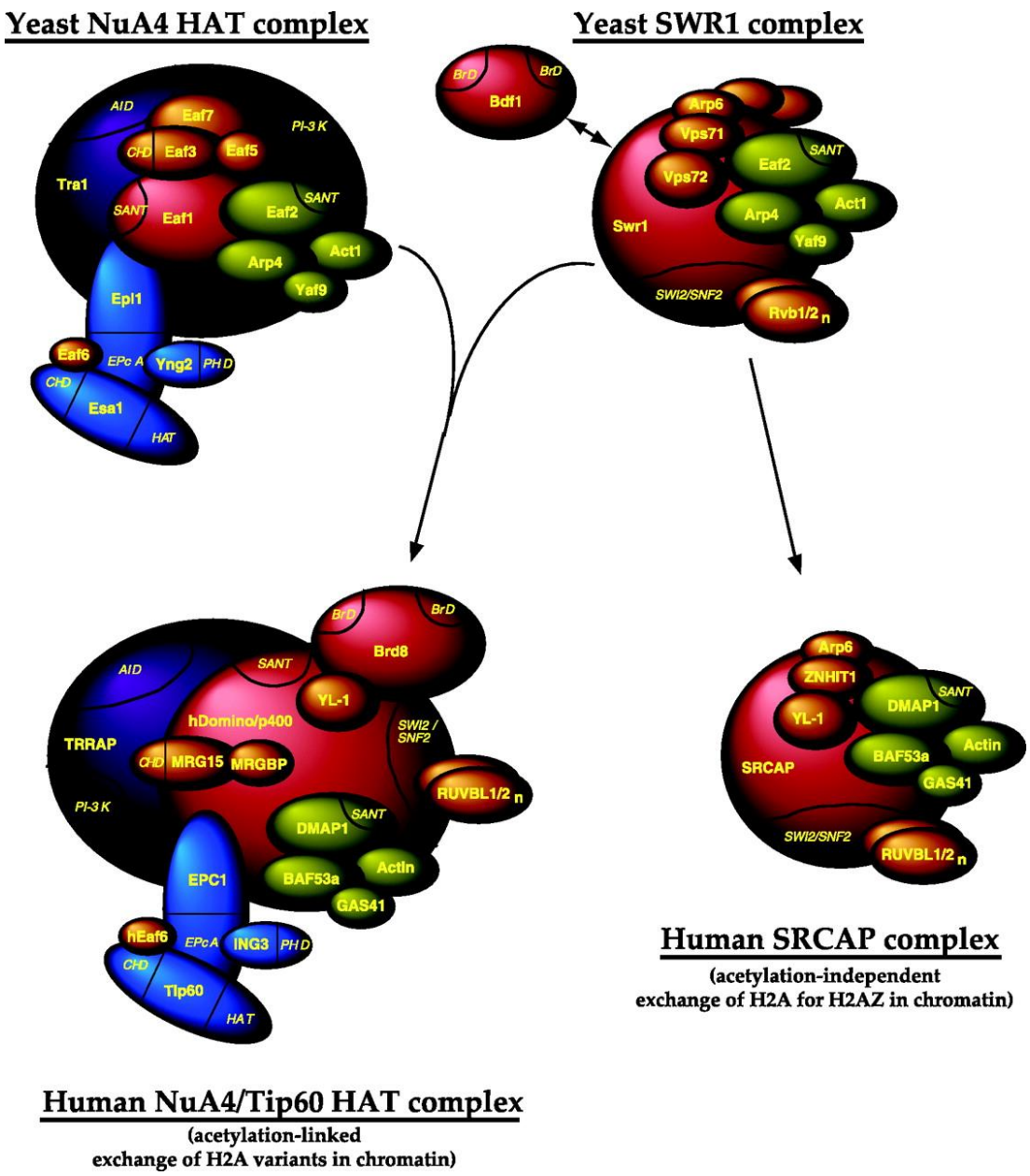

Figure 21. Model for the evolution of NuA4 HAT and SWR1 ATP-dependent remodeling complexes from yeast to human cells. The yeast NuA4 and SWR1 complexes are depicted. SWR1 could be present in two forms, with or without a bromodomain-containing Bdf1 subunit. These distinct complexes regulating histone H2AZ incorporation in chromatin would differentially reflect the link to NuA4-dependent chromatin acetylation. In human cells, SWR1 plus a Bdf1 equivalent is physically merged with NuA4 into the TIP60/hNuA4 complex (through the fusion of yeast Eaf1 and Swr1 platform proteins into human p400/Domino). The yeast SWR1 lacking Bdf1 corresponds to the human SRCAP complex, which should not be linked to chromatin acetylation (Auger, Galarneau et al. 2008).

presence of the platinum drugs to see if any others, besides BDF1, are important for survival in their presence.

It has been reported that Bdf1 also plays a role in mitochondrial retrograde signalling, a cellular quality control mechanism comprising a complex network of processes used to compensate for dysfunctional mitochondria. In yeast, damage to mitochondria induces an increase in the levels of

damaging reactive oxygen species (ROS) (which can act as signalling molecules) via the electron transport chain, which may be a route for eliminating those impaired cells. However, when the loss of respiratory function in mitochondria is due to a loss of cytochrome c oxidase (COX – this is encoded by mitochondrial DNA), cytosolic Ras protein is recruited to their outer membrane, which in turn induces ROS production via non-mitochondrial sources, prompting cell death signalling (Leadsham, Sanders et al. 2013) (this research was conducted in the Gourlay laboratory (Kent Fungal Group, UKC) where our yeast studies were performed). This recruitment of Ras to the mitochondria relies on Bdf1, but how Bdf1 does this is yet to be elucidated. When BDF1 is deleted in cells with no respiration (rho^0 zero stains), the accumulation of ROS is prevented; this is because Ras signalling can no longer occur without Bdf1, and there is also an increase in the expression of anti-oxidant defense genes (Leadsham, Sanders et al. 2013).

As previously mentioned, mitochondria and mitochondrial DNA have been shown to be targeted by cisplatin which can induce apoptosis, and this is partly responsible for the cytotoxicity of the drug (Gonzalez, Fuertes et al. 2001, Yang, Schumaker et al. 2006, Cullen, Yang et al. 2007). Mitochondrial DNA (mtDNA) has been shown to be more susceptible to damage and with the damage lasting longer than nuclear DNA (nDNA) (Yakes, VanHouten 1997), and this likely to be the case post-exposure of cells to the platinum drugs. The reason for this is mainly because the mitochondria lack their own DNA repair system, and mitochondrial DNA lacks protective histones and its lack of introns renders it susceptible to detrimental mutations (Preston, Abadi et al. 2001). Also in the Gourlay Laboratory (Kent Fungal Group, UKC), studies have been carried out (unpublished) which have demonstrated that cisplatin decreases respiratory activity in yeast but, intriguingly, this is not accompanied by an increase in ROS. In the same study, Gourlay et al have also shown that cisplatin initiates a PDR (pleiotropic drug resistance) mediated retrograde response as a cryoprotective mechanism (by assessing PDR5 expression), and partly an RTG (ReTrograde Regulation) (by assessing CIT2 expression); these are well defined retrograde pathways (Butow, Avadhani 2004). Intriguingly, in our initial screening using the higher ≤50 % cut off we hit PDR8 for cisplatin only, and PDR1 for oxaliplatin only, however PDR3 was not a hit, and surprisingly RTG1 or RTG3 were also not hits, which suggests that these pathways are not significantly important on an individual gene level for the resistance of yeast cells to cisplatin. It would be interesting to delete the genes of the PDR and RTG mediated responses together as gene groups and evaluate the resulting phenotype yeast cells on exposure to the platinum drugs to investigate platinum drug induced retrograde responses further; targeting such retrograde responses may enhance platinum drug cytotoxicity. Perhaps in the case of the BDF1 deletion strain in our studies, it is more the role of Bdf1 in DNA damage repair and chromatin remodelling than the Bdf1 mediated retrograde response that makes the cells more sensitive to the platinum drugs.

Bdf1, along with Bdf2, are members of the BET (Bromodomain and Extra-Terminal domain) family of transcriptional regulators that can be found in can be found in animals, plants and fungi (Matangkasombut, Buratowski et al. 2000, Florence, Faller 2001). These proteins all have sequence similarities concentrated in their bromodomain regions and C-terminal regions (designated the ET motif) (Florence, Faller 2001), and, unlike other bromodomain-containing proteins, they remain located on chromosomes during mitosis (CHUA, ROEDER 1995, Dey, Chitsaz et al. 2003, Kanno, Kanno et al. 2004, Garcia-Gutierrez, Mundi et al. 2012), due to the binding of the amino-terminal of acetylated histones (Matangkasombut, Buratowski et al. 2000, Dey, Chitsaz et al. 2003, Garcia-Gutierrez, Mundi et al. 2012). In humans, the BET family members include Brd2 (RING3), Brd3, Brd4 and Brdt (Brd6), which are the most studied, and also includes Brd7, Brd8, and Brd9; these proteins are widely expressed in all tissues except for Brdt, which is confined within the male germ line (Bunnage 2010, Garcia-Gutierrez, Mundi et al. 2012). Besides being involved in transcription via histone acetylation, BET proteins also strongly participate in the control of genes linked with the cell cycle (Dey, Chitsaz et al. 2003, Garcia-Gutierrez, Mundi et al. 2012), though specific functions are not well understood (Sanchez, Zhou 2009). Attempts to investigate their function, for example by using Brd2 and Brd4 knockout mice, have been confounded because these proteins are essential for early embryonic development (Garcia-Gutierrez, Mundi et al. 2012). BET proteins are implicated in oncogenesis, being overexpressed in certain cancers (Florence, Faller 2001), and can be cancer biomarkers, for example, BRD4 activation may predict the survival of patients with breast cancer because dysregulation of BRD4 associated pathways is believed to be involved in breast cancer progression (Crawford, Alsarraj et al. 2008, Sanchez, Zhou 2009). Considering all this, it is not surprising that they have recently been used as targets for cancer drugs in the form of BET inhibitors.

To date, BET inhibitors are termed as pan-BET inhibitors because these drugs target bromodomains rather than selectively targeting individual members of the BET family. Pan-BET inhibitors have been shown not just to have to have anti-cancer effects, but also others such as anti-inflammatory effects (Shi, Vakoc 2014) and they are very promising in the field of epigenetic drug treatments. However there is lack of understanding of the exact mechanism of action of BET inhibitors (Helin, Dhanak 2013). The first-published BET inhibitors were JQ1 and its use in NUT midline carcinoma, a cancer driven by translocations of Brd3 and Brd4 (Filippakopoulos, Qi et al. 2010, French 2014), and I-BET and its use in inflammation (the regulation of which is governed by Brd2, Brd3 and Brd4) and thus sepsis (Nicodeme, Jeffrey et al. 2010). These molecules have similar chemical structures and mechanism of action, which involves binding to the bromodomains of BET family members to compete out binding to acetylated histones, hence displacing them from chromatin (Shi, Vakoc 2014). This, in cancer, interrupts “reading” of abnormal histone acetylation, leading to the down-regulation of transcription of oncogenes, such as MYC (Khabele, Wilson et al. 2013, Helin, Dhanak 2013, Puissant, Frumm et al. 2013,

Filippakopoulos, Knapp 2014) and BCL2 (Helin, Dhanak 2013). Wyce et al have demonstrated this in both human neuroblastoma cell lines and mouse xenograft models of human neuroblastoma (which is associated with high frequency of MYCN amplifications) using the BET inhibitor I-BET726 (Wyce, Ganji et al. 2013).

The success of JQ1 and I-BET in models of cancer and inflammation respectively pushed the development of other highly related compounds called benzodiazepines and thienodiazapines, and pharmacological fragment screening has revealed molecules that are potential starting points for more novel BET inhibitor development. The search for more potent and selective BET inhibitors is ongoing and the consequence, in terms of side effects, explored in the clinic. Several of these drugs are currently being evaluated in phase I clinical trials (Mueller, Knapp 2014, Shi, Vakoc 2014). Besides reliably targeting individual BET family members, which to date has been unsuccessful (Filippakopoulos, Knapp 2014), it is also a focus to develop inhibitors that block one of the individual bromodomains, BD1 or BD2, to contribute to understanding of their specific functions in gene targeting and the treatment of disease; a BD1-specific chemical inhibitor, Olinone, has been shown to enhance oligodendrocyte differentiation (Chiang 2014).

There is a lack of biomarkers predictive of response or resistance to BET inhibitors (Helin, Dhanak 2013), though MYCN amplification has been suggested as a predictor of sensitivity (Puissant, Frumm et al. 2013). Anticipated resistance mechanisms of BET resistance have been more recently evaluated (Settleman 2016). Activation of the Wnt pathway, which is involved in proliferation and survival, has been associated with resistance to BET inhibitors, thus it could be useful to combine BET inhibitor therapy with Wnt-pathway inhibitors (Fong, Gilan et al. 2015, Rathert, Roth et al. 2015, Settleman 2016). For the first time, a recent study by Shu et al revealed that out of a panel of breast cancer cell lines, triple-negative breast cancers (TNBC) are preferentially sensitive to BET inhibition both *in vitro* and *in vivo* (Shu, Lin et al. 2016). Moreover, they created BET inhibitor (JQ1) resistant TNBCs and proteomics studies demonstrated JQ1 resistance to be linked to the transcription regulator protein MED1 and hyper-phosphorylation of BRD4 (due to decreased activity of a principle BRD4 serine phosphatase (PP2A) and increased activity of casein kinase 2 (CK2), which is helpful to anticipate clinical drug resistance to BET inhibitors. Thus it could be useful to combine BET and CK2 inhibitors to treat TNBCs and prevent drug resistance (Shu, Lin et al. 2016, Settleman 2016).

Our yeast BDF1 data contribute as supporting evidence for the Bdf1 related proteins of the human BET family as being possible targets to enhance sensitivity of cancer cells to the platinum drugs, or possibly to reverse platinum drug resistance, though studies to date regarding this are very limited. Considering existing BET inhibitors, pre-clinical studies for JQ1 have shown encouraging results in MYC-dependent cancers, but compatibility with platinum drug therapy has not been established (Wiedemeyer, Beach et al. 2014). Regarding reversal of resistance, one

study revealed that JQ1 could be a potentially effective drug for sensitising ovarian cancer cells to cisplatin therapy when resistance occurs (Khabele, Wilson et al. 2013).

Regarding Bdf1 in the yeast SWR1 complex, already discussed, it is interesting that Bdf1 shares functional homology with human Brd8, as previously illustrated in Figure 21 (Auger, Galarneau et al. 2008). Brd8 is an accessory subunit to human NuA4/Tip60 HAT complex, of which MRGBP (MRG-binding protein) is a subunit, and BRD8 is a downstream target for MRGBP. Short hairpin RNA suppression of expression of Brd8 inhibited proliferation of colorectal cancer cells, and the result was the same on suppressing MRGBP in the same way, suggesting MRGBP, and maybe Brd8 itself, should be possible future therapeutic targets for colorectal cancer (Yamaguchi, Sakai et al. 2010). Elevated levels of Brd8 in human metastatic colorectal cancer cells and a role of Brd8 in tumour progression have been shown (Yamada, Rao 2009) and this further evidences Brd8 as a future cancer drug target. Also, Brd8-knockdown cells are more sensitive to microtubule drugs, so a BRD8 inhibitor could be used alongside such drugs for a more effective therapy (Yamada, Rao 2009, Bunnage 2010). Based on this and our Bdf1 data, it may be useful to evaluate specifically targeting this Bdf1 human homologue, Brd8, to sensitise cancer cells to oxaliplatin.

It could be useful to test the use of BET inhibitors in combination with the platinum drugs using wild type yeast cells and our parental neuroblastoma cells to discover if BET inhibitors can be used in combination with the platinum drugs to enhance platinum cytotoxicity. Additionally, it may be of value to test BET inhibitors in combination with our platinum drug resistant neuroblastoma cell lines to evaluate their ability to reverse platinum drug resistance. Also, there is limited knowledge surrounding their mechanism of action, so it would be interesting to test BET inhibitors in the same way as our platinum drugs in our yeast screening system, and also study the acute affects by performing proteomics studies with our parental neuroblastoma cell lines, as we have with cisplatin.

4 Neuroblastoma cell lines

4.1 Materials and Methods – neuroblastoma cell lines

4.1.1 Platinum drugs

All stocks, described below, of platinum drugs were stored at room temperature in the dark/wrapped in foil.

Cisplatin 1 mg/mL solution used was prepared manually by diluting solid cisplatin (Sigma, Poole, Dorset, UK, Ref P4394) in 0.9 % sodium chloride. The 0.9 % sodium chloride solution (Fisons, Ipswich, Suffolk, UK, now part of Rhone-Poulenc, Inc., Ref S/3160/60) was prepared by dissolving 9 g sodium chloride with MQ H_20 up to 1000 mL and filter-sterilised (0.2 micron). Cisplatin was left to dissolve stirring on a magnetic stirrer (Bibby B212, Bibby Scientific Ltd, Stone, Staffordshire, UK) in the dark at room temperature for 5 days, after which it was adjusted to the final volume with diluent, filter-sterilised (0.2micron), and aliquoted into sterile tubes. All filtering was carried out in a Class II biological safety cabinet (Cellgard Energy Saver (ES) Model NU 480-400E, Nuaire, Plymouth, UK) because this cisplatin was also to be used in mammalian cell culture.

Carboplatin 10 mg/mL Concentrate for Solution for Infusion from Sun Pharmaceutical Industries (Leeds, Yorkshire, UK) and purchased from by Shakespeare Pharma Ltd. (Hilton, Derbyshire, UK), the diluent being water for injections, with a pH between 4 and 7. Oxaliplatin 5 mg/mL Concentrate for Solution for Infusion was purchased from TEVA (Castleford, West Yorkshire, UK) and sourced by Shakespeare Pharma Ltd. (Hilton, Derbyshire, UK). This solution contains 4.5 % lactose monohydrate. 1mg/mL aliquots were prepared for both drugs using filter-sterilised (0.2 micron) 5 % (w/v) glucose (D-glucose, Fisons, Ipswich, Suffolk, UK, now part of Rhone-Poulenc, Inc., Ref G/0500/61) solution and stored at -20 °C in the dark.

4.1.2 Tissue culture

4.1.2.1 Neuroblastoma cell lines

The human neuroblastoma cell lines UKF-NB-3 and UKF-NB-6 were established from bone marrow metastases of INSS stage 4 neuroblastoma patients (Kotchetkov, Driever et al. 2005) and are MYCN-amplified. The drug-resistant lines were derived from the RCCL (Resistance Cancer Cell Line) collection (2.3.1.2) (Cinatl, Michaelis et al.). UKF-NB-3 and UKF-NB-6 cells had been adapted

to cisplatin, carboplatin and oxaliplatin by continuous exposure to increasing drug concentrations, as described previously (Kotchetkov, Cinatl et al. 2003, Kotchetkov, Driever et al. 2005, Michaelis, Rothweiler et al. 2011, Michaelis, Agha et al. 2015). The resulting cisplatin-resistant cell lines were designated as UKF-NB-3^{r}CDDP^{1000} and UKF-NB-6^{r}CDDP^{2000}, the carboplatin-resistant cell lines as UKF-NB-3^{r}CARBO^{2000} and UKF-NB-6^{r}CARBO^{2000}, and the oxaliplatin-resistant cell lines UKF-NB-3^{r}OXALI^{2000} and UKF-NB-6^{r}OXALI^{4000}. The numbers in superscript indicate the drug concentrations that the resistant cells were continuously cultured with in ng/mL.

4.1.2.2 Media, reagents, continuous culture and passaging cells

The cell lines were cultured in Iscove's Modified Dulbecco's Medium (IMDM) (Gibco, as part of Thermo Fisher Scientific, Loughborough, Leicestershire, UK, Ref 21980065) supplemented with 10 % Foetal Bovine Serum (FBS) (Sigma, Poole, Dorset, UK, Ref F7524) and 100 U/mL penicillin/100 µg/mL streptomycin (Gibco, part of Thermo Fisher Scientific, Loughborough, Leicestershire, UK, Ref 15140) to make complete IMDM medium. The medium of the drug-resistant cell lines was also supplemented with the indicated drug concentrations (see 4.1.2.1) using the 1 mg/mL stocks prepared as described in 4.1.1; drug was added to media when passaging cells. Cells were routinely grown in 10 mL of their media in a T25 cm^2 culture flasks (Sarstedt AG & Co, Sarstedtstraße 1, 51588 Nümbrecht, Germany, Ref 1116035) in a 37°C/5 % CO_2 incubator. For passaging or experiments, cells were washed with Phosphate Buffered Saline (PBS) (Dulbecco A, with no Ca^{2+} or Mg^{2+}) (Oxoid, Fisher Scientific (part of Thermo Fisher Scientific), Loughborough, Leicestershire, UK, Ref BR0014G) and removed from the surface of cell culture flasks using 0.5 mL of 0.05 % Trypsin/EDTA (Gibco, as part of Thermo Fisher Scientific, Loughborough, Leicestershire, UK, Ref 25300) for approximately 2 minutes in a 37°C/5 % CO_2 incubator (Panasonic Biomedical, Loughborough, Leicestershire, UK, IncU Safe models MCO-20AIC and MCO-15AC) until all cells were detached, then medium was added up to the original medium volume to stop the enzymatic reaction. Cells were passaged once a week, when the cells had reached 80-100 % confluency and typical splitting ratios for weekly passaging are presented in Table 8.

Cell line	Passage ratio
UKF-NB-3 parentals	1 in 40
UKF-NB-3^{r}CDDP^{1000}	1 in 40
UKF-NB-3^{r}CARBO^{2000}	1 in 25
UKF-NB-3^{r}OXALI^{2000}	1 in 20
UKF-NB-6 parentals	1 in 20
UKF-NB-6^{r}CDDP^{2000}	1 in 20
UKF-NB-6^{r}CARBO^{2000}	1 in 25
UKF-NB-6^{r}OXALI^{4000}	1 in 30

Table 8. Neuroblastoma cell lines: typical splitting ratios for weekly passaging.

Separate media, PBS and 0.05 % Trypsin/EDTA were always used for each cell line and warmed to 37 °C in a waterbath (Grant JB series, Grant Instruments, Shepreth, Cambridge, UK) when used for the cells. The cell lines were always handled one at a time in a Class II biological safety flow cabinet (Cellgard Energy Saver (ES) Model NU 480-400E, Nuaire, Plymouth, UK).

4.1.2.3 Cryopreservation of cells

To expand enough cells for cryopreservation, cells were seeded into larger T75 cm^2 flasks per cell line which take 30 mL medium per flask. On reaching 70-80 % confluency 3 flasks of cells were washed with PBS, the cells detached using 1 mL 0.05 % Trypsin/EDTA, and then the cells from all 3 flasks were combined and resuspended in 10 mL complete IMDM (see 4.1.2.2 for reagent sources). After centrifugation for 5 minutes at 1000 rpm in an Eppendorf 5702 benchtop centrifuge (Eppendorf, Stevenage, Hertfordshire, UK) and removal of the supernatants, cells were resuspended in 6mL of cryoprotectant medium (IMDM supplemented with 10 % DMSO (Sigma, Poole, Dorset, UK, Ref P4394), 20 % FBS and 100 U/mL penicillin/100 µg/mL streptomycin), and 1 mL aliquots transferred into 1.8 mL cryotube vials (Nunc, as part of Thermo Fisher Scientific, Loughborough, Leicestershire, UK, Ref 368632). Note that all reagents were pre-warmed to 37 °C in a waterbath (Grant JB series, Grant Instruments, Shepreth, Cambridge, UK). Cryotube vials were sealed into cryoflex tubing (Nunc, as part of Thermo Fisher Scientific, Loughborough, Leicestershire, UK, Ref 343958) and then transferred to a Cryo 1 °C Freezing Container (Nalgene , as part of Thermo Fisher Scientific, Loughborough, Leicestershire, UK, Ref 5100-0001) at -80 °C overnight. The following day, the vials were transferred to liquid nitrogen containers for long term storage. For the drug-resistant sub-lines, if they were newly resuscitated, the required drug was introduced at the first passage and grown for a total of at least three passages with drug before cryopreservation.

4.1.2.4 Resuscitation of cells cryopreserved in liquid nitrogen

Frozen cells in a cryovial tube were thawed at 37 °C in a water bath and then immediately slowly transferred to 10 mL 37 °C complete IMDM medium and centrifuged at 1000 rpm for 5 mins in an Eppendorf 5702 benchtop centrifuge (Eppendorf, Stevenage, Hertfordshire, UK). The supernatant was removed and the cells were resuspended in 10 mL 37 °C complete IMDM medium and transferred into a T25 cm^2 flask and then into a 37 °C/5 % CO_2 incubator (Panasonic Biomedical, Loughborough, Leicestershire, UK, IncU Safe models MCO-20AIC and MCO-15AC). For the drug-resistant sub-lines the required drug was not introduced until the first passage, and they were cultured for at least 3 passages before using in experiments. See 4.1.2.2 for reagent sources.

4.1.2.5 Counting cells

To determine cell numbers, a sample of cells in suspension was diluted 1 in 2 with 0.4 % Trypan blue solution (Sigma, Poole, Dorset, UK, Ref 93595), and counted using a haemocytometer. The haemocytometer was viewed using an Olympus IM microscope, focussing on the gridlines. Unstained viable cells were counted, in each of the outer four quadrants (one quadrant is outlined in blue in Figure 22) of 16 squares. Regarding cells sat on boundary lines, only those on the right hand side boundary lines were included.

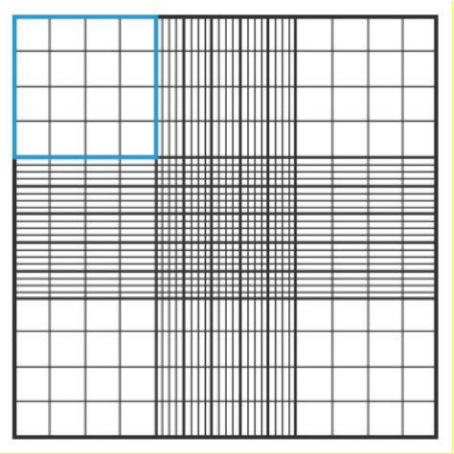

Figure 22. The gridlines of a haemocytometer.

To calculate the average number of viable cells/mL, the count from each of the four quadrants was averaged, multiplied by 10^4 and then multiplied by 2 to correct for the 1 in 2 dilution from the addition of Trypan Blue. If there were too many cells to accurately count the dilution was increased by diluting the cells with PBS first before diluting 1 in 2 with Trypan Blue, and then the final multiplication factor was changed accordingly. To determine the fraction of viable cells, the number of unstained cells was calculated relative to the total number of cells and expressed as a percentage.

4.1.3 Production of images of the neuroblastoma cell lines

Cells images were taken using a Zeiss IM 35 phase contrast light microscope (Carl Zeiss Microscopy GmbH, Kenam Germany) at a magnification of x 200. A Nikon D70 camera (Nikon UK Ltd, Kinsgton Upon Thames, Surrey, UK) was fitted to the microscope to take images using an exposure time of 1 second, resulting in 300 dpi resolution colour images.

4.1.4 Determination of cell growth kinetics

4.1.4.1 The Roche xCELLigence Real Time Cell Analyzer (RTCA)

Cell growth kinetics and doubling times were determined using the Roche xCELLigence system according to the manufacturer's instruction. The system comprises of an electronic sensor analyser and a device station with positions for three 16-well plates (called E-plates). The bottoms of the wells of E-plates are covered by gold microelectrodes which communicate impedance readings of the electrical circuit to the sensor analyser. The interaction of adherent mammalian cells with the microelectrodes generates a cell-substrate-impedance response that is proportional to the number of cells seeded into the wells, the cell viability, the morphology of the cells and the quality of the cell attachment. The electrode impedance is displayed as cell index (CI), which is a dimensionless parameter that represents a relative change in measure of electrical impedance to represent cell status (Acea Biosciences Inc.(San Diego, CA) , Witzel, Fritsche-Guenther et al. 2015) (www.bionity.com). Figure 23 illustrates the principles of impedance using E-plates.

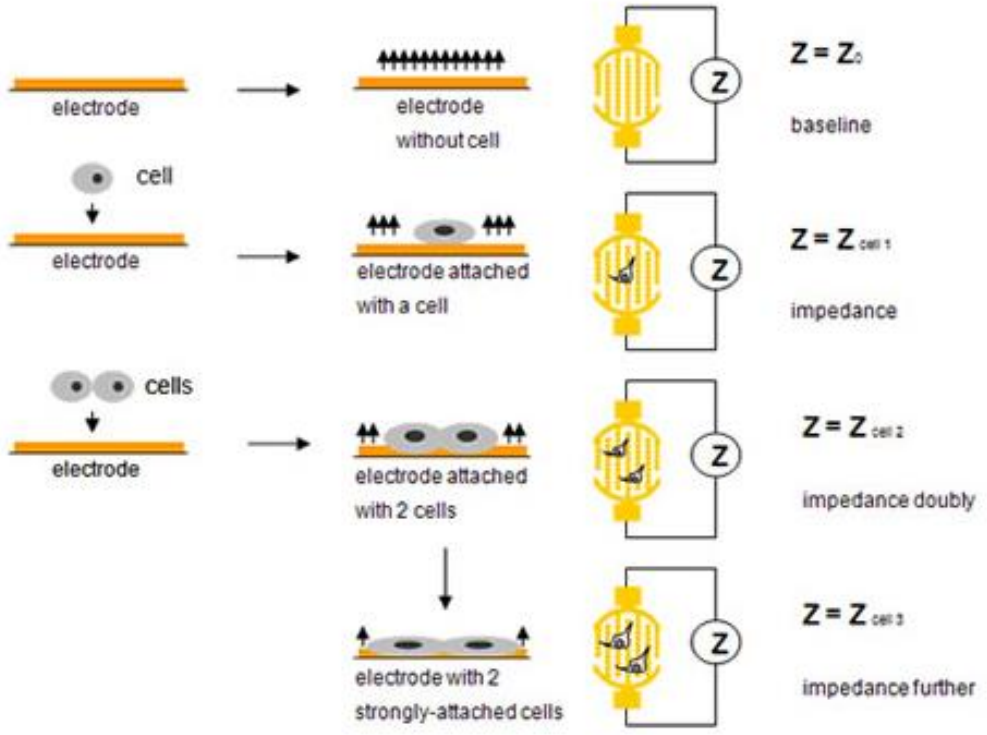

Figure 23. Schematic drawing of the interdigitated microelectrodes on the bottom of each well of the E-plates. The interaction of adherent mammalian cells with the microelectrodes generates a cell-substrate-impedance response that is proportional to the number of cells seeded into the wells, the morphology of the cells and the quality of the cell attachment. The signal generated is displayed by the arbitrary unit of cell index (CI). Z = impedence. (www.aceabio.com and www.bionity.com).

4.1.4.2 Generation of growth curves using the Roche xCELLigence Real Time Cell Analyzer (RTCA)

The Roche xCELLigence Real Time Cell Analyzer (RTCA) system (Roche Diagnostics Ltd., Burgess Hill, UK) was set up inside a 37 °C/5 % CO_2 incubator (Panasonic Biomedical, Loughborough, Leicestershire, UK, IncU Safe models MCO-20AIC and MCO-15AC). Impedance measurements (sweeps) were taken every 30 mins for 315 to 459 hours (13 to 19 days in total, so that death curves were also captured). Initially 100 µL 37 °C complete IMDM medium (4.1.2.2) was added to each of the 16 wells (two columns A and B of eight wells 1-8) of an xCELLigence E-Plate VIEW 16 Roche Diagnostics Ltd., (Burgess Hill, UK, Ref. 06324738001) and left for 30 mins inside a 37 °C/5 % CO_2 incubator to equilibrate before doing a scan of the E-plate on the xCELLigence RTCA system; this enables the software to measure the base-line impedance. A total of 3000 cells suspended in 100 µL complete IMDM medium were added to the 100 µL/well complete IMDM medium already used for calibration in each well (cells were counted as described in 4.1.2.5), and to blank wells complete IMDM medium only was added instead of cell suspension. All the surrounding gaps on the E-plate were then filled with 37 °C PBS to help to prevent evaporation of the media throughout the course of the growth curve. The prepared E-plate was not re-positioned onto the xCELLigence system until at least 30 minutes after adding the last cells to allow the cells to settle down onto the electrode, then the generation of growth curves was started.

In total, three biological repeats of duplicate growth curves were generated for each of the UKF-NB-3 and UKF-NB-6 parental cell lines and their corresponding platinum drug resistant cell lines (see 4.1.2.1 for cell line details). The resistant sub-lines were grown both in the presence and absence of their indicated drug concentrations (see 4.1.2.1).

4.1.4.3 Growth curve data analysis

Using the RTCA software, growth curves were plotted and the exponential parts of the growth curve (which were linear on the logging the y axis) were used to determine the doubling times. Each set of cell lines were run on three separate occasions, as described in 4.1.4.2., and the mean doubling times were calculated for each cell line and plotted as bar charts.

4.1.5 MTT cell viability assay

4.1.5.1 The MTT assay principle

This is a colourimetric test based on the reduction of yellow 3-(4,5-dimethylthiazol-2-yl)-2,5-diphenyltetrazolium bromide (MTT) to purple formazan (E,Z)-5-(4, 5-dimethylthiazol-2-yl)-1,3-diphenylformazan) by mitochondrial dehydrogenases (Figure 24). The protocol we used is an adaption from that of Mosmann (MOSMANN 1983), which has been regularly used for the determination of the viability when working with neuroblastoma cells (Michaelis, Fichtner et al.

2006, Michaelis, Cinatl et al. 2007, Michaelis, Bliss et al. 2008, Michaelis, Kleinschmidt et al. 2009, Michaelis, Rothweiler et al. 2009, Michaelis, Rothweiler et al. 2011, Fichtner, Cinatl et al. 2012, Michaelis, Hinsch et al. 2012, Loeschmann, Michaelis et al. 2013, Michaelis, Selt et al. 2014, Michaelis, Agha et al. 2015, Michaelis, Rothweiler et al. 2015).

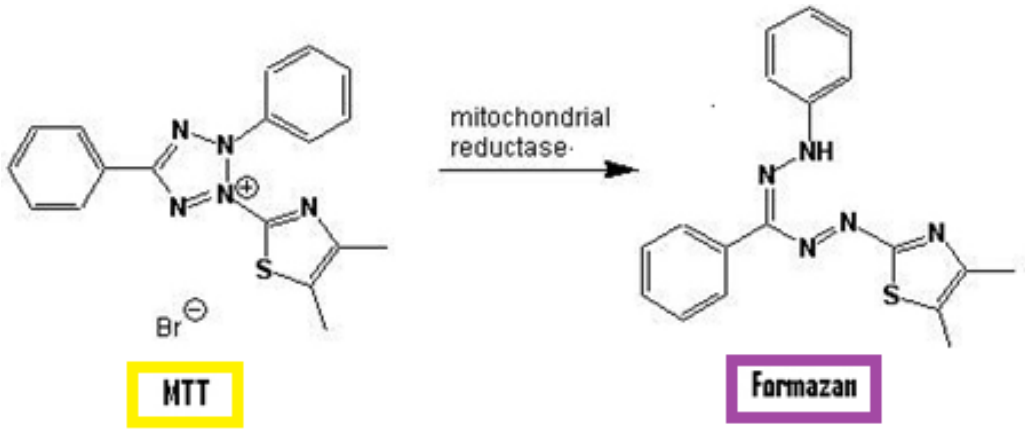

Figure 24. Conversion of yellow MTT to purple formazan by active mitochondrial dehydrogenases (www.biotek.com).

4.1.5.2 Performing the MTT assay

The MTT assay was always carried out in a Class II biological safety flow cabinet (Cellgard Energy Saver (ES) Model NU 480-400E, Nuaire, Plymouth, UK) with the light switched off when handling the platinum drugs. 0.4 g MTT (Serva Electropheresis GmbH, Heidelberg, Germany, Ref 20395.02) was dissolved with PBS up to 200 mL (Dulbecco A, with no Ca^{2+} or Mg^{2+}) (Oxoid, Fisher Scientific (part of Thermo Fisher Scientific), Loughborough, Leicestershire, UK, Ref BR0014G), then filter-sterilised (0.2 micron) and stored at 4 °C wrapped in foil.

Drugs were tested for their effects on cell viability using 8-point serial dilutions in 96-well plates (Greiner Bio-One Cellstar 96-well plates, Greiner BioOne Ltd, Stonehouse, UK, Ref 655 180) (refer to Figure 25C) using 3000 cells/well. One cell line was used per assay plate using cells harvested at 70 to 100 % confluency (4.1.2.2). Plates were set up by first adding complete IMDM medium (4.1.2.2) as in Figure 25A, and then cells were prepared at 2 x final assay concentration in complete IMDM medium and added as in Figure 25B. Finally, drug serial dilutions were prepared at 2 x final assay concentration in complete IMDM medium and added as in Figure 25C.

After 120 hours incubation in a 37 °C/5 % CO_2 incubator (Panasonic Biomedical, Loughborough, Leicestershire, UK , IncU Safe models MCO-20AIC and MCO-15AC), 25 µL MTT reagent was added per well and plates were incubated for a further 4 hours in a 37 °C/5 % CO_2 incubator. Then 100

µL of a 20 % (w/v) sodium dodecyl sulphate (SDS) (Fisher Scientific (part of Thermo Fisher Scientific), Loughborough, Leicestershire, UK, Ref S/P530/53) solution in 1:1 MQ H_20:DMF (Dimethylformamide (DMF) – Fisher Scientific: D/3840/17) adjusted to pH 4.7 was added per well to lyse cells and dissolve the precipitated formazan overnight in a 37 °C/5 % CO_2 incubator. The plates were then read in a BMG Labtech FLuostar Omega plate reader at an absorbance of 600 nm.

A. Addition of complete IMDM medium

	1	2	3	4	5	6	7	8	9	10	11	12
A	50	50	50	50	50	50	50	50	50	50	50	50
B	50	100									50	50
C	50	100									50	50
D	50	100									50	50
E	50	50									100	50
F	50	50									100	50
G	50	50									100	50
H	50	50	50	50	50	50	50	50	50	50	50	50

B. Addition of cells

	1	2	3	4	5	6	7	8	9	10	11	12
A	50	50	50	50	50	50	50	50	50	50	50	50
B	50		50	50	50	50	50	50	50	50	50	50
C	50		50	50	50	50	50	50	50	50	50	50
D	50		50	50	50	50	50	50	50	50	50	50
E	50	50	50	50	50	50	50	50	50	50		50
F	50	50	50	50	50	50	50	50	50	50		50
G	50	50	50	50	50	50	50	50	50	50		50
H	50	50	50	50	50	50	50	50	50	50	50	50

C.Addition of 8-point serial drug dilutions

	1	2	3	4	5	6	7	8	9	10	11	12
A												
B			1	2	3	4	5	6	7	8		
C			1	2	3	4	5	6	7	8		
D			1	2	3	4	5	6	7	8		
E			1	2	3	4	5	6	7	8		
F			1	2	3	4	5	6	7	8		
G			1	2	3	4	5	6	7	8		
H												

Figure 25. MTT assay plate set-up. Wells B2, C2, D2 and E11, F11, G11 (red boxed) = minimum signal (medium only), and wells E2, F2, G2 and B11, C11, D11 (blue boxed) = maximum signal (cells, no drug). A. Addition of medium only to orange wells only - numbers are µL/well added. B. Addition of cell suspension to yellow wells only- numbers are µL/well added. C. Addition of triplicate 8 point drug dilution series to coloured wells only, 50 µL/well – green and purple represent two different drugs.

The higher the absorbance value, the more converted formazan was present and so the higher the number of viable, proliferating cells.

4.1.5.3 MTT assay data analysis

The background absorbance derived from medium only (minimum) wells was subtracted from the absorbance of cell containing wells. Then the viability of drug-treated cells was calculated relative to non-treated cells in percent. From these data the IC_{50} values were determined using Calcusyn (Version 1.1, Biosoft 1996).

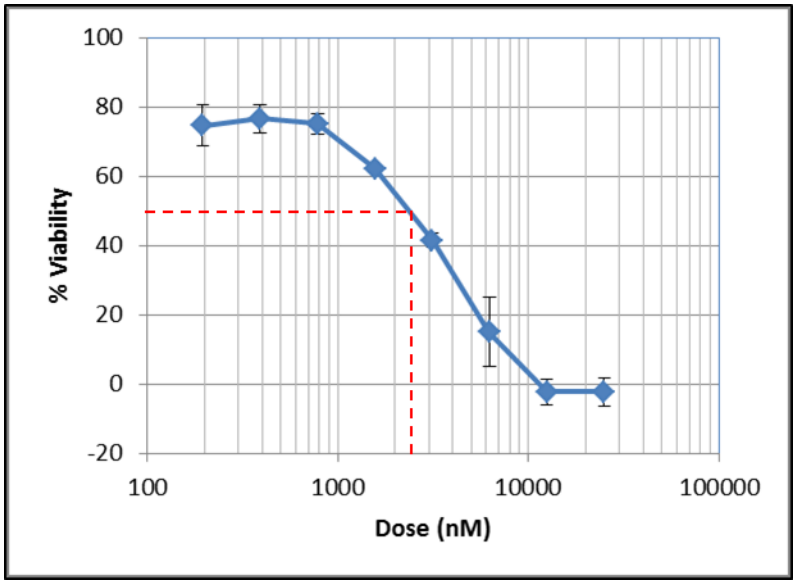

Figure 26. An example of a dose-response curve. Here the UKF-NB-3 parental cell line is challenged with carboplatin, resulting in an IC_{50} value of 2358nM (red dashed line). Data points represent the mean of 3 biological repeat, with bars representing standard deviation.

4.1.6 Generation of drug sensitivity profiles and investigating the effect of culturing drug resistant cell lines without drug

4.1.6.1 Culturing drug resistant cell lines with and without drug and generation of IC_{50} values

The UKF-NB-3 and UKF-NB-6 platinum drug resistant sub-lines (UKF-NB-3^{r}CDDP^{1000}, UKF-NB-3^{r}CARBO^{2000}, UKF-NB-3^{r}OXALI^{2000}, UKF-NB-6^{r}CDDP^{2000}, UKF-NB-6^{r}CARBO^{2000}, and UKF-NB-6^{r}OXALI^{4000}) were cultured both with and without drug for three months. The UKF-NB-3 and UKF-NB-6 chemosensitive parental cell lines were also cultivated alongside them. Refer to sections 4.1.2.1 and 4.1.2.2 for details of the cell lines and how to culture them. All cell lines were resuscitated as described in section 4.1.2.4, and the resistant sub-lines were split into two sets of flasks at the first passage; into one set drug was introduced to the continuous culture, and for the second set drug was not, and both sets were cultured from then on in parallel.

One month later the first MTT assay (4.1.5) was performed, for which each cell line was tested with each of cisplatin, carboplatin and oxaliplatin (4.1.1) to generate (IC_{50}) values, and this was carried out again one month later, and one month after that to give three datasets. Two further datasets of IC_{50} values were generated using the exactly the same parental cell lines and corresponding resistant sub-lines cultured with drug only.

4.1.6.2 Data analysis

The total of five datasets of IC_{50} values generated from the parental lines and the resistant sub-lines cultivated with drug only were used to construct drug sensitivity profiles for each cell line with each drug. Mean IC_{50} values were plotted for each cell line with each drug. Additionally, for the drug resistant sub-lines, the IC_{50}s were expressed as a fold difference over the corresponding drug IC_{50} of the parental cell line, by dividing the former by the latter, and the mean of these were also plotted. Fold differences of ≥2.0 were regarded as resistant. Data for UKF-NB-3 and UKF-NB-6 cell lines were plotted separately as bar charts. Using Minitab 17 statistical software, one-way ANOVA with a post hoc Tukey analysis was performed to compare each combination of cell line, drug tested and IC_{50} response to one another. This was to identify which mean IC_{50} value (for each cell line and drug combination) fell into a statistically different group compared to the others in terms of individual 95 % CIs for mean based on pooled STDEV: means that did not share a letter were significantly different ($p < 0.05$). Each group was labelled alphabetically on the chart bars. To determine whether a resistant subline retained drug resistance in the absence of drug in continuous culture we plotted, for each drug, the first three datasets of IC_{50} values generated from the parental lines and the resistant sub-lines cultivated in parallel with and without drug for three months (see 4.1.6.1). For each time point, we plotted the IC_{50} values for the cell lines cultured without drug expressed as a fold difference over the corresponding IC_{50} values for the same cell lines that were cultured with drug, by dividing the former by the latter. Data for UKF-NB-3 and UKF-NB-6 cell lines were plotted separately.

4.1.7 Proteomics

For proteomics studies, we investigated the acute and adaption effects of the platinum drug cisplatin on the neuroblastoma proteome using the UKF-NB-3 parental and UKF-NB-3rCDDP^{1000} cell lines and also the UKF-NB-6 parental and UKF-NB-6rCDDP^{2000} cell lines (see 4.1.2.1 for cell lines and 4.1.7.1 for the proteomics study set up). Cells were harvested and lysed (4.1.7.2), lysate protein content was measured (4.1.7.3), and proteins were separated on gels by 2D-gel electrophoresis (4.1.7.4). Differences in protein levels were identified using the Progenesis Samespots Software (4.1.7.5). Protein spots that significantly differed between cell lines or treatment were extracted from the gels and tryptically digested (4.1.7.6), and identified using matrix-assisted laser desorption /ionisation time of flight (MALDI-TOF and MALDI-TOF-TOF) and

tandem mass spectrometry (MS and MS/MS respectively) followed by data analysis using the human protein databases SwissProt (http://www.uniprot.org/) and (NCBInr http://www.ncbi.nlm.nih.gov/refseq/) (4.1.7.7).

4.1.7.1 Proteomics study plan and set up of cells for studies

To investigate the acute and adaption effects of cisplatin on the neuroblastoma proteome we set up two studies, one using the UKF-NB-3 parental and UKF-NB-3rCDDP^{1000} cell lines, and the other using the UKF-NB-6 parental and UKF-NB-6rCDDP^{2000} cell lines. For each study a total of three separate drug addition time course experiments were carried out, except for the UKF-NB-3 parental and UKF-NB-3rCDDP^{1000} 2 hour drug addition timepoints only, for which there were two. The cell lines were routinely cultured in between setting up the time course studies in T25 cm^2 flasks as described in 4.1.2.2, though for this study we used split ratios of 1 in 50 for both UKF-NB-3 cell lines and 1 in 25 for both UKF-NB-6 cell lines. All cell lines were grown for 120 hours with no drug to 60-90 % confluency and harvested, and cisplatin was added (at concentrations of 1000 ng/mL for both UKF-NB-3 cell lines and 2000 ng/mL for both UKF-NB-6 cell lines) at 24, 8, and 2 hours BEFORE harvesting, but no drug was added to control flasks (time 0 hours). Thus for each time course experiment at least two T75 cm^2 flasks of cells were set up for each of the cisplatin addition time points (24, 8, and 2 hour) and also control cells (no drug added) for both the parental and cisplatin resistant cell lines. The aim of these studies was to compare proteomes and identify differences for the following comparisons (vs = versus, CDDPr = cisplatin resistant):

Identification of changes associated with cisplatin acquired resistance;
Non-treated parental lines vs respective non-treated cisplatin resistant sub-lines
Parentals 0 hour control vs CDDPr 0 hour control

Identification of acute cisplatin effects in the parental cell lines and the cisplatin resistant cells;
Non-treated parental cell lines vs parental cell line after 2, 8, or 24 hours incubation with cisplatin
Parentals 0 hour con vs Parentals 2 hour
Parentals 0 hour con vs Parentals 8 hour
Parentals 0 hour con vs Parentals 24 hour
Non-treated cisplatin resistant sub-lines vs cisplatin resistant sub-lines after 2, 8, or 24 hrs of incubation with cisplatin
CDDPr 0 hour control vs CDDPr 2 hour
CDDPr 0 hour control vs CDDPr 8 hour
CDDPr 0 hour control vs CDDPr 24 hour

4.1.7.2 Harvesting of cells and cell lysis

60 mL Dunn lysis buffer was prepared by adding 36 g urea (Invitrogen (part of Thermo Fisher Scientific), Loughborough, Leicestershire, UK, Ref 15505-027), 1.2 g 3-[(3-Cholamidopropyl)dimethylammonio]-1-propanesulfonate hydrate (CHAPS) (Sigma, Poole, Dorset, UK, Ref C9426), and 0.6 g DTT (Melford Laboratories Ltd, Ipswich, Suffolk, Ref MB1015) to 24 mL MQ H_2O and stirring overnight on a magnetic stirrer (Bibby B212, Bibby Scientific Ltd, Stone, Staffordshire, UK). The following day, 1 mL volumes of MQ H_2O were added one at a time (about 6 mL total) until the solution was clear and the components in solution, at which point 1.2 mL Pharmalyte carrier ampholytes (pH 3-10) (Amersham Pharmacia, GE Healthcare Ltd., Buckinghamshire, UK Ref 17-0456-01) were added to the stirring solution. The volume was then adjusted to 60 mL with MQ H_2O, aliquoted and stored at -80°C. Urea (10 M) disrupts the non-covalent bonds in proteins and increases the solubility of some proteins; CHAPS (2 % w/v) is a non-denaturing zwitterionic detergent that solubilises membrane proteins; DTT (1 % w/v) disrupts protein disulphide bonds; carrier ampholytes (2 % v/v) are small soluble molecules with negative and positive charges and they both improve the solubility of some proteins and contribute to establishing the pH gradient for the first dimension of the 2D gel electrophoresis (4.1.7.4).

For each time point, cells in the two T75 cm^2 flasks were washed using PBS (no Ca^{2+} or Mg^{2+}) and detached using 1 mL 0.05 % Trypsin/EDTA (4.1.2.2), pooled and resuspended in 10 mL 37 °C complete IMDM medium. Then the cell suspensions were centrifuged in an Eppendorf 5702 benchtop centrifuge (Eppendorf, Stevenage, Hertfordshire, UK) at 1000 rpm for 5 mins. Cells were washed twice by resuspending in 10 mL PBS (no Ca^{2+} or Mg^{2+}) and centrifugation at 1000 rpm for 5 mins. Next the cells were resuspended in 5 mL 0.35 M sucrose, centrifuged at 1000 rpm for 5 mins and the supernatant discarded. One protease inhibitor (PI) tablet (Roche Complete, Mini Protease Inhibitor Cocktail Tablets, Roche Diagnostics Limited, Burgess Hill, West Sussex, UK Ref 11836153001) was dissolved into 1 mL MQ H_20 to make a 10 x concentration solution and kept on ice. This 10 x protease inhibitor solution was diluted to near a 1 x concentration by adding 100 µL of it to 1 mL DLB, and the cell pellet was resuspended using 220 µL of this protease inhibitor solution per $1x10^7$ cells by vortexing. Then the suspension was incubated on ice for 30 mins, vortexed again and sheared through a sterile 5 cm long Microlance 19G gauge needle (Becton Dickinson,UK Ltd, Oxford, England, Ref 301750) attached to a 5 mL sterile syringe (Henke Sass Wolf, Tuttlingen, Germany, Ref 5ML NORM-JECT), by aspirating and expelling rapidly five times. These lysed cells were then centrifuged at 4000 rpm at 4 °C for 20 mins in a cooling Thermo Electron Corporation centrifuge (Thermo Fisher Scientific), Loughborough, Leicestershire, UK, Ref IEC CL31R) to remove particulate material. The supernatant/lysate was then stored at -80°C.

4.1.7.3 Modified Bradford assay

The modified Bradford assay was used to measure the protein concentrations in our lysates (prepared as in 4.1.7.2) and the method is based on that described by (Ramagli 1999). In this method, acid is used to neutralise the alkaline lysate samples before adding dye because they contain urea and basic ampholytes that affect the binding of dye to the proteins.

Bovine serum albumin (BSA) (Sigma Cat# A7030) was dissolved in 1 x protease inhibitor solution in Dunn lysis buffer (prepared as in 4.1.7.2) at 5 mg/ml and stored at -80°C. 0.1 M HCl was prepared by adding 0.3 mL 32 % HCl (Fisher Scientific (part of Thermo Fisher Scientific), Loughborough, Leicestershire, UK, Ref H1100/PB17) to 29.7 mL MQ H_20, and 0.011 M HCl was freshly prepared on the day of testing by adding 1ml 0.1 M HCl to 8 ml ddH_2O. Then the BSA solution, protein inhibitor solution and 0.011 M HCl were mixed as indicated in Table 9 in order to generate a range of protein concentrations needed for preparing a standard curve for the detection of protein contents in sample. Triplicates were prepared, though only one blank (0 µg protein). The lysate samples from 4.1.7.2 were also prepared in triplicate, both undiluted and 1 in 2, as in Table 10.

Protein (µg)	5 mg/mL BSA (µl)	1 x protease inhibitor solution in Dunn lysis buffer (µl)	0.011 M HCl (µl)
0	0	10	90
5	1	9	90
10	2	8	90
15	3	7	90
20	4	6	90
25	5	5	90
30	6	4	90
40	8	2	90
50	10	0	90

Table 9. Preparation of the standard curve samples for the modified Bradford assay.

Dilution factor	Sample (µL)	1 x protease inhibitor solution in Dunn lysis buffer (µl)	0.011 M HCl (µL)
Undiluted	10	0	90
1 in 2	5	5	90

Table 10. Preparation of the lysate samples for the modified Bradford assay.

All tubes were vortexed to mix and then centrifuged in a Thermo Electron Corporation centrifuge (Thermo Fisher Scientific), Loughborough, Leicestershire, UK, Ref IEC CL31R) very briefly, to collect all liquid to the bottom of the tubes. BioRad Protein Assay reagent (Bio-Rad Laboratories Ltd., Hemel Hempstead, Hertsfordshire, UK, Ref 500-0006) was diluted 1 in 4 with MQ H_2O. Next, 3.5

ml of diluted Protein Assay reagent was added to each tube and the tubes were vortexed and left at room temperature for 5 mins. Then the absorbance was read at 595 nm using a spectrophotometer (Jenway 6705 UV/Vis, Barlow Scientific, Dunmow, Essex, UK) was blanked with 0 µg protein.

The standard curve was plotted using SigmaPlot software (an example of a standard curve is shown below in Figure 27). This standard curve was used to determine the protein concentrations in the undiluted and 1 in 2 diluted lysate samples. The protein concentration predicted for the samples diluted 1 in 2 was doubled to get their undiluted actual value. All the resulting protein concentrations were the amount of protein (µg) in 10 µL lysate. The mean concentration for each sample was calculated from the triplicate values. The decision between using the protein concentration values predicted for the undiluted or 1 in 2 diluted samples was based on the position of their A_{595} values on the standard curve; the more central to the curve the more accurate the protein determination.

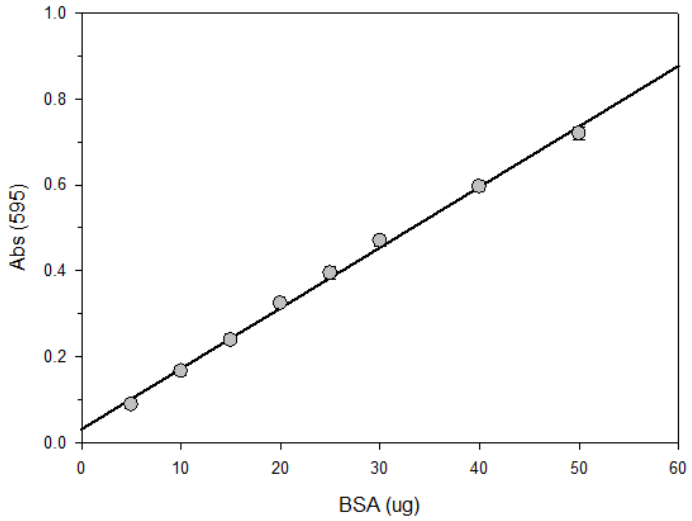

Figure 27. An example of a BSA standard curve for the modified Bradford Assay.

4.1.7.4 2D gel electrophoresis

4.1.7.4.1 The principle of 2D gel electrophoresis

The first dimension step, isoelectric focussing (also known as IEF), separates proteins according to their isoelectric points (pI), which is the pH at which the net charge of a protein is zero. Our samples were applied to a plastic-backed gel strip with an immobilized pH gradient (non-linear, pH 3-10), which was created by covalently incorporating a gradient of acidic and basic buffering groups (immobilines); the pH range of 3-10 covers most proteins found in eukaryotic cells and the

pH gradients at the extreme ends of the pH scale are nonlinear to distribute the proteins evenly over the gel length to obtain maximal resolution. On applying an electric potential across the strip, the proteins in the sample migrate and focus to their pI positions in the pH gradient, aided by the carrier ampholytes in the lysis buffer. Carrier ampholytes are a mixture of small, soluble amphoteric molecules, each with a different pI, so they also migrate and focus to their pI positions in the pH gradient - they have a high buffering capacity near their pI, and they buffer their environment to the corresponding pHs (*GE Healthcare Handbook 80-6429-60AC. 2-D Electrophoresis Principles and Methods.* 2004, Issaq, Veenstra 2008) . See Figure 28.

The second dimension step is sodium dodecyl sulphate-polyacrylamide gel electrophoresis (SDS-PAGE) which separates proteins according to their molecular weights (Mr) in a 90° direction from the first dimension. The pI resolved proteins in the IEF strips are again treated with DTT, a reducing agent that breaks disulphide bonds (also present in the lysis buffer, see 4.1.7.2) and also iodoacetic acid (IAA) that prevents the di-sulphide bonds reforming. SDS is a negatively charged anionic detergent which is used to denature the protein in the lysates further by binding to them and unfolding them into linear molecules. The resulting anionic complexes have a constant net negative charge per unit mass, which enables them to migrate through the polyacrylamide gel on application of an electrical potential. After such treatment, the degree of separation of the proteins in an SDS-PAGE gel mostly depends on their molecular weight, with larger proteins being retained higher in the gel and smaller proteins being able to migrate through the gel to lower positions. There is an approximately linear relationship between the logarithm of the molecular weight and the relative distance of migration of the SDS-polypeptide complex. The resulting 2D gel has protein spots distributed across it, each of which potentially represents a single type of protein (*GE Healthcare Handbook 80-6429-60AC. 2-D Electrophoresis Principles and Methods.* 2004, Issaq, Veenstra 2008) . See Figure 28.

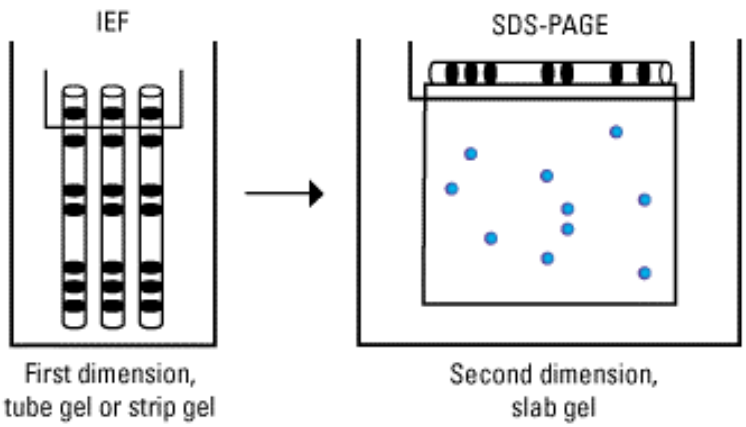

Figure 28 The first dimension (isoelectric focussing (IEF)) and second dimension (sodium dodecyl sulphate-polyacrylamide electrophoresis (SDS-PAGE)) of 2D gel electrophoresis (https://www.thermofisher.com).

4.1.7.4.2 Sample preparation for 2D gel electrophoresis

The resulting protein concentrations (µg) in 10 µL lysate values generated from the modified Bradford assay (4.1.7.3), were divided by 10 to get the resulting protein concentrations (µg) in 1 µL lysate. Then 180 was divided by this protein concentration (µg) in 1 µL lysate to get the volume of lysate that contains 180 µg total protein (180µg was a pre-optimised loading amount). This volume of lysate was adjusted to the loading volume of 125 µL with 1 x protease inhibitor solution in Dunn lysis buffer (prepared as in 4.1.7.2). The tiniest amount of bromophenol blue (Sigma, Poole, Dorset, UK, Ref B5525) was added to each sample and the samples were vortexed, resulting in a very pale blue sample colour. All samples were then briefly centrifuged in an Eppendorf minispin benchtop centrifuge (Eppendorf, Stevenage, Hertfordshire, UK) to collect sample at the bottom of the tubes before continuing to the first dimension step (IEF) (4.1.7.4.3).

4.1.7.4.3 First dimension step: isoelectric focussing (IEF)

The 125 uL volume of prepared sample containing 180 µg total protein (4.1.7.4.2) was pipetted along the length of a IEF ceramic strip holder (GE Healthcare Ltd., Buckinghamshire, UK Ref 80-6146-87) and a 7 cm Immobiline IPG DryStrip pH 3-10 NL (GE Healthcare Ltd., Buckinghamshire, UK Ref 17600112) was laid gel side down onto the sample with the marked + end pointing north in the + end of the strip holder. Any bubbles were gently pressed out using a pipette tip. The Immobiline IPG DryStrip was overlaid with 0.3 ml DryStrip cover fluid (Amersham Pharmacia, GE Healthcare Ltd., Buckinghamshire, UK, Ref 17-1335-01) and the strip holder lid gently put into position. The strip holders were all placed onto an Ettan IPGPhor system Isoelectric Focussing System (GE Healthcare Ltd., Buckinghamshire, UK) with the marked + at the top and - at the bottom, making sure the electrodes were on the gold plated electrode areas. The IPGphor conditions used for these 7 cm Immobiline IPG DryStrips is shown in Table 11. The system was run overnight and stopped when the last step reaches 8000 VhT.

Step	Voltage (V)	Time (h:min)
Step-n-hold	30	13:30
Gradient	200	00.45
Step-n-hold	500	00.45
Step-n-hold	1000	00.45
Gradient	8000	00.30
Step-n-hold	8000	07.30
Total Vhr (VhT)	**8000**	

Table 11. Focusing protocol for 7 cm IPG DryStrips pH 3-10 NL

The Immobiline IPG DryStrips were then washed in MQH_20. The washed strips that were not immediately progressed further were stored at -80°C.

4.1.7.4.4 Second dimension step: sodium dodecyl sulphate-polyacrylamide electrophoresis (SDS-PAGE)

4 X resolving gel buffer solution (1.5 M Tris (pH 8.8)) was prepared by dissolving 181.7 g Tris base (MW 121.1) (Fisons, Ipswich, Suffolk, UK, now part of Rhone-Poulenc, Inc.,Ref T/P360/60) in 750 ml MQ H_2O, adjusting to pH 8.8 with hydrochloric acid, and filling up to a final volume of 1 litre with MQ H_2O and stored long term at 4°C. 10 % (w/v) SDS solution was also prepared by dissolving 5 g SDS (Fisons, Ipswich, Suffolk, UK, now part of Rhone-Poulenc, Inc., Ref S/P530/53) with MQ H_2O up to 50 ml. 10 % (w/v) ammonium persulfate (APS) solution was prepared by dissolving 0.1 g APS (Bio-Rad Laboratories Ltd., Hemel Hempstead, Hertsfordshire, UK, Ref 161-0700) with MQ H_2O to to 1 ml.

12.5 % SDS gels were prepared in 1.0 mm gel cassettes (Invitrogen (part of Thermo Fisher Scientific), Loughborough, Leicestershire, UK, Ref NC2010). To prepare 50 mL of gel, the following reagents were added in the following order: 20.8 mL of 30 % (w/v) acrylamide/Bis solution 37.5:1 (2.7 % crosslinker) (Bio-Rad Laboratories Ltd., Hemel Hempstead, Hertsfordshire, UK, Ref 161-0158) (12.5 % w/v acrylamide final concentration), 12.5 mL of 4 x resolving gel buffer solution (1 x final concentration), 0.5 mL of 10 % (w/v) SDS solution (0.1 % w/v final concentration), 15.7 mL MQ H_2O, 0.5 mL 10 % (w/v) APS (0.1 % w/v final concentration), and 50 µl TEMED (Bio-Rad Laboratories Ltd., Hemel Hempstead, Hertsfordshire, UK, Ref. 161-0800) (0.1 % v/v final concentration). The resulting solution was thoroughly mixed by inversion and then transferred quickly into the gel cassettes, filling up near to their top, before carefully adding 400 µl water-saturated butanol to all the gels except for one gel into which a 2D-comb was added to give a position for the strip and also a well to add marker. Gels were left to set at room temperature for 30 mins.

SDS equilibration buffer consisted of 33.5 mL of 1.5 M Tris (pH 8.8) (this is 4 x resolving buffer as described above) (0.05 M final concentration), 360.35 g of urea (Invitrogen (part of Thermo Fisher Scientific) (6 M final concentration), Loughborough, Leicestershire, UK, Ref 15505-027), 345 mL of glycerol (Fisons, Ipswich, Suffolk, UK, now part of Rhone-Poulenc, Inc., Ref G/0650/17) (34.5 % v/v final concentration), 20 g SDS (Fisons, Ipswich, Suffolk, UK, now part of Rhone-Poulenc, Inc., Ref S/P530/53) (2 % w/v final concentration) and a couple of grains of bromophenol blue (Sigma, Poole, Dorset, UK, Ref B5525) all dissolving overnight stirring on a magnetic stirrer (Bibby B212, Bibby Scientific Ltd, Stone, Staffordshire, UK) up to 1 litre with MQ H_2O. Aliquots of 45 mL were stored at -80 °C for long term storage. 10 x Tris Glycine-SDS (TGS) running buffer was prepared by dissolving 144 g glycine (Fisons, Ipswich, Suffolk, UK, now part of Rhone-Poulenc, Inc., Ref G/0800/60) (192 mM final concentration as 1 x), 30.3 g Tris base (Fisons, Ipswich, Suffolk, UK, now part of Rhone-Poulenc, Inc., Ref T/P360/60) (25 mM final concentration when 1 x), 10 g SDS (0.1 % w/v final concentration when 1 x) with MQ H_2O up to 1 litre; there is no need to adjust the pH

as it will be pH 8.3. Agarose (0.5 %) sealing solution was prepared by dissolving 0.25 g agarose in 50 mL 1 x Tris Glycine-SDS (TGS) running buffer and storing 1 mL aliquots at room temperature.

The Immobiline IPG DryStrips generated in the first dimension (4.1.7.4.3) were equilibrated by soaking them at room temperature in 5 ml of SDS-equilibrium buffer containing 50 mg DTT (Melford Laboratories Ltd, Ipswich, Suffolk, Ref MB1015) per strip, which breaks protein disulphide bonds, in their individual tubes for 15 mins with gentle agitation on an IKA KS260 basic rotating table (IKA, GmBH & Co, Staufen, Germany). The strips were then each washed three times whilst in the tubes with MQ H_2O. The Immobiline IPG DryStrips were then incubated at room temperature for a further 15 mins with 5 ml of SDS-equilibrium buffer containing 125 mg iodoacetamide (IAA) (Sigma, Poole, Dorset, UK, Ref I1149) per strip, in their individual tubes for 15 minutes with gentle agitation on the rotating table. IAA alkylates the thiol groups and prevents their re-oxidation, and also alkylates any residual DTT to prevent streaking of the 2D gels. The strips were then each washed three times with MQ H_2O whilst in the tubes. Each strip was then laid on top of a 12.5 % Tris-glycine gel, gel side to the front and + end to the left, and overlaid with 0.5 mL agarose (0.5 %) sealing solution which had been previously heated to 100 °C in a Test Tube Heater SHT 1D (Stuart, Stone, Staffordshire, UK). For a set of strips from one time course experiment, there was a one gel for which a 2D-comb was used to give a position for the strip and also a well to add marker. For this gel the Immobiline IPG DryStrip used was cut off at each end where there is no gel to fit before sealing in. The markers used were Precision Plus Protein Standards (Dual Colour) (Bio-Rad Laboratories Ltd., Hemel Hempstead, Hertsfordshire, UK, Ref 161-0374), 5µL per well. The gels were run in an Invitrogen XCell Sure Lock Mini-Cell Electrophoresis System (Invitrogen (part of Thermo Fisher Scientific), Loughborough, Leicestershire, UK) in 1 x Tris Glycine-SDS (TGS) running buffer for 1 hour 30 mins (until the dye front reached the bottom of the gel) at a constant 125V, with amps set as high as possible (3.00).

The resulting 2D SDS PAGE gels were removed from the cassettes and individually stained with Coomassie Blue Stain for one hour on an IKA KS260 basic rotating table. This stain was prepared by dissolving 0.25 g Coomassie R-250 (Bio-Rad Laboratories Ltd., Hemel Hempstead, Hertsfordshire, UK, Ref 161-0400) (0.05 % w/v final) in 250 mL methanol (Fisons, Ipswich, Suffolk, UK, now part of Rhone-Poulenc, Inc., Ref M/4000/PC17) (50 % v/v final), 50 mL acetic acid (Fisons, Ipswich, Suffolk, UK, now part of Rhone-Poulenc, Inc., Ref A/03600PB17) (10 % v/v final) and 200 mL MQ H_2O (40 % v/v final). The stain was then poured off and the gels individually de-stained for two hours on a rotating table, until the background was clear and the spots and bands visible. The de-stain solution contained 25 mL methanol (Fisons, Ipswich, Suffolk, UK, now part of Rhone-Poulenc, Inc., Ref M/4000/PC17) (5 % v/v final), 35 mL acetic acid (Fisons, Ipswich, Suffolk, UK, now part of Rhone-Poulenc, Inc., Ref A/03600PB17) (7 % v/v final) and 440 mL MQ H_2O (88 % final). The de-stain was exchanged when it became too purple in colour. De-stained gels were

stored individually at 4 °C in 0.1 % acetic acid (1mL acetic acid (Fisons, Ipswich, Suffolk, UK, now part of Rhone-Poulenc, Inc., Ref A/03600PB17) in 1 litre MQ H_2O) in re-sealable bags, laid horizontally in a box which was wrapped in foil.

4.1.7.5 Analysis using Progenesis Samespots software

Progenesis SameSpots software by Non-Linear Dynamics (version 4; v4.0.3779.13732) (Nonlinear Dynamics Ltd., Newcastle upon Tyne, UK) was used to analyse the 2D SDS PAGE gels (4.1.7.4.4). Two experiments/Samespots files were created with the software, one to compare the UKF-NB-3 parental and UKF-NB-3rCDDP^{1000} cell lines, and the other one to compare the UKF-NB-6 parental and UKF-NB-6rCDDP^{2000} cell lines. The software has a guided workflow which was followed, in brief, as follows, described as for one of the experiments, with workflow steps in inverted commas (for more details refer to www.totallab.com (Total Lab Ltd (Newcastle upon Tyne, UK.) The next step was to upload images of the gels into their experiment under 'Image QC' and to select them to be included. All of the de-stained 2D SDS PAGE gels were scanned as 600dpi, bit depth of 8 and grey scale TIFF images using an Amersham Pharmacia Biotech Image Scanner (Amersham Pharmacia, GE Healthcare Ltd., Buckinghamshire, UK) with visualisation and appropriate cropping using Magiscan for Windows (version 4.3). Next, under 'Reference Image Selection', we assigned a gel, which had the clearest and most well defined spots, as the reference gel to align all the other gel images to. For our experiments no 'Mask of Disinterest' was added - nothing was cropped or not included 'Alignment' of each gel, one gel at a time, to the reference gel image, is a critical step in the workflow. The software initially aligns them using automatic alignment vectors, then manual alignment vectors were added to each of the other spots (and any individual automatic vectors discarded if judged as not appropriate). Spots are automatically assigned a number after alignment by the software, and no spots were filtered out under 'Filtering'. Spot volumes measured were automatically normalised to the spot intensity and background of a reference gel image that is selected by the software, to remove any system variation from differences between gels in, for example, sample preparation and loading, staining and de-staining, and/or image acquisition. The next stage was "Experimental Design Setup", and firstly an experiment was set up with all gels together. Then this experiment was viewed looking at multiple columns per condition so that, on scrolling through each spot one at a time, it was possible to see how it appears on all the gels together in the same frame and this was used to merge spots, split spots, redraw the spot outline, or just leave the spots as they were. Spots were only ever deleted if they were definitely not spots, but this was always avoided if possible. Then experiments were set up using the 'Between Subject Design' option, comparing two conditions, for example UKF-NB-3 parentals 0 hours and UKF-NB-3^{r}CDDP^{1000} 0 hours or UKF-NB-3 parentals 0 hours and UKF-NB-3 parentals 2 hours (all seven study comparisons are listed in 4.1.7.1), and the three gels from the three separate drug addition time course experiments were added for each

condition. In the 'view results' section, the expression profiles and spot details (with focus on the normalised spot volumes) can be analysed, as well as all collated images of all the spots in each of the comparisons, and a one-way ANOVA p-value and Fold increase value (the highest mean normalised spot volume/lowest mean spot volume) are displayed for each spot in each comparison. For each study comparison, spots were selected for further analysis. The selection criteria were that the ANOVA p-value was <0.05, the Fold increase value ≥1.5 (to 1 decimal place), and that the spot had reliable alignment and appearance on each gel.

4.1.7.6 Gel spot excision and in-gel tryptic digestion of proteins

Throughout the procedure, gloves were always worn and methanol (Analytical grade, Fisher Scientific (part of Thermo Fisher Scientific), Loughborough, Leicestershire, UK, Ref M/4000/PC17) washed (x3) 0.5 and 1.5 mL Eppendorf tubes were used.

4.1.7.6.1 Gel spot excision

Selected spots were cut out from at least two gels in which they were the strongest in terms of spot volume and clearest in terms of outline (4.1.7.5). A 2D SDS PAGE gel was initially washed twice with MQ H_2O in a sterile 150 mm petri dish with gentle agitation on a rotating table (IKA KS260 basic, IKA, GmBH & Co, Staufen, Germany). Using a suitable sized sterile filter pipette tip with the end cut off with a clean scalpel blade, the gel was positioned on a methanol wiped MEDALight flat light box and the spot of interest was excised, cutting as close to the edge of the spot as possible (it is important to reduce the amount of background gel). The excised spot was transferred into a 1.5 mL microfuge tube containing 0.5 mL 0.1 % acetic acid (1 mL acetic acid (Fisons, Ipswich, Suffolk, UK, now part of Rhone-Poulenc, Inc., Ref A/03600PB17) in 1 litre MQ H_2O). Batches of 12 spots at a time were taken through the following in gel digestion procedure, each spot in its own tube throughout.

4.1.7.6.2 In-gel tryptic digestion of proteins

The protocol was based on Shevchenko et al (Shevchenko, Wilm et al. 1996). Procedures were carried out in an ICN BSB48 laminar vertical flow recircling cabinet (MP Biomedicals, Irvine, California, USA, distributed by Fisher Scientific (part of Thermo Fisher Scientific), Loughborough, Leicestershire, UK) to reduce the chance of keratin contamination.

The proteins in the gel pieces were then reduced and alkylated. For this first stage the following buffers were required (note that all ammonium bicarbonate buffers were prepared fresh on the day of performing the digestions): 100 mM NH_4HCO_3 (Sigma, Poole, Dorset, UK, Ref A6141) (79.06 mg in 10 mL ddH_2O) filter-sterilised using 0.2 micron filters, which was used to prepare 50 mM NH_4HCO_3/acetonitrile (1:1) (for 12 samples: 350 µL 100 mM NH_4HCO_3, 350 µL MQ H_2O, and 700 µL

acetonitrile (Fisher Scientific (part of Thermo Fisher Scientific), Loughborough, Leicestershire, UK, Ref A/0627/17)), and 50 mM NH_4HCO_3 (for 12 samples: 1.4 mL 100 mM NH_4HCO_3 mixed with 1.4 mL ddH_2O, enough for 12 samples). 10 mM DTT (Melford Laboratories Ltd, Ipswich, Suffolk, Ref MB1015) solution was prepared in 50 mM NH_4HCO_3 (1.54 mg DTT in 1 mL). 55 mM iodoacetamide (IAA) (Sigma, Poole, Dorset, UK, Ref I1149) solution was prepared in 50 mM NH_4HCO_3 (10.17 mg IAA in 1 mL) and kept in the dark. Excised gel particles were washed with 100 μL of 50 mM NH_4HCO_3/acetonitrile (1:1) for 15 mins, then centrifuged for 1 min at 5000 rpm in a benchtop centrifuge (MSE Microcentaur MS13010.Cx1.5 centrifuge, MSE (UK) Ltd., Lower Sydenham, London, UK) and the liquid removed. Next, 100 μL acetonitrile was added and left for 15 mins until the gel pieces had dehydrated (they became white and stick together if more than one piece). Then they were centrifuged for 1 min at 5000 rpm and the acetonitrile was removed. The gel pieces were then rehydrated in 10 mM DTT in 50 mM NH_4HCO_3 solution by adding enough liquid to cover the gel piece (about 50 μL), and incubation for 30 mins in a Grant Y6 water bath at 56°C (Grant Instruments, Shepreth, Cambridge, UK). Next the gel pieces were centrifuged for 1 min at 5000 rpm and the DTT solution was removed. Then the gel pieces were then dehydrated again for 2 mins with 100 μL acetonitrile prior to centrifugation for 1 min at 5000 rpm to remove the acetonitrile. The next step was to rehydrate the gel pieces in 55 mM iodoacetamide solution in 50 mM NH_4HCO_3, adding enough liquid to cover the gel piece (about 50 μL), whilst in the dark for 20 mins at room temperature. They were then centrifuged for 1 min at 5000 rpm and the iodoacetamide solution was then removed. The gel pieces were then washed twice using 100 μL of 50 mM NH_4HCO_3 solution for 15 mins followed by centrifugation for 1 min @5000 rpm and removal of 50 mM NH_4HCO_3 solution. Next the gel pieces were again dehydrated for 15 mins with 100 μL acetonitrile, centrifuged for 1 min at 5000 rpm and acetonitrile was removed. The gel pieces then dried in a vacuum centrifuge for 15 mins at the lowest speed (SPD Speed Vac 11V-230, Thermo Savant (part of Thermo Fisher Scientific), Loughborough, Leicestershire, UK).

For in-gel tryptic protein digestion, the following reagents were prepared: 100 μL of Trypsin Resuspension Buffer (Promega, Southampton, UK, Ref V542A) was added to 20 μg freeze-dried Sequencing Grade Modified Trypsin (Promega, Southampton, UK, Ref V511A) resulting in a 0.2 μg/μL solution (aliquoted and stored at -20 °C long-term). Both enzyme and buffer were bought as a set (Promega, Southampton, UK, Ref V5111). Digestion buffer only (25 mM NH_4HCO_3, 10 % acetonitrile) was prepared by mixing 100 μL 100 mM NH_4HCO_3 solution (see above), 40 μL acetonitrile and 260 μL MQ H_2O. 10 ng/μL trypsin in digestion buffer was prepared by adding 20 μL 0.2 μg/μl trypsin (see above) to a mixture of 100 μL 100 mM NH_4HCO_3 (see above), 40 μL acetonitrile and 240 μL MQ H_2O. To digest the in-gel proteins, the gel pieces were rehydrated in 20 μL of the 10 ng/μL trypsin in digestion buffer solution at 4°C (on ice) for 30 mins. The remaining 10 ng/μL trypsin in digestion buffer solution was removed and 10 μl of the digestion

buffer only was added to cover the gel pieces. The samples were left at room temperature overnight in the dark.

After tryptic digestion, the proteins were extracted from the gel pieces. 5 µL acetonitrile was added to each gel piece. Then they were sonicated for 15 mins in a Decon FS minor sonicator, Ultrasonics Ltd., Hove, Sussed, UK), centrifuged for 1 min at 5000 rpm, and the supernatants collected. Next, 10 µL 50 % acetonitrile containing 5 % (v/v) formic acid (prepared using 7 µL formic acid (Fisher Chemical (part of Thermo Fisher Scientific), Loughborough, Leicestershire, UK, Ref 10559570), 70 µL acetonitrile, and 63 µL MQ H_2O) was added and the pieces sonicated again for 15 mins. After centrifugation for 1 min at 5000 rpm, the supernatant was collected and pooled with the first supernatant. The pooled supernatants were vortexed using a whirlimixer (Fisons Whirlimixer, Fisons Science equipment, Loughborough Leicestershire, UK, Ref SC-P-202-0105) and stored at -20 °C temporarily or -80 °C long-term.

4.1.7.7 Mass spectroscopy and identification of proteins

4.1.7.7.1 The principle of MALDI-TOF MS and MALDI-TOF-TOF MS/MS

A mass spectrometer comprises of an ion source which ionises analytes, an analyser to measure their mass-to-charge ratio (m/z), and a detector that quantifies the number of ions at each m/z value (Figure 29).

MALDI (Matrix-Assisted Laser Desorption/Ionisation) is a soft ionisation method which is commonly used to obtain large ions, like proteins, into gas phase with minimal fragmentation. Dried droplets of samples and calibration standards in a matrix solution are prepared as spots on a steel anchor plate (4.1.7.7.2). In the source of the instrument, desorption is triggered by pulses from a UV laser beam because the matrix material heavily absorbs UV laser light and converts it to heat energy. This causes ablation of the matrix upper layer and the transfer of a proton from the matrix to the analyte molecules, giving them a positive charge (positive ionisation) (Mann, Hendrickson et al. 2001, Cheng, Zhang 2010, Aebersold, Mann 2003). When analysing proteins digested with trypsin, each proteolytic fragment contains a basic arginine (R) or lysine (K) amino acid residue, and so this is highly suitable for positive ionisation mass spectrometric analysis (Cheng, Zhang 2010).

To generate time of flight (TOF) data (Figure 29A), the resulting charged ions of different sizes are accelerated in the source and again in a first time of flight tube (TOF-1) before entering the larger second time of flight (TOF-2) tube of the instrument, where they are subjected to an electronic/magnetic field. The time it takes for charged ions to fly through this tube to the detector depends on their mass-to-charge ratios. Smaller ions reach the detector more quickly. The result is a Peptide Mass Fingerprint (PMF) - a unique spectrum of abundance of all ions

detected for that sample. The most abundant peptides (most intense peaks in the PMF spectra) are selected to progress through to MALDI-TOF-TOF MS/MS. In the mass spectrometer, an ion can be narrowly electronically gated for selection based on the velocity with which it leaves the source in the TOF-1 tube of the instrument (Figure 29B). For MALDI-TOF-TOF MS/MS (Figure 29C), the samples are subjected to the laser again at the source, but at a higher intensity than for MALDI-TOF MS so that the peptides fall apart into even smaller fragments. In the TOF-1 tube the fragments fly at the original ion's velocity and are selected for its required mass by the gating before being accelerated through TOF-2 and reaching the detector. The result is a Peptide Fragment Fingerprint (PFF) for the selected mass, which can be used to derive the amino acid sequence of the original proteolytic fragment of that mass yielded from the trypsin digestion. This is carried out one at a time for the selected most abundant peptides (Aebersold, Mann 2003, Mann, Hendrickson et al. 2001, Cheng, Zhang 2010).

4.1.7.7.2 Target plate preparation for mass spectroscopy

The next stage was to prepare dried droplets of protein samples and calibration standards onto Anchorchip steel target plates ready for mass spectrometric analysis. AnchorChip standard 800µm target plates (MTP Anchorchip 384 TF Ref 209514 mounted on target frame Ref 74115, Bruker Daltronik GmbH, Bremen, Germany) are equipped with hydrophilic patches ("anchors") in hydrophobic surroundings - one plate has 384 anchors for samples and 96 anchors for calibrants (Calibanchors) for MALDI-TOF MS. Sample and calibration anchors are grouped in a manner, that always four sample anchors surround one calibration anchor which serves to calibrate those four sample runs.

HCCA (α-cyano-4-hydroxycinnamic acid) is a widely used MALDI matrix for peptides, especially in proteomics applications (Jaskolla, Papasotiriou et al. 2009). 0.7 mg/mL HCCA matrix solution was prepared by dissolving 1.4 mg HCCA (Sigma, Poole, Dorset, UK, Ref 144550-5 – re-crystallised twice) in 2 mL 80 % acetonitrile/0.09 % TFA solution (acetonitrile (Fisher Scientific (part of Thermo Fisher Scientific), Loughborough, Leicestershire, UK, Ref A/0627/17 and trifluoroacetic acid (TFA) (Rathburn Chemicals Ltd., Walkerburn, Scotland Ref PTS6045) to which 20 µL 100 mM $NH_4H_2PO_4$ (Sigma, Poole, Dorset, UK, Ref 216003) was added (final concentration 1 mM). Peptide Calibration Standard II (freeze-dried) (Bruker Daltronik GmbH, Bremen, Germany, Ref 222570) was prepared in 125 µL TA30 (30:70 (v/v) acetonitrile : TFA 0.1 % in water) and 10 µL of this calibrant solution was mixed with 2 mL of the HCCA matrix solution (aliquoted and stored at -20 °C for long-term storage). The Anchorchip target plate was cleaned according to manufacturer's instructions.

A. MALDI-TOF generation of Peptide Mass Fingerprint (PMF)

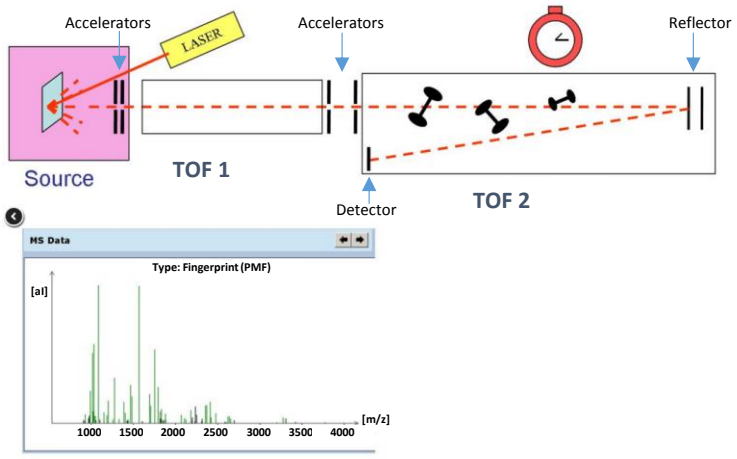

B. Mass selection

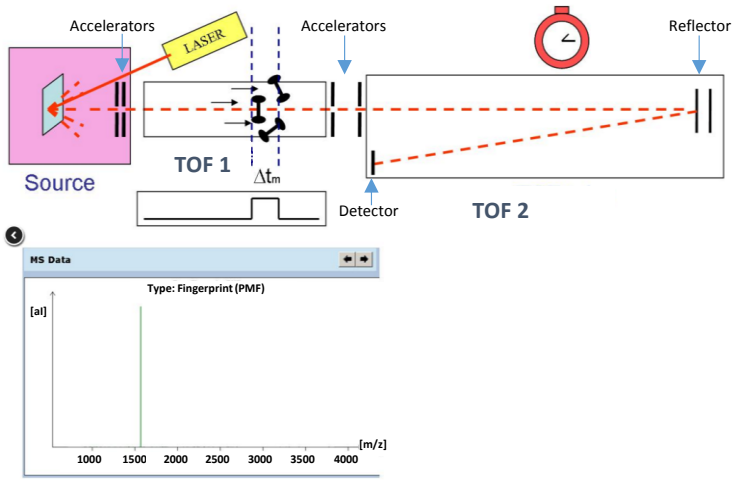

C. MALDI TOF-TOF generation of Peptide Fragment Fingerprint (PFF)

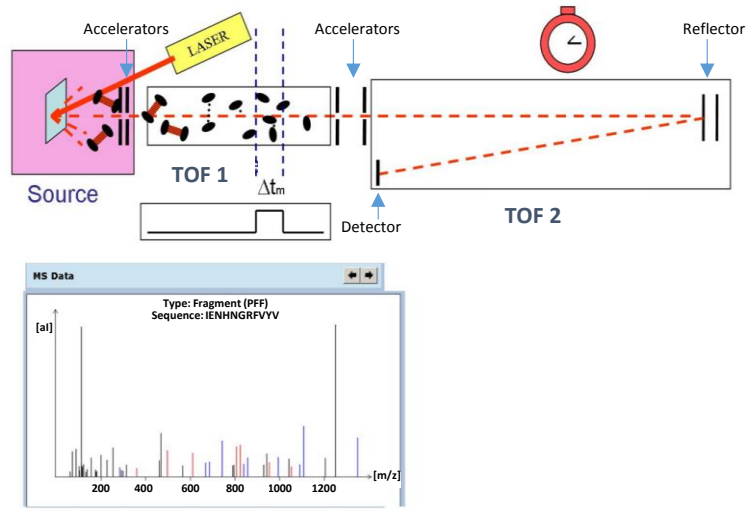

Figure 29. The generation of MALDI-TOF MS and MALDI-TOF-TOF MS/MS data by the Bruker UltraXtreme, a MALDI-TOF-TOF spectrometer. The legend for this figure is in the following text.

Figure 29. The generation of MALDI-TOF MS and MALDI-TOF-TOF MS/MS data by the Bruker UltraXtreme, a MALDI-TOF-TOF spectrometer. A. MALDI-TOF MS: Sample is ionised in the source by the laser and the ions are accelerated through Time of Flight (TOF) tubes 1 and 2. At the end of TOF2 the ions are reflected toward the detector which calculates ion mass, which is dependent on the mass-to-charge ratio - the smallest ions fly through the TOF tubes the quickest. What results is a PMF (Peptide Mass Fingerprint) which summarises the masses detected in a sample. B. An ion can be narrowly electronically gated for selection based on the velocity with which it leaves the source in the TOF-1 tube of the instrument. C. MALDI-TOF-TOF MS/MS: The most abundant peptides from MALDI-TOF MS are selected. The sample is ionised in the source by the laser again but at a higher intensity, causing the peptides to fall apart into smaller fragments. They are selected by gating at the original ion's velocity in the TOF1 tube and then the ion fragments are accelerated through the TOF2 tube. At the end of TOF2 the ions are reflected toward the detector which calculates ion mass. What results is a daughter PFF (Peptide Fragment Fingerprint) for the selected mass. (Figure adapted from Max Planck Institute for Plant Breeding Research website http://www.mpipz.mpg.de/44542/MALDI-TOF-TOF_MS_MS).

Tryptically digested protein samples prepared as in 4.1.7.6, were thawed on ice and vortexed using a Whirlimixer (Fisons Whirlimixer, Fisons Science equipment, Loughborough Leicestershire,UK, Ref SC-P-202-0105). All samples and the calibration solution were each vortexed again just before spotting them onto the Anchorchip target plate. 1 µL of tryptically digested protein sample solution was deposited onto each target sample anchor position and allow to dry, then 1 µL HCCA matrix solution was deposited over each sample spot and allow to dry. Then 1 µL of Peptide Calibration Standard II solution (which already contains the HCCA) was deposited onto each target calibranchor position and allow to air dry. 1 µL HCCA matrix solution only was deposited on three sample spots as a blank to check the Anchorchip plate was absolutely clean.

4.1.7.7.3 MALDI-TOF and MALDI-TOF-TOF analysis

For each sample, MALDI-TOF MS (generating protein mass fingerprints (PMF)) and MALDI-TOF-TOF MS/MS analyses (generating peptide fragment fingerprints (PFF)) were carried out using a Bruker UltrafleXtreme mass spectrometer (Bruker Daltronik, Bremen, Germany) in the positive ion mode, using monoisotopic mass. Flex control software (version 3.4, Bruker Daltronik, Bremen, Germany) was used to set up the instrument using the autoXecute feature for optimisation of laser energy and automated data collection. Spectra were collected in reflector mode with an acceleration voltage of 25 kV and a pulse ion extraction time of 80 ns. The protein mass range for MS was between 700 and 3500 m/z. The number of laser shots summed in MS was 3500, and for MS-MS it was 3000. Data generated was sent to Flex Analysis software (version 3.4, Bruker Daltronik, Bremen, Germany) for both external calibration in the protein mass range using the Peptide Calibration Standard II standard solution (described above), and for peak selection. The top five most intense peaks from the MALDI-TOF MS (PMF) data were subjected to MALDI TOF-TOF MS/MS to generate the PFF data.

4.1.7.7.4 Protein identification

The MS (PMF) and MS/MS (PFF) data (4.1.7.7.3) were then sent, using Biotools software (version 3.2, Bruker Daltronik, Bremen, Germany) to the standard Mascot search engine (version 2.4.1) (http://www.matrixscience.com/) and searched against both the human protein SwissProt database (http://www.uniprot.org/) (version 2014_01, and version 2014_03 for repeats) placed in the public domain by UNIprot (Bateman, Martin et al. 2015), and the human protein NCBInr database (version 20140122, and version 20140323 for repeats) (http://www.ncbi.nlm.nih.gov/refseq/). For MALDI-TOF MS (PMF) data the following search conditions were used; enzyme: trypsin, mixed modification: carbamidomethyl (C), variable modification: oxidation (M), mass values: monisotopic, protein mass: unrestricted, peptide mass tolerance: +/- 100 ppm, peptide charge state: 1+, max missed cleavages: 1. For MALDI-TOF-TOF MS/MS (PFF) data the search conditions used were as for the MALDI-TOF MS (PMF) data, but with the addition of fragment mass tolerance: +/- 0.5 Da. For details of the original database search algorithm that underpins the Mascot software refer to Pappin et al (Pappin, Hojrup et al. 1993).

Initially, for both MS and MS/MS data, the detailed data for all protein matches from both Swissprot and NCBInr from the search results that passed the score cut-off (which gives a p value <0.05 and indicates a significant match for MS and indicates identity or extensive homology for MS/MS) were collected in an Excel spreadsheet, irrespective of the expect value. It is important to note that for MS/MS data we focussed on the individual peptides (ion) scores, not the total protein score for all peptides together. Each protein score in a peptide mass fingerprint, and each ion score in an MS/MS search has an expectation value too, which indicates how often a match of this quality or better is expected to arise by chance alone; the lower the expectation value, the more significant the score. An expect value cut-off of 1×10^{-5} was taken as this represents a 1 in 100,000 chance that the match is random; we apply this strict criteria as for single spots from a 2D gel there is no reliable mechanism for measuring a false detection rate (http://www.matrixscience.com/).

Next a second spreadsheet was created, in which the names of the matched protein results passing the score cut-offs for both database searches were collated into a table and colour coded according to whether or not the expectation value was above or below 1×10^{-5}, resulting in a simplified and unbiased representation of all the data together. The NCBInr database is not as highly curated as the Swissprot database, so more likely for NCBInr many hits are frequently generated for a single query, and a single protein hit often consists of a list of proteins rather than a single protein (as for Swissprot) representing matches to, for example, different isoforms, partial sequences or subunits of the same protein. In Mascot MS data reports, proteins that match the same set or a sub-set of mass values are grouped into a single hit (listed in order of decreasing scores and expect values). For our MS data, the top scoring protein in the list for each hit was

transferred into the table. However, if a protein was unnamed, then the next named protein in the list for that hit was also transferred (if there was one). In Mascot MS/MS data reports, proteins matching the same set of peptides (therefore having the same score and expect values) are grouped as hits, so in this instance, the first protein in the list for each hit was transferred into the table, and if that protein was unnamed, then the next named protein in the list for that hit was also transferred (if there was one). A second protein in a list for an MS/MS hit was sometimes transferred too if its name made more sense relating to the names of corresponding MS hits for example VDAC2 was transferred as well as porin for spot 637. Colour coding was as follows. For the MS data, matches with an expect value $<1 \times 10^{-5}$ were colour coded green (strong match), and matches with an expect value $>1 \times 10^{-5}$ were colour coded orange (weak match). For the MS/MS data, matches were colour coded green (strong match) if 1. at least one of the five peptides passed the score cut-off (which gives a p value <0.05) as well as having a strong expect value $<1 \times 10^{-5}$, 2. two or more of the five peptides passed the score cut-off (which gives a p value <0.05) but had weaker expect values ($>1 \times 10^{-5}$), 3. just one of the five peptides passed the score cut-off (which gives a p value <0.05) with a weak expect value ($>1 \times 10^{-5}$) but accompanied by another one or more of the five peptides having (a) score (s) near to the score cut-off and weak expect value(s) ($>1 \times 10^{-5}$). An orange colour for the MS/MS data indicated a weaker match, and this was for when just a single peptide passed the score cut-off (which gives a p value <0.05) with a weak expect value ($>1 \times 10^{-5}$). The data in the table was then arranged together for the duplicate spots, then they were divided into one of the following groups; definite identifications, no identification, keratin identifications and unsure identifications. Generally speaking, spots were classed as definite identifications if each of the duplicates had strong identical identification in both databases, with more weighting given to MS/MS hits because MS/MS matches actual peptide sequences rather than masses.

4.2 Results – neuroblastoma cell lines

4.2.1 Characterisation of the neuroblastoma cell lines

4.2.1.1 Observed appearance and growth characteristics of the neuroblastoma cell lines

Representative images of each of the eight cell lines (4.1.2.1) used in these studies are shown in Figure 30, viewed on a phase contrast light microscope (4.1.3). Described below are observations of cell size, morphology and growth whilst continuously culturing in the laboratory (4.1.2.2).

All the UKF-NB-3 cell lines have projections and grow in monolayers. The UKF-NB-3 parentals are small and grow in clusters, and the UKF-NB-3^{r}OXALI^{2000} look very similar except when they die they merge together, and they die quite rapidly at a lower confluency than the other cell lines. The UKF-NB-3^{r}CDDP^{1000} cells are the largest of the UKF-NB-3 cell lines, growing uniquely in fan-shaped clusters. The UKF-NB-3^{r}CARBO^{2000} cells are smaller cells (compared to the UKF-NB-3 parentals and UKF-NB-3^{r}OXALI^{2000} cells) which grow more individually than as clusters, with a minimal number of larger cells too; interestingly these larger UKF-NB-3^{r}CARBO^{2000} cells reduce in number over time compared to those with the smaller morphology. The UKF-NB-3 parentals, UKF-NB-3^{r}CDDP^{1000} and UKF-NB-3^{r}OXALI^{2000} appear to be homogeneous populations compared to the UKF-NB-3^{r}CARBO^{2000} cells. The UKF-NB-3 parentals and UKF-NB-3^{r}CDDP^{1000} cells grew the fastest, followed by the UKF-NB-3^{r}CARBO^{2000} and UKF-NB-3^{r}OXALI^{2000} cells.

Compared to the UKF-NB-3 cell lines, the UKF-NB-6 cell lines have a more globular appearance. The UKF-NB-6 parentals and UKF-NB-6^{r}CDDP^{2000} are the smaller cells and resemble each other the most regarding cell size and morphology; they send out many processes to neighbouring cells and grow in multilayers the more confluent they get, however the UKF-NB-6^{r}CDDP^{2000} were more globular. The UKF-NB-6^{r}CARBO^{2000} and UKF-NB-6^{r}OXALI^{4000} grow not as much in multilayers with few processes. The UKF-NB-6^{r}CARBO^{2000} cells appear to be the most heterogeneous of all the cell lines, and (closely followed by the UKF-NB-6^{r}OXALI^{4000} cells) the hardest to trypsinise from the flask surface (particularly the distinctive larger flat cells in the cell population), and overall they are extremely pale and rounder in appearance. The UKF-NB-6^{r}OXALI^{4000} is the fastest growing of the UKF-NB-6 cell lines, with a larger and rounder morphology and are also pale, with a cobblestone growth pattern. The UKF-NB-6^{r}CARBO^{2000} do not grow as fast as the UKF-NB-6^{r}OXALI^{4000} cells, and the UKF-NB-6 parentals and UKF-NB-6^{r}CDDP^{2000} grow the slowest.

For one experiment (see 4.1.6), all the resistant sub-lines were also grown for three months without drug, and the only observed differences between the cells cultured with and without drug were that the UKF-NB-3^{r}CDDP^{1000} cells grew quicker without compared to with cisplatin, and that

the UKF-NB-6^{r}CDDP^{2000} cells cultured without cisplatin appeared less globular and looked flatter in morphology over time compared to those cultured with cisplatin.

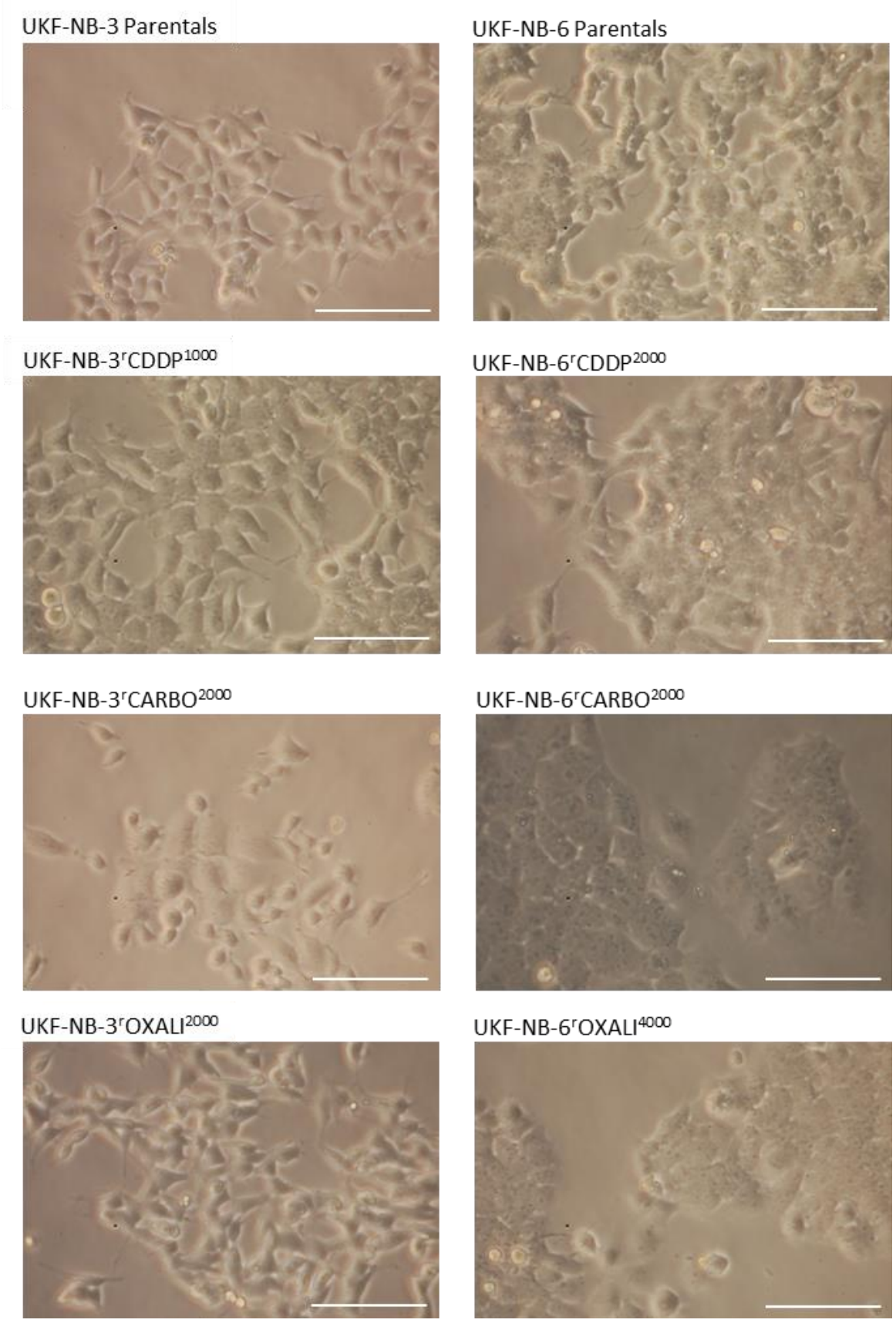

Figure 30. Images showing representative morphology of each of the eight neuroblastoma cell lines (images taken at x200 magnification, size bars represent 100 μm).

4.2.1.2 Real-time growth curves in the presence and absence of drugs

Growth curves were generated for all four UKF-NB-3 cell lines and the four UKF-NB-6 cell lines (4.1.2.1), using impedence based technology on the Roche xCELLigence system (4.1.4.1), in order to study their growth characteristics and to generate growth doubling times. For the resistant sub-lines, growth curves were generated in the presence of drug (at continuous culture concentrations), and in order to investigate the effects of removal of drug on their growth, curves were also set up with drug excluded from their media. A total of three biological repeats of duplicate growth curves were generated for each set of four cell lines (4.1.4.2). Figure 31 shows the growth curves for each of the UKF-NB-3 and UKF-NB6 cell lines (one representative biological repeat shown as an example, data not shown for the other two repeats), and Figure 32 shows bar charts of doubling times (4.1.4.3) (means of all three biological repeats).

For both the UKF-NB-3 and UKF-NB-6 sets of cell lines, the growth and death profiles of the curves for each drug resistant cell line all looked different compared to both that of the corresponding parental cell line (from which they were originally derived), and also compared to each other within the sets (Figure 31). This phenomenon was also demonstrated by the subsequently calculated mean doubling times in Figure 32.

For the UKF-NB-3 cell lines, focussing on doubling times (Figure 32) for cell lines cultured with and without drug, the fastest growing were the UKF-NB-3^{r}CDDP^{1000} cells (22.2 and 19.1 hours respectively), followed by the UKF-NB-3 parentals (32.3 hours) then the UKF-NB-3^{r}CARBO^{2000} (36.0 and 35.5 hours respectively) and UKF-NB-3^{r}OXALI^{2000} cells (38.7 and 35.7 hours respectively). For the UKF-NB-6 cell lines the fastest growing were the UKF-NB-6^{r}OXALI^{4000} cells (19.4 and 18.1 hours respectively) and the UKF-NB-6^{r}CARBO^{2000} cells (22.4 and 21.7 hours respectively), followed by the UKF-NB-6 parentals (27.4 hours) and UKF-NB-6^{r}CDDP^{2000} (32.0 and 27.3 hours respectively). Overall, the results generally reflected the growth observations of all the cell lines during continuous culture, as described in 4.2.1.1. It was interesting to note that the UKF-NB-6^{r}CARBO^{2000} and UKF-NB-6^{r}OXALI^{4000} cells were the most difficult to trypsinise from the surface of flasks (4.2.1.1), and in these experiments they always had the highest impedence (Cell Index (CI)) measurements. This makes sense because impedence measurements are not just proportional to the number of cells present and their viability, but also to cell morphology and attachment.

It was also demonstrated how the resistant sub-lines with drug removed still grew, on the whole, in parallel to when grown with drug, therefore the presence of drug is not essential for their viability and growth. However the resistant sub-lines all had marginally smaller mean doubling times than with drug present Figure 32. The actual percentage decreases of these mean doubling times are displayed below in Table 12, and interestingly it can be seen that the numbers are similar for the same drug resistant subline derived from each patient. The biggest mean doubling

time differences were between the cisplatin resistant sub-lines with and without drug (14.1 to 14.7 %), followed by the oxaliplatin resistant sub-lines with and without drug (6.5 to 7.8 %), and lastly, with minimal difference, the carboplatin resistant sub-lines with and without drug (1.4 to 3.3 %). In the laboratory, during routine continuous culture of the resistant sub-lines without drug, differences were only obvious for the cisplatin resistant sub-lines (see 4.2.1.1).

UKF-NB-3 cell line	% decrease in doubling time (no drug/+ drug)	UKF-NB-6 cell line	% decrease in doubling time (no drug/+ drug)
UKF-NB-3^{r}CDDP^{1000}	14.1	UKF-NB-6^{r}CDDP^{2000}	14.7
UKF-NB-3^{r}CARBO^{2000}	1.4	UKF-NB-6^{r}CARBO^{2000}	3.3
UKF-NB-3^{r}OXALI^{2000}	7.8	UKF-NB-6^{r}OXALI^{4000}	6.5

Table 12. The % decrease in mean doubling times (from Figure 32) of the drug resistant sub-lines grown with no drug compared to when grown with their corresponding drug.

A.

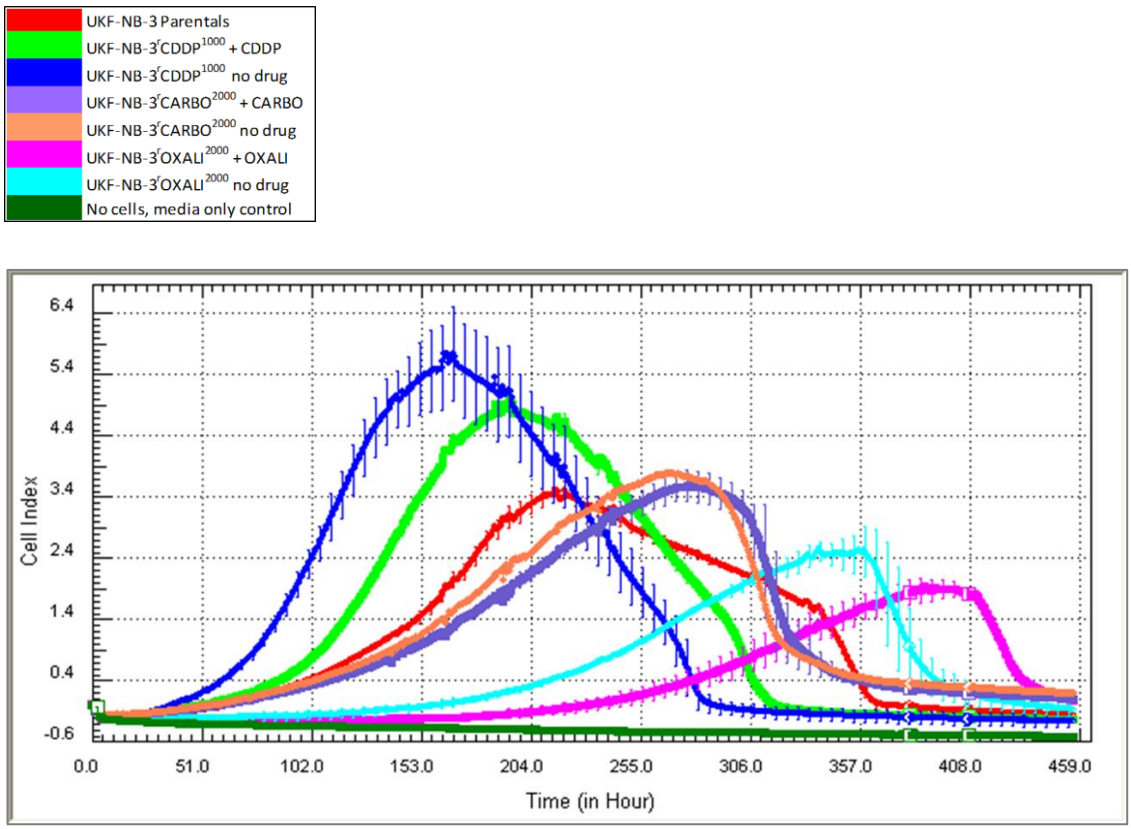

B.

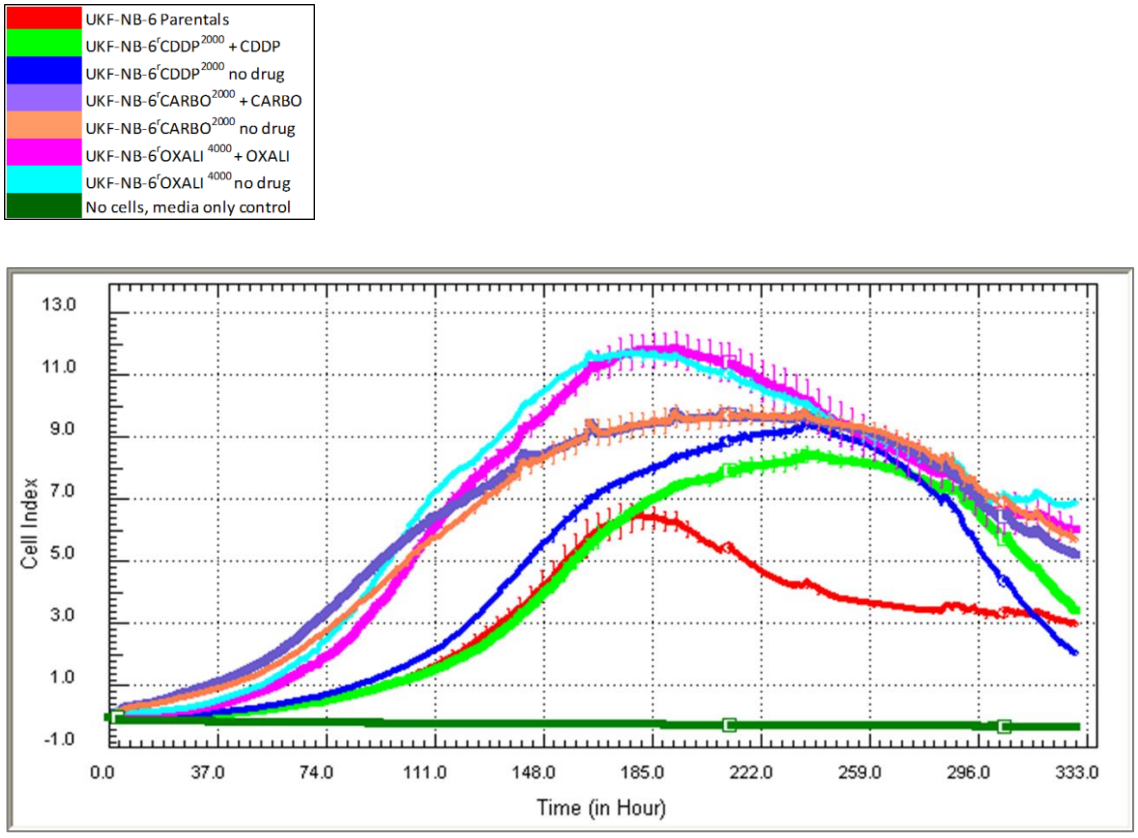

Figure 31. Representative growth curves generated using impedence technology (Roche xCelligence system) for the panels of UKF-NB-3 cell lines (A) and UKF-NB-6 cell lines (B). The drug resistant sub-lines were grown both in the presence and absence of drug (4.1.4). Data are the mean of duplicate curves and error bars represent standard deviation. This data set represents one of three biological repeats (other two not shown).

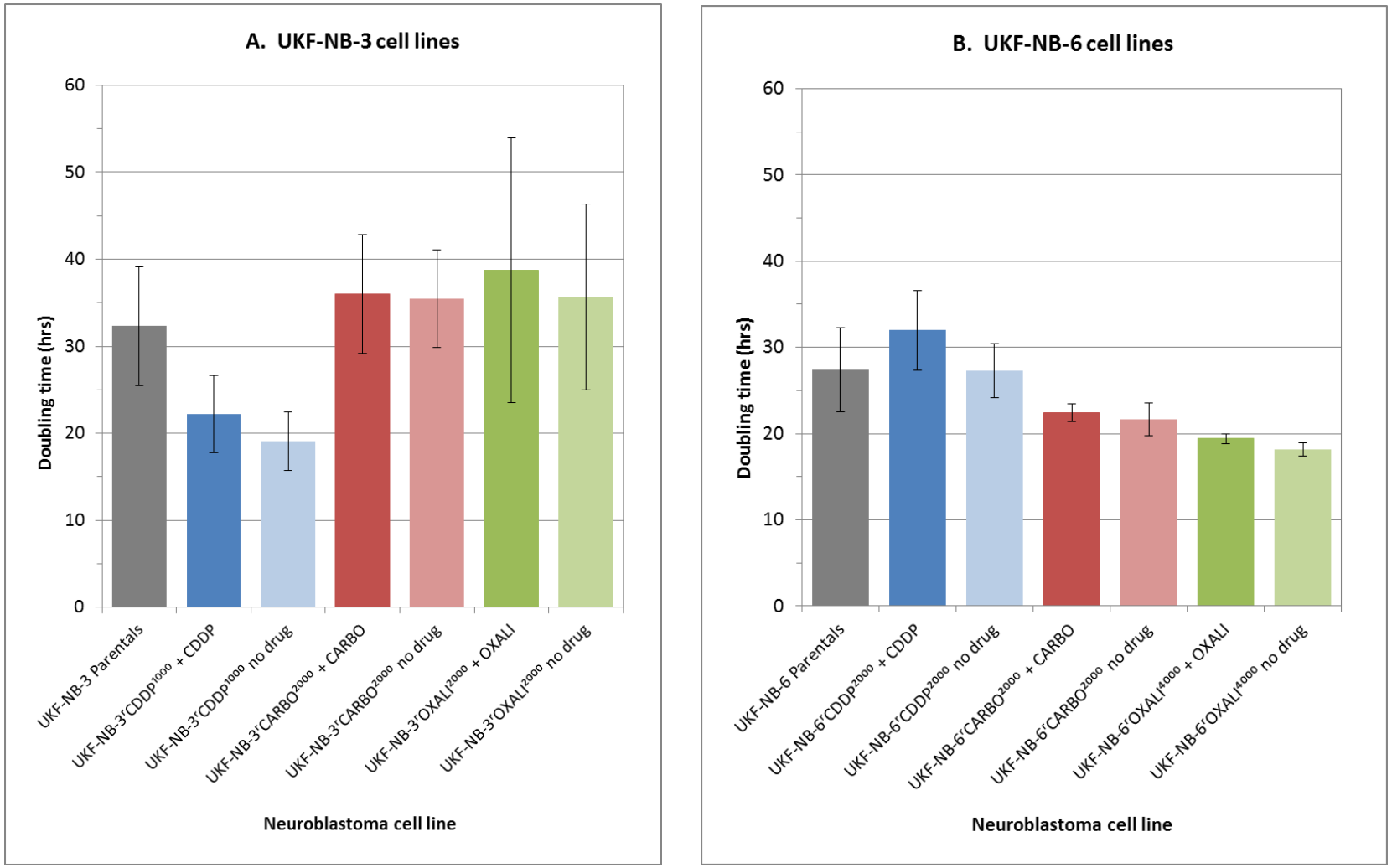

Figure 32. Mean doubling times (calculated as in 4.1.4.3) of three biological repeats of the growth curves (one of which is represented in Figure 31) generated using impedence technology (Roche xCelligence system) for the panels of UKF-NB-3 cell lines (A) and UKF-NB-6 cell lines (B). The drug resistant sub-lines were grown both in the presence and absence of drug (4.1.4). Error bars represent standard deviation.

4.2.1.3 Drug sensitivity profiles

The panels of UKF-NB-3 and UKF-NB-6 cell lines (4.1.2.1) were all tested by MTT assay (4.1.5) to generate five biological repeats of dose responses for each of the platinum drugs cisplatin, carboplatin, and oxaliplatin (4.1.6). The aim was to both assess the sensitivity of each cell line to each drug and to determine if there was any platinum drug cross-resistance. Cross-resistance means that even though the cancer cells have been cultured in the presence of one drug to which they have established resistance, they also demonstrate resistance to drugs to which they have never been exposed. Table 13 and Table 14 show the mean IC_{50} and mean fold difference data for the UKF-NB-3 cells and UKF-NB-6 cells respectively. Fold difference values were calculated for the drug resistant sub-lines only, by dividing the IC_{50}s by the corresponding drug IC_{50} of the parental cell line. Figure 33 shows these data plotted for the UKF-NB-3 cells and Figure 34 for the UKF-NB-6 cells.

Regarding Figure 33A and Figure 34A, sensitivity to each of the three platinum drugs was demonstrated for both the UKF-NB-3 and UKF-NB-6 parental cell lines, which have never been exposed to these drugs. Additionally, all drug-resistant sub-lines displayed substantially increased IC_{50} values to the drugs they had been adapted to. These data also clearly demonstrate a level of drug cross-resistance for the resistant UKF-NB-3 and UKF-NB-6 sub-lines, except for the UKF-NB-3^{r}OXALI^{2000} cells.

Focussing more on the fold differences values plotted in Figure 33B and Figure 34B, and classing a fold change ≥2.0 as resistant; both the UKF-NB-3^{r}CDDP^{1000} and UKF-NB-6^{r}CDDP^{2000} cell lines, besides having cisplatin resistance (8.3 and 19.9 fold respectively), also demonstrated resistance to carboplatin (6.3 and 9.6 fold respectively), but no, or lower levels of resistance to oxaliplatin (1 and 2.4 fold respectively). The UKF-NB-3^{r}CARBO^{2000} and UKF-NB-6^{r}CARBO^{2000} cell lines, besides having carboplatin resistance (7.6 and 8.5 fold respectively), also showed an interestingly higher level of resistance to cisplatin (10.6 and 12.9 fold respectively), but no, or lower levels of, resistance to oxaliplatin (1.1 and 4.1 fold respectively). The UKF-NB-3^{r}OXALI^{2000} and UKF-NB-6^{r}OXALI^{4000} cell lines, both showed oxaliplatin resistance (4.7 and 5.1 fold respectively), and whilst the UKF-NB-3^{r}OXALI^{2000} cells showed no cisplatin resistance (1.4 fold) and no carboplatin resistance (1.3 fold), the UKF-NB-6^{r}OXALI^{4000} cells showed a level of cross-resistance to cisplatin (3.9 fold) and carboplatin (4.1 fold). These data show that out of the drugs cisplatin, carboplatin and oxaliplatin, there is a higher level of cross-resistance between the drugs cisplatin and carboplatin in our panels of neuroblastoma cell lines.

		IC50 (nM)		Fold difference	
Cell line	Drug	Mean	STDEV	Mean	STDEV
UKF-NB-3 Parentals	CDDP	511	142	-	-
	CARBO	2540	771	-	-
	OXALI	1060	480	-	-
UKF-NB-3^{r}CDDP^{1000}	CDDP	4129	1374	8.3	3.0
	CARBO	15458	4620	6.3	2.2
	OXALI	1059	609	1.0	0.4
UKF-NB-3^{r}CARBO^{2000}	CDDP	5387	2112	10.6	3.8
	CARBO	18973	8182	7.6	3.1
	OXALI	1182	609	1.1	0.1
UKF-NB-3^{r}OXALI^{2000}	CDDP	660	208	1.4	0.5
	CARBO	3130	928	1.3	0.4
	OXALI	4669	1709	4.7	1.6

Table 13. Drug sensitivity profiling of the four UKF-NB-3 neuroblastoma cell lines with cisplatin, carboplatin and oxaliplatin by MTT assay: IC_{50} values and Fold differences. The table shows the mean IC_{50} values for each cell line for each drug and the mean fold differences of the IC_{50}s of the resistant sub-lines with each drug divided by the IC_{50} values for the same drug with the parental cell line. Fold differences below 2.0 were classed as no resistance. Data are the mean of five biological repeats with standard deviation.

		IC50 (nM)		Fold difference	
Cell line	Drug	Mean	STDEV	Mean	STDEV
UKF-NB-6 Parentals	CDDP	556	271	-	-
	CARBO	3275	1590	-	-
	OXALI	3704	1333	-	-
UKF-NB-6^{r}CDDP^{2000}	CDDP	9634	3579	19.9	8.5
	CARBO	29123	11157	9.6	3.2
	OXALI	8859	4500	2.4	0.6
UKF-NB-6^{r}CARBO^{2000}	CDDP	6211	2122	12.9	5.7
	CARBO	23829	6291	8.5	3.8
	OXALI	14086	5958	4.1	1.7
UKF-NB-6^{r}OXALI^{4000}	CDDP	2125	991	3.9	0.7
	CARBO	12079	4445	4.0	1.3
	OXALI	18033	6710	5.1	1.5

Table 14. Drug sensitivity profiling of the four UKF-NB-6 neuroblastoma cell lines with cisplatin, carboplatin and oxaliplatin by MTT assay: IC_{50} values and Fold differences. The table shows IC_{50} values for each cell line for each drug and fold differences of the IC_{50}s of the resistant sub-lines with each drug divided by the IC_{50} values for the same drug with the parental cell line. Fold differences below 2.0 were classed as no resistance. Data are the mean of five biological repeats with standard deviation.

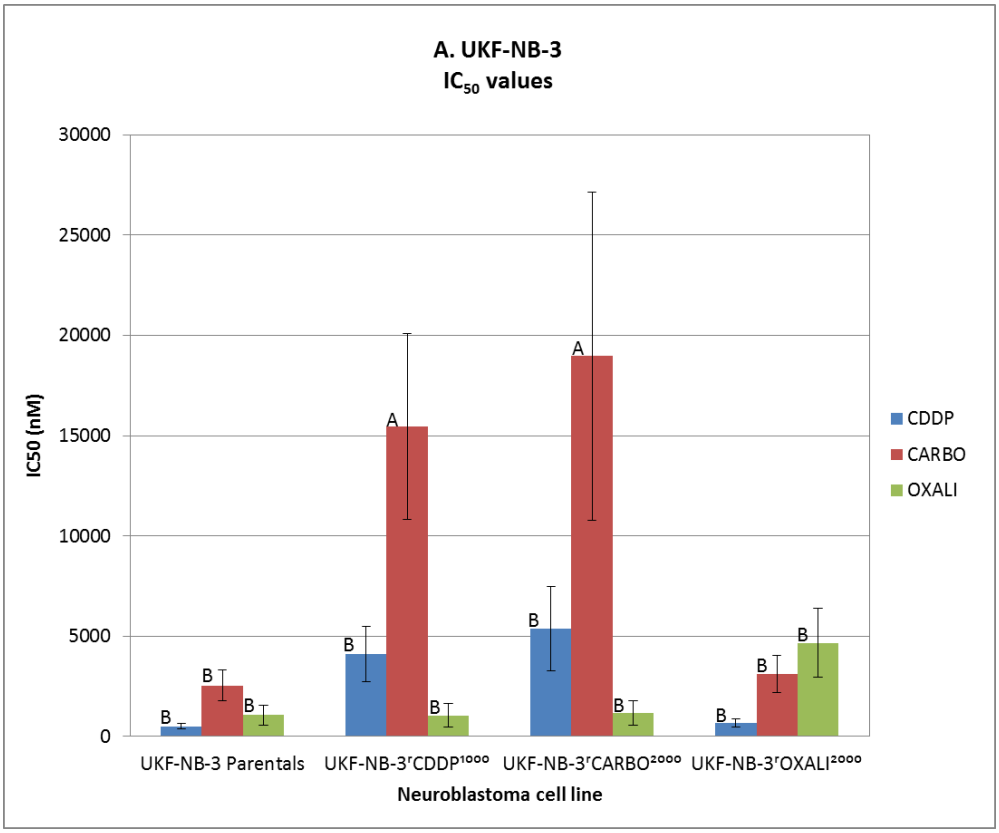

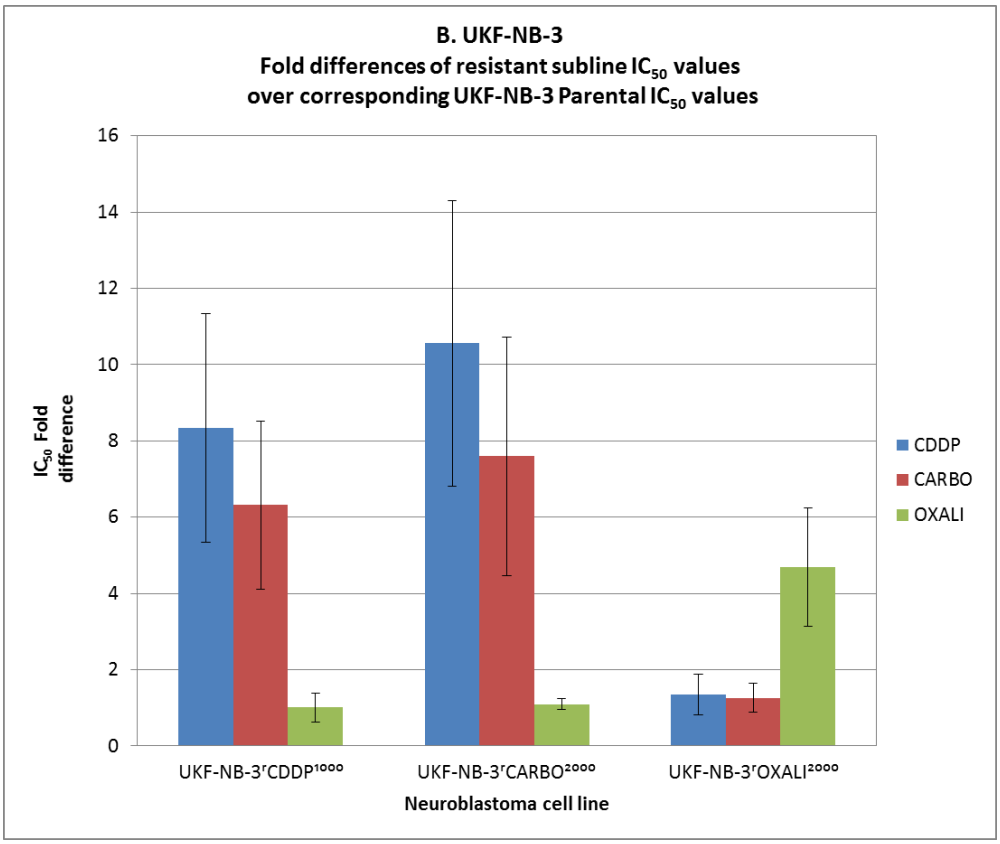

Figure 33. Drug sensitivity profiling of the four UKF-NB-3 neuroblastoma cell lines with cisplatin, carboplatin and oxaliplatin using the MTT assay: IC_{50} values and Fold differences. A. IC_{50} values for each cell line for each drug. Letters on bars represent grouping from ANOVA one-way analysis with post-hoc Tukey test, using individual 95 % CIs for mean IC_{50} based on pooled STDEV: means that do not share a letter are significantly different. B. The fold differences of the IC_{50}s (as in A) of the resistant sub-lines with each drug divided by the IC_{50} values (as in A) for the same drug with the parental cell line. For both A and B, data are the mean of five biological repeats; error bars represent standard deviation.

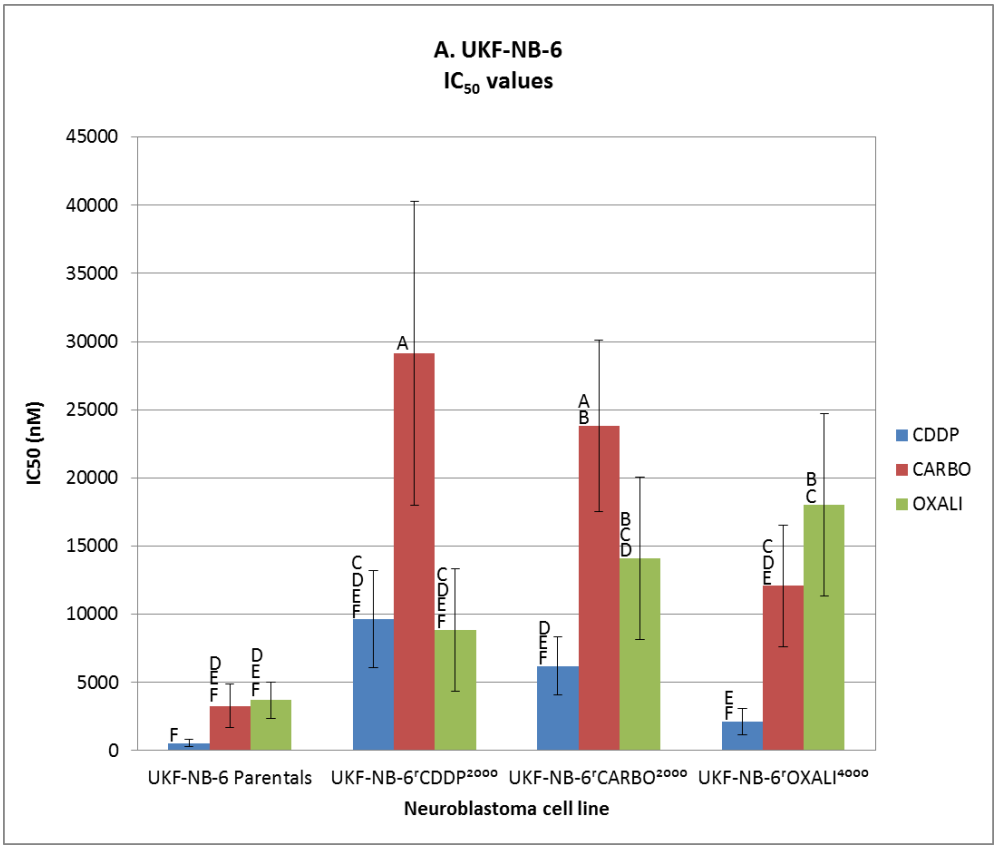

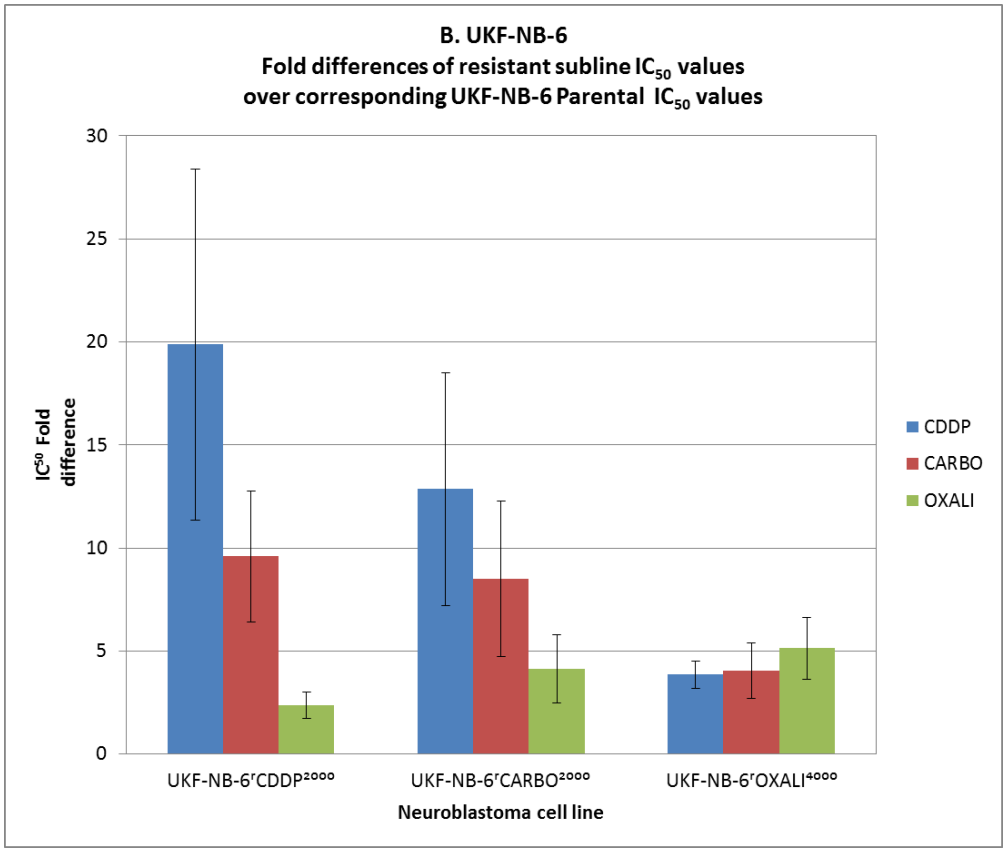

Figure 34. Drug sensitivity profiling of the four UKF-NB-6 neuroblastoma cell lines with cisplatin, carboplatin and oxaliplatin using the MTT assay: IC_{50} values and Fold differences. A. IC_{50} values for each cell line for each drug. Letters on bars represent grouping from ANOVA one-way analysis with post-hoc Tukey test, using individual 95 % CIs for mean IC_{50} based on pooled STDEV: means that do not share a letter are significantly different. B. The fold differences of the IC_{50}s (as in A) of the resistant sub-lines with each drug divided by the IC_{50} values (as in A) for the same drug with the parental cell line. For both A and B, data are the mean of five biological repeats; error bars represent standard deviation.

4.2.1.4 Assessment of culturing drug resistant cell lines with and without drug

To investigate the stability of the resistance phenotype of the UKF-NB-3 and UKF-NB-6 platinum drug resistant sub-lines in the absence of drug, they were cultured both with and without drug for three months. The parental cell lines were also cultivated alongside them. IC_{50} values were determined monthly for each drug with each cell line (4.1.6). Data for UKF-NB-3 and UKF-NB-6 cell lines were plotted separately in Figure 35 and Figure 36 respectively. These figures show time plots for IC_{50} values from all cell lines for cisplatin (A), carboplatin (B), and oxaliplatin (C), and additionally the fold differences (IC_{50} values for the cell lines cultured without drug divided by the corresponding IC_{50} values for the same cell lines cultured with drug) for cisplatin (D), carboplatin (E) and oxaliplatin (F).

A degree of variability in the MTT assay can be observed in the IC_{50} plots A, B and C for the UKF-NB-3 cell lines, but generally over the 3 months the IC_{50} values are stable. Regarding the fold differences in D, E and F, there is a decreasing trend for the UKF-NB-3^{r}CDDP^{1000} and UKF-NB-3^{r}OXALI^{2000} cell lines for each of the three platinum drugs, which could be translated as loss in drug resistance and cross resistance. However, the fold differences do not drop far below 1, thus giving no strong suggestion of a loss of resistance or cross-resistance of any cell line. Overall, the fold differences for Figure 35D, E and F ranged from 0.78 to 2.19. The four fold difference points that were over 1.5 can be explained by the variation in the corresponding IC_{50} values plotted in the corresponding IC_{50} plots. Assay variability was observed more so in the UKF-NB-6 IC_{50} plots in Figure 36A, B and C. However, the IC_{50} values for each cell line cultured without drug generally trend with the IC_{50} values for the corresponding cell line cultured with drug (Figure 36A, B and C). Therefore the fold differences plots (Figure 36D, E and F) all trended around the values of 1, suggesting no loss of resistance. A downward trend and the lowest fold difference (0.54) at month 3 was observed for the UKF-NB-6^{r}CDDP^{2000} cell line versus cisplatin in Figure 36D, however on referring to the cisplatin IC_{50} plot Figure 36A, this can be explained by a variable increase in IC_{50} of the UKF-NB-6^{r}CDDP^{2000} cell line + CDDP cell line versus cisplatin at the 3 month time point. Overall, the fold differences for Figure 36 plots D, E and F ranged from 0.54 to 1.43.

Taking into account variability of the MTT assay, there was no strong evidence that there was a loss of resistance for any of the UKF-NB-3 or UKF-NB-6 drug resistant sub-lines over three months of being cultured without drug. Hence resistance does not appear to be caused by the reversible enrichment of previously existing drug-resistant cell populations, but more likely that an irreversible genomic change occurred. .

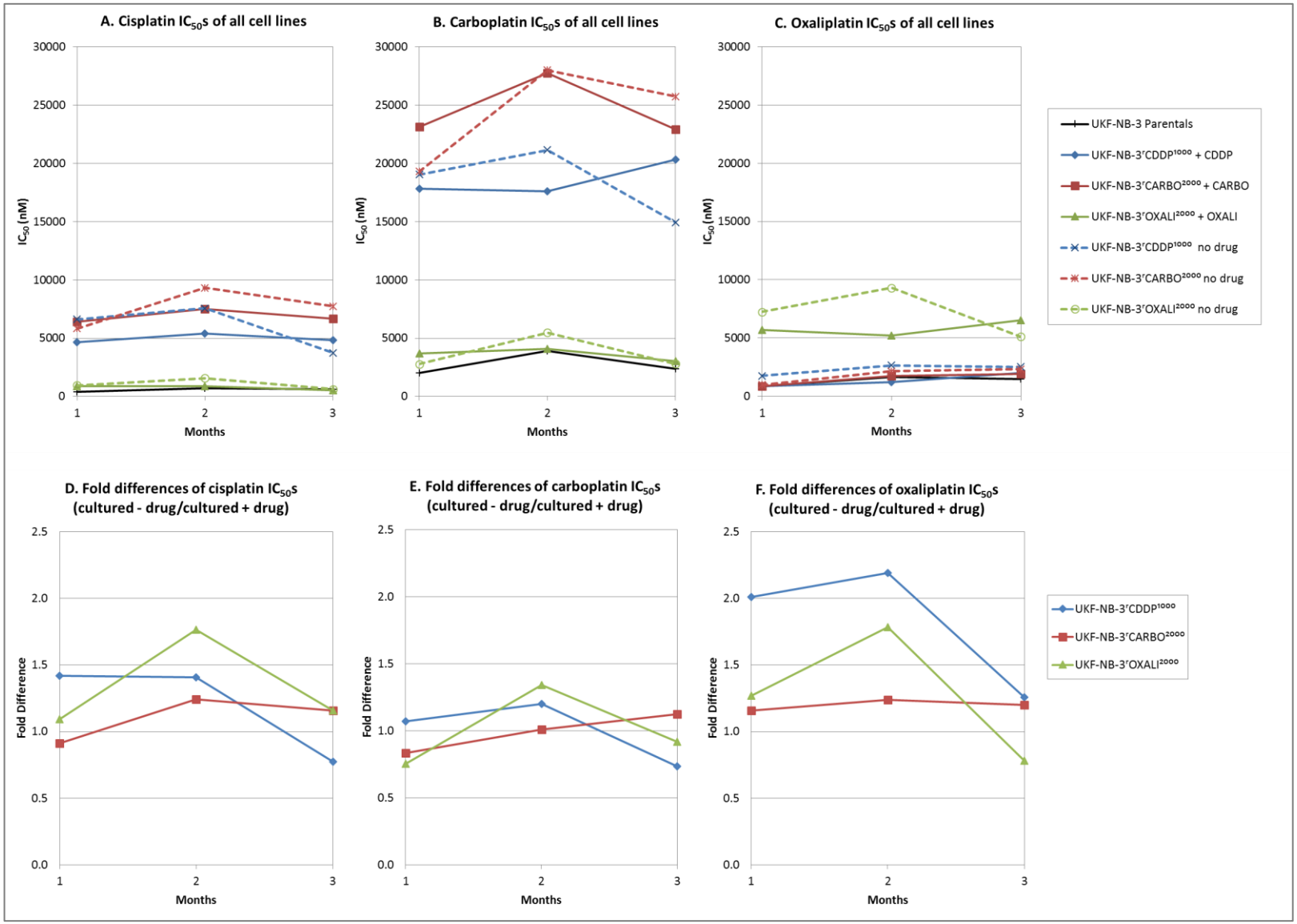

Figure 35. Assessment of culturing UKF-NB-3 drug resistant cell lines with and without drug for three months. Each month, by MTT assay, one biological repeat of IC_{50} values were generated for each cell line with each of the platinum drugs cisplatin, carboplatin, and oxaliplatin. Line graphs of the actual IC_{50} values for all cell lines are plotted over time for cisplatin (A), carboplatin (B), and oxaliplatin (C). Line graphs of the IC_{50} values for the cell lines cultured without drug expressed as a fold difference over the corresponding IC_{50} values for the same cell lines that were cultured with drug (by dividing the former by the latter) are plotted over time for cisplatin (D), carboplatin (E) and oxaliplatin (F).The key shows the cell line and the drug they were continuously cultured with or if not cultured with drug.

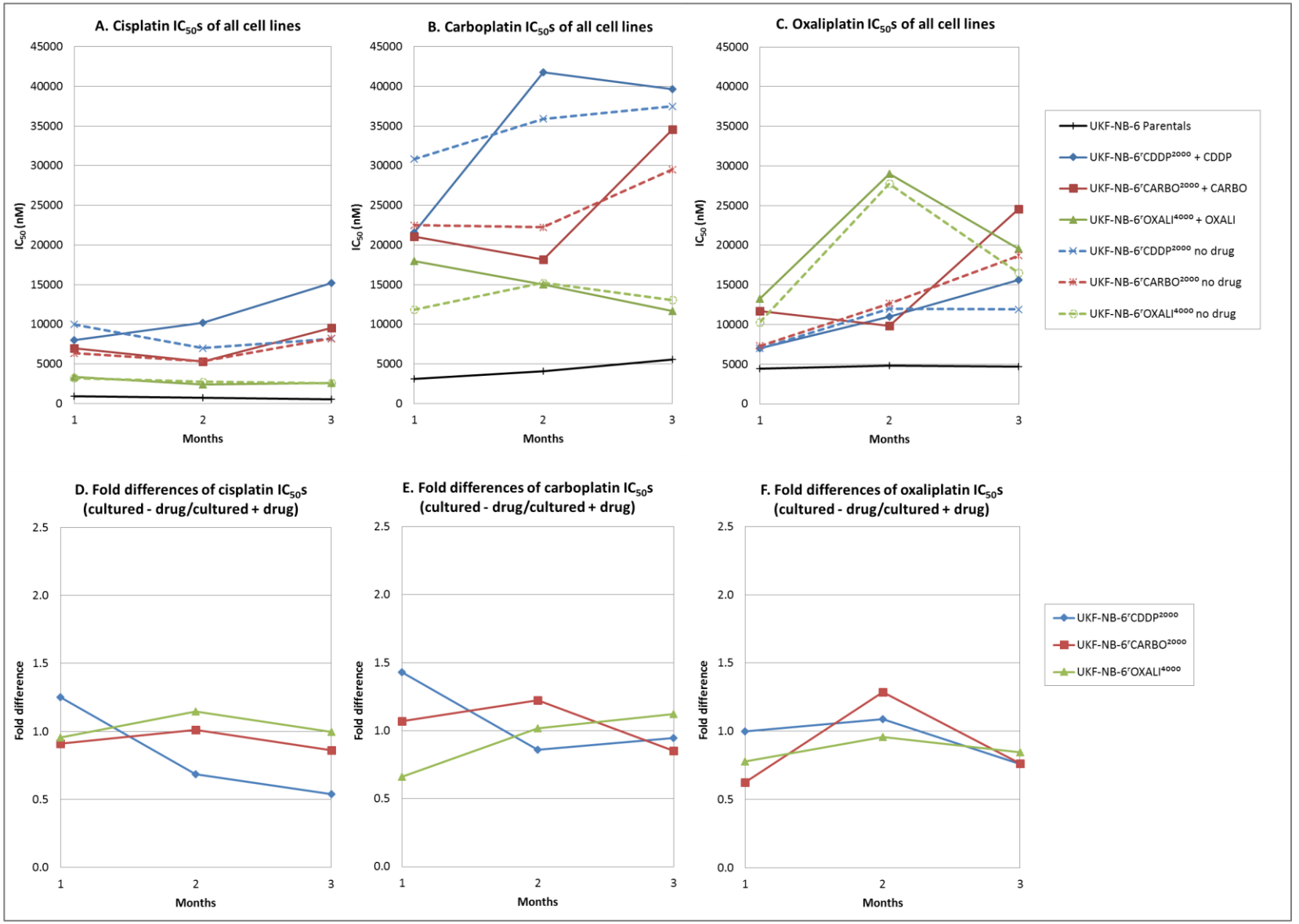

Figure 36. Assessment of culturing UKF-NB-6 drug resistant cell lines with and without drug for three months. Each month, by MTT assay, one biological repeat of IC_{50} values were generated for each cell line with each of the platinum drugs cisplatin, carboplatin, and oxaliplatin. Line graphs of the actual IC_{50} values for all cell lines are plotted over time for cisplatin (A), carboplatin (B), and oxaliplatin (C). Line graphs of the IC_{50} values for the cell lines cultured without drug expressed as a fold difference over the corresponding IC_{50} values for the same cell lines that were cultured with drug (by dividing the former by the latter) are plotted over time for cisplatin (D), carboplatin (E) and oxaliplatin (F). The key shows the cell line and the drug they were continuously cultured with or if not cultured with drug.

4.2.2 Proteomics

4.2.2.1 Overview

Proteomics is the large-scale study of the expression, localisations, functions, and interactions of the entire complement of proteins (the proteome) expressed by a cell, tissue or organism at a given time. Proteomics methodology was used to investigate the acute and adaption effects of cisplatin on the neuroblastoma proteome (4.1.7) using the UKF-NB-3 parental and UKF-NB-3^{r}CDDP^{1000} cell lines, and the UKF-NB-6 parental and UKF-NB-6^{r}CDDP^{2000} cell lines. Regarding the toxicity of cisplatin in these cells and the levels of resistance of the sub-lines, the UKF-NB-3 parental and UKF-NB-3^{r}CDDP^{1000} cell lines have mean (n=5) cisplatin IC_{50} values of 511 and 4129 nM respectively, with a mean (n=5) fold difference of 8.3; the UKF-NB-3^{r}CDDP^{1000} cell line is maintained in continuous culture with cisplatin at 3333 nM (1000 ng/mL) in the medium. The UKF-NB-6 parental and UKF-NB-6^{r}CDDP^{2000} cell lines have mean (n=5) cisplatin IC_{50} values of 556 and 9634 nM respectively, with a mean (n=5) fold difference of 19.9; the UKF-NB-6^{r}CDDP^{2000} cell line is maintained in continuous culture with cisplatin at 6666 nM (2000 ng/mL) in the medium (refer to both 4.2.1.3 and 4.1.2.2). Using the MTT assay (4.1.5), time kinetics of response to cisplatin were generated (courtesy of Joanna Bird) for UKF-NB-3 parental and UKF-NB-3^{r}CDDP^{1000} cell lines (1000 ng/mL cisplatin), and the UKF-NB-6 parental and UKF-NB-6^{r}CDDP^{2000} (2000 ng/mL cisplatin) (Figure 37). For this, to simulate the proteomics study (see below), cell lines were grown for 120 hours (at which point MTT reagent was added) with no drug to 60-90 % confluency, and drug was added individually for 2, 8, 24 or 48 hour timepoints prior to adding MTT reagent.

Two studies were set up, one using the UKF-NB-3 parental and UKF-NB-3rCDDP^{1000} cell lines, and the other using the UKF-NB-6 parental and UKF-NB-6^{r}CDDP^{2000} cell lines. For each study a total of three separate drug addition time course experiments were carried out, except for the UKF-NB-3 parental and UKF-NB-3rCDDP^{1000} 2 hour drug addition timepoints only, for which there were two (4.1.7.1). The time course experiments were named 3rd, 5th and 4th runs for the UKF-NB-3 studies, and n1, n2 and n3 for the UKF-NB-6 study. Cell lines were grown for 120 hours with no drug to 60-90 % confluency. Cisplatin (using the 1 mg/mL stocks prepared as described in 4.1.1) was added at concentrations of 1000ng/mL for the UKF-NB-3 cells and 2000 ng/mL for the UKF-NB-6 cells at 24, 8, and 2 hours prior to harvesting, but no drug was added to control cells (0 hours); note that for the UKF-NB-3 n1 (3rd run) study, there was no 2 hour drug addition time point. Cells were lysed (4.1.7.2), protein content was determined (4.1.7.3), and samples analysed by 2D gel electrophoresis (4.1.7.4). The resulting gels were scanned and images were analysed using Progenesis Samespots software (4.1.7.5), with experiments set up within the software that

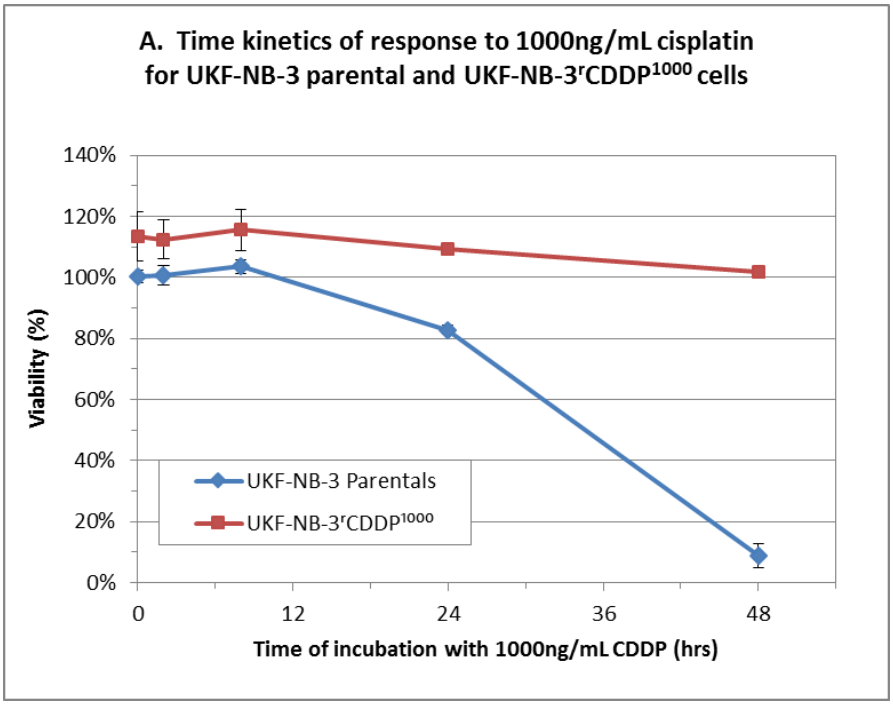

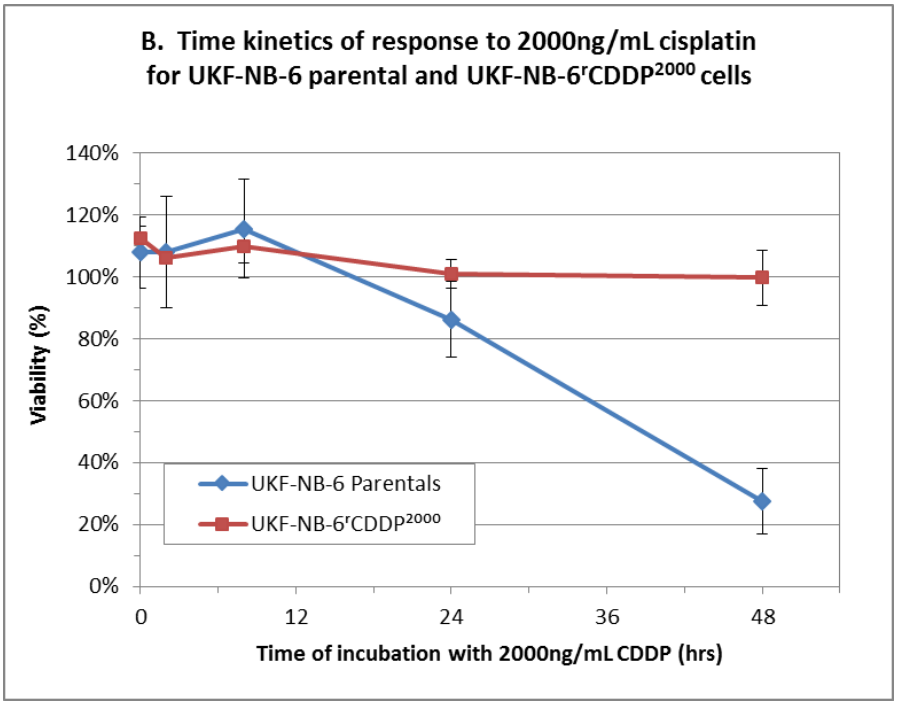

Figure 37. Time kinetics of response to cisplatin for A. UKF-NB-3 parental and UKF-NB-3^{r}CDDP^{1000} cell lines after treatment with 1000 ng/mL cisplatin, and B. UKF-NB-6 parental and UKF-NB-6^{r}CDDP^{2000} cell lines after treatment with 2000 ng/mL cisplatin. The data for these curves was generated by MTT assay (4.1.5). UKF-NB-3 parental and UKF-NB-3^{r}CDDP^{1000} lines were seeded at 3000 cells/well and UKF-NB-6 parental and UKF-NB-6^{r}CDDP^{2000} were seeded at 4000 cells/well in 96 well plates in 100 µL/well media in MTT assay, and grown for 120 hours with no drug to 60-90 % confluency and then MTT reagent was added. Cells were treated with cisplatin for 2, 8, 24 and or 48 hours and cell viability was determined relative to untreated control. Data are the mean of three biological repeats; error bars represent standard deviation. This data is courtesy of Joanna Bird. Our studies investigating the acute effects of cisplatin treatment in the same cell lines (4.2.2.4) were carried out over 24 hours.

compared the sets of gels from the different drug addition time points as follows (vs = versus, CDDPr = cisplatin resistant):

Identification of changes associated with cisplatin acquired resistance;

Non-treated parental lines vs respective non-treated cisplatin resistant sub-lines

Parentals 0 hour control vs CDDPr 0 hour control

Identification of acute cisplatin effects in the parental cell lines and the cisplatin resistant cells; Non-treated parental cell lines vs parental cell line after 2, 8, or 24 hours of incubation with cisplatin

Parentals 0 hour con vs Parentals 2 hour

Parentals 0 hour con vs Parentals 8 hour

Parentals 0 hour con vs Parentals 24 hour

Non-treated cisplatin resistant sub-lines vs cisplatin resistant sub-lines after 2, 8, or 24 hours of incubation with cisplatin

CDDPr 0 hour control vs CDDPr 2 hour

CDDPr 0 hour control vs CDDPr 8 hour

CDDPr 0 hour control vs CDDPr 24 hour

For archived Progenesis Samespots files for the UKF-NB-3 and UKF-NB-6 studies refer to the disc provided. Note that for the UKF-NB-3 study, we selected the gel named '020813 4 5th run NB3 Par 0 hr 73670 600dpi1' as the reference gel, and the software selected the gel named '020813 8 5th run NB3r CDDP 0hr 73675 600dpi0' for normalisation. For the UKF-NB-6 study, we selected the gel named 'n1 NB6par0h_020713_73683-600' as the reference gel, and the software selected the gel named 'n2 NB6rcis0hh_090713_73931_600dpi' for normalisation.

The criteria for selection of spots from the above comparisons were, using the average normalised spot volumes for one spot in each condition, that the ANOVA p-value was <0.05, and that the Fold increase value (the highest mean normalised spot volume/lowest mean spot volume) was ≥1.5 (to 1 decimal place), and that the spot had reliable alignment and appearance on each gel (4.1.7.5).

4.2.2.2 Summary of all identified proteins

48 spots (out of 574 per gel) indicated differences in protein levels for at least one comparison in the UKF-NB-3 cell lines and 32 spots (out of 675 per gel) indicated differences in protein levels for at least one comparison in the UKF-NB-6 cell lines. These spots were excised (4.1.7.6.1) from two different gels and then tryptically digested and extracted from the gel pieces (4.1.7.6.2). Each protein sample was subjected to the mass spectroscopy analytical methods MALDI-TOF MS (to

generate Protein mass fingerprints (PMF)) and MALDI-TOF-TOF MS/MS (to generate peptide fragment fingerprints (PFF)) (4.1.7.7). Protein identity was determined based on the resulting MS and MS/MS fingerprints which were searched against the human protein SwissProt database (http://www.uniprot.org/) (version 2014_01, and version 2014_03 for repeats), and the human protein NCBInr database (version 20140122, and version 20140323 for repeats) (http://www.ncbi.nlm.nih.gov/refseq/) (4.1.7.7.4). Subsequent data handling is described in detail in 4.1.7.7.4, and the resulting tables can be seen in Appendix I and J.

Of the 48 spots excised from the UKF-NB-3 study, 11 of these were recut from other gels and analysed again due to unsure identifications for which a re-cut could possibly help to achieve a definite identification, for which one did. Ultimately, the result was 20 definite identifications, 12 that were identified as keratin or that had no identification, and 16 unsure identifications. Of the 32 spots excised spots from the UKF-NB-6 study, 8 of these were recut from other gels and analysed again, although none achieved a definite identification. Ultimately, the result was 14 definite identifications, 4 that were identified as keratin or that had no identification, and 15 unsure identifications. Images of all spot n numbers for the 20 UKF-NB-3 study spots and 14 UKF-NB-6 study spots that were definitely identified (and what gels they were excised from) are shown in Appendix K and Appendix L respectively, tables showing normalised spot volumes and expression ratios are shown in Appendix M and Appendix N respectively. The original 2D SDS-PAGE (4.1.7.4.4) gel positions of these identified spots are shown for the UKF-NB-3 study in Figure 38 and for the UKF-NB-6 study in Figure 39 (on the pre-mentioned study reference gels).

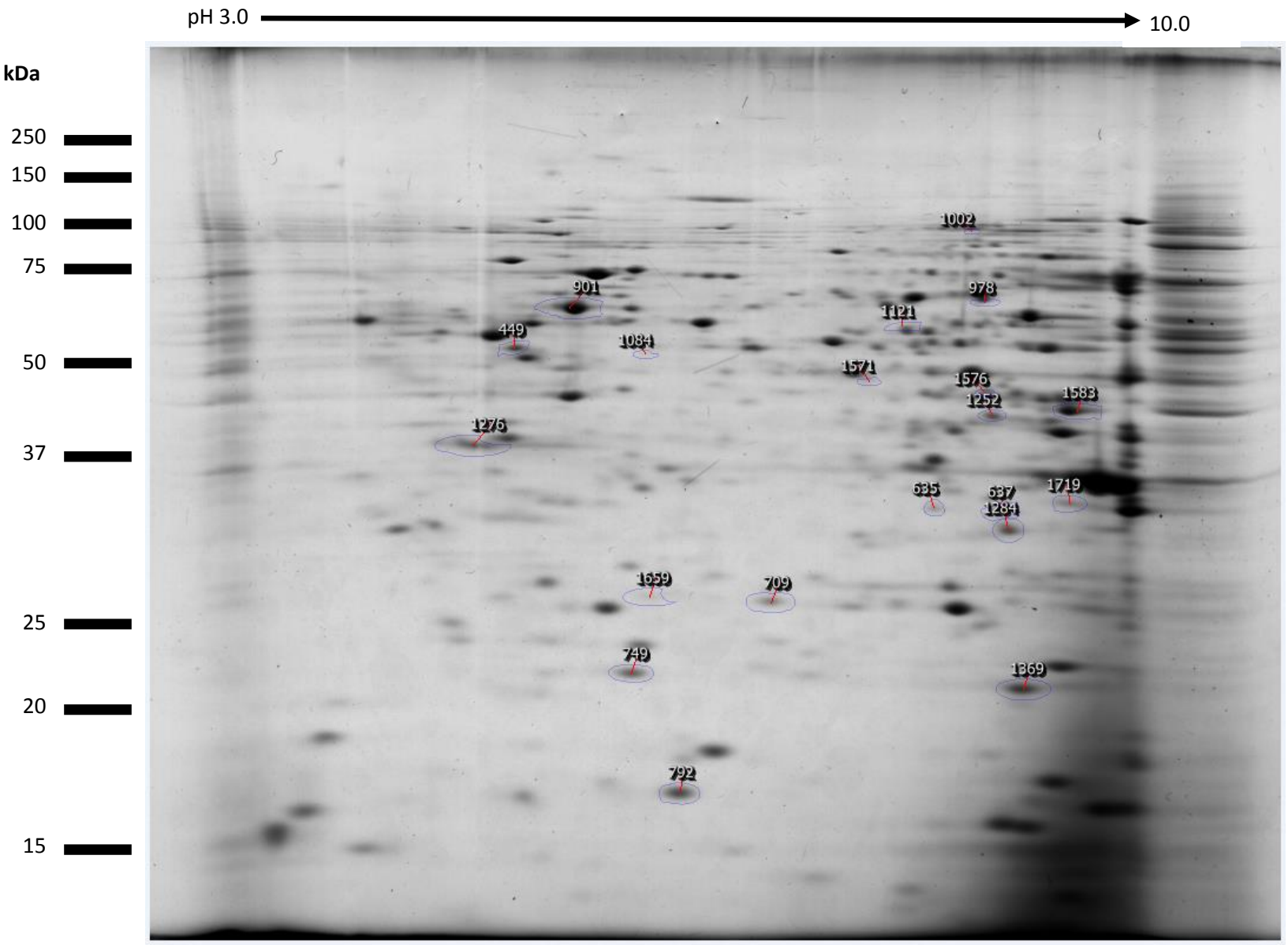

Figure 38. A 2D gel electrophoresis image showing the spot positions of the 20 proteins (pH 3 -10) resulting from the UKF-NB-3 study (4.1.7) that were excised and had definite identifications using mass spectroscopy methods and MASCOT searches of the the human protein Swiss-Prot and NCBInr databases. The gel shown is the selected reference gel '020813 4 5th run NB3 Par 0 hr 73670 600dpi1'.

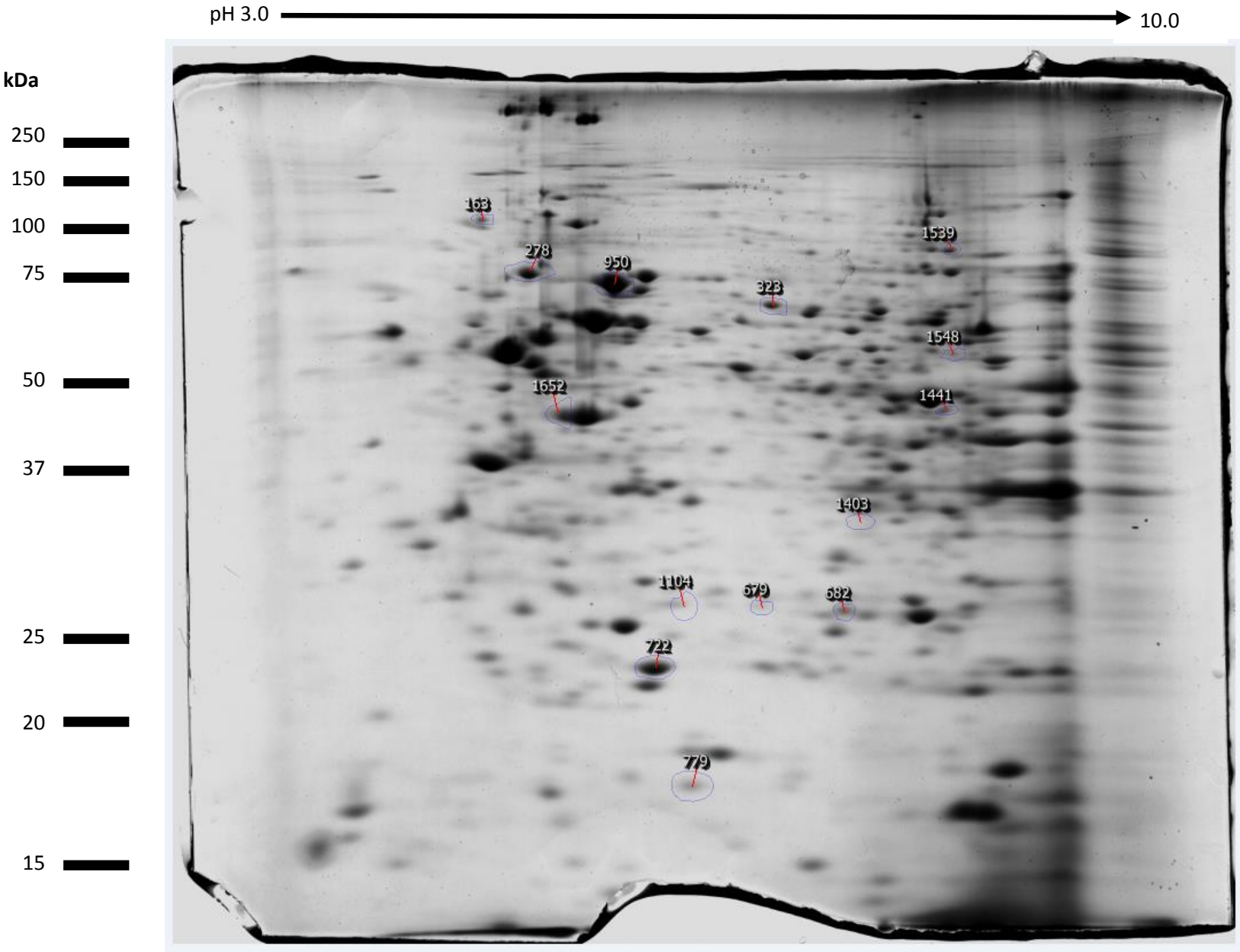

Figure 39. A 2D gel electrophoresis image showing the spot positions of the 14 proteins (pH 3-10) resulting from the UKF-NB-6 study (4.1.7) that were excised and had definite identifications using mass spectroscopy methods and MASCOT searches of the the human protein Swiss-Prot and NCBInr databases. The gel shown is the selected reference gel 'n1 NB6par0h_020713_73683-600'.

Table 15 and Table 16 are summary results tables for the twenty UKF-NB-3 and fourteen UKF-NB-6 identified proteins respectively. In these tables the spots are listed alongside their identified protein names, and with their Uniprot KB accession number and Uniprot KB name taken from the UNiprot knowledge base (http://www.uniprot.org/). The mature length of the proteins were also taken from Uniprot, and their theoretical average molecular weight (Mr) and theoretical isoelectric points were calculated from the mature length protein using the Compute pI/MW option. The gel positions of the identified proteins (Figure 38 and Figure 39) coincide with their expected positions with regard to their calculated molecular weights and pI values (Table 15 and Table 16). Minor variations were most likely due to post-translational modifications such as glycosylation, phosphorylation, and deamidation (Halligan, Ruotti et al. 2004). In Table 15 and Table 16 the mean normalised spot volumes for each set of gels are categorised into the highest or lowest for each comparison (see Appendix M and Appendix N for the individual and mean normalised spot volumes). This information, along with the ANOVA (p) and Fold increase (the highest mean normalised spot volume for the comparison expressed over the lowest mean normalised spot volume) originate from the Progenesis Samespots analysis. We have also expressed the mean spot volumes as a fold change ratio over the parental control cell lines (Par 0hr) for both the acquired cisplatin resistance study and the acute effects of cisplatin study in the parental cells, and then over the drug resistant control cell lines (CDDPr 0hr) for the acute effects of cisplatin study in the cisplatin resistant sub-lines. We shall focus on these fold change ratios rather than the fold increase values, Fold change ratios below 1.0 signified downregulation and above 1.0 upregulation of protein expression. Summarised roles were put together using Appendix O and Appendix P, where the main roles and matched Gene Ontology (GO) molecular function, biological process and cellular component terms (excluding those inferred by electronic annotation) are tabulated; all of this information was taken from UniProt Knowledge base (http://www.uniprot.org/).

Spot #	Protein name	Gene	UniprotKB accession #	UniprotKB name	Mature length (total length)	Average Mr *th* (Kda)	PI *th*	Highest mean normalised spot volume	Lowest mean normalised spot volume	Anova (p)	Fold increase (highest mean normalised spot volume/lowest mean spot volume)	Fold change ratio of mean normalised spot volumeas expressed / ….	Summarised role
Acquired cisplatin resistance												… Par 0hr	
749	Peroxiredoxin-2	PRDX2	P32119	PRDX2_HUMAN	2-198 (198)	21.8	5.67	Par 0hr	CDDPr 0hr	0.00847	2.04	0.49	Redox regulation, growth factor signalling, negative regulator of apoptosis
1369	Phosphatidylethanolamine-binding protein 1 / Neuropolypeptide h3	PEBP1	P30086	PEBP1_HUMAN	2-187 (187)	20.9	7.43	Par 0hr	CDDPr 0hr	0.02023	1.85	0.54	Enzyme inhibitor, neuronal function, promotes apoptosis, immune reponse
792	Stathmin	STMN1	P16949	STMN1_HUMAN	2-149 (149)	17.2	5.76	Par 0hr	CDDPr 0hr	0.04705	1.73	0.58	Microtubule regulation, signal transduction
978	Dihydropyrimidinase-related protein 5 /Collapsin response mediator protein-5	DPYSL5	Q9BPU6	DPYL5_HUMAN	1-564 (564)	61.4	6.73	Par 0hr	CDDPr 0hr	0.00170	1.71	0.58	Neuronal system development
635	S-formylglutathione hydrolase /Esterase D	ESD	P10768	ESTD_HUMAN	2-282 (282)	31.3	6.58	Par 0hr	CDDPr 0hr	0.03761	1.67	0.60	Detoxification of formaldehyde
709	Heat shock protein beta-1 /heat shock protein 27	HSPB1	P04792	HSPB1_HUMAN	1-205 (205)	22.8	5.98	CDDPr 0hr	Par 0hr	0.00525	2.72	2.72	Chaperone, stress resistance and actin organisation, immune response, negative regulator of apoptosis
1659	Heat shock protein beta-1 /heat shock protein 27	HSPB1	P04792	HSPB1_HUMAN	1-205 (205)	22.8	5.98	CDDPr 0hr	Par 0hr	0.01586	2.24	2.24	Chaperone, stress resistance and actin organisation, immune response, negative regulator of apoptosis
1719	Lactate dehydrogenase, A chain *	LDHA	P00338	LDHA_HUMAN	2-332 (332)	36.6	8.46	CDDPr 0hr	Par 0hr	0.01305	2.07	2.07	Carbohydrate metabolism
1276	Nucleophosmin **	NPM1	P06748	NPM_HUMAN	1-294 (294)	32.6	4.64	CDDPr 0hr	Par 0hr	0.01315	2.09	2.09	Chaperone, ribosome biogenesis, cell proliferation, DNA repair, tumour suppressor regulation, negative regulator of apoptosis
1571	Eukaryotic initiation factor 4A-III/Translation initiation factor	EIF4A3	P38919	IF4A3_HUMAN	1-411 (411)	46.9	6.30	CDDPr 0hr	Par 0hr	0.02673	1.93	1.93	Regulation of translation, mRNA metabolism, negative regulator of apoptosis
1583	Phosphoglycerate kinase 1	PGK1	P00558	PGK1_HUMAN	2-417 (417)	44.5	8.3	CDDPr 0hr	Par 0hr	0.00045	1.72	1.72	Carbohydrate metabolism, DNA replication
901	60 kDa heat shock protein, mitochondrial	HSPD1	P10809	CH60_HUMAN	27-573 (573)	58.0	5.24	CDDPr 0hr	Par 0hr	0.03634	1.50	1.50	Chaperone, stress resistance, mitochondrial protein import, regulation of apoptosis, immune reponse
1121	D-3-phosphoglycerate dehydrogenase	PHGDH	O43175	SERA_HUMAN	2-533 (533)	56.5	6.31	CDDPr 0hr	Par 0hr	0.02027	1.53	1.53	L-serine biosynthesis
Acute effects of cisplatin in cisplatin sensitive parental cells												… Par 0hr	
1084	RuvB-like 2	RUVBL2	Q9Y230	RUVB2_HUMAN	2-463 (463)	51.0	5.49	Par 2hr	Par 0hr	0.00357	1.67	1.67	Pos regulator of transcription; activation of cell proliferation, apoptosis, DNA repair and replication, negatively regulates expression of ER stress response genes (ERAD)
1276	Nucleophosmin **	NPM1	P06748	NPM_HUMAN	1-294 (294)	32.6	4.64	Par 8hr	Par 0hr	0.02465	1.61	1.61	Chaperone, ribosome biogenesis, cell proliferation, DNA repair, tumour suppressor regulation, negative regulator of apoptosis
449	ATP synthase subunit beta, mitochondrial	ATP5B	P06576	ATPB_HUMAN	48-529 (529)	51.8	5.00	Par 24hr	Par 0hr	0.02593	1.52	1.52	Cellular metabolism
Acute effects of cisplatin in corrresponding cisplatin resistant cells												… CDDPr 0hr	
1576	26S protease regulatory subunit 8 /Thyroid receptor interactor	PSMC5	P62195	PRS8_HUMAN	2-406 (406)	45.5	7.27	CDDPr 2hr	CDDPr 0hr	0.02232	1.58	1.58	Protein degradation
637	Voltage-dependent anion-selective channel protein 2	VDAC2	P45880	VDAC2_HUMAN	2-294 (294)	31.4	7.66	CDDPr 2hr	CDDPr 0hr	0.03104	1.61	1.61	Anion transport across the mitochondrial outer membrane, role in apoptosis
1284	Guanine nucleotide-binding protein subunit beta-2-like 1	GNB2L1	P63244	GBLP_HUMAN	1-317 (317)	35.1	7.60	CDDPr 2hr	CDDPr 0hr	0.04154	1.55	1.55	Cell signalling; repression of transcription and translation, protein turnover, protein transport, cell proliferation, promotes migration, promotes apoptosis
1252	26S protease regulatory subunit 10B /Proteasome subunit p42	PSMC6	P62333	PRS10_HUMAN	1-389 (389)	44.2	7.09	CDDPr 2hr	CDDPr 0hr	0.00522	1.54	1.54	Protein degradation
1002	Elongation factor 2	EEF2	P13639	EF2_HUMAN	2-858 (858)	95.2	6.42	CDDPr 0hr	CDDPr 24hr	0.01506	2.41	0.41	Translation elongation
1719	Lactate dehydrogenase , A chain *	LDHA	P00338	LDHA_HUMAN	2-332 (332)	36.6	8.46	CDDPr 0hr	CDDPr 24hr	0.03580	1.88	0.53	Carbohydrate metabolism

Table 15 The twenty identified UKF-NB-3 excised spots and their results for each comparison experiment in decreasing order of fold increase. For legend refer to Table 16 legend.

Spot #	Protein name	Gene	UniprotKB accession #	UniprotKB name	Mature length (total length)	Average Mr *th* (Kda)	PI *th*	Highest mean normalised spot volume	Lowest mean normalised spot volume	Anova (p)	Fold increase (highest mean normalised spot volume/lowest mean spot volume)	Fold change ratio of mean normalised spot volumeas expressed / ….	Summarised role
Acquired cisplatin resistance												… Par 0hr	
323	Dihydropyrimidinase-related protein 2	DPYSL2	Q16555	DPYL2_HUMAN	1-152 (152)	62.3	5.95	Par 0hr	CDDPr 0hr	0.00402	1.77	0.56	Neuronal system development, cytoskeleton remodelling for neuronal growth cone collapse and cell migration, endocytocis
722	Glutathione S-transferase P	GSTP1	P09211	GSTP1_HUMAN	2-210 (210)	23.2	5.44	Par 0hr	CDDPr 0hr	0.02040	1.72	0.58	Redox regulation, prevents neurodegeneration, negative regulator of apoptosis and proliferation
682	Proteasome subunit alpha type-6 /Macropain subunit iota *	PSMA6	P60900	PSA6_HUMAN	1-246 (246)	27.4	6.34	Par 0hr	CDDPr 0hr	0.00383	1.55	0.64	Protein degradation
1652	Actin cytoplasmic 1	ACTB	P60709	ACTB_HUMAN	1-375 (375)	41.7	5.29	Par 0hr	CDDPr 0hr	0.01803	1.50	0.66	Cell motility and cellular component organisation
679	Heat shock protein beta-1 /heat shock protein 27	HSPB1	P04792	HSPB1_HUMAN	1-205 (205)	22.8	5.98	CDDPr 0hr	Par 0hr	0.00409	2.35	2.35	Chaperone, stress resistance and actin organisation, immune response, negative regulator of apoptosis
779	Stathmin	STMN1	P16949	STMN1_HUMAN	2-149 (149)	17.2	5.76	CDDPr 0hr	Par 0hr	0.03179	2.24	2.24	Microtubule regulation, signal transduction
1403	Voltage-dependent anion-selective channel protein 2 (VDAC2)	VDAC2	P45880	VDAC2_HUMAN	2-294 (294)	31.4	7.66	CDDPr 0hr	Par 0hr	0.00009	1.97	1.97	Anion transport across the mitochondrial outer membrane, role in apoptosis
1441	26S protease regulatory subunit 8 /Thyroid receptor interactor **	PSMC5	P62195	PRS8_HUMAN	2-406 (406)	45.5	7.27	CDDPr 0hr	Par 0hr	0.01223	1.77	1.77	Protein degradation
1548	Pyruvate kinase (PKM) ***	PKM	P14618	KPYM_HUMAN	2-531 (531)	57.8	7.95	CDDPr 0hr	Par 0hr	0.02274	1.83	1.83	Carbohydrate metabolism, tumour cell proliferation and survival, role in caspase independent death of tumour cells
1539	Aconitate hydratase, mitochondrial	ACO2	Q99798	ACON_HUMAN	28-780 (780)	85.4	7.36	CDDPr 0hr	Par 0hr	0.00915	1.62	1.62	Carbohydrate metabolism
Acute effects of cisplatin in cisplatin sensitive parental cells												… Par 0hr	
163	Endoplasmin	HSP90B1	P14625	ENPL_HUMAN	22-803 (803)	90.2	4.73	Par 0hr	Par 2hr	0.04190	1.70	0.59	Chaperone; folding and transport of secreted proteins and Toll like receptors, ERAD, negative regulator of apoptosis
682	Proteasome subunit alpha type-6 /Macropain subunit iota *	PSMA6	P60900	PSA6_HUMAN	1-246 (246)	27.4	6.34	Par 0hr	Par 2hr	0.02157	1.45	0.69	Protein degradation
950	Heat shock cognate 71 kDa protein	HSPA8	P11142	HSP7C_HUMAN	2-646 (646)	70.8	5.37	Par 0hr	Par 8hr	0.00703	1.60	0.62	Repressor of transcriptional activation, chaperone, ERAD, component of the spliceosome
1104	Peroxiredoxin-4	PRDX4	Q13162	PRDX4_HUMAN	38-271 (271)	26.6	5.54	Par 0hr	Par 8hr	0.02249	1.47	0.68	Redox regulation
1548	Pyruvate kinase (PKM) ***	PKM	P14618	KPYM_HUMAN	2-531 (531)	57.8	7.95	Par 8 hr	Par 0hr	0.00104	1.47	1.47	Carbohydrate metabolism, tumour cell proliferation and survival, role in caspase independent death of tumour cells
278	78 kDa glucose-regulated protein	HSPA5	P11021	GRP78_HUMAN	19-654 (654)	70.5	5.01	Par 0hr	Par 24hr	0.01090	1.52	0.66	Chaperone, negative regulator of apoptosis
Acute effects of cisplatin in corrresponding cisplatin resistant cells												… CDDPr 0hr	
1548	Pyruvate kinase (PKM) ***	PKM	P14618	KPYM_HUMAN	2-531 (531)	57.8	7.95	CDDPr 0hr	CDDPr 2hr	0.02496	1.86	0.54	Carbohydrate metabolism, tumour cell proliferation and survival, role in caspase independent death of tumour cells
1441	26S protease regulatory subunit 8 /Thyroid receptor interactor **	PSMC5	P62195	PRS8_HUMAN	2-406 (406)	45.5	7.27	CDDPr 0hr	CDDPr 24hr	0.03220	1.45	0.69	Protein degradation

Table 16. The fourteen identified UKF-NB-6 excised spots and their results for each comparison experiment in decreasing order of fold increase. This legend is extended on the next page.

Table 16 legend continued. Spot # corresponds to those on the 2D gels (Figure 38 and Figure 39). Gene, Uniprot KB accession # and name, mature length of protein, Average Mr *th* (theoretical molecular weight) and PI th (theoretical isoelectric point) were all taken from the Uniprot KB (knowledge base) (http://www.uniprot.org/). Highest mean and lowest mean normalised spot volumes (see mean normalised spot volumes in Appendix M and N) for that comparison with the associated ANOVA p-value (all < 0.05) and Fold increase (all ≥1.5 to 1 decimal place), are all taken from the Progenesis Samespots analysis. Mean normalised spot volumes were also expressed as a Fold change ratio over the parental cell lines (Par 0hr) for both the acquired cisplatin resistance study and the acute effects of cisplatin study in the parental cells, and then over the cisplatin resistant control cell lines (CDDPr 0hr) for the acute effects of cisplatin study in the cisplatin resistant sub-lines. Fold change ratio values below 1.0 signified downregulation and above 1.0 upregulation of protein expression. Par = parental cell line, CDDPr = cisplatin resistant cell line, and hr values are the cisplatin addition timepoints (note no drug was added to 0 hr controls). Summarised roles have been constructed using Appendix O and P. Shaded in grey are proteins that appear in both the UKF-NB-3 and UKF-NB-6 studies; Heat shock protein beta-1, stathmin, VDAC2, and 26S protease regulatory subunit 8. Asterisks denote if a protein was a result in more than one study comparison in the table; lactate dehydrogenase, A chain (*) and nucleophosmin (**) each appear twice in Table 15 and proteasome subunit alpha type-6 (*) and 26S protease regulatory subunit 8 (**) each appear twice and pyruvate kinase (PKM) (***) appears three times in Table 16.

4.2.2.3 Investigation of changes associated with acquired cisplatin resistance

This investigation was carried out by comparing the proteomes of the non-treated parental cells to the corresponding cisplatin resistant sub-lines.

Regarding the UKF-NB-3 acquired cisplatin resistance study (top section of Table 15), there were 12 proteins found differentially regulated; 5 proteins displayed decreased levels in the UKF-NB-3^{r}CDDP^{1000} cells relative to the UKF-NB-3 parental cells (peroxiredoxin-2, phosphatidylethanolamine-binding protein 1, stathmin, dihydropyrimidinase-related protein 5, and S-formylglutathione hydrolase), and 7 proteins displayed increased levels in the UKF-NB-3^{r}CDDP^{1000} cells relative to the UKF-NB-3 parental cells (heat shock protein beta-1, lactate dehydrogenase, nucleophosmin, eukaryotic initiation factor 4A III, phosphoglycerate kinase 1, 60 kDa heat shock protein (mitochondrial), and D-3-phosphoglycerate dehydrogenase). As indicated by GO term analysis, the identified proteins are involved in many processes including chaperone activity, stress resistance, redox and detoxification, cell growth, apoptosis, DNA repair, protein turnover, carbohydrate metabolism, cytoskeletal organisation and neuronal function and development (Table 15 and Appendix O). Fold change ratio values below 1.0 signified downregulation and above 1.0 upregulation of protein expression, and we considered the largest changes in protein expression to be for proteins with a fold change ratio over the UKF-NB-3 parental cells below 0.5 or above 2.0. The redox regulator peroxiredoxin-2 was downregulated with a fold change ratio of 0.49, whilst the chaperone heat shock protein beta-1, lactate dehydrogenase (A chain), which is a player in sugar metabolism, and the multifunctional protein nucleophosmin were all upregulated with fold change ratios of 2.72/2.24, 2.07 and 2.09 respectively; note that in this study, heat shock protein beta-1 was identified as two spots appearing at different isoelectric points on the gel (Figure 38), which could be explained by differences in post-translational modifications.

Regarding the UKF-NB-6 acquired cisplatin resistance study (Table 16) there were 10 proteins that were found differentially regulated; 4 proteins displayed decreased levels in the UKF-NB-6^{r}CDDP^{2000} cells relative to the UKF-NB-6 parental cells (dihydropyrimidinase-related protein 2, glutathione S-transferase P, proteasome subunit alpha type-6, and actin cytoplasmic 1), and 6 proteins displayed increased levels in the UKF-NB-6^{r}CDDP^{2000} cells relative to the UKF-NB-6 parental cells (heat shock protein beta-1, stathmin, voltage-dependent anion-selective channel protein 2 (VDAC2), 26S protease regulatory subunit 8, pyruvate kinase, and aconitate hydratase (mitochondrial)). GO term analysis revealed that these identified proteins are involved in similar processes as those found differentially regulated between the UKF-NB-3^{r}CDDP^{1000} and UKF-NB-3 parental cells, including chaperone activity, stress resistance, redox and detoxification, cell growth, apoptosis, DNA repair, protein turnover, carbohydrate metabolism, cytoskeletal organisation and neuronal function and development (Table 16 and Appendix P). Regarding fold change ratios over the UKF-NB-3 parental cells falling below 0.5 or above 2.0, there were none below 0.5, but above 2.0 were heat shock protein beta-1 (also high in the UKF-NB-3 study), along with the microtubule system regulator stathmin, and the voltage-dependent anion-selective channel protein 2 (VDAC2), with fold change ratios of 2.3, 2.2 and 2.0 respectively. VDAC2 is involved in both anion transport across the outer mitochondrial membrane and apoptosis, and had the smallest ANOVA p-value. It appeared to be switched on in the UKF-NB-6^{r}CDDP^{2000} cells compared to switched off in the UKF-NB-6 parental cells (see spot 1403 in Appendix L).

At the individual protein level, heat shock protein beta-1 was found to be upregulated in both comparisons, UKF-NB-3^{r}CDDP^{1000} cells vs UKF-NB-3 parental cells, and the UKF-NB-6^{r}CDDP^{2000} cells vs UKF-NB-6 parental cells. Stathmin was also differentially regulated in both comparisons. However, stathmin was downregulated in the comparison UKF-NB-3^{r}CDDP^{1000} cells vs UKF-NB-3 parental cells and upregulated in the comparison UKF-NB-6^{r}CDDP^{2000} cells vs UKF-NB-6 parental cells.

Differences in up and downregulation were observed when we compared our results with those from two other proteomic investigations into cisplatin resistance using neuroblastoma cell lines; one that was published previous to our work (D'Aguanno, D'Alessandro et al. 2011), and a second that was published after (Piskareva, Harvey et al. 2015). D'Aguanno et al carried out expression analysis in SH-SY5Y parental and corresponding cisplatin resistant neuroblastoma cells using, in parallel, 2D gel electrophoresis coupled to mass spectrometry and the more sophisticated label-free nLC-MS^{E} (nanoflow liquid chromatography mass spectroscopy). Piskareva et al used similar methodology (nLC-MS-MS), to generate protein expression data for three neuroblastoma cell lines (Kelly, CHP-212 and SK-N-AS cells) and their corresponding cisplatin resistant sub-lines. From these publications we took their results for all the proteins that we found to be differentially expressed in our acquired cisplatin resistance investigations and presented it altogether, with our

Table 17. A comparison of the differentially regulated proteins in our UKF-NB-3 and UKF-NB-6 studies (resistance only: Par 0hr vs CDDPr 0hr from Table 15 and Table 16) alongside the results for the same proteins in two other proteomics studies investigating platinum resistance in neuroblastoma cell lines (D'Aguanno, D'Alessandro et al. 2011, Piskareva, Harvey et al. 2015). This legend is extended on the next page.

Our studies					D'Aguanno et al (2011)		Piskareva et al (2015)			
2D electrophoresis					2D electrophoresis	nLC-MS^{E}	nLC-MS-MS			
Spot #	Protein name	UniprotKB accession #	Fold change ratio UKF-NB-3^{r}CDDP^{1000} / UKF-NB-3 Par	Fold change ratio UKF-NB-6^{r}CDDP^{2000} / UKF-NB-6 Par	Fold change ratio SH-SY5Ycp / SH-SY5Ywt		Fold change ratio KellyCis83 / Kelly	Fold change ratio CHP-212Cis100 / CHP-212	Fold change ratio SK-N-ASCis24 / SK-N-AS	Of the 6 cell lines, the # that the protein is modulated in (# agreeing with us in terms of expression direction)
UKF-NB-3 study										
749	Peroxiredoxin-2	P32119	0.49	none	none	none	0.57	none	none	2 (2)
1369	Phosphatidylethanolamine-binding protein 1 / Neuropolypeptide h3	P30086	0.54	none	none	none	none	none	none	1
792	Stathmin	P16949	0.58	2.24	none	highly represented in SH-SY5Ywt	0.61	none	none	4 (3)
978	Dihydropyrimidinase-related protein 5 /Collapsin response mediator protein-5	Q9BPU6	0.58	none	none	none	none	none	none	1
635	S-formylglutathione hydrolase /Esterase D	P10768	0.60	none	none	none	none	none	none	1
709	Heat shock protein 27/Heat shock protein beta-1	P04792	2.72	2.35	none	none	none	0.43	0.41	4 (2)
1659	Heat shock protein 27/Heat shock protein beta-1	P04792	2.24	2.35	none	none	none	0.43	0.41	4 (2)
1719	Lactate dehydrogenase, A chain	P00338	2.07	none	none	9.09	none	none	0.50	3 (2)
1276	Nucleophosmin	P06748	2.09	none	none	9.09	none	none	none	2 (2)
1571	Eukaryotic initiation factor 4A-III/Translation initiation factor	P38919	1.93	none	none	none	none	none	none	1
1583	Phosphoglycerate kinase 1	P00558	1.72	none	none	highly represented in SH-SY5Ycp	1.48	none	0.47	4 (3)
901	60 kDa heat shock protein, mitochondrial	P10809	1.50	none	none	3.70	none	1.75	none	3 (3)
1121	D-3-phosphoglycerate dehydrogenase	O43175	1.53	none	none	none	none	0.55	none	2 (1)
UKF-NB-6 study										
323	Dihydropyrimidinase-related protein 2	Q16555	none	0.56	none	none	none	none	none	1
722	Glutathione S-transferase P	P09211	none	0.58	0.30	none	1.67	none	none	3 (2)
682	Proteasome subunit alpha type-6 /Macropain subunit iota	P60900	none	0.64	none	none	none	none	none	1
1652	Actin cytoplasmic 1	P60709	none	0.66	none	none	none	none	none	1
679	Heat shock protein beta-1 /heat shock protein 27	P04792	2.72 2.24	2.35	none	none	none	0.43	0.41	4 (2)
779	Stathmin	P16949	0.58	2.24	none	highly represented in SH-SY5Ywt	0.61	none	none	4 (1)
1403	Voltage-dependent anion-selective channel protein 2 (VDAC2)	P45880	none	1.97	2.22	none	none	none	none	2 (2)
1441	26S protease regulatory subunit 8 /Thyroid receptor interactor	P62195	none	1.77	none	none	none	none	none	1
1548	Pyruvate kinase (PKM)	P14618	none	1.83	none	none	1.49	0.66	none	3 (2)
1539	Aconitate hydratase, mitochondrial	Q99798	none	1.62	none	none	0.64	none	none	2 (1)

Table 17 legend continued. Fold change ratios were calculated by dividing the mean normalised spot volume of the cisplatin resistance subline over that of its parental line. Note that all the proteins presented in this table had a one way ANOVA p-value <0.05 and a fold increase (highest mean/lowest mean spot volumes) of ≥1.5 to 1 decimal place for each comparison, except for the D'Aguanno 2D gel electrophoresis results, which used more stringent cut-offs, p value <0.02 and a fold increase (highest mean/lowest mean spot volumes) of ≥2.0. Blue = proteins with higher expression in parentals cells, green = proteins with higher expression in corresponding cisplatin resistant sub-lines, grey = proteins appearing in both the UKF-NB-3 and UKF-NB-6 studies. Red text = 12 proteins with a result in at least one of the cell lines of the D'Aguanno et al or Piskareva et al studies.

data, in Table 17, making a total of 6 neuroblastoma cell line, including our two. It is important to note the major neuroblastoma-relevant difference between these cell lines; UKF-NB-3, UKF-NB-6, and Kelly are MYCN-amplified, and SH-SY5Y, CHP-212 and SK-N-AS are non-amplified (refer to 2.1.2 and 2.1.3 for MYCN information). Since a limited amount of such studies has been performed so far, it is not really clear what level of overlap we would expect.

Of our total of 20 modulated proteins in one or both of the UKF-NB-3 and UKF-NB-6 acquired cisplatin resistance studies, 8 (40 %) (in black text in Table 17) gave no result in any of the other neuroblastoma cell line comparisons. The remaining 12 (60 %) (in red text in Table 17) were discovered to have a result in at least one of the other neuroblastoma cell line comparisons by the other two research groups. Of these 12 proteins, 4 (33 %) (peroxiredoxin-2, nucleophosmin, the chaperone 60 kDa mitochondrial heat shock protein, and the voltage-dependent anion-selective channel protein 2 (VDAC-2)) were the same in terms of up or downregulation (in a total of 2, 2, 3, 2 cell lines respectively; see last column of the table) across all 6 cell line comparisons. The remaining 8 out of these 12 proteins (67 %), including heat shock protein beta-1, were both up and downregulated.

Focussing more on the results of the individual cell lines in the D'Aguanno et al and Piskareva et al studies, there were 5/12 (42 %) UKF-NB-3 proteins (including stathmin) that were also modulated in the SH-SY5Y studies and all with the same direction of expression to our study, and there were 3/10 (33 %) UKF-NB-6 proteins also modulated in the SH-SY5Y studies, two of which had the same direction of expression to our study whilst stathmin was different. There were 3/12 (25 %) UKF-NB-3 proteins that were also modulated in the Kelly study and all with the same direction of expression, and there were 4/10 (40 %) UKF-NB-6 proteins that were also modulated in the Kelly study, one (stathmin) with the same direction of expression to our study. There were 3/12 (25 %) UKF-NB-3 proteins that were modulated in the CHP-212 study of which one had the same direction of expression to our study, and there were 2/10 (20 %) UKF-NB-6 proteins that were modulated in the CHP-212 study and both had different directions of expression to our studies. There were 3/12 (25 %) UKF-NB-3 proteins that were modulated in the SK-N-AS study and they had a different direction of expression to our study, which was also the case for the one (10 %) UKF-NB-6 protein. Regarding both the number of modulated proteins and direction of expression,

the SH-SY5Y study generated the most similar results to our UKF-NB-3 and UKF-NB-6 studies, and overall our UKF-NB-6 cell line was more different than our UKF-NB-3 cell line was to the cell lines of the other studies.

4.2.2.4 Investigating the acute effects of cisplatin

The parental cell lines and the cisplatin-resistant sub-lines were treated with cisplatin (UKF-NB-3 parentals, UKF-NB-3^{r}CDDP^{1000}: 1000 ng/mL; UKF-NB-6 parentals, UKF-NB-6^{r}CDDP^{2000}: 2000 ng/mL) for 2, 8 or 24 hours and the cisplatin-mediated effects were determined by 2D gel-based proteomics. No drug was added to the 0hr time point (control cells) (4.1.7.1). The identified proteins are shown for the UKF-NB-3 studies in Table 15 and for the UKF-NB-6 studies in Table 16. In these tables, the main roles of these proteins were summarised using Appendix O and Appendix P, where their main roles and matched Gene Ontology (GO) molecular function, biological process and cellular component terms (excluding those inferred by electronic annotation) are tabulated; all of this information was taken from the UniProt Knowledge base (http://www.uniprot.org/). The Progenesis Samespots data for these proteins are also shown for the UKF-NB-3 studies in Table 18 and Table 19, and for the UKF-NB-6 studies in Table 20 and Table 21, but here the tables include the results for these proteins at all the other time points, even though at these time points the ANOVA p value was not <0.05, except for peroxiredoxin-4 at 2 hours (Table 20) and the 26S protease regulatory subunit 8 at 8 hours (Table 21), and Fold increase values were not always above our cut off (≥1.5 (to 1 decimal place)). Despite this, we used these extra time point data to get an overall idea of expression over 24 hours for each protein. We focussed on fold change ratios (quoted in parentheses in the following text).

Cisplatin treatment resulted in the differential regulation of 3 proteins in the UKF-NB-3 parental cells (refer to Table 18). RuvB-like 2, a protein that plays a key role in DNA repair and metabolism (Table 15), displayed enhanced levels after 2 hours of incubation with cisplatin with a fold change ratio over the UKF-NB-3 parental cells at 0 hours of 1.67. This appears to be a short acting response because the fold change ratio decreases after 8hr (1.32) and then by 24 hours (1.16) it is nearly back to control cell levels. The multifunctional protein nucleophosmin (Table 15) (which was also identified in the UKF-NB-3 acquired resistance study as having elevated expression levels in the resistant compared to the parental cells (4.2.2.3 and Table 15)), was upregulated during the 8 hours post addition of cisplatin with a fold change ratio over the UKF-NB-3 parental cells 0 hours of 1.61. Expression levels were also elevated after 2 hours (1.58), but by 24 hours (1.33) they had decreased, overall suggesting a longer acting response. ATP synthase subunit beta (mitochondrial), a cellular metabolism protein (Table 15), was upregulated during the 24 hours post addition of cisplatin with a fold change ratio over the UKF-NB-3 parental cells 0 hours of 1.52. It was also upregulated at the 2 hours (1.70) and 8 hours (1.49) time points, suggesting a long acting response.

Cisplatin treatment resulted in the differential regulation of 6 proteins in the UKF-NB-3^{r}CDDP^{1000} cells (refer to Table 19), 4 of which were upregulated during 2 hours post cisplatin addition; the 26S protease regulatory subunit 8 and 26S protease regulatory subunit 10B, VDAC2 (which appeared as upregulated in resistant cells in the UKF-NB-6 acquired resistance study (4.2.2.3 and Table 16)) and the multifunctional protein guanine nucleotide-binding protein subunit beta-2-like 1 with fold change ratios over the UKF-NB-3^{r}CDDP^{1000} cells at 0 hours of 1.58, 1.54, 1.61 and 1.55 respectively. 26S protease regulatory subunit 8 appeared to be downregulated by 8 hours (1.18) but then levels increased again at 24 hours (1.40), 26S protease regulatory subunit 10B was downregulated near to the control cell levels by 8 hours (1.07) and 24 hours (1.10) which suggests a short acting response, VDAC2 expression levels were also elevated at 8 hours (1.43) and 24 hours (1.51) suggesting a long acting response, and guanine nucleotide-binding protein subunit beta-2-like 1 was also longer acting with upregulated expression at 8 hours (1.36) and 24 hours (1.36). These proteins all play a key role in protein degradation except for VDAC2, which is involved in both anion transport across the outer mitochondrial membrane and apoptosis (Table 15). 24 hours post cisplatin addition we identified translational elongation factor 2 and lactate dehydrogenase (A chain), a protein involved in sugar metabolism (Table 15) (which appeared as upregulated in resistant cells in the UKF-NB-3 acquired resistance study (4.2.2.3 and Table 15)) that were downregulated with fold change ratios over the UKF-NB-3^{r}CDDP^{1000} cells at 0 hours of 0.41 and 0.53 respectively. Elongation factor 2 was not modulated at 2 hours (1.00), and at 8 hours (0.78) expression had begun to downregulate, overall suggesting a slow starting response to cisplatin for this protein. A decrease in expression levels of lactate dehydrogenase (A chain) also appeared to be slow starting because of its higher expression levels at 2 hours (0.79) and 8 hours (0.95).

We observed mostly downregulation of expression levels of the identified proteins post addition of cisplatin to the UKF-NB-6 parental cells (refer to Table 20). Two proteins were identified post 2 hours cisplatin addition; the chaperone endoplasmin and proteasome subunit alpha type-6 (which was identified as downregulated in resistant cells in the UKF-NB-6 acquired resistance study (4.2.2.3 and Table 16)), with fold change ratios over the UKF-NB-6 parental cells at 0 hours of 0.59 and 0.69 respectively. At 8 hours (0.66) and 24 hours (0.77), endoplasmin expression began to increase again, but not back up to the levels of the UKF-NB-6 parental cells at 0 hours, therefore endoplasmin downregulation appears to be a long acting effect. At 8 hours (0.85) and 24 hours (0.90), proteasome subunit alpha type-6 expression had increased nearly back up to the levels of the UKF-NB-6 parental cells at 0hr suggesting a short acting cisplatin effect. Also downregulated, but post 8 hours cisplatin addition, was the chaperone heat-shock cognate 71Kda protein, a repressor of transcription, and the redox regulator peroxiredoxin-4 (Table 16) with fold change ratios over the UKF-NB-6^{r}CDDP^{2000} cells 0 hours of 0.62 and 0.68 respectively. Heat-shock cognate 71Kda protein expression levels were slightly decreased after 2 hours (0.74), but by 24 hours

(0.85) expression had increased nearly back up to the levels of the UKF-NB-6 parental cells at 0 hours so overall this suggested a short acting downregulatory effect. The response was similar regarding peroxiredoxin-4, protein expression levels were slightly decreased after 2 hours (0.73), but by 24 hours (0.92) expression had increased nearly back up to the levels of the UKF-NB-6 parental cells at 0hr. Pyruvate kinase was also identified at this time point though, in contrast, with elevated expression and a fold change ratio over the UKF-NB-6 parental cells 0 hours of 1.47. The other time point data, 2 hours (1.03) and 24 hours (1.32), suggested that this response did not occur within the first 2 hours and was starting to decrease by 24 hours. Pyruvate kinase is involved in sugar metabolism and both tumour cell proliferation and death (Table 16) and also appeared as upregulated in resistant cells in the UKF-NB-6 acquired resistance study (4.2.2.3 and Table 16). Post 24 hours cisplatin addition we also observed downregulation of the ER chaperone and negative apoptotic regulator 78Kda glucose-regulated protein (Table 16) with a fold change ratio over the UKF-NB-6 parental cells at 0 hours of 0.66. Regarding the time points prior to this, 2 hours (0.79) and 8 hours (0.58), it appears that this protein was downregulated over the 24 hours and suggests a long acting effect.

Two proteins were modulated post addition of cisplatin in the UKF-NB-6^{r}CDDP^{2000} cells (refer to Table 21). Firstly, downregulated after 2 hours, was pyruvate kinase with a fold change ratio over the UKF-NB-6^{r}CDDP^{2000} cells at 0 hours of 0.54. The fold change ratios at 8 hours (0.62) and 24 hours (0.64) suggest that this downregulation was a long acting effect. This protein also appeared, but upregulated, in the UKF-NB-6 parental time course study (see above), and also as upregulated in resistant cells in the UKF-NB-6 acquired resistance study (4.2.2.3 and Table 16). Secondly, also downregulated but after 24 hours, was 26S protease regulatory subunit 8, with a fold change ratio over the UKF-NB-6^{r}CDDP^{2000} cells at 0hr of 0.69. At 2 hours (0.64) and 8 hours (0.76) the expression was increasing again but levels remained low, suggestive of a long acting cisplatin effect. This protein was upregulated in the resistant cells in the UKF-NB-6 acquired resistance study (4.2.2.3 and Table 16), and also post 2 hours cisplatin addition in the UKF-NB-3^{r}CDDP^{1000} cells (see above).

Overall, for the UKF-NB-3 parental time course, there were 3 proteins that were identified that did not appear in the UKF-NB-3^{r}CDDP^{1000} cells time course, and also there were 5 proteins identified in the UKF-NB-6 parental time course (excluding pyruvate kinase) that did not appear in the UKF-NB-6^{r}CDDP^{2000} time course. There were 6 proteins unique to the UKF-NB-3^{r}CDDP^{1000} time course and one of these proteins, 26S protease regulatory subunit 8, was shared with the UKF-NB-6^{r}CDDP^{2000} time course. Pyruvate kinase is an overlapping protein in the UKF-NB-6 study, appearing in both UKF-NB-6 parental (elevated with a fold change ratio over the UKF-NB-6^{r}CDDP^{2000} cells 0 hours of 1.47) and UKF-NB-6^{r}CDDP^{2000} (decreased with a fold change ratio over the UKF-NB-6^{r}CDDP^{2000} cells 0 hours hr of 0.69) time courses.

#	Protein name	Highest mean normalised spot volume	Lowest mean normalised spot volume	Anova (p)	Fold increase (highest mean normalised spot volume/lowest mean normalised spot volume	Fold change ratio of mean normalised spot volumes expressed / Par 0hr
1084	RuvB-like 2	Par 2hr	Par 0 hr	0.00357	1.67	1.67
		Par 8hr	Par 0 hr	0.24073	1.32	1.32
		Par 24hr	Par 0 hr	0.60616	1.16	1.16
1276	Nucleophosmin	Par 2hr	Par 0 hr	0.50046	1.58	1.58
		Par 8hr	Par 0 hr	0.02465	1.61	1.61
		Par 24hr	Par 0 hr	0.18422	1.33	1.33
449	ATP synthase subunit beta, mitochondrial	Par 2hr	Par 0 hr	0.24611	1.70	1.70
		Par 8hr	Par 0 hr	0.18563	1.49	1.49
		Par 24hr	Par 0 hr	0.02593	1.52	1.52

Table 18. The acute effects in UKF-NB-3 parental cells after 2, 8 and 24 hours 1000 ng/mL cisplatin incubation. Spot # corresponds to those on the 2D gels (Figure 38). Highest mean and lowest mean normalised spot volumes for each comparison, with the associated ANOVA p-value and Fold increase, are all taken from the Progenesis Samespots analysis. Highlighted green are the time points where both the ANOVA p-value was <0.05 (red type)) and Fold increase was ≥1.5 (red type); these data are included in Table 15. Mean normalised spot volumes were also expressed as a Fold change ratio over the parental cell lines (Par 0hr). Fold change ratio values below 1.0 signified downregulation and above 1.0 upregulation of protein expression. Par = parental cell line, CDDPr = cisplatin resistant cell line, and hr values are the cisplatin addition timepoints (note no drug was added to 0 hr controls).

#	Protein name	Highest mean normalised spot volume	Lowest mean normalised spot volume	Anova (p)	Fold increase (highest mean normalised spot volume/lowest mean normalised spot volume	Fold change ratio of mean normalised spot volumes expressed / CDDPr 0hr
1576	26S protease regulatory subunit 8 isoforma 2/Thyroid receptor interactor	CDDPr 2hr	CDDPr 0 hr	0.02232	1.58	1.58
		CDDPr 8hr	CDDPr 0 hr	0.56242	1.18	1.18
		CDDPr 24hr	CDDPr 0 hr	0.21404	1.40	1.40
637	Voltage-dependent anion-selective channel protein 2	CDDPr 2hr	CDDPr 0 hr	0.03104	1.61	1.61
		CDDPr 8hr	CDDPr 0 hr	0.13316	1.43	1.43
		CDDPr 24hr	CDDPr 0 hr	0.15980	1.51	1.51
1284	Guanine nucleotide binding protein subunit beta-like 2	CDDPr 2hr	CDDPr 0 hr	0.04154	1.55	1.55
		CDDPr 8hr	CDDPr 0 hr	0.18564	1.36	1.36
		CDDPr 24hr	CDDPr 0 hr	0.27203	1.36	1.36
1252	26S proteasome regulatory subunit 10B/Proteasome subunit p42	CDDPr 2hr	CDDPr 0 hr	0.00522	1.54	1.54
		CDDPr 8hr	CDDPr 0 hr	0.67688	1.07	1.07
		CDDPr 24hr	CDDPr 0 hr	0.57984	1.10	1.10
1002	Elongation factor 2	CDDPr 0 hr	CDDPr 2hr	0.93164	1.00	1.00
		CDDPr 0 hr	CDDPr 8hr	0.43824	1.27	0.78
		CDDPr 0 hr	CDDPr 24hr	0.01506	2.41	0.41
1719	Lactate dehydrogenase, A chain	CDDPr 0 hr	CDDPr 2hr	0.57129	1.27	0.79
		CDDPr 0 hr	CDDPr 8hr	0.82908	1.05	0.95
		CDDPr 0 hr	CDDPr 24hr	0.03580	1.88	0.53

Table 19 The acute effects in UKF-NB-3^{r}CDDP^{1000} cells after 2, 8 and 24 hours 1000 ng/mL cisplatin incubation. Spot # corresponds to those on the 2D gels (Figure 38) Highest mean and lowest mean normalised spot volumes for each comparison, with the associated ANOVA p-value and Fold increase, are all taken from the Progenesis Samespots analysis. Highlighted green are the time points where the both the ANOVA p-value was <0.05 (red type)) and Fold increase was ≥1.5 to 1 decimal place (red type); these data are included in Table 15. Mean normalised spot volumes were also expressed as a Fold change ratio over the cisplatin resistant control cell lines (CDDPr 0hr). Fold change ratio values below 1.0 signified downregulation and above 1.0 upregulation of protein expression. Par = parental cell line, CDDPr = cisplatin resistant cell line, and hr values are the cisplatin addition timepoints (note no drug was added to 0 hr controls).

#	Protein name	Highest mean normalised spot volume	Lowest mean normalised spot volume	Anova (p)	Fold increase (highest mean normalised spot volume/lowest mean normalised spot volume	Fold change ratio of mean normalised spot volumes expressed / Par 0hr
163	Endoplasmin	Par 0hr	Par 2hr	0.04190	1.70	0.59
		Par 0hr	Par 8hr	0.18465	1.51	0.66
		Par 0hr	Par 24hr	0.29311	1.29	0.77
682	Proteasome subunit alpha type-6/Macropain subunit iota	Par 0hr	Par 2hr	0.02157	1.45	0.69
		Par 0hr	Par 8hr	0.40042	1.17	0.85
		Par 0hr	Par 24hr	0.36837	1.11	0.90
950	Heat shock cognate 71 kDa glucose-regulated protein	Par 0hr	Par 2hr	0.14432	1.35	0.74
		Par 0hr	Par 8hr	0.00703	1.60	0.62
		Par 0hr	Par 24hr	0.34044	1.18	0.85
1104	Peroxiredoxin-4	Par 0hr	Par 2hr	0.00049	1.36	0.73
		Par 0hr	Par 8hr	0.02249	1.47	0.68
		Par 0hr	Par 24hr	0.43498	1.09	0.92
1548	Pyruvate kinase	Par 2hr	Par 0hr	0.84425	1.03	1.03
		Par 8hr	Par 0hr	0.00104	1.47	1.47
		Par 24hr	Par 0hr	0.90448	1.32	1.32
278	78 kDa glucose-regulated protein	Par 0hr	Par 2hr	0.39414	1.27	0.79
		Par 0hr	Par 8hr	0.19863	1.72	0.58
		Par 0hr	Par 24hr	0.01090	1.52	0.66

Table 20. The acute effects in UKF-NB-6 parental cells after 2, 8 and 24 hours 2000 ng/mL cisplatin incubation. Spot # corresponds to those on the 2D gels (Figure 39). Highest mean and lowest mean normalised spot volumes for each comparison, with the associated ANOVA p-value and Fold increase, are all taken from the Progenesis Samespots analysis. Highlighted green are the time points where both the ANOVA p-value was <0.05 (red type)) and Fold increase was ≥1.5 (red type); these data are included in Table 16. Mean normalised spot volumes were also expressed as a Fold change ratio over the parental cell lines (Par 0hr). Fold change ratio values below 1.0 signified downregulation and above 1.0 upregulation of protein expression. Par = parental cell line, CDDPr = cisplatin resistant cell line, and hr values are the cisplatin addition timepoints (note no drug was added to 0 hr controls).

#	Protein name	Highest mean normalised spot volume	Lowest mean normalised spot volume	Anova (p)	Fold increase (highest mean normalised spot volume/lowest mean normalised spot volume	Fold change ratio of mean normalised spot volumes expressed / CDDPr 0hr
1548	Pyruvate kinase	CDDPr 0hr	CDDPr 2hr	0.02496	1.86	0.54
		CDDPr 0hr	CDDPr 8hr	0.10637	1.62	0.62
		CDDPr 0hr	CDDPr 24hr	0.26811	1.56	0.64
1441	26S protease regulatory subunit 8/Thyroid receptor interactor	CDDPr 0hr	CDDPr 2hr	0.12078	1.57	0.64
		CDDPr 0hr	CDDPr 8hr	0.01975	1.32	0.76
		CDDPr 0hr	CDDPr 24hr	0.03220	1.45	0.69

Table 21. The acute effects in UKF-NB-6^{r}CDDP^{2000} cells after 2, 8 and 24 hours 2000 ng/mL cisplatin incubation. Spot # corresponds to those on the 2D gels (Figure 39) Highest mean and lowest mean normalised spot volumes for each comparison, with the associated ANOVA p-value and Fold increase, are all taken from the Progenesis Samespots analysis. Highlighted green are the time points where the both the ANOVA p-value was <0.05 (red type)) and Fold increase was ≥1.5 to 1 decimal place (red type); these data are included in Table 16. Mean normalised spot volumes were also expressed as a Fold change ratio over the cisplatin resistant control cell lines (CDDPr 0hr). Fold change ratio values below 1.0 signified downregulation and above 1.0 upregulation of protein expression. Par = parental cell line, CDDPr = cisplatin resistant cell line, and hr values are the cisplatin addition timepoints (note no drug was added to 0 hr controls).

4.3 Discussion – neuroblastoma cell lines

Platinum drug resistance, both intrinsic and acquired, is a major cause of treatment failure (Lippert, Ruoff et al. 2011, Holohan, Van Schaeybroeck et al. 2013, Hu, Zhang 2016, Gottesman, Lavi et al. 2016). Resistance mechanisms are complex and only partly understood (Shahzad, Lopez-Berestein et al. 2009). It is important to gain further insight into the mechanisms underlying platinum drug action and resistance in order to identify novel, effective (biomarker-guided) therapies for the treatment of cancers, like neuroblastoma, that are prone to platinum drug resistance (2.1.3, 2.1.4, 2.2).

Our understanding of the processes underlying the acquisition of resistance to therapy in cancer is limited (Sharma, Haber et al. 2010, Holohan, Van Schaeybroeck et al. 2013). Preclinical models such as cancer cell lines (2.3.1.1) enable a detailed systems level investigation of resistance formation in cancer cell populations that cannot be determined in patients suffering from multiple metastases in which not all cancer cells are accessible. Notably, intra-tumour heterogeneity is a limitation for cancer biopsies (Burrell, McGranahan et al. 2013). Pre-clinical models enable the systematic performance of functional studies that can only be performed to a very limited extent by the use of clinical samples. Resistance mechanisms in drug-adapted cancer cell line models have been shown to reflect drug resistance mechanisms in patients (Sharma, Haber et al. 2010, Domingo-Domenech, Vidal et al. 2012, Korpal, Korn et al. 2013, Joseph, Lu et al. 2013, Bucheit, Davies 2014, Crystal, Shaw et al. 2014).

To study acquired platinum drug resistance in human neuroblastoma cells we used a panel of eight neuroblastoma cell lines (4.1.2.1), consisting of the MYCN-amplified neuroblastoma cell lines UKF-NB-3 and UKF-NB-6 (drug-sensitive parentals) and their sub-lines adapted to growth in the presence of therapeutic concentrations of cisplatin, carboplatin or oxaliplatin. The cell lines were characterised for morphology, growth kinetics and drug sensitivity/resistance profiles to the three platinum drugs. In parallel, drug was removed from continuous culture for the drug resistant sub-lines to see whether resistance remained. Finally, a proteomics study was carried out, using both UKF-NB-3 and UKF-NB-6 parental lines and their cisplatin-resistant sub-lines, to identify proteins that potentially play a part in cisplatin resistance and the acute mode of action of cisplatin in neuroblastoma. Modulated proteins could be possible biomarkers for drug resistance or actual drug targets for the treatment of cisplatin-resistant neuroblastoma.

4.3.1 Characterisation of the neuroblastoma cell lines

Cell size and morphological changes, as we have observed (4.2.1.1, cell images in Figure 30) on acquiring platinum drug resistance are not unexpected, considering the numerous genomic and epigenetic changes that take place in cancer cells to assume the resistance phenotype (Sharma, Haber et al. 2010, Holohan, Van Schaeybroeck et al. 2013). Changes in morphology may indicate resistance mechanisms and have functional roles. For example, modification of the organisation of the cytoskeletal proteins is a recognised cisplatin resistance mechanism (Shen, Liang et al. 2004, Shen, Pouliot et al. 2012). In concordance with previous studies (IRELAND, PITTMAN et al. 1994, Piskareva, Harvey et al. 2015), resistance acquisition to platinum drugs was associated with substantial changes in morphology. We did not observe a consistent pattern, suggesting that the different resistant cell lines may have developed different resistance mechanisms.

Resistance formation to platinum drugs may be associated with changes in cell proliferation patterns due to changes in the cellular energy requirements or changes in molecules that are involved in resistance and in cell cycle regulation (Stewart 2007). Growth curves were generated for all cell lines (4.2.1.2 and Figure 31) using impedence-based technology on the Roche xCELLigence system (4.1.4.1) and doubling times were generated (Figure 32). There was no consistent proliferation pattern in the platinum drug-resistant neuroblastoma cell lines, further suggesting heterogeneity in the individual cell line resistance mechanisms. In a previous study, Piskareva et al also found that the doubling times differed between parental neuroblastoma cell lines and their corresponding cisplatin resistant sub-lines (Piskareva, Harvey et al. 2015). However, resistance formation to cisplatin may not always be associated with a change in proliferation rate since Ireland et al found no differences in cell growth of their two cisplatin resistant neuroblastoma cell lines compared to the sensitive lines (IRELAND, PITTMAN et al. 1994). Interestingly, the platinum drug resistant cells proliferated marginally quicker in the absence of drug (Figure 31 and Figure 32), indicating that the drugs still exerted anti-proliferative effects in the resistant cell lines. Interestingly, the change in proliferation rates on removal of drug was by the same percentage in the same resistant cell lines of UKF-NB-3 cells and UKF-NB-6 cells (Table 12).

Cultivation of the resistant cell lines for three months in the absence of drug did not result in their re-sensitisation to the drugs of adaption (4.2.1.4) This suggests that resistance formation is not the result of a reversible enrichment of a pre-existing drug-resistant sub-population. It may rather be the consequence of an irreversible adaption process resulting in durable genetic and epigenetic changes (Figure 40).

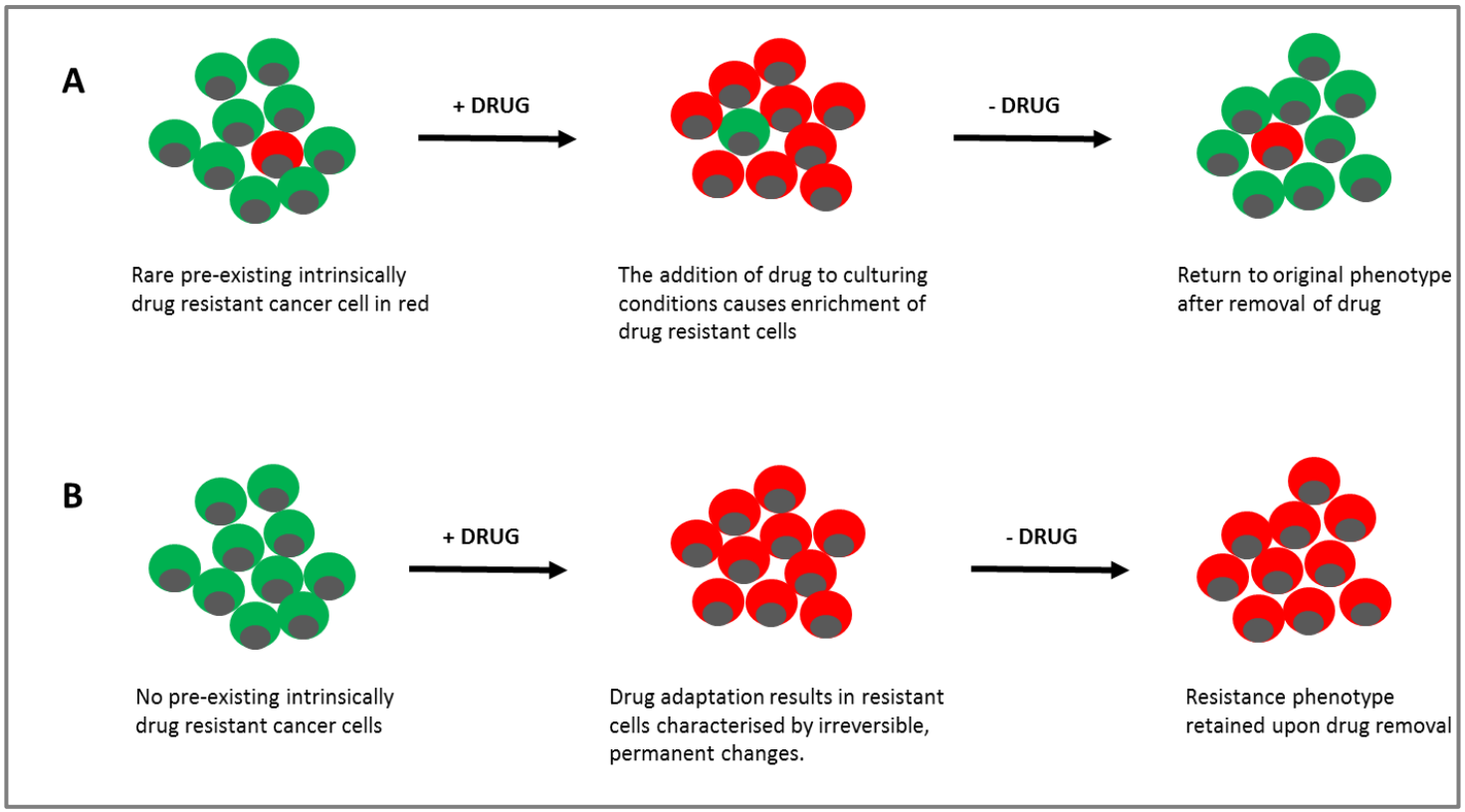

Figure 40. Two possible outcomes from continuously culturing cancer cells in the presence of drug. A. An enrichment of previously existing intrinsically drug-resistant cells, that is ultimately reversible if drug were to be removed. B. There are no previously existing intrinsically drug-resistant cell populations, and resistance is acquired due to a permanent, irreversible genomic change which remains if drug is removed.

Drug sensitivity profiles were generated by challenging each cell line with dose-responses of cisplatin, carboplatin and oxaliplatin by MTT assay (see Figure 33 and Figure 34, and section 4.2.1.3). Both UKF-NB-3 and UKF-NB-6 parental lines exhibited sensitivity to all three drugs. The platinum drug-adapted parental cells displayed generally increased resistance not just to the drug to which they were adapted, but to all three platinum drugs. However, UKF-NB-3^{r}CDDP^{1000} and UKF-NB-3^{r}CARBO^{2000} did not display substantial cross-resistance to oxaliplatin and UKF-NB-3^{r}OXALI^{2000} displayed limited resistance to cisplatin and carboplatin. This is the first time that these three platinum drugs have been tested in parallel in this way, and in cell lines from two sources, to demonstrate cross-resistance. Overall, this again shows some heterogeneity in the resistance mechanisms among the cell lines. As discussed in the introduction (2.2.2), many drug-resistance mechanisms common to the platinum drugs have been reported, though cisplatin has been studied in more depth compared to the other two drugs.

Such platinum drug cross-reactivity, along with cross-reactivity to other anti-cancer therapeutics has been demonstrated in other cell lines. Multi-drug resistance is one of the biggest problems to date when it comes to successful treatment with anti-cancer agents (Wu, Yang et al. 2014). Cisplatin resistant oral carcinoma cells were shown, using the MTT assay and a clonogenecity assay, to have strong cross-resistance to carboplatin, nedaplatin and oxaliplatin (Negoro, Yamano et al. 2009). Endorsing our results, Rixe et al took cisplatin resistant cervical cancer and ovarian cancer cell lines and, using a dye-staining method, established that these cells were also cross-resistant to carboplatin, but very minimally cross-resistant to oxaliplatin and tetraplatin (Rixe, Ortuzar et al. 1996). Using neuroblastoma cell lines established at different points of therapy, Keshelava et al clinically demonstrated cross-resistance between cisplatin and doxorubicin, between carboplatin and cisplatin, or etoposide, or melphalan, also between etoposide and cisplatin, melphalan, or doxorubicin - these are all drugs usually used in the treatment of neuroblastoma (Keshelava, Seeger et al. 1998). This demonstrates how common some of the modes of actions, cellular targets and resistance mechanisms to different drugs must be.

We have observed a high level of cross reactivity between cisplatin and carboplatin from the drug sensitivity profiles. These drugs are used to treat similar types of cancer, and studies overall strongly suggest that they share similar, although not always identical, resistance mechanisms (Stewart 2007) (2.2.1). This is likely due to their similar chemical structures, which means that they form similar DNA adducts and bind to analogous cellular components, resulting in a comparable mode of action and molecular response. In contrast, oxaliplatin is more structurally dissimilar to cisplatin and carboplatin, therefore it forms different DNA adducts and binds to different cellular components, thus ultimately being more different to them in its mode of action (Rabik, Dolan 2007, Heffeter, Jungwirth et al. 2008, Wheate, Walker et al. 2010, Martinez-Balibrea, Martinez-Cardus et al. 2015); this explains the lower level of cross-reactivity that we

observed for this drug. Evidencing this further is that, unlike for the other two drugs, the oxaliplatin DNA adducts are not recognised by DNA mismatch repair proteins (Fink, Nebel et al. 1996, Trudu, Amato et al. 2015, Martinez-Balibrea, Martinez-Cardus et al. 2015); the DACH ligand of the compound is thought to prevent the binding of the mismatch repair complex (MMR) (Mehmood 2014). Moreover, research involving CTR1, involved in the uptake of platinum drugs, has shown that oxaliplatin is different to the other two drugs; the uptake of cisplatin, carboplatin is reduced by a much larger extent compared to that of oxaliplatin in CTR1 knockout murine cells (Holzer, Manorek et al. 2006). Research investigating cancer treatment using combinations of cisplatin and oxaliplatin have highlighted how these two drugs are additive and maybe even synergistic due to the low cross reactivity between them (Rixe, Ortuzar et al. 1996). Therefore researchers suggested to consider oxaliplatin to treat cisplatin-resistant cancer (Rixe, Ortuzar et al. 1996, Rabik, Dolan 2007, Wheate, Walker et al. 2010).

Regarding our yeast studies, the majority of the results indicated that, if anything, cisplatin and carboplatin are not necessarily the most similar of the three platinum drugs we have investigated. The gene hit distribution for both our yeast screen and the Yeast Fitness Database screen showed that they were not the most similar (Figure 7, 3.2.1.1), as did the gene hit distribution for our yeast screen once analysed with a reduced cut off value of ≤30 % (Figure 10, 3.2.1.3), as did our hit conformation screen (Figure 11, 3.2.2), the strongest hits of which indicated that cisplatin and oxaliplatin are most similar (3.2.2). The distribution between drugs of Yeast Go-Slim 'function' and 'process' terms matched to gene hits from the Yeast Fitness Database screen (Figure 8/Appendix C and Figure 9/Appendix D respectively, both in section 3.2.1.2) also showed that cisplatin and carboplatin are not necessarily the more similar. In fact the majority of processes were shared by all three drugs or by cisplatin with oxaliplatin. In terms of the distribution of matched 'process' terms to our own screening data (Appendix F), this also showed that cisplatin and carboplatin are not necessarily the most alike. Yeast data suggesting that oxaliplatin may be more unique compared to cisplatin and carboplatin was from the Yeast Fitness Database screen analysis of processes; oxaliplatin had overall much higher fold enrichment values, and these processes were more orchestrated around vesicle and membrane trafficking, whereas the processes with the highest fold enrichment values for cisplatin and carboplatin were quite varied (Appendix D). It was also interesting that, when evaluating BDF1, oxaliplatin generated growth curves of a different nature to the other two drugs, suggesting it is different to the other two drugs (for example see 3.2.3.1 and Figure 13).

4.3.2 Proteomics

Proteomics approaches are regarded as suitable techniques for studying drug action and resistance mechanisms to anti-cancer drugs (Zhang, Liu 2007, Wang, Chiu 2008, Gabbiani, Magherini et al. 2010). They have been used to examine resistance to the platinum drug cisplatin using a variety of human cancer cell lines, including neuroblastoma (D'Aguanno, D'Alessandro et al. 2011, Piskareva, Harvey et al. 2015), melanoma (Sinha, Poland et al. 2003), bladder cancer (Miura, Takemori et al. 2012), ovarian cancer (Yan, Pan et al. 2007, Gong, Peng et al. 2011, Lincet, Guevel et al. 2012, Stewart, White et al. 2006, Jin, Huo et al. 2014), and cervical cancer cells (Castagna, Antonioli et al. 2004, Chavez, Hoopmann et al. 2011). The acute effects of cisplatin have been studied in cell lines from various cancer entities, including neuroblastoma (Tabata, Sakai et al. 2011), cervical cancer (Castagna, Antonioli et al. 2004), ovarian cancer (Li, Zhao et al. 2005) and renal cell carcinoma (Vasko, Mueller et al. 2011).

We used a well-established proteomics method (2D gel electrophoresis coupled with MALDI-TOF MS and MALDI-TOF-TOF MS/MS) to resolve, analyse, and identify proteins of the proteomes of parental neuroblastoma cell lines and the corresponding cisplatin resistant sub-lines (UKF-NB-3 parental and UKF-NB-3^{r}CDDP^{1000}, and UKF-NB-6 parental and UKF-NB-6^{r}CDDP^{2000}), with the aim of studying both the adaption and acute effects of cisplatin (4.1.7). To investigate the acquired resistance mechanisms, we compared the proteomes of the parental cells and the corresponding cisplatin resistant sub-lines directly to each other. To investigate the acute cisplatin effects in both the parental and cisplatin resistant cells, time course cisplatin addition studies were set up, where cisplatin was added at 24, 8, and 2 hours before lysing cells and comparing the results to those of control cells to which no drug was added. It is important to be aware of limitations to a proteomics approach like ours, in that it reveals minimum numbers of spots because there will be proteins below our detection limits. Also, we solely focussed on proteins with a fold difference cut-off of 1.5, and additionally not all spots that were excised were identified; for UKF-NB-3 42 % (20/48) were identified, and for the UKF-NB-6 study, 44 % were identified (14/32). Further work would be to use western blot analysis to confirm the modulation of expression of our identified proteins.

D'Aguanno et al (D'Aguanno, D'Alessandro et al. 2011) carried out expression analysis in SH-SY5Y parental and corresponding cisplatin resistant neuroblastoma cells using, in parallel, 2D gel electrophoresis coupled to mass spectrometry and the more sophisticated label-free nLC-MS^{E} (nanoflow liquid chromatography mass spectroscopy), published before our studies were carried out. The identified proteins (13 by 2-D gel electrophoresis, 88 by label-free nLC-MS^{E}), of which some had overlap with those identified in our studies (see 4.3.2.1), were then organised into biological functions and were mostly classified into cytoskeletal proteins, nucleic acid binding proteins, and chaperones. Next, bioinformatics pathway analysis was carried out to identify

processes in which the proteins modulated in resistance partake. This was followed by a meta-mining investigation in an effort to identify main pathways involved in resistance to cisplatin in other cancer cell lines that have been published to date, including their results too. The most frequent occurrence was the oxidative stress response pathway mediated by Nrf2, which they investigated further and concluded that this pathway is possibly involved in cisplatin resistance. In non-cancerous cells a protein called Keap1 directs the proteasomal degradation of Nrf2, but in oxidative stress conditions, Nrf2 translocates to the nucleus where it activates the transcription of genes regulated by AREs (AU-rich elements) (D'Aguanno, D'Alessandro et al. 2011). However, a recent publication claims that the Nrf2-Keap1 pathway does not have an important role in cisplatin resistance in neuroblastoma (Tanoshima, Yang et al. 2014). Some of their modulated proteins were also modulated in our acquired cisplatin resistance study (see Table 17 in 4.2.2.3).

Piskareva et al (Piskareva, Harvey et al. 2015) recently carried out a large proteomics study, post our studies, using similar methodology (nLC-MS-MS) to generate protein expression data for three neuroblastoma cell lines (Kelly, CHP-212 and SK-N-AS cells) and their corresponding cisplatin resistant sub-lines to examine resistance molecular pathways and integrate this with accompanying characterisation data including cell behaviour, genomic alterations and cytotoxicity. They found that most of the proteins with modulated expression levels in the resistance cell lines were cytoskeletal, nucleic acid binding and chaperones and that the pathways in which they were mostly involved indicated that epithelial to mesenchymal transition (EMT) is a characteristic of the development of cisplatin resistance in neuroblastoma to enable invasion and metastasis. As for the D'Aguanno study, some of their modulated proteins were also modulated in our acquired cisplatin resistance study (see Table 17 in 4.2.2.3).

Another proteomics study in neuroblastoma (IMR-32) cells, by Tabata et al (Tabata, Sakai et al. 2011), was to investigate the acute mode of action of cisplatin, administered at a dose of 3 μg/mL for 24 hours. 2D gel electrophoresis demonstrated elevation of T-complex protein 1 β-subunit (CCT-β), elongation factor 1-γ (EF-1- γ), actin cytoplasmic 1 (β-actin), and adenosylhomocysteinase (adoHcy hydrolase), and a decrease in expression levels of splicing factor arigine/serine-rich 3 (SRP20). AdoHcy hydrolase, involved in methylation metabolism, showed the largest modulation and the results from subsequent investigation into the methylation of histones in these cells implied that methylation status is altered by acute cisplatin exposure. None of their modulated proteins appeared in our acute studies (4.2.2.4).

Comparing our studies to the D'Aguanno, Piskareva and Tabata investigations just described, our studies extend their own. This is because we used two different neuroblastoma cell lines, and in parallel we carried out a multiple cisplatin addition time course over 24hrs with the same parental and cisplatin resistant cell lines.

4.3.2.1 Investigation of acquired cisplatin resistance

Our investigation into the adaption mechanisms of cisplatin revealed 12 differentially expressed proteins in the UKF-NB-3^{r}CDDP^{1000} cells relative to the UKF-NB-3 parental cells, and 10 in the UKF-NB-6^{r}CDDP^{2000} relative to the UKF-NB-6 parental cells (see results 4.2.2.3). The identified proteins from both comparative studies covered a similar variety of functions and processes, which highlighted the complexity of cisplatin resistance. These were mainly chaperone activity, stress resistance, redox and detoxification, cell growth, apoptosis, DNA repair, protein turnover, carbohydrate metabolism, cytoskeletal organisation and neuronal function and development. The summarised identified proteins can be found in Table 15 and Table 16. Their roles in these tables were put together using Appendix O and Appendix P, in which both the main roles and matched Gene Ontology (GO) molecular function, biological process and cellular component terms that they are matched to (excluding those inferred by electronic annotation) are tabulated; all of this information was taken from the UniProt Knowledge base (http://www.uniprot.org/). Similar roles were reported for proteins that had been found differentially regulated in other studies, (which have been summarised in 4.3.2), reporting on proteomics comparisons of parental neuroblastoma cell lines and their cisplatin-resistant sub-lines (D'Aguanno, D'Alessandro et al. 2011, Piskareva, Harvey et al. 2015). We tabulated their results for our identified proteins alongside ours in Table 17 (section 4.2.2.3), making a total of six neuroblastoma cell lines, including our two. Table 17 notably shows how the overlap of individual proteins associated with cisplatin resistance and their direction of expression is limited, indicating how cisplatin resistance formation may be complicated and cell line specific.

4.3.2.1.1 Chaperones

Our results show that chaperone activity plays a role in acquisition of cisplatin resistance, and this was also demonstrated in the other two neuroblastoma studies (D'Aguanno, D'Alessandro et al. 2011, Piskareva, Harvey et al. 2015). Of the seven proteins found upregulated in the UKF-NB-3^{r}CDDP^{1000} cells vs UKF-NB-3 parental cells, three were chaperones: nucleophosmin, heat shock protein beta-1 (HSP27/HSPB1) and 60 kDa heat shock protein (mitochondrial) (HSP60/HSPD1). Heat shock protein beta-1 and nucleophosmin were both upregulated with a large fold change ratio over the parentals above 2.0. Heat shock protein beta-1 was also found upregulated in the UKF-NB-6^{r}CDDP^{2000} cells vs UKF-NB-6 parentals (with a large fold change ratio over the parentals above 2.0), as well as in cisplatin-adapted ovarian cancer (Yan, Pan et al. 2007) and in cisplatin-adapted melanoma cells (Sinha, Poland et al. 2003). Interestingly, heat shock protein beta-1 was, however, down-regulated in cisplatin resistant CHP-212 and SK-N-AS neuroblastoma cells compared to their corresponding parental cells in the Piskereva et al study (Table 17), and was also downregulated in cisplatin resistant bladder cancer cells compared to their corresponding parental cells (Miura, Takemori et al. 2012). 60 kDa heat shock protein was also found

upregulated in cisplatin-adapted SH-SY5Y and CHP-212 neuroblastoma cells in the D'Aguanno et al and Piskereva et al studies (Table 17), and in cisplatin-adapted melanoma cancer cells (Sinha, Poland et al. 2003) .

Chaperones are involved in the correct folding and assembly of proteins, and the three that we identified also have roles in the stress response and apoptosis. These proteins could therefore mechanistically contribute to cisplatin resistance by supporting the functions of proteins involved in resistance, and by playing anti-stress and anti-apoptotic roles. Regarding the heat shock proteins (see 2.2.2.4), both 60 kDa heat shock protein and heat shock protein beta-1 have been reported to be over-expressed during carcinogenesis ((Cappello, Bellafiore et al. 2003) and (Katsogiannou, Andrieu et al. 2014) respectively). Mitochondrial 60 kDa heat shock protein has previously been associated with cisplatin (and oxaliplatin) resistance (Abu-Hadid, Wilkes et al. 1997). Mitochondria and mitochondrial DNA have been shown to be targeted by cisplatin (Gonzalez, Fuertes et al. 2001, Yang, Schumaker et al. 2006, Cullen, Yang et al. 2007) (2.2.1). Hence, it may not be too surprising that a mitochondrial heat shock protein such as the 60 kDa heat shock protein may be involved in cisplatin resistant cells. However, this protein can also been found in extra-mitochondrial locations in cancer and may exert extra-mitochondrial functions in cancer cells (Cappello, de Macario et al. 2008). Heat shock protein beta-1, which has many client proteins, had been previously associated with cisplatin resistance (Yamamoto, Okamoto et al. 2001, Ciocca, Cappello et al. 2015). It protected mouse fibroblasts against cisplatin-induced apoptosis (Zhang, Shen 2007). It is interesting that two spots of the same molecular weight but different pI values were identified as being heat shock protein beta-1 in the UKF-NB-3 study (Table 15), but this could be explained by this protein also having a phosphorylated state (Zhu, Zhao et al. 2005), which is known to function in cancer progression (Katsogiannou, Andrieu et al. 2014). These heat shock proteins were suggested as therapeutic targets in cancer, which could also alleviate resistance to drugs like cisplatin. However, to date, only a few compounds have been shown to bind the 60 kDa heat shock protein but, because they inhibit its folding activity, further development work is required. Regarding targeting heat shock protein beta-1, research has mainly utilised RNA interference approaches. An antisense nucleotide directed against heat shock protein beta-1 (Apatorsen), is currently being evaluated in clinical trials (Ciocca, Cappello et al. 2015).

Overexpression of nucleophosmin has been demonstrated in highly proliferating cells and in many cancer types (Grisendi, Mecucci et al. 2006, Di Fiore 2008, Lindstrom 2011, Lo, Fan et al. 2013), but it has not been directly associated with cisplatin resistance so far. However, it was found upregulated in the UKF-NB-3^{r}CDDP^{1000} cells relative to the UKF-NB-3 parental cells, and in cisplatin adapted SH-SY5Y neuroblastoma cells (D'Aguanno, D'Alessandro et al. 2011) (Table 17). In contrast it was found downregulated in cisplatin-adapted ovarian cancer cells (Jin, Huo et al.

2014). Nucleophosmin is a nucleolar protein with intrinsic RNase activity that continuously shuttles between the nucleus and the cytoplasm, playing a key role in ribosome biogenesis and is a histone chaperone in chromatin remodelling (Lindstrom 2011). It also contributes to the response to DNA damage, and a novel role in base excision repair has recently been proposed (Poletto, Lirussi et al. 2014). Furthermore, nucleophosmin is involved in DNA replication and transcription, acts as a controller of centrosome replication (Grisendi, Mecucci et al. 2006, Poletto, Lirussi et al. 2014), and its overexpression leads to indirect inhibition of apoptosis (Ye 2005). Moreover, nucleophosmin can mediate tumour suppression (Grisendi, Mecucci et al. 2006).

Taking our findings and these functions together, it appears plausible that nucleophosmin could contribute to cisplatin resistance in neuroblastoma cells. Nucleophosmin silencing by RNA interference was demonstrated to sensitise human hepatoma cells to cisplatin treatment (Lo, Fan et al. 2013). In the same study, a novel interaction of nucleophosmin with BAX was demonstrated that regulates death evasion. BAX is a pro-apoptotic protein of the BCL2 family that is required for mitochondrial mediated apoptosis (Wei, Zong et al. 2001, Roy, Ehrlich et al. 2009) (see VDAC2 in section 4.3.2.1.7), and Lo et al showed that by directly blocking BAX mitochondrial translocation and activation, nucleophosmin facilitates evasion of apoptosis independently of p53-mediated cell death (Lo, Fan et al. 2013). Anti-cancer peptides and small molecules that knock down nucleophosmin in an attempt to stop proliferation have shown promise (Lindstrom 2011), and it would be of worth to utilise such drugs to explore their ability to reverse cisplatin resistance in our resistant neuroblastoma cells, in particularly UKF-NB-3^{r}CDDP^{1000}, to support the results from our proteomics analysis.

4.3.2.1.2 Cytoskeletal proteins

Our results support possible roles for the cytoskeleton in acquired cisplatin resistance in neuroblastoma cells. Cytoskeletal proteins are important for the intracellular structure and dynamic behaviour of cells during carcinogenesis and the process of apoptosis (Zhang, Liu 2007), and also intracellular drug transport. Heat shock protein beta-1, previously mentioned as upregulated in cisplatin resistant cells (4.3.2.1.1), is also involved in the organisation of actin (Kostenko, Johannessen et al. 2009). The other protein besides heat shock protein beta-1 that was found differentially regulated in both the UKF-NB-3^{r}CDDP^{1000} cells and UKF-NB-6^{r}CDDP^{2000} relative to the respective parental lines was stathmin. However, stathmin was downregulated in UKF-NB-3^{r}CDDP^{1000} cells compared to upregulated in the UKF-NB-6^{r}CDDP^{2000} cells. Such discrepancies in up and down-regulation of proteins in different neuroblastoma cell lines was apparent when comparing the acquired cisplatin resistance studies of six cell lines from both our studies and the D'Aguanno et al and Piskareva et al studies (see 4.2.2.3 and Table 17). Stathmin was downregulated in cisplatin-adapted SH-SY5Y and Kelly neuroblastoma cell lines in these studies.

Stathmin was also downregulated in cisplatin-adapted cervical cancer cells compared to corresponding parental cells (Castagna, Antonioli et al. 2004), but upregulated in cisplatin-adapted ovarian cancer cells (Gong, Peng et al. 2011).

Stathmin is expressed at high levels in many types of tumour cells and plays a role in cancer progression (Sherbet, Cajone 2005). It is important in mediating the microtubule filament system by preventing assembly and promoting disassembly of microtubules (Figure 41) for example, of the mitotic spindle. This enables its role as an important signal transduction factor in the mitogen activated protein kinase (MAPK) signalling pathway and its involvement in cell cycle and cell division (Lin, Tang et al. 2012). Microtubule alterations may also have an effect on the formation of endocytic recycling compartments, leading to reduced cisplatin uptake and resistance (Liang, Mukherjee et al. 2006, Stewart 2007), and decreased endocytosis is often a cisplatin resistance mechanism in cancer (Shen, Pouliot et al. 2012). Stathmin, at high levels, negatively regulates the sensitivity of cancer cells to microtubule targeting drugs (Meng, Tao 2015). However, little is known about the role of stathmin in the sensitivity or resistance of cancer cells to cisplatin. Our data is inclusive and may indicate that a role of stathmin in the context of cisplatin resistance may depend on the individual cellular context. Functional studies that investigate the effects of stathmin silencing using RNA interference or CRISPR methods and stathmin upregulation by forced expression on cellular cisplatin sensitivity are needed to further its role in cisplatin resistance.

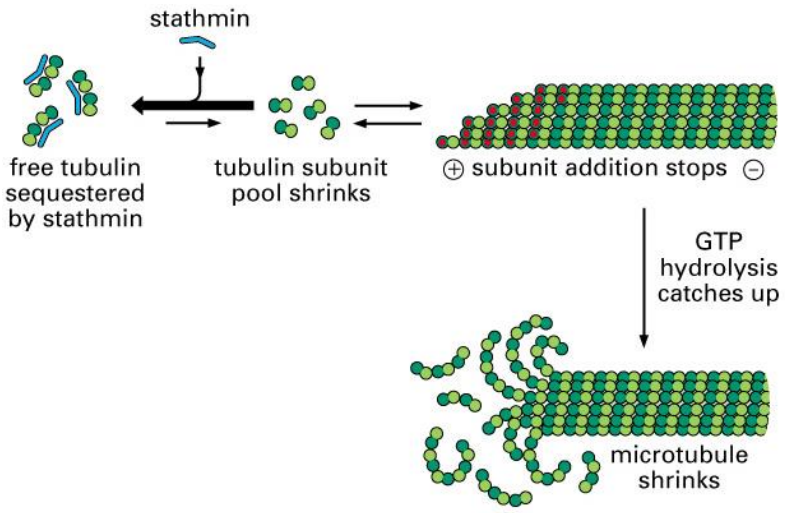

Figure 41. Stathmin prevents assembly of microtubules by sequestering free tubulin and reducing cytosolic tubulin levels; this stops the addition of tubulin to the microtubules and ultimately causes microtubule collapse. Diagram is Figure 16-31 taken from (Alberts, Johnson et al. 2002)

Cytoplasmic actin 1 (beta-actin) and dihydropyrimidinase-related protein 2, which is involved in cytoskeletal remodelling, were found downregulated in UKF-NB-6^{r}CDDP^{2000} cells relative to UKF-NB-6 parental cells. Neither of these proteins were found to be modulated in the D'Aguanno et al

and Piskareva et al proteomics studies in cisplatin-adapted neuroblastoma cells (see 4.2.2.3 and Table 17). Actin is key to cell motility and cellular component organisation and also plays a role in endocytosis which, as already mentioned, is a route of cellular entry of cisplatin. Decreased endocytosis is often a cisplatin resistance mechanism in cancer cells (Shen, Pouliot et al. 2012). Decreased actin and filamin levels in parallel with actin and filamin disorganisation was demonstrated in cisplatin-adapted human epidermoid and liver carcinoma cell lines (Shen, Liang et al. 2004), which supports our findings. Interestingly, the actin cytoskeleton has been reported as being more robust in cisplatin resistant ovarian cancer cells compared to their sensitive parental cells due to an actin remodelling mechanism mediated by Rho GTPase (Sharma, Santiskulvong et al. 2012, Sharma, Santiskulvong et al. 2014). A denser actin network may physically disrupt drug uptake in resistant cells (Mokady, Meiri 2015), but this may not necessarily be accompanied by a change in actin expression levels as we have observed. In our yeast studies we identified the gene SLA1 to be essential for growth in the presence of cisplatin (3.2.2 and Figure 7). SLA1 encodes a cytoskeletal protein binding protein which is a central player in actin cytoskeleton assembly, and has effects on proteins essential for endocytosis (Gardiner, Costa et al. 2007) (3.3.3). Beta-actin is also a component of the human SRCAP, TIP60 histone acetyltransferase and INO80 chromatin remodelling complexes, which are also involved in processes such as DNA repair and replication (Ikura, Ogryzko et al. 2000, Morrison, Shen 2009) (see the discussion for RuvB-like 2 protein, another component, in 4.3.2.2.1). The SRCAP complex is the human equivalent of the yeast SWR1 chromatin remodelling complex of which Bdf1 can be a component. Bdf1-deficient yeast cells displayed increased sensitivity to cisplatin, as well as carboplatin, and oxaliplatin (see the yeast discussion (3.3)). Upregulation of DNA repair is a known cisplatin resistance mechanism (2.2.2.3), therefore upregulation of the levels and activity of these chromatin remodelling complexes, including their subunits such as beta-actin (which has weak ATPase activity) would be expected in our cisplatin-adapted cells (Ikura, Ogryzko et al. 2000, Morrison, Shen 2009), rather than beta-actin downregulation, as we have observed.

Dihydropyrimidinase-related protein 2, also known a collapsing response mediator protein 2, plays a role in neuronal development and polarity and axon growth, neuronal growth cone collapse, and cell migration and endocytosis (Inagaki, Chihara et al. 2001, Chi, Schmutzler et al. 2009, Rahajeng, Giridharan et al. 2010) and altered expression has been observed in several malignant cancers, inclusing colorectal, lung and breast cancer (Tan, Thiele et al. 2014). Its role in endocytosis, which is a route of cellular entry of cisplatin, may explain the downregulation of this protein in UKF-NB-6^{r}CDDP^{2000} cells. Its role in cisplatin resistance is poorly understood and functional studies would gain further insights into this.

4.3.2.1.3 Redox proteins

Proteins of the redox system are necessary for keeping the intracellular redox state levels of reactive oxygen species (ROS) balanced. They are often detected in drug resistant cells where they are involved in combating cellular stress (Zhang, Liu 2007). Cisplatin induces an increase in ROS levels that causes DNA damage and cell death (Dasari, Tchounwou 2014). Peroxiredoxin-2 was downregulated in UKF-NB-3^{r}CDDP^{1000} cells relative to UKF-NB-3 parental cells, and also in the case of cisplatin-adapted Kelly neuroblastoma cells in the Piskareva et al proteomics study (Table 17) (Piskareva, Harvey et al. 2015). Peroxiredoxin-2, as well as the other isoforms 4 and 6, were also found to be downregulated in cisplatin-resistant ovarian cancer cell lines (Jin, Huo et al. 2014). Peroixiredoxin-2 was also reported by Zhang et al. as being generally downregulated in proteomics studies looking at resistance to various cancer treatments in different cancer cell lines (Zhang, Liu 2007). Interestingly, peroxiredoxin-2 is involved in redox regulation (by reducing peroxides (ROS) using reducing equivalents generated via the thioredoxin system), in cell proliferation and differentiation, intracellular signalling, and is also a negative regulator of apoptosis (Sanchez-Font, Sebastia et al. 2003, Sharapov, Ravin et al. 2014, Perkins, Nelson et al. 2015) (Table 15). Overexpression of peroxiredoxin-2 in gastric carcinoma cells inhibited cisplatin-induced apoptosis, suggesting that peroxiredoxin-2 contributes to cisplatin resistance (Chung, Yoo et al. 2001, Sharapov, Ravin et al. 2014) and a decrease in the expression of peroxiredoxin-2 in gastric carcinoma cells by an siRNA approach increased their sensitivity to cisplatin-induced apoptosis (Yoo, Chung et al. 2002, Sharapov, Ravin et al. 2014). Therefore it might have been expected to be upregulated in resistant cells, as it indeed was in cisplatin resistant bladder cells (Miura, Takemori et al. 2012). Functional studies will be needed to further elucidate the role of peroxiredoxin-2 in cisplatin resistance.

Another redox regulatory protein modulated in our studies was the enzyme glutathione-S-transferase P (GSTP) which, like peroxiredoxin-2, was downregulated in UKF-NB-6^{r}CDDP^{2000} cells relative to UKF-NB-6 parental cells. This was unexpected because glutathione-S-transferase P is reported to catalyse the conjugation of drugs like cisplatin to the endogenous thiol glutathione to facilitate their elimination from the cell, to prevent neurodegeneration and to be a negative regulator of apoptosis and proliferation (Townsend, Tew 2003). Detoxification involving glutathione-S-transferase P is a well-documented platinum drug resistance mechanism (Townsend, Tew 2003, Siddik 2003, Stewart 2007, Heffeter, Jungwirth et al. 2008, Koeberle, Tomicic et al. 2010, Galluzzi, Vitale et al. 2014). Recently, knockdown of glutathione-S-transferase P was shown to enhance the cisplatin and carboplatin sensitivity of ovarian cancer cell lines (Sawers, Ferguson et al. 2014). Therefore this protein could be expected to be upregulated, rather than downregulated, in resistant cells, as it has been shown in cisplatin resistant bladder cells (Miura, Takemori et al. 2012). However, as was the case in our experiments, it was also

downregulated in SH-SY5Y cisplatin resistant neuroblastoma cells in the D'Aguanno et al study (Table 17) (D'Aguanno, D'Alessandro et al. 2011), but in contrast upregulated in CHP-212 cisplatin resistant neuroblastoma cells in the Piskareva et al study (Table 17) (Piskareva, Harvey et al. 2015). D'Aguanno et al quote that GSTP1 is controlled by a different element compared to other detoxification enzymes, which may explain downregulation (Usami, Kusano et al. 2005). Glutathione-S-transferase P was also found to be downregulated in cisplatin resistant bladder cancer cells (Miura, Takemori et al. 2012) and cisplatin resistant ovarian cancer cells (Jin, Huo et al. 2014). Similar inconsistent observations regarding the direction of regulation of this protein across studies have been discussed (Rabik, Dolan 2007, Sawers, Ferguson et al. 2014) and it has been suggested that whilst such detoxification involving glutathione-S-transferase P may be important for some cancers regarding cisplatin resistance, it does not appear to be a global indicator of cisplatin resistance (Rabik, Dolan 2007). The reason for both up and down regulation in resistance cells is not understood and it may be of worth to investigate this further in our panel of cell lines, for which there are tool compounds available. One example is the diuretic drug ethacrynic acid, which inhibits glutathione-S-transferase by both binding directly to the substrate-binding site and depleting its cofactor glutathione (Townsend, Tew 2003, Xu, Zheng et al. 2013). Another example is the drug buthionine sulfoximine (BSO) is a synthetic amino acid that inhibits glutathione-S-transferase indirectly by irreversibly inhibiting an enzyme, γ-glutamylcysteine synthetase (γ-GCS), which is a critical step in glutathione biosynthesis. (YOKOMIZO, KOHNO et al. 1995).

4.3.2.1.4 Glycolytic enzymes

In terms of carbohydrate metabolism, we identified four proteins involved in this process, and all were upregulated in cisplatin resistant cells. Interestingly, a glycolytic regulator (GCR2) with a human functional equivalent (hSGT1) was a hit in our carboplatin and oxaliplatin yeast screens (3.3.3) (Table 7). Lactate dehydrogenase and phosphoglycerate kinase 1 were both upregulated (lactate dehydrogenase highly) in UKF-NB-3^{r}CDDP^{1000} cells compared to UKF-NB-3 parental cells. Pyruvate kinase and mitochondrial aconitate hydratase were both upregulated in UKF-NB-6^{r}CDDP^{2000} cells compared to UKF-NB-6 parental cells. The 'Warburg effect' (Figure 42) describes cancer cells as persistently converting glucose to pyruvate to lactic acid even in the presence of oxygen (termed aerobic glycolysis), rather than oxidation of pyruvate via the tricarboxylic acid (TCA) cycle, which has been suggested to offer a growth advantage and is a hallmark of invasive cancers (Gatenby, Gillies 2004, Xu, Pelicano et al. 2005, Pelicano, Martin et al. 2006, Vasko, Mueller et al. 2011). The causes of this effect are thought to be inherent changes such as mitochondrial respiration injury (there are high mutation rates in mitochondrial DNA in cancer), oncogenic signalling, alterations in metabolic enzymes, and also tumour environmental constraints such as hypoxia and acidosis (Gatenby, Gillies 2004, Pelicano, Martin et al. 2006).

Inhibition of glycolysis for the treatment of cancer has been explored and suggested to be a promising approach to kill cancer cells with mitochondrial defects (Xu, Pelicano et al. 2005, Pelicano, Martin et al. 2006), and the inhibition of glycolysis has also been shown to enhance cisplatin-induced apoptosis in ovarian cancer cells (Loar, Wahl et al. 2010). Our results showing elevation of the enzymes phosphoglycerate kinase 1, pyruvate kinase and lactate dehydrogenase in our cisplatin resistant neuroblastoma cells suggest a shift of cisplatin-resistant cells towards 'Warburg'. This could be explained by the cisplatin-induced mitochondrial DNA damage in resistant cells, which causes a malfunction of mitochondrial oxidative phosphorylation resulting in a need to rely on glycolysis for energy. The TCA cycle enzyme aconitate hydratase was also upregulated in UKF-NB-6^{r}CDDP^{2000} cells. However, aconitate hydratase may also be upregulated due to its secondary function, which is to maintain the stability of mtDNA. Aconitate hydratase was suggested, possibly, by reversibly remodelling nucleoids, to directly affect the expression of mitochondrial genes in response to changes in cellular metabolism, including oxidative stress, caused by genotoxic drugs like cisplatin (Shadel 2005).

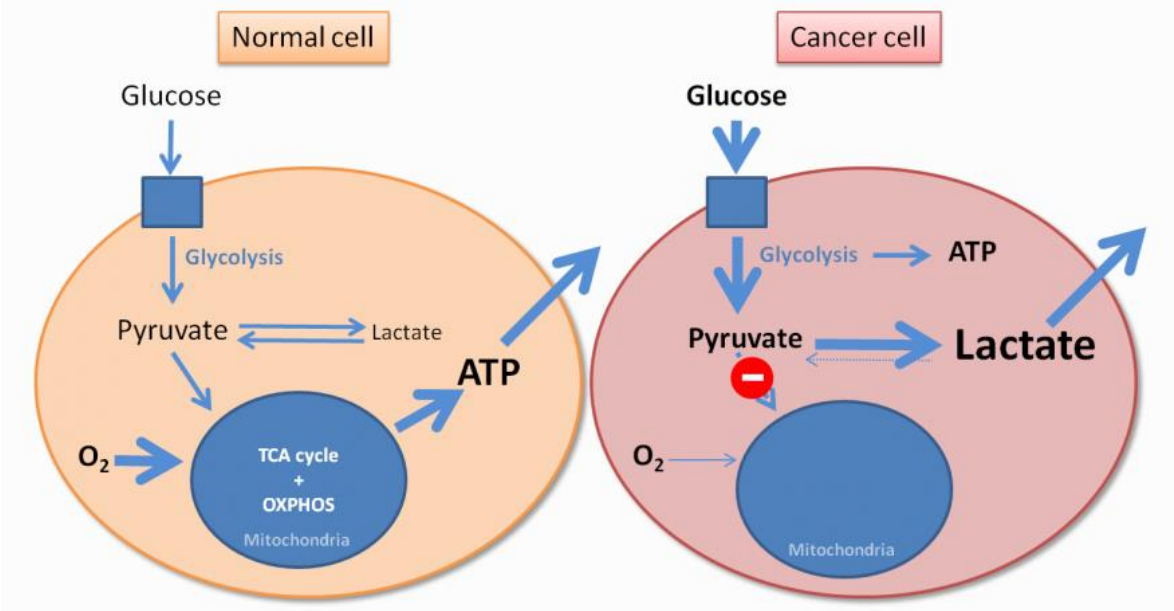

Figure 42 A diagrammatic representation of the 'Warburg effect'. This describes cancer cells as persistently converting glucose to pyruvate to lactic acid even in the presence of oxygen (termed aerobic glycolysis), rather than oxidation of pyruvate via the tricarboxylic acid (TCA) cycle, which offers a growth advantage and is a hallmark of invasive cancers (Gatenby, Gillies 2004, Xu, Pelicano et al. 2005, Pelicano, Martin et al. 2006, Vasko, Mueller et al. 2011). Heavier arrows indicate more reliance on that particular part of the pathway. Diagram taken from www.biochemikon.com.

Notably, the regulation of lactate dehydrogenase, phosphoglycerate kinase and pyruvate kinase does not appear to be consistent in different neuroblastoma models of acquired cisplatin resistance. Lactate dehydrogenase was upregulated in cisplatin-adapted SH-SY5Y neuroblastoma cells, but downregulated in cisplatin-adapted neuroblastoma SK-N-AS cells. Phosphoglycerate

kinase was upregulated in cisplatin-adapted SH-SY5Y and Kelly neuroblastoma cells, but downregulated in cisplatin-adapted SK-N-AS neuroblastoma cells. Pyruvate kinase was upregulated in cisplatin-adapted Kelly neuroblastoma cells, but downregulated in cisplatin-adapted CH-212 neuroblastoma cells. Mitochondrial aconitate hydratase was downregulated in cisplatin-adapted Kelly neuroblastoma cells (D'Aguanno, D'Alessandro et al. 2011, Piskareva, Harvey et al. 2015) (Table 17). In line with our findings in cisplatin-adapted UKF-NB-3 and UKF-NB-6 cells, phosphoglycerate kinase was shown to be upregulated in cisplatin-adapted ovarian carcinoma cells (Gong, Peng et al. 2011, Lincet, Guevel et al. 2012) and cervical cancer cells (Castagna, Antonioli et al. 2004), and pyruvate kinase was shown to be upregulated in cisplatin-adapted ovarian carcinoma cells (Lincet, Guevel et al. 2012). In contrast, the expression levels of glycolytic enzymes (including lactate dehydrogenase, phosphoglycerate kinase and pyruvate kinase) was decreased in cisplatin resistant ovarian cancer cells, suggesting that resistance formation to cisplatin was linked to a decrease in glycolysis (Jin, Huo et al. 2014). Also, a decrease in expression and activity of pyruvate kinase has been linked to cisplatin resistance in gastric carcinoma cell lines, and RNA interfering inhibition of pyruvate kinase expression increased resistance to cisplatin (Yoo, Ku et al. 2004). Conversely, though, RNA interfering inhibition of pyruvate kinase expression enhanced the cytotoxic effects of cisplatin by upregulating apoptosis and preventing cell proliferation in a lung cancer xenograft model (Guo, Zhang et al. 2011). These apparently conflicting findings emphasise the complexity of the drug resistance formation process in cancer cell populations and the need to better understand the role of particular resistance-associated changes in a given, individual cellular background. To do so, the role of the individual metabolic enzymes needs to be further elucidated in different models of acquired cisplatin resistance by functional studies.

4.3.2.1.5 Proteasomal proteins

Two proteins that are involved in protein turnover were found to be differentially regulated between UKF-NB-6^{r}CDDP^{2000} and UKF-NB-6 parental cells: proteasome subunit alpha type-6 (a component of the 20S proteasome), was downregulated in UKF-NB-6^{r}CDDP^{2000} cells compared to the parental cells, and 26S protease regulatory subunit 8 (a component of the 26S proteasome), displayed enhanced levels in UKF-NB-6^{r}CDDP^{2000}cells. No differentially-regulated proteasomal proteins were identified according to our criteria in the other studies investigating cisplatin-adapted neuroblastoma cells (D'Aguanno, D'Alessandro et al. 2011, Piskareva, Harvey et al. 2015) (Table 17). However, supporting our findings, proteasome subunit alpha type-6 was found downregulated and 26S protease regulatory subunit 8 was found upregulated in cisplatin-adapted ovarian cancer cells (Jin, Huo et al. 2014). There is a substantial amount of evidence that may link changes in proteasomal function to cisplatin resistance. Proteasomes are very abundant protein complexes and are required for ubiquitin-dependent degradation of proteins, besides being

essential to numerous processes such as cell cycle progression, gene expression, and apoptosis (Gu, Enenkel 2014, Tundo, Sbardella et al. 2015). Proteasomal activity is necessary for cancer cells to proliferate (Tundo, Sbardella et al. 2015). Recently, cisplatin has been shown *in vitro* to inhibit the three enzymatic activities of proteasome (chymotryspsin-like activity, trypsin-like activity and caspase-like activity) in a dose-dependent fashion and also to inhibit proteasome activity in SH-SY5Y neuroblastoma cells (Tundo, Sbardella et al. 2015). Furthermore, the proteasome inhibitor lactacystin increased cisplatin-induced apoptosis in neuroblastoma cells (Tundo, Sbardella et al. 2015). Additionally, a combination of cisplatin and the proteasome inhibitor bortezomib enhanced apoptosis in bladder cancer cells, compared to treatment with either drug alone, and thus to be a potential treatment for bladder cancer (Konac, Varol et al. 2015). As part of the 26S proteasome, 26S protease regulatory subunit 8 is involved in the regulation of Wnt–β-catenin signalling (Hwang, Yu et al. 2005), a proliferation pathway that has been implicated in cisplatin resistance (Gao, Liu et al. 2013, Nagaraj, Joseph et al. 2015) (2.2.2.4). However, the roles of proteasome subunit alpha type-6 and 26S protease regulatory subunit 8 need to be studied by functional investigations in the individual cellular contexts in order to learn more about their actual roles in cisplatin resistance.

4.3.2.1.6 Neuronal proteins

Two neuronal proteins were found differentially regulated between UKF-NB-3^{r}CDDP^{1000} cells and UKF-NB-3 parental cells; phosphatidylethanolamine-binding protein 1 and dihydropyrimidinase-related protein 5 were both downregulated in UKF-NB-3^{r}CDDP^{1000} cells. They are involved in neuronal function and neuronal system development respectively. As discussed in section 4.3.2.1.2 (because it is also involved in cytoskeletal remodelling), a different dihydropyrimidinase-related protein (dihydropyrimidinase-related protein 2) was identified as being downregulated in in UKF-NB-6^{r}CDDP^{2000}cells. Dihydropyrimidinase-related protein 5, also known as collapsin mediator protein-5, plays a role in nervous system development, and is a novel biomarker of lung tumour samples to distinguish between highly aggressive neuroendocrine carcinoma and other lung cancers, such as poorly differentiated non-small cell carcinoma or carcinoid lung tumors (Meyronet, Massoma et al. 2008). Nuclear dihydropyrimidinase-related protein 5 may also play a role in glioblastoma proliferation (Tan, Thiele et al. 2014), though a role in drug resistance is unclear. Phosphatidylethanolamine-binding protein 1, also known as Raf kinase inhibitor protein (RKIP), is a selective modulator of the Raf1/MEK/ERK growth factor pathway, as well as G-protein signalling and NF-κB and so has multiple cellular roles aside from neuronal function, including membrane biosynthesis and spermatogenesis, and promotion of apoptosis (Keller, Fu et al. 2005, Wang, Wang et al. 2010, Farooqi, Li et al. 2015). Phosphatidylethanolamine-binding protein 1 has been reported to be a suppressor of metastasis and is frequently downregulated in cancers. It is a prognostic biomarker for prostate, breast, melanoma, gastrointestinal stromal, and epithelial

ovarian cancer (Keller, Fu et al. 2005, Wang, Wang et al. 2010, Farooqi, Li et al. 2015) and has also been found to be downregulated in pancreatic cancer (Wang, Wang et al. 2010) and ovarian cancer (Martinho, Pinto et al. 2013). Phosphatidylethanolamine-binding protein 1 expression, which is controlled by various proteins (Farooqi, Li et al. 2015), was shown to be downregulated in cisplatin-adapted gastric cancer cells, and overexpression was demonstrated to can enhance cisplatin-induced apoptosis, possibly via the NF-κB/Snail signaling pathway y (Liu, Li et al. 2015). Also, phosphatidylethanolamine-binding protein 1 inhibition by shRNA methodology induced apoptotic resistance to cisplatin treatment in cervical cancer cells (Martinho, Pinto et al. 2013). Furthermore, up-regulation of the miRNA molecule miR-27a was reported to possibly suppress phosphatidylethanolamine-binding protein 1 expression and hence contribute to cisplatin resistance in lung adenocarcinoma cells (Li, Wang et al. 2014, Farooqi, Li et al. 2015). Taking these roles and studies together, the downregulation of phosphatidylethanolamine-binding protein 1 levels in UKF-NB-3^{r}CDDP^{1000} cells makes sense. Natural agents that increase phosphatidylethanolamine-binding protein 1 expression are also potential cancer therapeutics for the future, as well as nanotechnological delivery of phosphatidylethanolamine-binding protein 1 (Farooqi, Li et al. 2015). Neither phosphatidylethanolamine-binding protein 1 or dihydropyrimidinase-related protein 5 were identified above our cut off criteria in the proteomics studies by D'Aguanno et al and Piskareva et al (D'Aguanno, D'Alessandro et al. 2011, Piskareva, Harvey et al. 2015) (Table 17). Functional studies are required to draw further conclusions about the role of these proteins in cisplatin resistance in the individual cellular contexts.

4.3.2.1.7 Other modulated proteins, including VDAC2

Other proteins that were found differentially regulated in cisplatin-adapted cells included S-formylglutathione hydrolase (Esterase D) (an enzyme that detoxifies formaldehyde downregulated in UKF-NB-3^{r}CDDP^{1000} cells) and eukaryotic initiation factor 4A-III (a protein involved in translation and a negative regulator of apoptosis, upregulated in UKF-NB-3^{r}CDDP^{1000} cells). However, neither of these proteins fell above our cut off criteria in the proteomics studies by D'Aguanno et al and Piskareva et al (D'Aguanno, D'Alessandro et al. 2011, Piskareva, Harvey et al. 2015) (Table 17). Eukaryotic initiation factor 4A-III was also found to be upregulated in cisplatin resistant ovarian cancer cell lines (Jin, Huo et al. 2014). D-3-phosphoglycerate dehydrogenase is an enzyme involved in L-serine biosynthesis that was found upregulated in in UKF-NB-3^{r}CDDP^{1000} cells. It was also found to be upregulated in cisplatin-adapted ovarian cancer cell lines (Lincet, Guevel et al. 2012). However, it was found downregulated in cisplatin-adapted CHP-212 neuroblastoma in the Piskareva study (Piskareva, Harvey et al. 2015).

The voltage-dependent anion channel protein 2 (VDAC2) displayed enhanced levels in UKF-NB-6^{r}CDDP^{2000} cells compared to in UKF-NB-6 parentals (see spot 1403 in Appendix L). Upregulation

of VDAC2 was also observed in cisplatin-adapted SH-SY5Y neuroblastoma cells in the D'Aguanno 2D gel electrophoresis study (D'Aguanno, D'Alessandro et al. 2011).

There are three VDAC isoforms, VDAC1, VDAC2, VDAC3, that have been characterised in higher eukaryotes. VDAC1 is the most abundant one. All three isoforms are mainly located in the outer mitochondrial membrane, being evenly spread across the mitochondrial surface. The transcript levels of all three isoforms were shown to be significantly higher in rat liver cancer cells compared to normal liver cells (Shinohara, Ishida et al. 2000, Shoshan-Barmatz, Ben-Hail 2012). These anion channels may play a role in the mitochondrial mediated (intrinsic) apoptosis pathway, existing in different oligomerization states. They possess the ability to complex with other proteins and form pores (such as the mitochondrial permeability transition (MPT) pore complex (PTPC)) that permeabilise the outer mitochondrial membrane (OMM) (Shoshan-Barmatz, Ben-Hail 2012) (Figure 43).

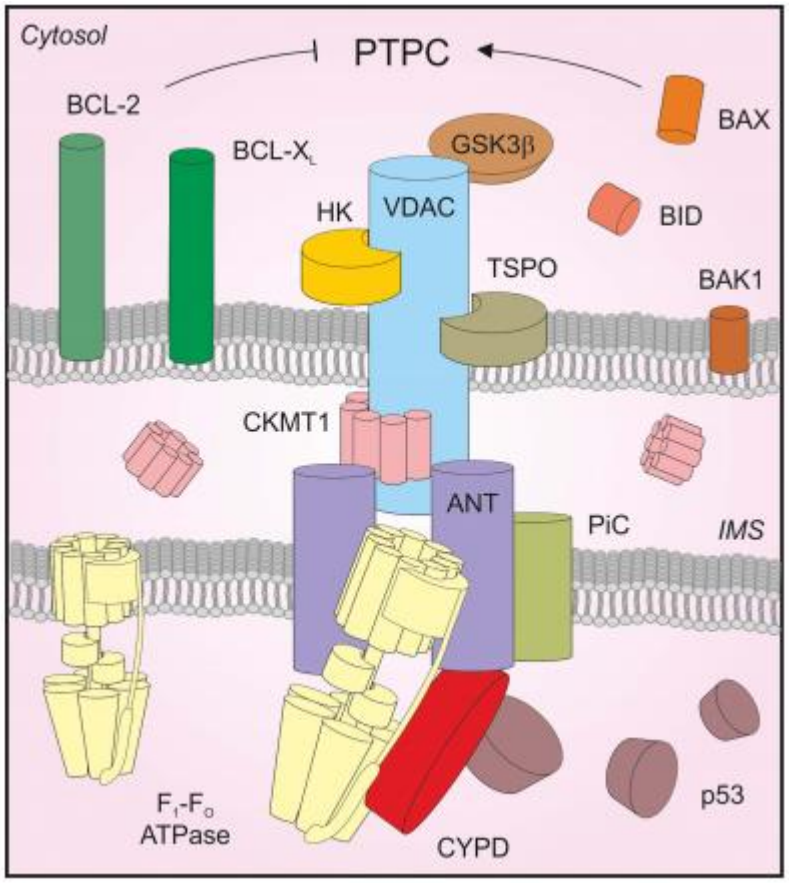

Figure 43. A representation of the possible of architecture of the permeability transition pore complex (PTPC). This is a large multiprotein complex that is assembled across the outer and inner mitochondrial membranes and its opening mediates mitochondrial permeability transition (MPT). Numerous mitochondrial and cytosolic proteins intervene in the formation or regulation of this pore complex, but its actual pore-forming unit is yet to be defined. These proteins include (but are not limited to): various isoforms of VDAC, ANT and HK (hexokinase), CYPD (cyclophilin D), PiC (SLC25A3), TSPO (translocator protein), CKMT1 (mitochondrial creatine kinase), GSK3β (glycogen synthase kinase 3β), p53, as well as several members of the Bcl-2 protein family (B-Cell Leukaemia-2). IMS, mitochondrial intermembrane space. Diagram lifted and legend adapted from (Bonora, Wieckowski et al. 2015)

BAX (Bcl2 Associated X-protein) and BAK (Bcl2 Antagonist Killer-1) are pro-apoptotic proteins of the BCL2 (B-Cell Leukaemia-2) family that play key roles in mitochondrial dysfunction, which is neccessary for mitochondrial mediated apoptosis (Wei, Zong et al. 2001, Roy, Ehrlich et al. 2009). BAK is an integral OMM protein where it controls its permeabilisation (Wei, Lindsten et al. 2000), whereas BAX is located in the cytosol from which it is redirected to the OMM to do the same (Wolter, Hsu et al. 1997). This permeabilisation results in the release of proteins such as cytochrome C, an intermediate of apoptosis leading to cell death. BAK and BAX control OMM permeabilisation in response to truncated BID (tBID), another pro-apoptotic protein of the BCL2 family. Truncation of cytosolic BID is catalysed by caspases, calpain, cathepsins or granzyme B, and this can be initiated by a variety of stress conditions such as direct DNA damage by chemotherapeutics such as cisplatin, or via death receptors such as tumour necrosis factor receptor 1 (TNFR1) or FAS (Wei, Lindsten et al. 2000, Roy, Ehrlich et al. 2009).

There are conflicting studies regarding the role of VDAC2 in apoptosis. Roy et al (Roy, Ehrlich et al. 2009) demonstrated that VDAC2 has a pro-apoptotic role, being crucial for the OMM permeabilisation mediated by tBID (whilst VDAC1 and VDAC3 are not), not necessarily as a membrane pore, but by mediating both the control of recruitment of BAK to the OMM, and also BAK dependent regulation of BAX expression. In contrast, previous work by Cheng et al (Cheng, Sheiko et al. 2003) support an anti-apoptotic role for VDAC2, but not VDAC1, specifically as an inhibitor of BAK-dependent mitochondrial apoptosis by interacting with BAK and maintaining it in an inactive form. Consistent with these findings, both *vdac1*-deficient and *vdac3*-deficient mice are viable, whereas *vdac2*-deficient mouse embryos are non-viable (Cheng, Sheiko et al. 2003). Furthermore, studies by Baines et al (Baines, Kaiser et al. 2007) indicate that all three VDAC isoforms are actually dispensable for both MPT pore and BCl-2 family orchestrated apoptosis. Roy et al (Roy, Ehrlich et al. 2009) suggest that a pro-apoptotic role for VDAC2 was not recognised in these earlier studies by Cheng et al and Baines et al due to the variation in the way both BID dependent and other apoptosis pathways are regulated. Perhaps our data, demonstrating elevated VDAC2 levels in UKF-NB-6^{r}CDDP^{2000} cells, supports an anti-apoptotic role of VDAC2, as suggested by the Cheng et al study. Besides directly damaging mitochondrial DNA, cisplatin also damages nuclear DNA and initiates the mitochondrial apoptosis pathway via p53 dependent or independent damage responses (Yang, Schumaker et al. 2006), and VDAC2 could possibly protect from this by inhibiting BAK-dependent mitochondrial apoptosis in the UKF-NB-6^{r}CDDP^{2000} cells.

In head and neck cancer, cisplatin has been shown to preferentially bind to both mitochondrial DNA and VDAC itself. The quantity of cisplatin bound to VDAC was more than 200 fold higher than the amount bound by total cellular proteins (Yang, Schumaker et al. 2006). This binding of VDAC by cisplatin can directly assist the release of cytochrome c by disrupting the mitochondrial permeability transition pore and in turn induce apoptosis in cancer cells, irrespective of

mitochondrial DNA damage by cisplatin (Gonzalez, Fuertes et al. 2001, Yang, Schumaker et al. 2006, Cullen, Yang et al. 2007). It should be noted, though, that the VDAC in these experiments comprised of all 3 isoforms and so it is not known what proportion, if any, of specific binding was to VDAC2. Maybe the levels of VDAC2 are elevated in the UKF-NB-6^{r}CDDP^{2000} cells in an attempt to circumvent direct VDAC2 cisplatin binding and maintain its anti-apoptotic effects. The exact role of the VDAC2 isoform in the mode of action and resistance to cisplatin remains to be elucidated. The VDAC1 isoform, though, has been shown to be involved in cisplatin-induced apoptosis via OMM permeabilisation (acting downstream of BAK and upstream of BAX) (2.2.1 and Figure 2. Downregulation or inhibition of VDAC1 reduced cisplatin-induced apoptosis-associated modifications of both mitochondrial and plasma membranes in non-small cell lung cancer cells (Tajeddine, Galluzzi et al. 2008). Also, the protein adseverin (SCIN) was identified as a cisplatin resistance marker in human bladder cancer cells in a proteomics study, and SCIN binds to VDACs in the mitochondria. This interaction may inhibit the mitochondrial apoptosis pathway in cancer cells that are resistant to cisplatin (Miura, Takemori et al. 2012).

It is also interesting that VDACs, by partaking in the binding of the glycolytic enzyme hexokinase to the mitochondrial outer compartment, have been proposed to play a key role in the 'Warburg effect' (high rates of glycolysis in the presence of oxygen) in cancer cells, whilst the mitochondrially-associated hexokinase activity simultaneously protects against apoptosis (Pedersen 2008, Shoshan-Barmatz, De Pinto et al. 2010). We have discussed that the 'Warburg effect' may be further driven in the UKF-NB-3^{r}CDDP^{1000} and UKF-NB-6^{r}CDDP^{2000} cells due to the upregulation of glycolytic enzymes (4.3.2.1.4), but the direct involvement of the VDAC2 isoform in this phenomenom is also not known. Nevertheless, if VDAC2 is involved, it could be another explanation for elevated levels of VDAC2 is elevated in the UKF-NB-6^{r}CDDP^{2000} cells.

Ultimately, elevated VDAC2 could be a biomarker for cisplatin resistance in neuroblastoma cells, and a target for inhibitors to alleviate cisplatin resistance, though further functional studies in cisplatin-adapted cells and in the individual cellular contexts are required.

4.3.2.2 Investigating the acute effects of cisplatin

We also investigated the effects of acute cisplatin treatment in parental and cisplatin-adapted neuroblastoma cell lines by performing a multiple cisplatin addition time course over 24 hours, adding cisplatin to cells at 2, 8 and 24 hours before harvesting, with no drug added to the 0 hour time point (control cells) (4.1.7.1), see results (4.2.2.4). As for the acquired resistance studies, summarised identified proteins can be found in Table 15 and Table 16 and their roles were put together using Appendix O and Appendix P, where the main roles and matched Gene Ontology (GO) molecular function, biological process and cellular component terms that they are matched to (excluding those inferred by electronic annotation) are tabulated; all of this information was

taken from the UniProt Knowledge base (http://www.uniprot.org/). Table 18, Table 19, Table 20, and Table 21 show the ANOVA p-values and fold change ratios of the proteins at each time point over 24 hours. In the acute studies we unveiled a mixture of proteins that were a combination of different, similar and the same as those found in the acquired resistance studies.

4.3.2.2.1 The acute response study in parental cells

RuvB-like 2 protein, nucleophosmin, and ATP synthase subunit beta (mitochondrial) were upregulated in response to cisplatin treatment after 2 hours, 8 hours and 24 hours incubation respectively of UKF-NB-3 parental cells with 1000 ng/mL cisplatin compared to the control (no drug) cells. RuvB-like 2 appeared to be a short acting response, whereas nucleophosmin, and ATP synthase subunit beta appeared to be longer acting responses over the 24 hours (Table 18).

RuvB-like 2, along with RuvB-like 1, are components of the human SRCAP, NuA4/TIP60 histone acetyltransferase, INO80 chromatin and BAF remodelling complexes. The RuvB-like proteins are functionally related to bacterial RuvB helicase which is involved in DNA repair (HOLLIDAY 1974, Ikura, Ogryzko et al. 2000). As part of human SRCAP and NuA4/TIP60 histone acetyltransferase they are involved in the transcriptional regulation of genes, possibly including those involved in oncogene-mediated growth or tumour suppressor-growth arrest, via nucleosomal histone modification. The SRCAP complex is the human equivalent of the yeast SWR1 chromatin remodelling complex, of which Bdf1 can be a component. Interestingly, Bdf1 deletion resulted in increased yeast cell sensitivity to cisplatin, as well as to carboplatin and oxaliplatin (3.3). Figure 21 illustrates a model for the evolution of the yeast chromatin remodelling complexes SWR1 and also NuA4 HAT (histone acetyltransferase) (responsible for histone H4 and H2A acetylation) to the human SRCAP (responsible for acetylation-independent exchange of 2A for H2AZ) and human NuA4/ Tip60 HAT (responsible for acetylation-linked exchange of H2A variants) complexes (Auger, Galarneau et al. 2008). As part of the NuA4/TIP60 histone acetyltransferase complex, the Ruv-B like proteins (which contribute ATPase and DNA helicase activity) are also involved in DNA repair and the signalling of the existence of DNA damage to the apoptotic system (Ikura, Ogryzko et al. 2000). As part of the INO80 complex, the RuvB-like proteins are also involved in transcriptional regulation, DNA replication and repair. Therefore, the upregulation of RuvB-like 2 may antagonise cisplatin-induced DNA damage (2.2.1). It is not surprising regarding that damaging DNA resulting in apoptosis is a known mode of cisplatin action. However, functional studies are needed to further investigate the role of RuvB-like 2 in cisplatin resistance, in particularly because cytoplasmic actin-1 (beta actin), another component of the human SRCAP and INO80 complexes, was found downregulated in UKF-NB-6^{r}CDDP^{2000} cells (Ikura, Ogryzko et al. 2000, Morrison, Shen 2009) (4.3.2.1.2.). Nucleophosmin was found upregulated both in this acute response study in UKF-NB-3 parental cells, and in the UKF-NB-3^{r}CDDP^{1000} vs UKF-NB-3 parental cell comparison

(4.3.2.1.1, where it is described). Therefore, it may be involved in the acute response to cisplatin and play a role in acquired cisplatin resistance. ATP synthase subunit beta, also known as F_1F_0 ATP synthase or Complex V, is a mitochondrial membrane protein that produces ATP form ADP in the presence of a proton gradient that is generated across the membrane by electron transport complexes of the respiratory chain. The role in the context of cisplatin treatment is unclear.

Six proteins were differentially regulated in UKF-NB-6 parental cells in response to cisplatin treatment. Three of these were heat shock chaperones, which were downregulated: endoplasmin (HSP90B1/GRP94/GP96), heat shock cognate 71 kDa protein (HSP71/HSC70/HSPA8) and 78 kDa glucose related protein (GRP78/HSPA5) after 2 hours, 8 hours and 24 hours (respectively) incubation with 2000 ng/mL cisplatin compared to the control (no drug) cells. Endoplasmin appeared to be a longer-acting response, heat shock cognate 71 kDa protein a short term response, and 78 kDa glucose related protein a long-acting effect over the 24 hours (Table 20).

Endoplasmin is a constitutive and cytosolic HSP90 isoform that is required for proper folding of proteins involved in tumourigenesis such as Toll-like receptors, and also plays a key role in the innate function of macrophages (Yang, Liu et al. 2007). It is overexpressed in certain cancers, playing a key role in tumour cell survival, and is a negative regulator of apoptosis (Wu, Chu et al. 2015). An endoplasmin peptide complex derived from tumours, named vitespen, has been trialled successfully as a vaccine for a range of cancers (Wood, Mulders 2009). Heat shock cognate 71 kDa protein is a member of the HSP70 family that is overexpressed in tumours and is involved in many cellular processes such as protein folding, protein degradation, autophagy (Stricher, Macri et al. 2013). Additionally, it is required for activating pre-mRNA splicing as part of the splicesome (van Maldegem, Maslen et al. 2015). There is a drug called apoptozole which inhibits the ATPase activity of both HSP70A1 and HSPA8, resulting in the induction of apoptosis in human embryonic carcinoma and lung cancer cells (Braunstein, Scott et al. 2007, Ciocca, Cappello et al. 2015). Both endoplasmin and 78 kDa glucose related protein, of which there are several inhibitors available, are classed as stress-inducible glucose-regulated proteins (GRPs) which are mainly located in the ER and mitochondria, both being positive regulators of the unfolded protein response (UPR), the cell cycle regulating PI3K–AKT pathway, Wnt–β-catenin proliferative signalling, suppressors of apoptosis and are linked to drug resistance (Lee 2014). Hence down-regulation of each of these three heat shock proteins may contribute to the anti-neuroblastoma effects of cisplatin. Notable the effects may be isoform specific. One proteomics study in cervix squamous cell carcinoma cells demonstrated that three isoforms of heat shock cognate 71 kDa were differentially regulated in response to cisplatin treatment (30 µg/mL for 1 hour) (Castagna, Antonioli et al. 2004).

Also after 2 hours incubation with cisplatin, proteasome subunit alpha type-6 (a component of the 20S proteasome) was downregulated in UKF-NB-6 parental cells, which is concordant with recent work showing that cisplatin inhibits proteasome activity in SH-SY5Y neuroblastoma cells (Tundo,

Sbardella et al. 2015). This downregulation appeared to be short acting (Table 20). Notably, this protein was also found downregulated in the comparison UKF-NB-6^{r}CDDP^{2000} vs UKF-NB-6 parental cells in the acquired resistance study, as already discussed (4.3.2.1.5). Overall, our data suggests that downregulation of proteasome subunit alpha type-6 is both a resistance mechanism and an acute effect of cisplatin at least in UKF-NB-6 neuroblastoma cells.

Another protein that was found downregulated after 8 hours cisplatin treatment was a redox protein, peroxiredoxin-4. By 24 hours this downregulation had returned back up to near the levels of the control UKF-NB-6 parental cells at 0 hours (Table 20). Since cisplatin is anticipated to induce higher ROS levels that contribute to DNA damage and cell death (Dasari, Tchounwou 2014) (2.2.1), peroxiredoxin-4 downregulation may contribute to the anti-neuroblastoma effects of cisplatin. Notably, peroxiredoxin-2 was found downregulated in UKF-NB-3^{r}CDDP^{1000} in the acquired resistance study (4.3.2.1.3).

Pyruvate kinase (PKM) was found upregulated in UKF-NB-6 cells in response to 8 hours cisplatin incubation (Table 20). Pyruvate kinase was also upregulated in the UKF-NB-6^{r}CDDP^{2000} cells compared to the parental cells in the acquired resistance study (4.3.2.1.4). Hence a shift towards a 'Warburg' metabolism, likely resulting from cisplatin-induced mitochondrial respiration injury (4.3.2.1.4), may be an acute protective and also an acquired resistance mechanism against cisplatin.

Functional studies are required to further elucidate the roles of the identified proteins.

4.3.2.2.2 The acute response study in cisplatin-adapted cells

There was no overlap between the proteins that were differentially regulated in response to cisplatin in UKF-NB-3 and UKF-NB-3^{r}CDDP^{1000} cells (4.3.2.2.1). Four proteins were found short-term upregulated in response to 2 hour cisplatin (1000 ng/mL) treatment in UKF-NB-3^{r}CDDP^{1000} cells (Table 19). 26S protease regulatory subunit 8, which was modulated in the UKF-NB-6^{r}CDDP^{2000} cells in the acquired resistance study (4.3.2.1.5), and also 26S protease regulatory subunit 10B are both components of the 26S proteasome (refer to 4.3.2.1.5).

VDAC2 was also upregulated in UKF-NB-3^{r}CDDP^{1000} cells after 2 hours cisplatin treatment which appeared to be a long term response (Table 19). Since VDAC2 was switched on in UKF-NB-6^{r}CDDP^{2000} cells compared UKF-NB-6 parental cells, it has been discussed previously (4.3.2.1.7). It has been discussed how in head and neck cancer, cisplatin has been shown to preferentially bind to VDAC itself, directly assisting the release of cytochrome c by disrupting the mitochondrial permeability transition pore and in turn inducing apoptosis (Yang, Schumaker et al. 2006, Cullen, Yang et al. 2007) (4.3.2.1.7). If part of this binding is to the VDAC2 isoform, then VDAC2 elevation in the cisplatin resistant cells could also be an immediate defence against this cisplatin mode of

action. Maybe VDAC2 has an alternative, yet unknown, role in the stress response to drug challenge.

The fourth protein that was found upregulated in UKF-NB-3^{r}CDDP^{1000} cells in response to 2 hours cisplatin treatment was guanine nucleotide-binding protein subunit beta-2-like-1, also known as RACK1 (receptor of activated protein C kinase 1). RACK1 is involved in many cellular processes, including a dual roles in apoptosis and proliferation (Li, Xie 2015). RACK1 has been implicated in negative regulation of Wnt–β-catenin signalling (Li, Esterberg et al. 2011, Deng, Yao et al. 2012), a proliferation pathway that has been implicated in cisplatin resistance (Gao, Liu et al. 2013, Nagaraj, Joseph et al. 2015) (2.2.2.4). Regarding neuroblastoma, it has been documented that RACK1 is expressed in neuroblastoma cells and in contrast positively regulates cell migration and proliferation via modulating the activation of Src (Lu, Zhang et al. 2012). However, in response to cisplatin, RACK1 has been shown to target ΔNp63α (a member of the p53 family) for proteasome degradation in head and neck cancer cells (Fomenkov, Zangen et al. 2004), disrupting the role of ΔNp63α in cell proliferation and oncogenic growth (Patturajan, Nomoto et al. 2002).

Elongation factor 2 and lactate dehydrogenase (A chain) were downregulated in UKF-NB-3^{r}CDDP^{1000} cells after 24 hours treatment with cisplatin (Table 19). Lactate dehydrogenase was previously discussed because it was upregulated in UKF-NB-3^{r}CDDP^{1000} cells in the acquired resistance study (4.3.2.1.4). During translation elongation, elongation factor 2 catalyses the GTP-dependent ribosomal translocation step, and silencing of elongation factor 2 in lung adenocarcinoma cells resulted in increased sensitivity to cisplatin (Chen, Fang et al. 2011).

The relevance of these six proteins in the response of UKF-NB-3^{r}CDDP^{1000} cells to cisplatin remains unclear.

In the UKF-NB-6^{r}CDDP^{2000} cells, pyruvate kinase was downregulated after 2 hours treatment with cisplatin (2000 ng/mL) which appeared to be a long-term response (Table 21). This protein was upregulated in UKF-NB-6^{r}CDDP^{2000}cells relative to UKF-NB-6 parentals cells in the acquired resistance study (4.3.2.1.4) and also in the UKF-NB-6 parental cells in the acute study after 8 hours cisplatin treatment (4.3.2.2.1). In addition, 26S protease regulatory subunit 8 was downregulated after 24 hours cisplatin treatment in UKF-NB-6^{r}CDDP^{2000} cells, also appearing to be a long-term response (Table 21). This protein has already been discussed due to its upregulation in UKF-NB-6^{r}CDDP^{2000}cells relative to UKF-NB-6 parental cells in the acquired resistance study (4.3.2.1.5) and also in this section (4.3.2.2.2) because it was upregulated in the acute response study in the UKF-NB-3^{r}CDDP^{1000} cells in response to cisplatin.

Again, the relevance of these proteins in the response of UKF-NB-6^{r}CDDP^{2000}cells to cisplatin remains to be elucidated.

5 Conclusions

In conclusion, our findings shed additional light on the (complexity of the) mechanisms underlying resistance (formation) to the clinically approved platinum drugs cisplatin, carboplatin and oxaliplatin.

Growth profiling studies of a yeast (*S.cerevisiae*) heterozygous gene deletion strains in the presence of cisplatin, carboplatin and oxaliplatin on agar containing drug versus no drug (3.2.1 and 3.2.2), as well as proteomics studies of human parental and cisplatin-resistant neuroblastoma cell lines using 2D gel electrophoresis (coupled with MALDI-TOF MS and MALDI-TOF-TOF MS/MS) (4.2.2), both revealed a number of novel candidates that may contribute to platinum drug resistance or mode of platinum drug action, being potential biomarkers, or future drug targets to reverse resistance or enhance platinum drug sensitivity. The most obvious differences between these approaches were the, just described, methodologies and the model organisms. Also, the yeast screen was a gene deletion/loss of function analysis approach compared to the analysis of protein overexpression and down-regulation for the proteomics studies. Furthermore, the yeast screen was of a pre-selected group of strains with genes encoding transcription factors deleted, whereas proteomics was of the whole cell proteome. The yeast study was also extended by examining fitness data generated from screening a whole-genome homozygous gene deletion library versus the same platinum drugs (3.2.1.1 and 3.2.1.2); these data was extracted from the Yeast Fitness Database, produced from pooled competitive growth of gene deletion strains in the presence of drug, with growth quantified by PCR and tag micro-array technology.

Comparing screening figures, in yeast a total of 14 genes were confirmed from our initial screen of 209 (transcription factor/regulator) gene deletion strains, as important for survival in the presence of platinum drugs (3.2.2); 4 for cisplatin, 6 for carboplatin, and 13 for oxaliplatin (Figure 11). From the Yeast Fitness Database (3.2.1.1), derived from screening the whole genome, there were 1656 hits for cisplatin, 582 for carboplatin, and 657 for oxaliplatin (Figure 7B). Both our screen and the Yeast Fitness Database screen, from studying the distribution of both the hit strains (3.2.1.1) and their functions and processes (3.2.1.2), demonstrated that the three platinum drugs have both exclusively individual and shared (between two or all three drugs) modes of actions and potential resistance mechanisms. Of the hit strains confirmed in our screening, BDF1 was investigated in more detail (3.2.3), confirming that it antagonises the effects of all three platinum drugs. Notably, BET inhibitors that target the human analogues of BDF1 are under clinical development for cancer and may sensitise cancer cells to platinum drugs, and it would be useful to explore whether such drugs sensitise our neuroblastoma cell lines to the platinum agents. As an accessory to the SWR1 complex, Bdf1 shares functional homology with human Brd8, an accessory subunit of the human NuA4/Tip60 HAT complex (Figure 21) (Auger, Galarneau et al.

2008); both complexes regulate histone H2AZ incorporation into chromatin and ultimately regulate transcriptional processes. Targeting Brd8 specifcally may be a worthwhile consideration for future therapy to sensitise cancer cells to platinum agents. In contrast, we carried out solely cisplatin studies in neuroblastoma, and 20 differentially expressed proteins were implicated in acquired cisplatin resistance and 15 in all the acute cisplatin responses (combined figures from the UKF-NB-3 and UKF-NB-6 studies). Originally, 20/48 excised spots (out of 574 per gel) were identified in the UKF-NB-3 cell lines and 14/32 spots (out of 675 per gel) the UKF-NB-6 cell lines. Excised spots were those that indicated differences in protein levels for at least one of the comparisons (4.2.2.2).

Even though the yeast studies and proteomics were two quite different approaches, they were both data mining exercises with some interesting overlaps in results. Proteomics hits for cisplatin resistance (4.2.2.3) and the acute responses (4.2.2.4) were matched to a variety of functions and processes, mainly chaperone activity, stress resistance, redox and detoxification, cell growth, apoptosis, DNA repair and replication, protein turnover, carbohydrate metabolism, cytoskeletal organisation and neuronal functional and development. Most of these were in agreement with those of the gene deletion hits (both for cisplatin only and for all three drugs) from the yeast studies (3.2.1.2). It was also very interesting that proteomics hits RuvB-like 2 (identified as upregulated in the cisplatin acute response in UKF-NB-3 parental cells) and beta-actin (identified as downregulated in UKF-NB-6 acquired cisplatin resistance) are both part of the human NuA4/TIP60 histone acetyltransferase (as for Brd8, see above), INO80 and SRCAP chromatin remodelling complexes, which are also involved in DNA repair and replication (Ikura, Ogryzko et al. 2000, Morrison, Shen 2009). The SRCAP complex is the human equivalent of the yeast SWR1 chromatin remodelling complex with which Bdf1, our key hit from the yeast studies, is associated. It would be very interesting to further investigate the role of all these complexes, and their individual components, in platinum drug resistance and as potential drug targets, in particularly to enhance platinum toxicity.

Focussing on the proteomics studies, it would be interesting and worthwhile to further investigate the role of nucleophosmin and VDAC2 in cisplatin resistance because both of these proteins were upregulated with high fold change ratios in cisplatin resistant cells (UKF-NB-3^{r}CDDP^{1000} and UKF-NB-6^{r}CDDP^{2000} respectively) (4.2.2.3), and both appeared in the UKF-NB-3 acute responses (4.2.2.4), and both were upregulated in one of the other external acquired resistance studies in neuroblastoma (SH-SY5Y cells) with the same direction of expression (4.2.2.2). Furthermore, there is limited literature implicating them in cisplatin resistance, which would add to their novelty as potential biomarkers or drug targets.

Cisplatin and carboplatin, which have similar modes of cellular uptake, were described to induce similar DNA adducts and to differ from oxaliplatin in their modes of interaction with DNA and

subsequent cascade of events leading to cell death. However, the majority of our results obtained from the yeast deletion strains suggested that they are not the most similar (3.2). In contrast to these findings in the yeast model, cross-resistance profiles in our cell line panel (consisting of the neuroblastoma cell lines UKF-NB-3 and UKF-NB-6 and their sub-lines adapted to cisplatin, carboplatin or oxaliplatin) were more pronounced between cisplatin- and carboplatin-resistant neuroblastoma cells than between cisplatin- or carboplatin-resistant neuroblastoma cells and oxaliplatin-resistant neuroblastoma cells (4.2.1.3). This finding suggests that yeast-derived data may only transferred to human cancer (models) with caution.

The comparison of platinum drug-resistance profiles (4.2.1.3), cell doubling times (4.2.1.2) and cell morphology (4.2.1.1) indicated significant differences between the different platinum drug-adapted neuroblastoma cell lines, indicating that, despite a substantial level of cross-resistance, resistance formation is a complex, cell line-specific (individual) process. The individuality of the resistance formation process in a given cancer cell line was confirmed by our proteomics study investigating the cisplatin-resistant sub-lines of UKF-NB-3 and UKF-NB-6 and the comparison of the resulting data to the results of two other external studies that had investigated additional cisplatin-adapted neuroblastoma cell lines by proteomics (4.2.2).

Taken together, our data overall suggests that an in depth systems biology understanding of the processes underlying resistance (formation) to platinum drugs (and probably also other anti-cancer drugs) will be needed to develop improved therapies for each individual cancer patient.

6 Bibliography

GE Healthcare Handbook 80-6429-60AC. 2-D Electrophoresis Principles and Methods. 2004. Third edn.

ABU-HADID, M., WILKES, J.D., ELAKAWI, Z., PENDYALA, L. and PEREZ, R.P., 1997. Relationship between heat shock protein 60 (HSP60) mRNA expression and resistance to platinum analogues in human ovarian and bladder carcinoma cell lines. *Cancer letters,* **119**(1), pp. 63-70.

ACEA BIOSCIENCES INC.(SAN DIEGO, CA), . Available: http://www.aceabio.com/main.aspx.

AEBERSOLD, R. and MANN, M., 2003. Mass spectrometry-based proteomics. *Nature,* **422**(6928), pp. 198-207.

AHMAD, S., 2010. Platinum-DNA Interactions and Subsequent Cellular Processes Controlling Sensitivity to Anticancer Platinum Complexes. *Chemistry & Biodiversity,* **7**(3), pp. 543-566.

ALBERTS, B., JOHNSON, A., LEWIS, J., RAFF, M., ROBERTS, K. and WALTER, P., 2002. *Molecular Biology of the Cell, 4th edition.* 4th edn. New York: Garland Science.

ALBULESCU, L., SABET, N., GUDIPATI, M., STEPANKIW, N., BERGMAN, Z.J., HUFFAKER, T.C. and PLEISS, J.A., 2012. A Quantitative, High-Throughput Reverse Genetic Screen Reveals Novel Connections between Pre-mRNA Splicing and 5 ' and 3 ' End Transcript Determinants. *Plos Genetics,* **8**(3), pp. e1002530.

AMBUDKAR, S., DEY, S., HRYCYNA, C., RAMACHANDRA, M., PASTAN, I. and GOTTESMAN, M., 1999. Biochemical, cellular, and pharmacological aspects of the multidrug transporter RID B-5964-2008. *Annual Review of Pharmacology and Toxicology,* **39**, pp. 361-398.

ANDREOTTI, P., CREE, I., KURBACHER, C., HARTMANN, D., LINDER, D., HAREL, G., GLEIBERMAN, I., CARUSO, P., RICKS, S., UNTCH, M., SARTORI, C. and BRUCKNER, H., 1995. Chemosensitivity Testing of Human Tumors using a Microplate Adenosine-Triphosphate Luminescence Assay - Clinical Correlation for Cisplatin Resistance of Ovarian-Carcinoma. *Cancer research,* **55**(22), pp. 5276-5282.

APETOH, L., GHIRINGHELLI, F., TESNIERE, A., OBEID, M., ORTIZ, C., CRIOLLO, A., MIGNOT, G., MAIURI, M.C., ULLRICH, E., SAULNIER, P., YANG, H., AMIGORENA, S., RYFFEL, B., BARRAT, F.J., SAFTIG, P., LEVI, F., LIDEREAU, R., NOGUES, C., MIRA, J., CHOMPRET, A., JOULIN, V., CLAVEL-CHAPELON, F., BOURHIS, J., ANDRE, F., DELALOGE, S., TURSZ, T., KROEMER, G. and ZITVOGEL, L., 2007. Toll-like receptor 4-dependent contribution of the immune system to anticancer chemotherapy and radiotherapy. *Nature medicine,* **13**(9), pp. 1050-1059.

AUGER, A., GALARNEAU, L., ALTAF, M., NOURANI, A., DOYON, Y., UTLEY, R.T., CRONIER, D., ALLARD, S. and COTE, J., 2008. Eaf1 is the platform for NuA4 molecular assembly that evolutionarily links chromatin acetylation to ATP-dependent exchange of histone H2A variants. *Molecular and cellular biology,* **28**(7), pp. 2257-2270.

BAETZ, K., MCHARDY, L., GABLE, K., TARLING, T., REBERIOUX, D., BRYAN, J., ANDERSEN, R., DUNN, T., HIETER, P. and ROBERGE, M., 2004. Yeast genome-wide drug-induced haploinsufficiency screen to determine drug mode of action. *Proceedings of the National Academy of Sciences of the United States of America,* **101**(13), pp. 4525-4530.

BAINES, C.P., KAISER, R.A., SHEIKO, T., CRAIGEN, W.J. and MOLKENTIN, J.D., 2007. Voltage-dependent anion channels are dispensable for mitochondrial-dependent cell death. *Nature cell biology,* **9**(5), pp. 550-U122.

BANDYOPADHYAY, S., MEHTA, M., KUO, D., SUNG, M., CHUANG, R., JAEHNIG, E.J., BODENMILLER, B., LICON, K., COPELAND, W., SHALES, M., FIEDLER, D., DUTKOWSKI, J., GUENOLE, A., VAN ATTIKUM, H., SHOKAT, K.M., KOLODNER, R.D., HUH, W., AEBERSOLD, R., KEOGH, M., KROGAN, N.J. and IDEKER, T., 2010. Rewiring of Genetic Networks in Response to DNA Damage. *Science,* **330**(6009), pp. 1385-1389.

BARKER, A.D., SIGMAN, C.C., KELLOFF, G.J., HYLTON, N.M., BERRY, D.A. and ESSERMAN, L.J., 2009. I-SPY 2: An Adaptive Breast Cancer Trial Design in the Setting of Neoadjuvant Chemotherapy. *Clinical Pharmacology & Therapeutics,* **86**(1), pp. 97-100.

BARRETINA, J., CAPONIGRO, G., STRANSKY, N., VENKATESAN, K., MARGOLIN, A.A., KIM, S., WILSON, C.J., LEHAR, J., KRYUKOV, G.V., SONKIN, D., REDDY, A., LIU, M., MURRAY, L., BERGER, M.F., MONAHAN, J.E., MORAIS, P., MELTZER, J., KOREJWA, A., JANE-VALBUENA, J., MAPA, F.A., THIBAULT, J., BRIC-FURLONG, E., RAMAN, P., SHIPWAY, A., ENGELS, I.H., CHENG, J., YU, G.K., YU, J., ASPESI, P., Jr., DE SILVA, M., JAGTAP, K., JONES, M.D., WANG, L., HATTON, C., PALESCANDOLO, E., GUPTA, S., MAHAN, S., SOUGNEZ, C., ONOFRIO, R.C., LIEFELD, T., MACCONAILL, L., WINCKLER, W., REICH, M., LI, N., MESIROV, J.P., GABRIEL, S.B., GETZ, G., ARDLIE, K., CHAN, V., MYER, V.E., WEBER, B.L., PORTER, J., WARMUTH, M., FINAN, P., HARRIS, J.L., MEYERSON, M., GOLUB, T.R., MORRISSEY, M.P., SELLERS, W.R., SCHLEGEL, R. and GARRAWAY, L.A., 2012. The Cancer Cell Line Encyclopedia enables predictive modelling of anticancer drug sensitivity. *Nature,* **483**(7391), pp. 603-607.

BASEHOAR, A., ZANTON, S. and PUGH, B., 2004. Identification and distinct regulation of yeast TATA box-containing genes. *Cell,* **116**(5), pp. 699-709.

BASU, A., BODYCOMBE, N.E., CHEAH, J.H., PRICE, E.V., LIU, K., SCHAEFER, G.I., EBRIGHT, R.Y., STEWART, M.L., ITO, D., WANG, S., BRACHA, A.L., LIEFELD, T., WAWER, M., GILBERT, J.C., WILSON, A.J., STRANSKY, N., KRYUKOV, G.V., DANCIK, V., BARRETINA, J., GARRAWAY, L.A., HON, C.S., MUNOZ, B., BITTKER, J.A., STOCKWELL, B.R., KHABELE, D., STERN, A.M., CLEMONS, P.A., SHAMJI, A.F. and SCHREIBER, S.L., 2013. An Interactive Resource to Identify Cancer Genetic and Lineage Dependencies Targeted by Small Molecules. *Cell,* **154**(5), pp. 1151-1161.

BATEMAN, A., MARTIN, M.J., O'DONOVAN, C., MAGRANE, M., APWEILER, R., ALPI, E., ANTUNES, R., ARGANISKA, J., BELY, B., BINGLEY, M., BONILLA, C., BRITTO, R., BURSTEINAS, B., CHAVALI, G., CIBRIAN-UHALTE, E., DA SILVA, A., DE GIORGI, M., DOGAN, T., FAZZINI, F., GANE, P., CAS-TRO, L.G., GARMIRI, P., HATTON-ELLIS, E., HIETA, R., HUNTLEY, R., LEGGE, D., LIU, W., LUO, J., MACDOUGALL, A., MUTOWO, P., NIGHTIN-GALE, A., ORCHARD, S., PICHLER, K., POGGIOLI, D., PUNDIR, S., PUREZA, L., QI, G., ROSANOFF, S., SAIDI, R., SAWFORD, T., SHYPITSYNA, A., TURNER, E., VOLYNKIN, V., WARDELL, T., WATKINS, X., ZELLNER, H., COWLEY, A., FIGUEIRA, L., LI, W., MCWILLIAM, H., LOPEZ, R., XENARIOS, I., BOUGUELERET, L., BRIDGE, A., POUX, S., REDASCHI, N., AIMO, L., ARGOUD-PUY, G., AUCHINCLOSS, A., AXELSEN, K., BANSAL, P., BARATIN, D., BLATTER, M., BOECKMANN, B., BOLLEMAN, J., BOUTET, E., BREUZA, L., CASAL-CASAS, C., DE CASTRO, E., COUDERT, E., CUCHE, B., DOCHE, M., DORNEVIL, D., DUVAUD, S., ESTREICHER, A., FAMIGLIETTI, L., FEUERMANN, M., GASTEIGER, E., GEHANT, S., GERRITSEN, V., GOS, A., GRUAZ-GUMOWSKI, N., HINZ, U., HULO, C., JUNGO, F., KELLER, G., LARA, V., LEMERCIER, P., LIEBERHERR, D., LOMBARDOT, T., MARTIN, X., MASSON, P., MORGAT, A., NETO, T., NOUSPIKEL, N., PAESANO, S., PEDRUZZI, I., PILBOUT, S., POZZATO, M., PRUESS, M., RIVOIRE, C., ROECHERT, B., SCHNEIDER, M., SIGRIST, C., SONESSON, K., STAEHLI, S., STUTZ, A., SUNDARAM, S., TOGNOLLI, M., VERBREGUE, L., VEUTHEY, A., WU, C.H., ARIGHI, C.N., ARMINSKI, L., CHEN, C., CHEN, Y., GARAVELLI, J.S., HUANG, H., LAIHO, K., MCGARVEY, P., NATALE, D.A., SUZEK, B.E., VINAYAKA, C.R., WANG, Q., WANG, Y., YEH, L., YERRAMALLA, M.S., ZHANG, J. and UNIPROT CONSORTIUM, 2015. UniProt: a hub for protein information. *Nucleic acids research,* **43**(D1), pp. D204-D212.

BEALE, P., ROGERS, P., BOXALL, F., SHARP, S. and KELLAND, L., 2000. BCL-2 family protein expression and platinum drug resistance in ovarian carcinoma. *British journal of cancer,* **82**(2), pp. 436-440.

BEROUKHIM, R., MERMEL, C.H., PORTER, D., WEI, G., RAYCHAUDHURI, S., DONOVAN, J., BARRETINA, J., BOEHM, J.S., DOBSON, J., URASHIMA, M., MC HENRY, K.T., PINCHBACK, R.M., LIGON, A.H., CHO, Y., HAERY, L., GREULICH, H., REICH, M., WINCKLER, W., LAWRENCE, M.S., WEIR, B.A., TANAKA, K.E., CHIANG, D.Y., BASS, A.J., LOO, A., HOFFMAN, C., PRENSNER, J., LIEFELD, T., GAO, Q., YECIES, D., SIGNORETTI, S., MAHER, E., KAYE, F.J., SASAKI, H., TEPPER, J.E., FLETCHER, J.A., TABERNERO, J., BASELGA, J., TSAO, M., DEMICHELIS, F., RUBIN, M.A., JANNE, P.A., DALY, M.J., NUCERA, C., LEVINE, R.L., EBERT, B.L., GABRIEL, S., RUSTGI, A.K., ANTONESCU, C.R., LADANYI, M., LETAI, A., GARRAWAY, L.A., LODA, M., BEER, D.G., TRUE, L.D., OKAMOTO, A., POMEROY, S.L., SINGER, S., GOLUB, T.R., LANDER, E.S., GETZ, G., SELLERS, W.R. and MEYERSON, M., 2010. The landscape of somatic copy-number alteration across human cancers RID E-2437-2011. *Nature,* **463**(7283), pp. 899-905.

BERTHELET, S., USHER, J., SHULIST, K., HAMZA, A., MALTEZ, N., JOHNSTON, A., FONG, Y., HARRIS, L.J. and BAETZ, K., 2010. Functional Genomics Analysis of the Saccharomyces cerevisiae Iron Responsive Transcription Factor Aft1 Reveals Iron-Independent Functions. *Genetics,* **185**(3), pp. 1111-1128.

BIANCHI, M., COSTANZO, G., CHELSTOWSKA, A., GRABOWSKA, D., MAZZONI, C., PICCINNI, E., CAVALLI, A., CICERONI, F., RYTKA, J., SLONIMSKI, P., FRONTALI, L. and NEGRI, R., 2004. The bromodomain-containing protein Bdf1p acts as a phenotypic and transcriptional multicopy suppressor of YAF9 deletion in yeast. *Molecular microbiology,* **53**(3), pp. 953-968.

BIANKIN, A.V., PIANTADOSI, S. and HOLLINGSWORTH, S.J., 2015. Patient-centric trials for therapeutic development in precision oncology. *Nature,* **526**(7573), pp. 361-370.

BIGNELL, G.R., GREENMAN, C.D., DAVIES, H., BUTLER, A.P., EDKINS, S., ANDREWS, J.M., BUCK, G., CHEN, L., BEARE, D., LATIMER, C., WIDAA, S., HINTON, J., FAHEY, C., FU, B., SWAMY, S., DALGLIESH, G.L., TEH, B.T., DELOUKAS, P., YANG, F., CAMPBELL, P.J., FUTREAL, P.A. and STRATTON, M.R., 2010. Signatures of mutation and selection in the cancer genome. *Nature,* **463**(7283), pp. 893-U61.

BILD, A., YAO, G., CHANG, J., WANG, Q., POTTI, A., CHASSE, D., JOSHI, M., HARPOLE, D., LANCASTER, J., BERCHUCK, A., OLSON, J., MARKS, J., DRESSMAN, H., WEST, M. and NEVINS, J., 2006. Oncogenic pathway signatures in human cancers as a guide to targeted therapies. *Nature,* **439**(7074), pp. 353-357.

BIRRELL, G., BROWN, J., WU, H., GIAEVER, G., CHU, A., DAVIS, R. and BROWN, J., 2002. Transcriptional response of Saccharomyces cerevisiae to DNA-damaging agents does not identify the genes that protect against these agents. *Proceedings of the National Academy of Sciences of the United States of America,* **99**(13), pp. 8778-8783.

BIRRELL, G., GIAEVER, G., CHU, A., DAVIS, R. and BROWN, J., 2001. A genome-wide screen in Saccharomyces cerevisiae for genes affecting UV radiation sensitivity. *Proceedings of the National Academy of Sciences of the United States of America,* **98**(22), pp. 12608-12613.

BJORNSTI, M. and HOUGHTON, P., 2004. The TOR pathway: A target for cancer therapy. *Nature Reviews Cancer,* **4**(5), pp. 335-348.

BONORA, M., WIECKOWSKI, M.R., CHINOPOULOS, C., KEPP, O., KROEMER, G., GALLUZZI, L. and PINTON, P., 2015. Molecular mechanisms of cell death: central implication of ATP synthase in mitochondrial permeability transition. *Oncogene,* **34**(12), pp. 1475-1486.

BORRELL, B., 2010. How accurate are cancer cell lines? *Nature,* **463**(7283), pp. 858-858.

BRAUNSTEIN, M.J., SCOTT, C.M., BERMAN, S., WALTER, P., WIPF, P., BRODSKY, J.L. and BATUMAN, O., 2007. In vitro antimyeloma effects of inhibitors of the heat shock protein 70 (Hsp70) molecular chaperone. *Blood,* **110**(11), pp. 456A-456A.

BRODEUR, G., 2003. Neuroblastoma: Biological insights into a clinical enigma. *Nature Reviews Cancer,* **3**(3), pp. 203-216.

BROWN, R., CURRY, E., MAGNANI, L., WILHELM-BENARTZI, C.S. and BORLEY, J., 2014. Poised epigenetic states and acquired drug resistance in cancer. *Nature Reviews Cancer,* **14**(11), pp. 747-753.

BUCHEIT, A.D. and DAVIES, M.A., 2014. Emerging insights into resistance to BRAF inhibitors in melanoma. *Biochemical pharmacology,* **87**(3), pp. 381-389.

BUNNAGE, M.E., 2010. Chapter 5: Chemical Biology of Histone Modifications Section 5.2.3 Bromodomains. In: M.E. BUNNAGE, ed, ***New Frontiers in Chemical Biology: Enabling Drug DiscoveryIssue 5 of RSC drug discovery series****.* Royal Society of Chemistry, pp. 169-173.

BURRELL, R.A., MCGRANAHAN, N., BARTEK, J. and SWANTON, C., 2013. The causes and consequences of genetic heterogeneity in cancer evolution. *Nature,* **501**(7467), pp. 338-345.

BUTOW, R. and AVADHANI, N., 2004. Mitochondrial signaling: The retrograde response. *Molecular cell,* **14**(1), pp. 1-15.

BYUN, S., KIM, S., CHOI, H., LEE, C. and LEE, E., 2005. Augmentation of cisplatin sensitivity in cisplatin-resistant human bladder cancer cells by modulating glutathione concentrations and glutathione-related enzyme activities. *BJU international,* **95**(7), pp. 1086-1090.

CAPPELLO, F., BELLAFIORE, M., PALMA, A., DAVID, S., MARCIANO, V., BARTOLOTTA, T., SCIUME, C., MODICA, G., FARINA, E., ZUMMO, G. and BUCCHIERI, F., 2003. 60KDa chaperonin (HSP60) is over-expressed during colorectal carcinogenesis. *European Journal of Histochemistry,* **47**(2), pp. 105-109.

CAPPELLO, F., DE MACARIO, E.C., MARASA, L., ZUMMO, G. and MACARIO, A.J.L., 2008. Hsp60 expression, new locations, functions and perspectives for cancer diagnosis and therapy. *Cancer Biology & Therapy,* **7**(6), pp. 801-809.

CAREN, H., KRYH, H., NETHANDER, M., SJOBERG, R.M., TRAGER, C., NILSSON, S., ABRAHAMSSON, J., KOGNER, P. and MARTINSSON, T., 2010. High-risk neuroblastoma tumors with 11q-deletion display a poor prognostic, chromosome instability phenotype with later onset. *Proceedings of the National Academy of Sciences of the United States of America,* **107**(9), pp. 4323-4328.

CARROLL, S.Y., STIRLING, P.C., STIMPSON, H.E.M., GIESSELMANN, E., SCHMITT, M.J. and DRUBIN, D.G., 2009. A Yeast Killer Toxin Screen Provides Insights into A/B Toxin Entry, Trafficking, and Killing Mechanisms. *Developmental Cell,* **17**(4), pp. 552-560.

CARROZZA, M.J., FLORENS, L., SWANSON, S.K., SHIA, W.J., ANDERSON, S., YATES, J., WASHBURN, M.P. and WORKMAN, J.L., 2005. Stable incorporation of sequence specific repressors Ash1 and Ume6 into the Rpd3L complex. *Biochimica et biophysica acta,* **1731**(2), pp. 77-87; discussion 75-6.

CASTAGNA, A., ANTONIOLI, P., ASTNER, H., HAMDAN, M., RIGHETTI, S., PEREGO, P., ZUNINO, F. and RIGHETTI, P., 2004. A proteomic approach to cisplatin resistance in the cervix squamous cell carcinoma cell line A431. *Proteomics,* **4**(10), pp. 3246-3267.

CHANG, X., MONITTO, C.L., DEMOKAN, S., KIM, M.S., CHANG, S.S., ZHONG, X., CALIFANO, J.A. and SIDRANSKY, D., 2010. Identification of Hypermethylated Genes Associated with Cisplatin Resistance in Human Cancers. *Cancer research,* **70**(7), pp. 2870-2879.

CHAO, S., CHIANG, J., HUANG, A.-. and CHANG, W., 2011. An integrative approach to identifying cancer chemoresistance-associated pathways. *Bmc Medical Genomics,* **4**, pp. 23.

CHAVEZ, J.D., HOOPMANN, M.R., WEISBROD, C.R., TAKARA, K. and BRUCE, J.E., 2011. Quantitative Proteomic and Interaction Network Analysis of Cisplatin Resistance in HeLa Cells. *Plos One,* **6**(5), pp. e19892.

CHEN, C., FANG, H., CHIOU, S., YI, S., HUANG, C., CHIANG, S., CHANG, H., LIN, T., CHIANG, I. and CHOW, K., 2011. Sumoylation of eukaryotic elongation factor 2 is vital for protein stability and anti-apoptotic activity in lung adenocarcinoma cells. *Cancer Science,* **102**(8), pp. 1582-1589.

CHEN, H.H.W. and KUO, M.T., 2013. Overcoming Platinum Drug Resistance with Copper-lowering Agents. *Anticancer Research,* **33**(10), pp. 4157-4161.

CHENG, L. and ZHANG, D.Y., 2010. Diagnostics Methodology and Technology (section of Molecular Genetic Pathology). In: L. CHENG and D.Y. ZHANG, eds, *Molecular Genetic Pathology.* Illustrated edn. Springer Science & Business Media, pp. 65-133.

CHENG, E., SHEIKO, T., FISHER, J., CRAIGEN, W. and KORSMEYER, S., 2003. VDAC2 inhibits BAK activation and mitochondrial apoptosis. *Science,* **301**(5632), pp. 513-517.

CHEUNG, N.V. and DYER, M.A., 2013. Neuroblastoma: developmental biology, cancer genomics and immunotherapy. *Nature Reviews Cancer,* **13**(6), pp. 397-411.

CHEUNG-ONG, K., GIAEVER, G. and NISLOW, C., 2013. DNA-Damaging Agents in Cancer Chemotherapy: Serendipity and Chemical Biology. *Chemistry & biology,* **20**(5), pp. 648-659.

CHI, X.X., SCHMUTZLER, B.S., BRITTAIN, J.M., WANG, Y., HINGTGEN, C.M., NICOL, G.D. and KHANNA, R., 2009. Regulation of N-type voltage-gated calcium channels (Cav2.2) and transmitter release by collapsin response mediator protein-2 (CRMP-2) in sensory neurons. *Journal of cell science,* **122**(23), pp. 4351-4362.

CHIANG, C., 2014. Nonequivalent Response to Bromodomain-Targeting BET Inhibitors in Oligodendrocyte Cell Fate Decision. *Chemistry & biology,* **21**(7), pp. 804-806.

CHRISTIANSON, T., SIKORSKI, R., DANTE, M., SHERO, J. and HIETER, P., 1992. Multifunctional Yeast High-Copy-Number Shuttle Vectors. *Gene,* **110**(1), pp. 119-122.

CHUA, P. and ROEDER, G., 1995. Bdfl, a Yeast Chromosomal Protein Required for Sporulation. *Molecular and cellular biology,* **15**(7), pp. 3685-3696.

CHUNG, Y.M., YOO, Y.D., PARK, J.K., KIM, Y.T. and KIM, H.J., 2001. Increased expression of peroxiredoxin II confers resistance to cisplatin. *Anticancer Research,* **21**(2A), pp. 1129-1133.

CINATL, J.,Jr., MICHAELIS, M. and WASS, M.N., , The Resistant Cancer Cell Line (RCCL) collection. Available: http://www.kent.ac.uk/stms/cmp/RCCL/RCCLabout.html.

CIOCCA, D.R., CAPPELLO, F., CUELLO-CARRIÓN, F.D. and ARRIGO, A., 2015. Molecular Approaches to Target Heat Shock Proteins for Cancer Treatment. *Frontiers in Clinical Drug Research - Anti-Cancer Agents,* **2**, pp. 3-47.

CIPOLLINA, C., VAN DEN BRINK, J., DARAN-LAPUJADE, P., PRONK, J.T., PORRO, D. and DE WINDE, J.H., 2008. Saccharomyces cerevisiae SFP1: at the crossroads of central metabolism and ribosome biogenesis. *Microbiology-Sgm,* **154**, pp. 1686-1699.

CLINE, S.D., 2012. Mitochondrial DNA damage and its consequences for mitochondrial gene expression. *Biochimica Et Biophysica Acta-Gene Regulatory Mechanisms,* **1819**(9-10), pp. 979-991.

COIC, E., SUN, K., WU, C. and HABER, J.E., 2006. Cell cycle-dependent regulation of Saccharomyces cerevisiae donor preference during mating-type switching by SBF (Swi4/Swi6) and Fkh1. *Molecular and cellular biology,* **26**(14), pp. 5470-5480.

COSTANZO, M., BARYSHNIKOVA, A., BELLAY, J., KIM, Y., SPEAR, E.D., SEVIER, C.S., DING, H., KOH, J.L.Y., TOUFIGHI, K., MOSTAFAVI, S., PRINZ, J., ONGE, R.P.S., VANDERSLUIS, B., MAKHNEVYCH, T., VIZEACOUMAR, F.J., ALIZADEH, S., BAHR, S., BROST, R.L., CHEN, Y., COKOL, M., DESHPANDE, R., LI, Z., LIN, Z., LIANG, W., MARBACK, M., PAW, J., LUIS, B.S., SHUTERIQI, E., TONG, A.H.Y., VAN DYK, N., WALLACE, I.M., WHITNEY, J.A., WEIRAUCH, M.T., ZHONG, G., ZHU, H., HOURY, W.A., BRUDNO, M., RAGIBIZADEH, S., PAPP, B., PAL, C., ROTH, F.P., GIAEVER, G., NISLOW, C., TROYANSKAYA, O.G., BUSSEY, H., BADER, G.D., GINGRAS, A., MORRIS, Q.D., KIM, P.M., KAISER, C.A., MYERS, C.L., ANDREWS, B.J. and BOONE, C., 2010. The Genetic Landscape of a Cell. *Science,* **327**(5964), pp. 425-431.

COUGHLIN, C.M., JOHNSTON, D.S., STRAHS, A., BURCZYNSKI, M.E., BACUS, S., HILL, J., FEINGOLD, J.M., ZACHARCHUK, C. and BERKENBLIT, A., 2010. Approaches and limitations of phosphatidylinositol-3-kinase pathway activation status as a predictive biomarker in the clinical development of targeted therapy. *Breast cancer research and treatment,* **124**(1), pp. 1-11.

CRAWFORD, N.P.S., ALSARRAJ, J., LUKES, L., WALKER, R.C., OFFICEWALA, J.S., YANG, H.H., LEE, M.P., OZATO, K. and HUNTER, K.W., 2008. Bromodomain 4 activation predicts breast cancer survival. *Proceedings of the National Academy of Sciences of the United States of America,* **105**(17), pp. 6380-6385.

CRYSTAL, A.S., SHAW, A.T., SEQUIST, L.V., FRIBOULET, L., NIEDERST, M.J., LOCKERMAN, E.L., FRIAS, R.L., GAINOR, J.F., AMZALLAG, A., GRENINGER, P., LEE, D., KALSY, A., GOMEZ-CARABALLO, M., ELAMINE, L., HOWE, E., HUR, W., LIFSHITS, E., ROBINSON, H.E., KATAYAMA, R., FABER, A.C., AWAD, M.M., RAMASWAMY, S., MINO-KENUDSON, M., IAFRATE, A.J., BENES, C.H. and ENGELMAN, J.A., 2014. Patient-derived models of acquired resistance can identify effective drug combinations for cancer. *Science (New York, N.Y.),* **346**(6216), pp. 1480-1486.

CULLEN, K.J., YANG, Z., SCHUMAKER, L. and GUO, Z., 2007. Mitochondria as a critical target of the chemotheraputic agent cisplatin in head and neck cancer. *Journal of Bioenergetics and Biomembranes,* **39**(1), pp. 43-50.

D'AGUANNO, S., D'ALESSANDRO, A., PLERONI, L., ROVERI, A., ZACCARIN, M., MARZANO, V., DE CANIO, M., BERNARDINI, S., FEDERICI, G. and URBANI, A., 2011. New Insights into Neuroblastoma Cisplatin Resistance: A Comparative Proteomic and Meta-Mining Investigation. *Journal of Proteome Research,* **10**(2), pp. 416-428.

DANCEY, J., 2004. Predictive factors for epidermal growth factor receptor inhibitors - The bull's-eye hits the arrow. *Cancer Cell,* **5**(5), pp. 411-415.

DASARI, S. and TCHOUNWOU, P.B., 2014. Cisplatin in cancer therapy: Molecular mechanisms of action. *European journal of pharmacology,* **740**, pp. 364-378.

DE BONO, J.S. and ASHWORTH, A., 2010. Translating cancer research into targeted therapeutics. *Nature,* **467**(7315), pp. 543-549.

DENG, Y.Z., YAO, F., LI, J.J., MAO, Z.F., HU, P.T., LONG, L.Y., LI, G., JI, X.D., SHI, S., GUAN, D.X., FENG, Y.Y., CUI, L., LI, D.S., LIU, Y., DU, X., GUO, M.Z., XU, L.Y., LI, E.M., WANG, H.Y. and XIE, D., 2012. RACK1 suppresses gastric tumorigenesis by stabilizing the beta-catenin destruction complex. *Gastroenterology,* **142**(4), pp. 812-823.e15.

DENIS, G. and GREEN, M., 1996. A novel, mitogen-activated nuclear kinase is related to a Drosophila developmental regulator. *Genes & development,* **10**(3), pp. 261-271.

DEY, A., CHITSAZ, F., ABBASI, A., MISTELI, T. and OZATO, K., 2003. The double bromodomain protein Brd4 binds to acetylated chromatin during interphase and mitosis. *Proceedings of the National Academy of Sciences of the United States of America,* **100**(15), pp. 8758-8763.

DI FIORE, P.P., 2008. Playing both sides: nucleophosmin between tumor suppression and oncogenesis. *Journal of Cell Biology,* **182**(1), pp. 7-9.

DIKSTEIN, R., RUPPERT, S. and TJIAN, R., 1996. TAF(11)250 is a bipartite protein kinase that phosphorylates the basal transcription factor RAP74. *Cell,* **84**(5), pp. 781-790.

DMITRIEV, O.Y., 2011. Mechanism of tumor resistance to cisplatin mediated by the copper transporter ATP7B. *Biochemistry and Cell Biology-Biochimie Et Biologie Cellulaire,* **89**(2), pp. 138-147.

DOMINGO-DOMENECH, J., VIDAL, S.J., RODRIGUEZ-BRAVO, V., CASTILLO-MARTIN, M., QUINN, S.A., RODRIGUEZ-BARRUECO, R., BONAL, D.M., CHARYTONOWICZ, E., GLADOUN, N., DE LA IGLESIA-VICENTE, J., PETRYLAK, D.P., BENSON, M.C., SILVA, J.M. and CORDON-CARDO, C., 2012. Suppression of Acquired Docetaxel Resistance in Prostate Cancer through Depletion of Notch- and Hedgehog-Dependent Tumor-Initiating Cells. *Cancer Cell,* **22**(3), pp. 373-388.

DONG, K., ADDINALL, S.G., LYDALL, D. and RUTHERFORD, J.C., 2013. The Yeast Copper Response Is Regulated by DNA Damage. *Molecular and cellular biology,* **33**(20), pp. 4041-4050.

DORNFELD, K. and LIVINGSTON, D., 1991. Effects of Controlled Rad52 Expression on Repair and Recombination in Saccharomyces-Cerevisiae. *Molecular and cellular biology,* **11**(4), pp. 2013-2017.

DUNPHY, M.P.S. and LEWIS, J.S., 2009. Radiopharmaceuticals in Preclinical and Clinical Development for Monitoring of Therapy with PET. *Journal of Nuclear Medicine,* **50**, pp. 106S-121S.

EASTMAN, A., 1986. Reevaluation of Interaction of Cis-Dichloro(ethylenediamine)platinum(ii) with Dna. *Biochemistry,* **25**(13), pp. 3912-3915.

EASWARAN, H., TSAI, H. and BAYLIN, S.B., 2014. Cancer Epigenetics: Tumor Heterogeneity, Plasticity of Stem-like States, and Drug Resistance. *Molecular cell,* **54**(5), pp. 716-727.

FALASCA, M. and LINTON, K.J., 2012. Investigational ABC transporter inhibitors. *Expert opinion on investigational drugs,* **21**(5), pp. 657-666.

FALCHOOK, G.S., FU, S., NAING, A., HONG, D.S., HU, W., MOULDER, S., WHELER, J.J., SOOD, A.K., BUSTINZA-LINARES, E., PARKHURST, K.L. and KURZROCK, R., 2013. Methylation and histone deacetylase inhibition in combination with platinum treatment in patients with advanced malignancies. *Investigational new drugs,* **31**(5), pp. 1192-1200.

FARMER, H., MCCABE, N., LORD, C., TUTT, A., JOHNSON, D., RICHARDSON, T., SANTAROSA, M., DILLON, K., HICKSON, I., KNIGHTS, C., MARTIN, N., JACKSON, S., SMITH, G. and ASHWORTH, A.,

2005. Targeting the DNA repair defect in BRCA mutant cells as a therapeutic strategy. *Nature,* **434**(7035), pp. 917-921.

FAROOQI, A.A., LI, Y. and SARKAR, F.H., 2015. The biological complexity of RKIP signaling in human cancers. *Experimental and Molecular Medicine,* **47**, pp. e185.

FERRY, K., HAMILTON, T. and JOHNSON, S., 2000. Increased nucleotide excision repair in cisplatin-resistant ovarian cancer cells - Role of ERCC1-XPF. *Biochemical pharmacology,* **60**(9), pp. 1305-1313.

FICHTNER, I., CINATL, J., Jr., MICHAELIS, M., SANDERS, L.C., HILGER, R., KENNEDY, B.N., REYNOLDS, A.L., HACKENBERG, F., LALLY, G., QUINN, S.J., MCRAE, I. and TACKE, M., 2012. In Vitro and In Vivo Investigations into the Carbene Silver Acetate Anticancer Drug Candidate SBC1. *Letters in Drug Design & Discovery,* **9**(9), pp. 815-822.

FILIPPAKOPOULOS, P. and KNAPP, S., 2014. Targeting bromodomains: epigenetic readers of lysine acetylation. *Nature Reviews Drug Discovery,* **13**(5), pp. 339-358.

FILIPPAKOPOULOS, P., QI, J., PICAUD, S., SHEN, Y., SMITH, W.B., FEDOROV, O., MORSE, E.M., KEATES, T., HICKMAN, T.T., FELLETAR, I., PHILPOTT, M., MUNRO, S., MCKEOWN, M.R., WANG, Y., CHRISTIE, A.L., WEST, N., CAMERON, M.J., SCHWARTZ, B., HEIGHTMAN, T.D., LA THANGUE, N., FRENCH, C.A., WIEST, O., KUNG, A.L., KNAPP, S. and BRADNER, J.E., 2010. Selective inhibition of BET bromodomains. *Nature,* **468**(7327), pp. 1067-1073.

FINK, D., NEBEL, S., AEBI, S., ZHENG, H., CENNI, B., NEHME, A., CHRISTEN, R. and HOWELL, S., 1996. The role of DNA mismatch repair in platinum drug resistance. *Cancer research,* **56**(21), pp. 4881-4886.

FLIS, S., GNYSZKA, A. and SPLAWINSKI, J., 2009. HDAC inhibitors, MS275 and SBHA, enhances cytotoxicity induced by oxaliplatin in the colorectal cancer cell lines. *Biochemical and biophysical research communications,* **387**(2), pp. 336-341.

FLORENCE, B. and FALLER, D., 2001. You BET-CHA: A novel family of transcriptional regulators. *Frontiers in Bioscience,* **6**, pp. D1008-D1018.

FOMENKOV, A., ZANGEN, R., HUANG, Y., OSADA, M., GUO, Z., FOMENKOV, T., TRINK, B., SIDRANSKY, D. and RATOVITSKI, E., 2004. RACK1 and stratifin target Delta Np63 alpha for a proteasome degradation in head and neck squamous cell carcinoma cells upon DNA damage. *Cell Cycle,* **3**(10), pp. 1285-1295.

FONG, C.Y., GILAN, O., LAM, E.Y.N., RUBIN, A.F., FTOUNI, S., TYLER, D., STANLEY, K., SINHA, D., YEH, P., MORISON, J., GIOTOPOULOS, G., LUGO, D., JEFFREY, P., LEE, S.C., CARPENTER, C., GREGORY, R., RAMSAY, R.G., LANE, S.W., ABDEL-WAHAB, O., KOUZARIDES, T., JOHNSTONE, R.W., DAWSON, S., HUNTLY, B.J.P., PRINJHA, R.K., PAPENFUSS, A.T. and DAWSON, M.A., 2015. BET inhibitor resistance emerges from leukaemia stem cells. *Nature,* **525**(7570), pp. 538-+.

FRENCH, C., 2014. NUT midline carcinoma. *Nature Reviews Cancer,* **14**(3), pp. 149-150.

FU, J., HOU, J., LIU, L., CHEN, L., WANG, M., SHEN, Y., ZHANG, Z. and BAO, X., 2013. Interplay between BDF1 and BDF2 and their roles in regulating the yeast salt stress response. *Febs Journal,* **280**(9), pp. 1991-2001.

FU, S., NAING, A., FU, C., KUO, M.T. and KURZROCK, R., 2012. Overcoming Platinum Resistance through the Use of a Copper-Lowering Agent. *Molecular Cancer Therapeutics,* **11**(6), pp. 1221-1225.

FUERTES, M., CASTILLA, J., ALONSO, C. and PEREZ, J., 2003. Cisplatin biochemical mechanism of action: From cytotoxicity to induction of cell death through interconnections between apoptotic and necrotic pathways. *Current medicinal chemistry,* **10**(3), pp. 257-266.

FUJIE, Y., YAMAMOTO, H., NGAN, C., TAKAGI, A., HAYASHI, T., SUZUKI, R., EZUMI, K., TAKEMASA, I., IKEDA, M., SEKIMOTO, M., MATSUURA, N. and MONDEN, M., 2005. Oxaliplatin, a potent inhibitor of survivin, enhances paclitaxel-induced apoptosis and mitotic catastrophe in colon cancer cells. *Japanese journal of clinical oncology,* **35**(8), pp. 453-463.

GABBIANI, C., MAGHERINI, F., MODESTI, A. and MESSORI, L., 2010. Proteomic and Metallomic Strategies for Understanding the Mode of Action of Anticancer Metallodrugs. *Anti-Cancer Agents in Medicinal Chemistry,* **10**(4), pp. 324-337.

GALDIERI, L., MEHROTRA, S., YU, S. and VANCURA, A., 2010. Transcriptional Regulation in Yeast during Diauxic Shift and Stationary Phase. *Omics-a Journal of Integrative Biology,* **14**(6), pp. 629-638.

GALLUZZI, L., VITALE, I., MICHELS, J., BRENNER, C., SZABADKAI, G., HAREL-BELLAN, A., CASTEDO, M. and KROEMER, G., 2014. Systems biology of cisplatin resistance: past, present and future. *Cell Death & Disease,* **5**, pp. e1257.

GAO, G., CHEN, L. and HUANG, C., 2014. Anti-cancer drug discovery: update and comparisons in yeast, Drosophila, and zebrafish. *Current molecular pharmacology,* **7**(1), pp. 44-51.

GAO, Y., LIU, Z., ZHANG, X., HE, J., PAN, Y., HAO, F., XIE, L., LI, Q., QIU, X. and WANG, E., 2013. Inhibition of cytoplasmic GSK-3 beta increases cisplatin resistance through activation of Wnt/beta-catenin signaling in A549/DDP cells. *Cancer letters,* **336**(1), pp. 231-239.

GARABEDIAN, M.V., NOGUCHI, C., ZIEGLER, M.A., DAS, M.M., SINGH, T., HARPER, L.J., LEMAN, A.R., KHAIR, L., MOSER, B.A., NAKAMURA, T.M. and NOGUCHI, E., 2012. The Double-Bromodomain Proteins Bdf1 and Bdf2 Modulate Chromatin Structure to Regulate S-Phase Stress Response in Schizosaccharomyces pombe. *Genetics,* **190**(2), pp. 487-U301.

GARCIA-GUTIERREZ, P., MUNDI, M. and GARCIA-DOMINGUEZ, M., 2012. Association of bromodomain BET proteins with chromatin requires dimerization through the conserved motif B. *Journal of cell science,* **125**(15), pp. 3671-3680.

GARDINER, F.C., COSTA, R. and AYSCOUGH, K.R., 2007. Nucleocytoplasmic trafficking is required for functioning of the adaptor protein Sla1p in endocytosis. *Traffic,* **8**(4), pp. 347-358.

GASCH, A., SPELLMAN, P., KAO, C., CARMEL-HAREL, O., EISEN, M., STORZ, G., BOTSTEIN, D. and BROWN, P., 2000. Genomic expression programs in the response of yeast cells to environmental changes. *Molecular biology of the cell,* **11**(12), pp. 4241-4257.

GATENBY, R. and GILLIES, R., 2004. Why do cancers have high aerobic glycolysis? *Nature Reviews Cancer,* **4**(11), pp. 891-899.

GATTI, L., CASSINELLI, G., ZAFFARONI, N., LANZI, C. and PEREGO, P., 2015. New mechanisms for old drugs: Insights into DNA-unrelated effects of platinum compounds and drug resistance determinants. *Drug Resistance Updates,* **20**, pp. 1-11.

GEWIRTZ, D.A., HOLT, S.E. and ELMORE, L.W., 2008. Accelerated senescence: An emerging role in tumor cell response to chemotherapy and radiation. *Biochemical pharmacology,* **76**(8), pp. 947-957.

GHIRINGHELLI, F., APETOH, L., TESNIERE, A., AYMERIC, L., MA, Y., ORTIZ, C., VERMAELEN, K., PANARETAKIS, T., MIGNOT, G., ULLRICH, E., PERFETTINI, J., SCHLEMMER, F., TASDEMIR, E., UHL, M., GENIN, P., CIVAS, A., RYFFEL, B., KANELLOPOULOS, J., TSCHOPP, J., ANDRE, F., LIDEREAU, R., MCLAUGHLIN, N.M., HAYNES, N.M., SMYTH, M.J., KROEMER, G. and ZITVOGEL, L., 2009. Activation of the NLRP3 inflammasome in dendritic cells induces IL-1 beta-dependent adaptive immunity against tumors. *Nature medicine,* **15**(10), pp. 1170-U99.

GIAEVER, G., CHU, A., NI, L., CONNELLY, C., RILES, L., VERONNEAU, S., DOW, S., LUCAU-DANILA, A., ANDERSON, K., ANDRE, B., ARKIN, A., ASTROMOFF, A., EL BAKKOURY, M., BANGHAM, R., BENITO, R., BRACHAT, S., CAMPANARO, S., CURTISS, M., DAVIS, K., DEUTSCHBAUER, A., ENTIAN, K., FLAHERTY, P., FOURY, F., GARFINKEL, D., GERSTEIN, M., GOTTE, D., GULDENER, U., HEGEMANN, J., HEMPEL, S., HERMAN, Z., JARAMILLO, D., KELLY, D., KELLY, S., KOTTER, P., LABONTE, D., LAMB, D., LAN, N., LIANG, H., LIAO, H., LIU, L., LUO, C., LUSSIER, M., MAO, R., MENARD, P., OOI, S., REVUELTA, J., ROBERTS, C., ROSE, M., ROSS-MACDONALD, P., SCHERENS, B., SCHIMMACK, G., SHAFER, B., SHOEMAKER, D., SOOKHAI-MAHADEO, S., STORMS, R., STRATHERN, J., VALLE, G., VOET, M., VOLCKAERT, G., WANG, C., WARD, T., WILHELMY, J., WINZELER, E., YANG, Y., YEN, G., YOUNGMAN, E., YU, K., BUSSEY, H., BOEKE, J., SNYDER, M., PHILIPPSEN, P., DAVIS, R. and JOHNSTON, M., 2002. Functional profiling of the Saccharomyces cerevisiae genome. *Nature,* **418**(6896), pp. 387-391.

GIAEVER, G. and NISLOW, C., 2014. The Yeast Deletion Collection: A Decade of Functional Genomics. *Genetics,* **197**(2), pp. 451-465.

GILLET, J.P., CALCAGNO, A.M., VARMA, S., MARINO, M., GREEN, L.J., VORA, M.I., PATEL, C., ORINA, J.N., ELISEEVA, T.A., SINGAL, V., PADMANABHAN, R., DAVIDSON, B., GANAPATHI, R., SOOD, A.K., RUEDA, B.R., AMBUDKAR, S.V. and GOTTESMAN, M.M., 2011. Redefining the relevance of established cancer cell lines to the study of mechanisms of clinical anti-cancer drug resistance. *Proceedings of the National Academy of Sciences of the United States of America,* .

GONG, F., PENG, X., ZENG, Z., YU, M., ZHAO, Y. and TONG, A., 2011. Proteomic analysis of cisplatin resistance in human ovarian cancer using 2-DE method. *Molecular and cellular biochemistry,* **348**(1-2), pp. 141-147.

GONZALEZ, V., FUERTES, M., ALONSO, C. and PEREZ, J., 2001. Is cisplatin-induced cell death always produced by apoptosis? *Molecular pharmacology,* **59**(4), pp. 657-663.

GOODSELL, D.S., 2006. The molecular perspective: Cisplatin. *Oncologist,* **11**(3), pp. 316-317.

GOODSPEED, A., HEISER, L.M., GRAY, J.W. and COSTELLO, J.C., 2016. Tumor-Derived Cell Lines as Molecular Models of Cancer Pharmacogenomics. *Molecular Cancer Research,* **14**(1), pp. 3-13.

GOSSAGE, L. and MADHUSUDAN, S., 2007. Current status of excision repair cross complementing-group 1 (ERCC1) in cancer. *Cancer treatment reviews,* **33**(6), pp. 565-577.

GOTTESMAN, M.M., LAVI, O., HALL, M.D. and GILLET, J., 2016. Toward a Better Understanding of the Complexity of Cancer Drug Resistance. *Annual Review of Pharmacology and Toxicology, Vol 56,* **56**, pp. 85-102.

GOURDIER, I., CRABBE, L., ANDREAU, K., PAU, B. and KROEMER, G., 2004. Oxaliplatin-induced mitochondrial apoptotic response of colon carcinoma cells does not require nuclear DNA. *Oncogene,* **23**(45), pp. 7449-7457.

GRANT, P., DUGGAN, L., COTE, J., ROBERTS, S., BROWNELL, J., CANDAU, R., OHBA, R., OWENHUGHES, T., ALLIS, C., WINSTON, F., BERGER, S. and WORKMAN, J., 1997. Yeast Gcn5

functions in two multisubunit complexes to acetylate nucleosomal histones: Characterization of an Ada complex and the SAGA (Spt/Ada) complex. *Genes & development,* **11**(13), pp. 1640-1650.

GRAY, J., PETSKO, G., JOHNSTON, G., RINGE, D., SINGER, R. and WERNER-WASHBURNE, M., 2004. "Sleeping beauty": Quiescence in Saccharomyces cerevisiae. *Microbiology and Molecular Biology Reviews,* **68**(2), pp. 187-+.

GRIFFITH, O. and MEISTER, A., 1985. Origin and Turnover of Mitochondrial Glutathione. *Proceedings of the National Academy of Sciences of the United States of America,* **82**(14), pp. 4668-4672.

GRISENDI, S., MECUCCI, C., FALINI, B. and PANDOLFI, P.P., 2006. Nucleophosmin and cancer. *Nature Reviews Cancer,* **6**(7), pp. 493-505.

GU, Z.C. and ENENKEL, C., 2014. Proteasome assembly. *Cellular and molecular life sciences : CMLS,* **71**(24), pp. 4729-4745.

GUO, W., ZHANG, Y., CHEN, T., WANG, Y., XUE, J., ZHANG, Y., XIAO, W., MO, X. and LU, Y., 2011. Efficacy of RNAi targeting of pyruvate kinase M2 combined with cisplatin in a lung cancer model. *Journal of cancer research and clinical oncology,* **137**(1), pp. 65-72.

HALLIGAN, B., RUOTTI, V., JIN, W., LAFFOON, S., TWIGGER, S. and DRATZ, E., 2004. ProMoST (Protein Modification Screening Tool): a web-based tool for mapping protein modifications on two-dimensional gels. *Nucleic acids research,* **32**, pp. W638-W644.

HARRIES, M. and SMITH, I., 2002. The development and clinical use of trastuzumab (Herceptin). *Endocrine-related cancer,* **9**(2), pp. UNSP 1351-0088/02/009-075.

HARTMAN, J. and TIPPERY, N., 2004. Systematic quantification of gene interactions by phenotypic array analysis. *Genome biology,* **5**(7), pp. R49.

HARVEY, H., PISKAREVA, O., CREEVEY, L., ALCOCK, L.C., BUCKLEY, P.G., O'SULLIVAN, M.J., SEGURA, M.F., GALLEGO, S., STALLINGS, R.L. and BRAY, I.M., 2015. Modulation of chemotherapeutic drug resistance in neuroblastoma SK-N-AS cells by the neural apoptosis inhibitory protein and miR-520f. *International Journal of Cancer,* **136**(7), pp. 1579-1588.

HAYDEN, E.C., 2011. Targeted treatment tested as potential cancer cure. *Nature,* **479**(7373), pp. 281-281.

HEFFETER, P., JUNGWIRTH, U., JAKUPEC, M., HARTINGER, C., GALANSKI, M., ELBLING, L., MICKSCHE, M., KEPPLER, B. and BERGER, W., 2008. Resistance against novel anticancer metal compounds: Differences and similarities RID B-7085-2011. *Drug Resistance Updates,* **11**(1-2), pp. 1-16.

HELIN, K. and DHANAK, D., 2013. Chromatin proteins and modifications as drug targets. *Nature,* **502**(7472), pp. 480-488.

HERMAN, P., 2002. Stationary phase in yeast. *Current opinion in microbiology,* **5**(6), pp. 602-607.

HILLENMEYER, M.E., FUNG, E., WILDENHAIN, J., PIERCE, S.E., HOON, S., LEE, W., PROCTOR, M., ST ONGE, R.P., TYERS, M., KOLLER, D., ALTMAN, R.B., DAVIS, R.W., NISLOW, C. and GIAEVER, G., 2008. The chemical genomic portrait of yeast: Uncovering a phenotype for all genes. *Science,* **320**(5874), pp. 362-365.

HO, W., COSTANZO, M., MOORE, L., KOBAYASHI, R. and ANDREWS, B., 1999. Regulation of transcription at the Saccharomyces cerevisiae start transition by Stb1, a Swi6-binding protein. *Molecular and cellular biology,* **19**(8), pp. 5267-5278.

HOLLENHORST, P., BOSE, M., MIELKE, M., MULLER, U. and FOX, C., 2000. Forkhead genes in transcriptional silencing, cell morphology and the cell cycle: Overlapping and distinct functions for FKH1 and FKH2 in Saccharomyces cerevisiae. *Genetics,* **154**(4), pp. 1533-1548.

HOLLIDAY, R., 1974. Molecular Aspects of Genetic Exchange and Gene Conversion. *Genetics,* **78**(1), pp. 273-287.

HOLOHAN, C., VAN SCHAEYBROECK, S., LONGLEY, D.B. and JOHNSTON, P.G., 2013. Cancer drug resistance: an evolving paradigm. *Nature Reviews Cancer,* **13**(10), pp. 714-726.

HOLZER, A.K., MANOREK, G.H. and HOWELL, S.B., 2006. Contribution of the major copper influx transporter CTR1 to the cellular accumulation of cisplatin, carboplatin, and oxaliplatin. *Molecular pharmacology,* **70**(4), pp. 1390-1394.

HU, X. and ZHANG, Z., 2016. Understanding the Genetic Mechanisms of Cancer Drug Resistance Using Genomic Approaches. *Trends in Genetics,* **32**(2), pp. 127-137.

HUISINGA, K. and PUGH, B., 2004. A genome-wide housekeeping role for TFIID and a highly regulated stress-related role for SAGA in Saccharomyces cerevisiae. *Molecular cell,* **13**(4), pp. 573-585.

HWANG, S.G., YU, S.S., RYU, J.H., JEON, H.B., YOO, Y.J., EOM, S.H. and CHUN, J.S., 2005. Regulation of beta-catenin signaling and maintenance of chondrocyte differentiation by ubiquitin-independent proteasomal degradation of alpha-catenin. *The Journal of biological chemistry,* **280**(13), pp. 12758-12765.

IBRAHIM, M.A., SRIVENUGOPAL, K.S. and RASUL, K.I., 2013. Platinum Resistance: The Role of Molecular, Genetic and Epigenetic Factors. *Journal of Medical Sciences,* **13**, pp. 160-168.

IHRLUND, L.S., HERNLUND, E., KHAN, O. and SHOSHAN, M.C., 2008. 3-Bromopyruvate as inhibitor of tumour cell energy metabolism and chemopotentiator of platinum drugs. *Molecular Oncology,* **2**(1), pp. 94-101.

IKURA, T., OGRYZKO, V.V., GRIGORIEV, M., GROISMAN, R., WANG, J., HORIKOSHI, M., SCULLY, R., QIN, J. and NAKATANI, Y., 2000. Involvement of the TIP60 histone acetylase complex in DNA repair and apoptosis. *Cell,* **102**(4), pp. 463-473.

INAGAKI, N., CHIHARA, K., ARIMURA, N., MENAGER, C., KAWANO, Y., MATSUO, N., NISHIMURA, T., AMANO, M. and KAIBUCHI, K., 2001. CRMP-2 induces axons in cultured hippocampal neurons. *Nature neuroscience,* **4**(8), pp. 781-782.

IRELAND, C., PITTMAN, S., JONES, S. and HARNETT, P., 1994. Establishment of an In-Vitro Model for Cisplatin Resistance in Human Neuroblastoma Cell-Lines. *Anticancer Research,* **14**(6B), pp. 2397-2403.

IRLBACHER, H., FRANKE, J., MANKE, T., VINGRON, M. and EHRENHOFER-MURRAY, A., 2005. Control of replication initiation and heterochromatin formation in Saccharomyces cerevisiae by a regulator of meiotic gene expression. *Genes & development,* **19**(15), pp. 1811-1822.

ISHIDA, S., LEE, J., THIELE, D. and HERSKOWITZ, I., 2002. Uptake of the anticancer drug cisplatin mediated by the copper transporter Ctr1 in yeast and mammals. *Proceedings of the National Academy of Sciences of the United States of America,* **99**(22), pp. 14298-14302.

ISSAQ, H.J. and VEENSTRA, T.D., 2008. Two-dimensional polyacrylamide gel electrophoresis (2D-PAGE): advances and perspectives. *BioTechniques,* **44**(5), pp. 697-+.

IVANOVA, T., ZOURIDIS, H., WU, Y., CHENG, L.L., TAN, I.B., GOPALAKRISHNAN, V., OOI, C.H., LEE, J., QIN, L., WU, J., LEE, M., RHA, S.Y., HUANG, D., LIEM, N., YEOH, K.G., YONG, W.P., TEH, B.T. and TAN, P., 2013. Integrated epigenomics identifies BMP4 as a modulator of cisplatin sensitivity in gastric cancer. *Gut,* **62**(1), pp. 22-33.

IYER, V., HORAK, C., SCAFE, C., BOTSTEIN, D., SNYDER, M. and BROWN, P., 2001. Genomic binding sites of the yeast cell-cycle transcription factors SBF and MBF. *Nature,* **409**(6819), pp. 533-538.

JAMIESON, E. and LIPPARD, S., 1999. Structure, recognition, and processing of cisplatin-DNA adducts. *Chemical reviews,* **99**(9), pp. 2467-2498.

JASKOLLA, T.W., PAPASOTIRIOU, D.G. and KARAS, M., 2009. Comparison between the Matrices alpha-Cyano-4-hydroxycinnamic Acid and 4-Chloro-alpha-cyanocinnamic Acid for Trypsin, Chymotrypsin, and Pepsin Digestions by MALDI-TOF Mass Spectrometry. *Journal of Proteome Research,* **8**(7), pp. 3588-3597.

JELINSKY, S., ESTEP, P., CHURCH, G. and SAMSON, L., 2000. Regulatory networks revealed by transcriptional profiling of damaged Saccharomyces cerevisiae cells: Rpn4 links base excision repair with proteasomes. *Molecular and cellular biology,* **20**(21), pp. 8157-8167.

JIANG, C.C., MAO, Z.G., AVERY-KIEJDA, K.A., WADE, M., HERSEY, P. and ZHANG, X.D., 2009. Glucose-regulated protein 78 antagonizes cisplatin and adriamycin in human melanoma cells. *Carcinogenesis,* **30**(2), pp. 197-204.

JIN, L., HUO, Y., ZHENG, Z., JIANG, X., DENG, H., CHEN, Y., LIAN, Q., GE, R. and DENG, H., 2014. Down-regulation of Ras-related Protein Rab 5C-dependent Endocytosis and Glycolysis in Cisplatin-resistant Ovarian Cancer Cell Lines. *Molecular & Cellular Proteomics,* **13**(11), pp. 3138-3151.

JOHNSTONE, T.C., SUNTHARALINGAM, K. and LIPPARD, S.J., 2016. The Next Generation of Platinum Drugs: Targeted Pt(II) Agents, Nanoparticle Delivery, and Pt(IV) Prodrugs. *Chemical reviews,* **116**(5), pp. 3436-3486.

JOSEPH, J.D., LU, N., QIAN, J., SENSINTAFFAR, J., SHAO, G., BRIGHAM, D., MOON, M., MANEVAL, E.C., CHEN, I., DARIMONT, B. and HAGER, J.H., 2013. A clinically relevant androgen receptor mutation confers resistance to second-generation antiandrogens enzalutamide and ARN-509. *Cancer discovery,* **3**(9), pp. 1020-1029.

KALA, R., PEEK, G.W., HARDY, T.M. and TOLLEFSBOL, T.O., 2013. MicroRNAs: an emerging science in cancer epigenetics. *Journal of clinical bioinformatics,* **3**(1), pp. 6-9113-3-6.

KANNO, T., KANNO, Y., SIEGEL, R., JANG, M., LENARDO, M. and OZATO, K., 2004. Selective recognition of acetylated histones by bromodomain proteins visualized in living cells. *Molecular cell,* **13**(1), pp. 33-43.

KATSOGIANNOU, M., ANDRIEU, C. and ROCCHI, P., 2014. Heat shock protein 27 phosphorylation state is associated with cancer progression. *Frontiers in Genetics,* **5**, pp. 346-Article No.: 346.

KELLAND, L., 2007. The resurgence of platinum-based cancer chemotherapy. *Nature Reviews Cancer,* **7**(8), pp. 573-584.

KELLER, E., FU, Z. and BRENNAN, M., 2005. The biology of a prostate cancer metastasis suppressor protein: Raf kinase inhibitor protein. *Journal of cellular biochemistry,* **94**(2), pp. 273-278.

KERN, D. and WEISENTHAL, L., 1990. Highly Specific Prediction of Antineoplastic Drug-Resistance with an Invitro Assay using Suprapharmacologic Drug Exposures. *Journal of the National Cancer Institute,* **82**(7), pp. 582-588.

KESHELAVA, N., SEEGER, R., GROSHEN, S. and REYNOLDS, C., 1998. Drug resistance patterns of human neuroblastoma cell lines derived from patients at different phases of therapy. *Cancer research,* **58**(23), pp. 5396-5405.

KHABELE, D., WILSON, A.J., SASKOWSKI, J. and HIEBERT, S.W., 2013. ***Abstract B52: The bromodomain inhibitor JQ1 enhances cisplatin-mediated cytotoxicity in ovarian cancer cells***. Clin Cancer Res: .

KIM, E.S., HERBST, R.S., WISTUBA, I.I., LEE, J.J., BLUMENSCHEIN, G.R., Jr., TSAO, A., STEWART, D.J., HICKS, M.E., ERASMUS, J., Jr., GUPTA, S., ALDEN, C.M., LIU, S., TANG, X., KHURI, F.R., TRAN, H.T., JOHNSON, B.E., HEYMACH, J.V., MAO, L., FOSSELLA, F., KIES, M.S., PAPADIMITRAKOPOULOU, V., DAVIS, S.E., LIPPMAN, S.M. and HONG, W.K., 2011. The BATTLE Trial: Personalizing Therapy for Lung Cancer. *Cancer Discovery,* **1**(1), pp. 44-53.

KIM, J., KIM, K., LEE, E., LIM, J., CHO, H., YOON, H., CHO, M., BAEK, K., PARK, Y., PAIK, S., CHOE, Y. and LEE, H., 2004. Up-regulation of Bfl-1/A1 via NF-kappa B activation in cisplatin-resistant human bladder cancer cell line. *Cancer letters,* **212**(1), pp. 61-70.

KIM, M., PAK, J.H., CHOI, W.H., PARK, J., NAM, J. and KIM, J., 2012. The relationship between cisplatin resistance and histone deacetylase isoform overexpression in epithelial ovarian cancer cell lines. *Journal of Gynecologic Oncology,* **23**(3), pp. 182-189.

KIMURA, A., OHASHI, K. and NAGANUMA, A., 2007. Cisplatin upregulates Saccharomyces cerevisiae genes involved in iron homeostasis through activation of the iron insufficiency-responsive transcription factor Aft1. *Journal of cellular physiology,* **210**(2), pp. 378-384.

KLEIN, A.V. and HAMBLEY, T.W., 2009. Platinum Drug Distribution in Cancer Cells and Tumors. *Chemical reviews,* **109**(10), pp. 4911-4920.

KOBOR, M., VENKATASUBRAHMANYAM, S., MENEGHINI, M., GIN, J., JENNINGS, J., LINK, A., MADHANI, H. and RINE, J., 2004. A protein complex containing the conserved Swi2/Snf2-related ATPase Swr1p deposits histone variant H2A.Z into euchromatin. *Plos Biology,* **2**(5), pp. 587-599.

KOEBERLE, B., TOMICIC, M.T., USANOVA, S. and KAINA, B., 2010. Cisplatin resistance: Preclinical findings and clinical implications. *Biochimica Et Biophysica Acta-Reviews on Cancer,* **1806**(2), pp. 172-182.

KONAC, E., VAROL, N., KILICCIOGLU, I. and BILEN, C.Y., 2015. Synergistic effects of cisplatin and proteasome inhibitor bortezomib on human bladder cancer cells. *Oncology Letters,* **10**(1), pp. 560-564.

KORPAL, M., KORN, J.M., GAO, X., RAKIEC, D.P., RUDDY, D.A., DOSHI, S., YUAN, J., KOVATS, S.G., KIM, S., COOKE, V.G., MONAHAN, J.E., STEGMEIER, F., ROBERTS, T.M., SELLERS, W.R., ZHOU, W. and ZHU, P., 2013. An F876L mutation in androgen receptor confers genetic and phenotypic resistance to MDV3100 (enzalutamide). *Cancer discovery,* **3**(9), pp. 1030-1043.

KOSTENKO, S., JOHANNESSEN, M. and MOENS, U., 2009. PKA-induced F-actin rearrangement requires phosphorylation of Hsp27 by the MAPKAP kinase MK5. *Cellular signalling,* **21**(5), pp. 712-718.

KOTCHETKOV, R., CINATL, J., BLAHETA, R., VOGEL, J.U., KARASKOVA, J., SQUIRE, J., DRIEVER, P.H., KLINGEBIEL, T. and CINATL, J., 2003. Development of resistance to vincristine and doxorubicin in neuroblastoma alters malignant properties and induces additional karyotype changes: A preclinical model. *International Journal of Cancer,* **104**(1), pp. 36-43.

KOTCHETKOV, R., DRIEVER, P.H., CINATL, J., MICHAELIS, M., KARASKOVA, J., BLAHETA, R., SQUIRE, J.A., VON DEIMLING, A., MOOG, J. and CINATL, J., 2005. Increased malignant behavior in neuroblastoma cells with acquired multi-drug resistance does not depend on P-gp expression. *International journal of oncology,* **27**(4), pp. 1029-1037.

KROGAN, N., KEOGH, M., DATTA, N., SAWA, C., RYAN, O., DING, H., HAW, R., POOTOOLAL, J., TONG, A., CANADIEN, V., RICHARDS, D., WU, X., EMILI, A., HUGHES, T., BURATOWSKI, S. and GREENBLATT, J., 2003. A Snf2 family ATPase complex required for recruitment of the histone H2A variant Htz1. *Molecular cell,* **12**(6), pp. 1565-1576.

KROL, K., BROZDA, I., SKONECZNY, M., BRETNE, M. and SKONECZNA, A., 2015. A Genomic Screen Revealing the Importance of Vesicular Trafficking Pathways in Genome Maintenance and Protection against Genotoxic Stress in Diploid Saccharomyces cerevisiae Cells. *Plos One,* **10**(3), pp. UNSP e0120702.

KRYSTON, T.B., GEORGIEV, A.B., PISSIS, P. and GEORGAKILAS, A.G., 2011. Role of oxidative stress and DNA damage in human carcinogenesis. *Mutation Research-Fundamental and Molecular Mechanisms of Mutagenesis,* **711**(1-2), pp. 193-201.

KUO, M.T., CHEN, H.H.W., SONG, I., SAVARAJ, N. and ISHIKAWA, T., 2007. The roles of copper transporters in cisplatin resistance. *Cancer and metastasis reviews,* **26**(1), pp. 71-83.

KURDZIEL, K.A. and KIESEWETTER, D.O., 2010. PET Imaging of Multidrug Resistance in Tumors Using F-18-Fluoropaclitaxel. *Current Topics in Medicinal Chemistry,* **10**(17), pp. 1792-1798.

LABBE, S., ZHU, Z. and THIELE, D., 1997. Copper-specific transcriptional repression of yeast genes encoding critical components in the copper transport pathway. *Journal of Biological Chemistry,* **272**(25), pp. 15951-15958.

LADURNER, A., INOUYE, C., JAIN, R. and TJIAN, R., 2003. Bromodomains mediate an acetyl-histone encoded antisilencing function at heterochromatin boundaries. *Molecular cell,* **11**(2), pp. 365-376.

LAGE, H., 2008. An overview of cancer multidrug resistance: a still unsolved problem. *Cellular and Molecular Life Sciences,* **65**(20), pp. 3145-3167.

LANDEN, C.N., Jr., LIN, Y.G., IMMANENI, A., DEAVERS, M.T., MERRITT, W.M., SPANNUTH, W.A., BODURKA, D.C., GERSHENSON, D.M., BRINKLEY, W.R. and SOOD, A.K., 2007. Overexpression of the centrosomal protein Aurora-A kinase is associated with poor prognosis in epithelial ovarian cancer patients. *Clinical Cancer Research,* **13**(14), pp. 4098-4104.

LANGE, S.S. and VASQUEZ, K.M., 2009. HMGB1: The Jack-of-All-Trades Protein Is a Master DNA Repair Mechanic. *Molecular carcinogenesis,* **48**(7), pp. 571-580.

LARDENOIS, A., BECKER, E., WALTHER, T., LAW, M.J., XIE, B., DEMOUGIN, P., STRICH, R. and PRIMIG, M., 2015. Global alterations of the transcriptional landscape during yeast growth and

development in the absence of Ume6-dependent chromatin modification. *Molecular Genetics and Genomics,* **290**(5), pp. 2031-2046.

LEADSHAM, J.E., SANDERS, G., GIANNAKI, S., BASTOW, E.L., HUTTON, R., NAEIMI, W.R., BREITENBACH, M. and GOURLAY, C.W., 2013. Loss of Cytochrome c Oxidase Promotes RAS-Dependent ROS Production from the ER Resident NADPH Oxidase, Yno1p, in Yeast. *Cell Metabolism,* **18**(2), pp. 279-286.

LEE, A.S., 2014. Glucose-regulated proteins in cancer: molecular mechanisms and therapeutic potential. *Nature Reviews Cancer,* **14**(4), pp. 263-276.

LEE, W., ONGE, R., PROCTOR, M., FLAHERTY, P., JORDAN, M., ARKIN, A., DAVIS, R., NISLOW, C. and GIAEVER, G., 2005. Genome-wide requirements for resistance to functionally distinct DNA-damaging agents. *Plos Genetics,* **1**(2), pp. 235-246.

LEONHARDT, K., GEBHARDT, R., MOESSNER, J., LUTSENKO, S. and HUSTER, D., 2009. Functional Interactions of Cu-ATPase ATP7B with Cisplatin and the Role of ATP7B in the Resistance of Cells to the Drug. *Journal of Biological Chemistry,* **284**(12), pp. 7793-7802.

LESLIE, E., DEELEY, R. and COLE, S., 2005. Multidrug resistance proteins: role of P-glycoprotein, MRP1, MRP2, and BCRP (ABCG2) in tissue defense. *Toxicology and applied pharmacology,* **204**(3), pp. 216-237.

LESTERHUIS, W.J., PUNT, C.J.A., HATO, S.V., ELEVELD-TRANCIKOVA, D., JANSEN, B.J.H., NIERKENS, S., SCHREIBELT, G., DE BOER, A., VAN HERPEN, C.M.L., KAANDERS, J.H., VAN KRIEKEN, J.H.J.M., ADEMA, G.J., FIGDOR, C.G. and DE VRIES, I.J.M., 2011. Platinum-based drugs disrupt STAT6-mediated suppression of immune responses against cancer in humans and mice. *Journal of Clinical Investigation,* **121**(8), pp. 3100-3108.

LI, J., LEE, B. and LEE, A.S., 2006. Endoplasmic reticulum stress-induced apoptosis: multiple pathways and activation of p53-up-regulated modulator of apoptosis (PUMA) and NOXA by p53. *The Journal of biological chemistry,* **281**(11), pp. 7260-7270.

LI, J., WANG, Y., SONG, Y., FU, Z. and YU, W., 2014. miR-27a regulates cisplatin resistance and metastasis by targeting RKIP in human lung adenocarcinoma cells. *Molecular Cancer,* **13**, pp. 193.

LI, J. and XIE, D., 2015. RACK1, a versatile hub in cancer. *Oncogene,* **34**(15), pp. 1890-1898.

LI, S., ESTERBERG, R., LACHANCE, V., REN, D., RADDE-GALLWITZ, K., CHI, F., PARENT, J., FRITZ, A. and CHEN, P., 2011. Rack1 is required for Vangl2 membrane localization and planar cell polarity signaling while attenuating canonical Wnt activity. *Proceedings of the National Academy of Sciences of the United States of America,* **108**(6), pp. 2264-2269.

LI, Y., HU, W., SHEN, D., KAVANAGH, J.J. and FU, S., 2009. Azacitidine enhances sensitivity of platinum-resistant ovarian cancer cells to carboplatin through induction of apoptosis. *American Journal of Obstetrics and Gynecology,* **200**(2), pp. 177.e1.

LI, Z., ZHAO, X., YANG, J. and WEI, Y., 2005. Proteomics profile changes in cisplatin-treated human ovarian cancer cell strain. *Science in China.Series C, Life sciences / Chinese Academy of Sciences,* **48**(6), pp. 648-657.

LIANG, X.J., MUKHERJEE, S., SHEN, D.W., MAXFIELD, F.R. and GOTTESMAN, M.M., 2006. Endocytic recycling compartments altered in cisplatin-resistant cancer cells. *Cancer research,* **66**(4), pp. 2346-2353.

LIN, W.M., BAKER, A.C., BEROUKHIM, R., WINCKLER, W., FENG, W., MARMION, J.M., LAINE, E., GREULICH, H., TSENG, H., GATES, C., HODI, F.S., DRANOFF, G., SELLERS, W.R., THOMAS, R.K., MEYERSON, M., GOLUB, T.R., DUMMER, R., HERLYN, M., GETZ, G. and GARRAWAY, L.A., 2008. Modeling genomic diversity and tumor dependency in malignant melanoma. *Cancer research,* **68**(3), pp. 664-673.

LIN, X., TANG, M., TAO, Y., LI, L., LIU, S., GUO, L., LI, Z., MA, X., XU, J. and CAO, Y., 2012. Epstein-Barr virus-encoded LMP1 triggers regulation of the ERK-mediated Op18/stathmin signaling pathway in association with cell cycle. *Cancer Science,* **103**(6), pp. 993-999.

LIN, Y.G., IMMANENI, A., MERRITT, W.M., MANGALA, L.S., KIM, S.W., SHAHZAD, M.M.K., TSANG, Y.T.M., ARMAIZ-PENA, G.N., LU, C., KAMAT, A.A., HAN, L.Y., SPANNUTH, W.A., NICK, A.M., LANDEN, C.N., Jr., WONG, K.K., GRAY, M.J., COLEMAN, R.L., BODURKA, D.C., BRINKLEY, W.R. and SOOD, A.K., 2008. Targeting Aurora kinase with MK-0457 inhibits ovarian cancer growth. *Clinical Cancer Research,* **14**(17), pp. 5437-5446.

LINCET, H., GUEVEL, B., PINEAU, C., ALLOUCHE, S., LEMOISSON, E., POULAIN, L. and GAUDUCHON, P., 2012. Comparative 2D-DIGE proteomic analysis of ovarian carcinoma cells: Toward a reorientation of biosynthesis pathways associated with acquired platinum resistance. *Journal of Proteomics,* **75**(4), pp. 1157-1169.

LINDSTROM, M.S., 2011. NPM1/B23: A Multifunctional Chaperone in Ribosome Biogenesis and Chromatin Remodeling. *Biochemistry research international,* **2011**, pp. 195209.

LIPPERT, T.H., RUOFF, H. and VOLM, M., 2011. Current Status of Methods to Assess Cancer Drug Resistance. *International Journal of Medical Sciences,* **8**(3), pp. 245-253.

LIU, D. and XU, Y., 2011. P53, Oxidative Stress, and Aging. *Antioxidants & redox signaling,* **15**(6), pp. 1669-1678.

LIU, H., LI, P., LI, B., SUN, P., ZHANG, J., WANG, B. and JIA, B., 2015. RKIP promotes cisplatin-induced gastric cancer cell death through NF-kappa B/Snail pathway. *Tumor Biology,* **36**(3), pp. 1445-1453.

LIU, Y., KAO, H. and BAMBARA, R., 2004. Flap endonuclease 1: A central component of DNA metabolism. *Annual Review of Biochemistry,* **73**, pp. 589-615.

LO, S., FAN, L., TSAI, Y., LIN, K., HUANG, H., WANG, T., LIU, H., CHEN, T., HUANG, S., CHANG, C., LIN, Y., YUNG, B.Y. and HSIEH, S., 2013. A Novel Interaction of Nucleophosmin with BCL2-Associated X Protein Regulating Death Evasion and Drug Sensitivity in Human Hepatoma Cells. *Hepatology,* **57**(5), pp. 1893-1905.

LOAR, P., WAHL, H., KSHIRSAGAR, M., GOSSNER, G., GRIFFITH, K. and LIU, J.R., 2010. Inhibition of glycolysis enhances cisplatin-induced apoptosis in ovarian cancer cells. *American Journal of Obstetrics and Gynecology,* **202**(4), pp. 371.e1.

LOESCHMANN, N., MICHAELIS, M., ROTHWEILER, F., ZEHNER, R., CINATL, J., VOGES, Y., SHARIFI, M., RIECKEN, K., MEYER, J., VON DEIMLING, A., FICHTNER, I., GHAFOURIAN, T., WESTERMANN, F. and CINATL, J., Jr., 2013. Testing of SNS-032 in a Panel of Human Neuroblastoma Cell Lines with Acquired Resistance to a Broad Range of Drugs. *Translational Oncology,* **6**(6), pp. 685-U314.

LOPEZ-MAURY, L., MARGUERAT, S. and BAEHLER, J., 2008. Tuning gene expression to changing environments: from rapid responses to evolutionary adaptation. *Nature Reviews Genetics,* **9**(8), pp. 583-593.

LU, F., ZHANG, C., WU, W. and WU, Y., 2012. RACK1 downregulation suppresses migration and proliferation of neuroblastoma cell lines. *Oncology reports,* **27**(5), pp. 1646-1652.

LUM, P., ARMOUR, C., STEPANIANTS, S., CAVET, G., WOLF, M., BUTLER, J., HINSHAW, J., GARNIER, P., PRESTWICH, G., LEONARDSON, A., GARRETT-ENGELE, P., RUSH, C., BARD, M., SCHIMMACK, G., PHILLIPS, J., ROBERTS, C. and SHOEMAKER, D., 2004. Discovering modes of action for therapeutic compounds using a genome-wide screen of yeast heterozygotes. *Cell,* **116**(1), pp. 121-137.

LYGEROU, Z., CONESA, C., LESAGE, P., SWANSON, R., RUET, A., CARLSON, M., SENTENAC, A. and SERAPHIN, B., 1994. The Yeast Bdf1 Gene Encodes a Transcription Factor Involved in the Expression of a Broad Class of Genes Including Snrnas. *Nucleic acids research,* **22**(24), pp. 5332-5340.

MACISAAC, K., WANG, T., GORDON, D., GIFFORD, D., STORMO, G. and FRAENKEL, E., 2006. An improved map of conserved regulatory sites for Saccharomyces cerevisiae. *Bmc Bioinformatics,* **7**, pp. 113.

MANDIC, A., HANSSON, J., LINDER, S. and SHOSHAN, M., 2003. Cisplatin induces endoplasmic reticulum stress and nucleus-independent apoptotic signaling. *Journal of Biological Chemistry,* **278**(11), pp. 9100-9106.

MANGALA, L.S., ZUZEL, V., SCHMANDT, R., LESHANE, E.S., HAIDER, J.B., ARMAIZ-PENA, G.N., SPANNUTH, W.A., TANAKA, T., SHAHZAD, M.M.K., LIN, Y.G., NICK, A.M., DANES, C.G., LEE, J., JENNINGS, N.B., VIVAS-MEJIA, P.E., WOLF, J.K., COLEMAN, R.L., SIDDIK, Z.H., LOPEZ-BERESTEIN, G., LUTSENKO, S. and SOOD, A.K., 2009. Therapeutic Targeting of ATP7B in Ovarian Carcinoma. *Clinical Cancer Research,* **15**(11), pp. 3770-3780.

MANN, M., HENDRICKSON, R. and PANDEY, A., 2001. Analysis of proteins and proteomes by mass spectrometry. *Annual Review of Biochemistry,* **70**, pp. 437-473.

MANOHAR, C., BRAY, J., SALWEN, H., MADAFIGLIO, J., CHENG, A., FLEMMING, C., MARSHALL, G., NORRIS, M., HABER, M. and COHN, S., 2004. MYCN-mediated regulation of the MRP1 promoter in human neuroblastoma. *Oncogene,* **23**(3), pp. 753-762.

MARRACHE, S., PATHAK, R.K. and DHAR, S., 2014. Detouring of cisplatin to access mitochondrial genome for overcoming resistance. *Proceedings of the National Academy of Sciences of the United States of America,* **111**(29), pp. 10444-10449.

MARTINEZ-BALIBREA, E., MARTINEZ-CARDUS, A., GINES, A., RUIZ DE PORRAS, V., MOUTINHO, C., LAYOS, L., LUIS MANZANO, J., BUGES, C., BYSTRUP, S., ESTELLER, M. and ABAD, A., 2015. Tumor-Related Molecular Mechanisms of Oxaliplatin Resistance. *Molecular Cancer Therapeutics,* **14**(8), pp. 1767-1776.

MARTINHO, O., PINTO, F., GRANJA, S., MIRANDA-GONCALVES, V., MOREIRA, M.A.R., RIBEIRO, L.F.J., DI LORETO, C., ROSNER, M.R., LONGATTO-FILHO, A. and REIS, R.M., 2013. RKIP Inhibition in Cervical Cancer Is Associated with Higher Tumor Aggressive Behavior and Resistance to Cisplatin Therapy. *Plos One,* **8**(3), pp. e59104.

MARTINS, I., KEPP, O., SCHLEMMER, F., ADJEMIAN, S., TAILLER, M., SHEN, S., MICHAUD, M., MENGER, L., GDOURA, A., TAJEDDINE, N., TESNIERE, A., ZITVOGEL, L. and KROEMER, G., 2011. Restoration of the immunogenicity of cisplatin-induced cancer cell death by endoplasmic reticulum stress. *Oncogene,* **30**(10), pp. 1147-1158.

MATANGKASOMBUT, O., BURATOWSKI, R., SWILLING, N. and BURATOWSKI, S., 2000. Bromodomain factor 1 corresponds to a missing piece of yeast TFIID. *Genes & development,* **14**(8), pp. 951-962.

MATUO, R., SOUSA, F.G., SOARES, D.G., BONATTO, D., SAFFI, J., ESCARGUEIL, A.E., LARSEN, A.K. and PEGAS HENRIQUES, J.A., 2012. Saccharomyces cerevisiae as a model system to study the response to anticancer agents. *Cancer chemotherapy and pharmacology,* **70**(4), pp. 491-502.

MCDERMOTT, U., SHARMA, S.V., DOWELL, L., GRENINGER, P., MONTAGUT, C., LAMB, J., ARCHIBALD, H., RAUDALES, R., TAM, A., LEE, D., ROTHENBERG, S.M., SUPKO, J.G., SORDELLA, R., ULKUS, L.E., IAFRATE, A.J., MAHESWARAN, S., NJAUW, C.N., TSAO, H., DREW, L., HANKE, J.H., MA, X., ERLANDER, M.G., GRAY, N.S., HABER, D.A. and SETTLEMAN, J., 2007. Identification of genotype-correlated sensitivity to selective kinase inhibitors by using high-throughput tumor cell line profiling. *Proceedings of the National Academy of Sciences of the United States of America,* **104**(50), pp. 19936-19941.

MCDERMOTT, U., SHARMA, S.V. and SETTLEMAN, J., 2008. High-throughput lung cancer cell line screening for genotype-correlated sensitivity to an EGFR kinase inhibitor. *Small Gtpases in Disease, Part a,* **438**, pp. 331-341.

MEHMOOD, R.K., 2014. Review of Cisplatin and oxaliplatin in current immunogenic and monoclonal antibody treatments. *Oncology reviews,* **8**(2), pp. 256.

MENG, Z. and TAO, K., 2015. Enhancement of Chemosensitivity by Stathmin-1 Silencing in Gastric Cancer Cells In Situ and In Vivo. *Oncology research,* **23**(1-2), pp. 35-41.

MEYRONET, D., MASSOMA, P., THIVOLET, F., CHALABREYSSE, L., ROGEMOND, V., SCHLAMA, A., HONNORAT, J. and THOMASSET, N., 2008. Extensive Expression of Collapsin Response Mediator Protein 5 (CRMP5) is a Specific Marker of High-grade Lung Neuroendocrine Carcinoma. *American Journal of Surgical Pathology,* **32**(11), pp. 1699-1708.

MICHAELIS, M., FICHTNER, I., BEHRENS, D., HAIDER, W., ROTHWEILER, F., MACK, A., CINATLI, J., DOERR, H.W. and CINATL, J., 2006. Anti-cancer effects of bortezomib against chemoresistant neuroblastoma cell lines in vitro and in vivo. *International journal of oncology,* **28**(2), pp. 439-446.

MICHAELIS, M., KLASSERT, D., BARTH, S., SUHAN, T., BREITLING, R., MAYER, B., HINSCH, N., DOERR, H.W., CINATL, J. and CINATL, J.,Jr, 2009. Chemoresistance acquisition induces a global shift of expression of aniogenesis-associated genes and increased pro-angogenic activity in neuroblastoma cells. *Molecular cancer,* **8**, pp. 80.

MICHAELIS, M., KLEINSCHMIDT, M.C., BARTH, S., BREITLING, R., MAYER, B., DEUBZER, H., WITT, O., DOERR, H.W., CINATL, J. and CINATL, J.,Jr., 2009. Anti-cancer effects of artesunate in a panel of chemoresistant neuroblastoma cell lines. *Ejc Supplements,* **7**(2), pp. 124-124.

MICHAELIS, M., ROTHWEILER, F., BARTH, S., CINATL, J., VAN RIKXOORT, M., LOESCHMANN, N., VOGES, Y., BREITLING, R., VON DEIMLING, A., ROEDEL, F., WEBER, K., FEHSE, B., MACK, E., STIEWE, T., DOERR, H.W., SPEIDEL, D. and CINATL, J., Jr., 2011. Adaptation of cancer cells from different entities to the MDM2 inhibitor nutlin-3 results in the emergence of p53-mutated multi-drug-resistant cancer cells. *Cell Death & Disease,* **2**, pp. e243.

MICHAELIS, M., AGHA, B., ROTHWEILER, F., LOESCHMANN, N., VOGES, Y., MITTELBRONN, M., STARZETZ, T., HARTER, P.N., ABHARI, B.A., FULDA, S., WESTERMANN, F., RIECKEN, K., SPEK, S., LANGER, K., WIESE, M., DIRKS, W.G., ZEHNER, R., CINATL, J., WASS, M.N. and CINATL, J., Jr., 2015. Identification of flubendazole as potential anti-neuroblastoma compound in a large cell line screen. *Scientific Reports,* **5**, pp. 8202.

MICHAELIS, M., BLISS, J., ARNOLD, S.C., HINSCH, N., ROTHWEILER, F., DEUBZER, H.E., WITT, O., LANGER, K., DOERR, H.W., WELS, W.S. and CINATL, J.,Jr., 2008. Cisplatin-Resistant Neuroblastoma Cells Express Enhanced Levels of Epidermal Growth Factor Receptor (EGFR) and Are Sensitive to Treatment with EGFR-Specific Toxins. *Clinical Cancer Research,* **14**(20), pp. 6531-6537.

MICHAELIS, M., CINATL, J., ANAND, P., ROTHWEILER, F., KOTCHETKOV, R., VON DEIMLING, A., DOERR, H.W., SHOGEN, K. and CINATL, J.,Jr., 2007. Onconase induces caspase-independent cell death in chemoresistant neuroblastoma cells. *Cancer letters,* **250**(1), pp. 107-116.

MICHAELIS, M., HINSCH, N., MICHAELIS, U.R., ROTHWEILER, F., SIMON, T., DOERR, H.W.I., CINATL, J. and CINATL, J., Jr., 2012. Chemotherapy-Associated Angiogenesis in Neuroblastoma Tumors. *American Journal of Pathology,* **180**(4), pp. 1370-1377.

MICHAELIS, M., ROTHWEILER, F., KLASSERT, D., VON DEIMLING, A., WEBER, K., FEHSE, B., KAMMERER, B., DOERR, H.W. and CINATL, J.,Jr., 2009. Reversal of P-glycoprotein-Mediated Multidrug Resistance by the Murine Double Minute 2 Antagonist Nutlin-3. *Cancer research,* **69**(2), pp. 416-421.

MICHAELIS, M., ROTHWEILER, F., LOESCHMANN, N., SHARIFI, M., GHAFOURIAN, T. and CINATL, J., Jr., 2015. Enzastaurin inhibits ABCB1-mediated drug efflux independently of effects on protein kinase C signalling and the cellular p53 status. *Oncotarget,* **6**(19), pp. 17605-17620.

MICHAELIS, M., SELT, F., ROTHWEILER, F., LOESCHMANN, N., NUESSE, B., DIRKS, W.G., ZEHNER, R. and CINATL, J., Jr., 2014. Aurora Kinases as Targets in Drug-Resistant Neuroblastoma Cells. *Plos One,* **9**(9), pp. e108758.

MICHELS, J., VITALE, I., SENOVILLA, L., ENOT, D.P., GARCIA, P., LISSA, D., OLAUSSEN, K.A., BRENNER, C., SORIA, J., CASTEDO, M. and KROEMER, G., 2013. Synergistic interaction between cisplatin and PARP inhibitors in non-small cell lung cancer. *Cell Cycle,* **12**(6), pp. 877-883.

MIURA, N., TAKEMORI, N., KIKUGAWA, T., TANJI, N., HIGASHIYAMA, S. and YOKOYAMA, M., 2012. Adseverin: A novel cisplatin-resistant marker in the human bladder cancer cell line HT1376 identified by quantitative proteomic analysis. *Molecular Oncology,* **6**(3), pp. 311-322.

MIZUGUCHI, G., SHEN, X., LANDRY, J., WU, W., SEN, S. and WU, C., 2004. ATP-Driven exchange of histone H2AZ variant catalyzed by SWR1 chromatin remodeling complex. *Science,* **303**(5656), pp. 343-348.

MIZUTANI, S., MIYATO, Y., SHIDARA, Y., ASOH, S., TOKUNAGA, A., TAJIRI, T. and OHTA, S., 2009. Mutations in the mitochondrial genome confer resistance of cancer cells to anticancer drugs. *Cancer Science,* **100**(9), pp. 1680-1687.

MIZZEN, C., YANG, X., KOKUBO, T., BROWNELL, J., BANNISTER, A., OWENHUGHES, T., WORKMAN, J., WANG, L., BERGER, S., KOUZARIDES, T., NAKATANI, Y. and ALLIS, C., 1996. The TAF(II)250 subunit of TFIID has histone acetyltransferase activity. *Cell,* **87**(7), pp. 1261-1270.

MOHAMMED, M. and RETSAS, S., 2000. Oxaliplatin is active in vitro against human melanoma cell lines: comparison with cisplatin and carboplatin. *Anti-Cancer Drugs,* **11**(10), pp. 859-863.

MOKADY, D. and MEIRI, D., 2015. RhoGTPases - A novel link between cytoskeleton organization and cisplatin resistance. *Drug Resistance Updates,* **19**, pp. 22-32.

MORRISON, A.J. and SHEN, X., 2009. Chromatin remodelling beyond transcription: the INO80 and SWR1 complexes. *Nature Reviews Molecular Cell Biology,* **10**(6), pp. 373-384.

MOSMANN, T., 1983. Rapid Colorimetric Assay for Cellular Growth and Survival - Application to Proliferation and Cyto-Toxicity Assays. *Journal of immunological methods,* **65**(1-2), pp. 55-63.

MOUTINHO, C., MARTINEZ-CARDUS, A., SANTOS, C., NAVARRO-PEREZ, V., MARTINEZ-BALIBREA, E., MUSULEN, E., JAVIER CARMONA, F., SARTORE-BIANCHI, A., CASSINGENA, A., SIENA, S., ELEZ, E., TABERNERO, J., SALAZAR, R., ABAD, A. and ESTELLER, M., 2014. Epigenetic Inactivation of the BRCA1 Interactor SRBC and Resistance to Oxaliplatin in Colorectal Cancer. *Jnci-Journal of the National Cancer Institute,* **106**(1), pp. djt322.

MUELLER, S. and KNAPP, S., 2014. Discovery of BET bromodomain inhibitors and their role in target validation. *Medchemcomm,* **5**(3), pp. 288-296.

MURPHY, M. and STORDAL, B., 2011. Erlotinib or gefitinib for the treatment of relapsed platinum pretreated non-small cell lung cancer and ovarian cancer: A systematic review. *Drug Resistance Updates,* **14**(3), pp. 177-190.

MYMRYK, J.S., ZANIEWSKI, E. and ARCHER, T.K., 1995. Cisplatin Inhibits Chromatin Remodeling, Transcription Factor-Binding, and Transcription from the Mouse Mammary-Tumor Virus Promoter In-Vivo. *Proceedings of the National Academy of Sciences of the United States of America,* **92**(6), pp. 2076-2080.

NAGARAJ, A.B., JOSEPH, P., KOVALENKO, O., SINGH, S., ARMSTRONG, A., REDLINE, R., RESNICK, K., ZANOTTI, K., WAGGONER, S. and DIFEO, A., 2015. Critical role of Wnt/beta-catenin signaling in driving epithelial ovarian cancer platinum resistance. *Oncotarget,* **6**(27), pp. 23720-23734.

NAGATANI, G., NOMOTO, M., TAKANO, H., ISE, T., KATO, K., IMAMURA, T., IZUMI, H., MAKISHIMA, K. and KOHNO, K., 2001. Transcriptional activation of the human HMG1 gene in cisplatin-resistant human cancer cells. *Cancer research,* **61**(4), pp. 1592-1597.

NEGORO, K., YAMANO, Y., NAKASHIMA, D., SAITO, K., NAKATANI, K., SHIIBA, M., BUKAWA, H., YOKOE, H., UZAWA, K., WADA, T., TANZAWA, H. and FUJITA, S., 2009. Cross-resistance of platinum derivatives in H-1R, a cisplatin-resistant cell line. *Oncology reports,* **21**(2), pp. 443-449.

NEVE, R.M., CHIN, K., FRIDLYAND, J., YEH, J., BAEHNER, F.L., FEVR, T., CLARK, L., BAYANI, N., COPPE, J., TONG, F., SPEED, T., SPELLMAN, P.T., DEVRIES, S., LAPUK, A., WANG, N.J., KUO, W., STILWELL, J.L., PINKEL, D., ALBERTSON, D.G., WALDMAN, F.M., MCCORMICK, F., DICKSON, R.B., JOHNSON, M.D., LIPPMAN, M., ETHIER, S., GAZDAR, A. and GRAY, J.W., 2006. A collection of breast cancer cell lines for the study of functionally distinct cancer subtypes RID B-8085-2009. *Cancer Cell,* **10**(6), pp. 515-527.

NICODEME, E., JEFFREY, K.L., SCHAEFER, U., BEINKE, S., DEWELL, S., CHUNG, C., CHANDWANI, R., MARAZZI, I., WILSON, P., COSTE, H., WHITE, J., KIRILOVSKY, J., RICE, C.M., LORA, J.M., PRINJHA, R.K., LEE, K. and TARAKHOVSKY, A., 2010. Suppression of inflammation by a synthetic histone mimic. *Nature,* **468**(7327), pp. 1119-1123.

NOMURA, T., YAMASAKI, M., NOMURA, Y. and MIMATA, H., 2005. Expression of the inhibitors of apoptosis proteins in cisplatin-resistant prostate cancer cells. *Oncology reports,* **14**(4), pp. 993-997.

OHASHI, K., KAJIYA, K., INABA, S., HASEGAWA, T., SEKO, Y., FURUCHI, T. and NAGANUMA, A., 2003. Copper(II) protects yeast against the toxicity of cisplatin independently of the induction of metallothionein and the inhibition of platinum uptake. *Biochemical and biophysical research communications,* **310**(1), pp. 148-152.

OHTA, T., OHMICHI, M., HAYASAKA, T., MABUCHI, S., SAITOH, M., KAWAGOE, J., TAKAHASHI, K., IGARASHI, H., DU, B., DOSHIDA, M., MIREI, I., MOTOYAMA, T., TASAKA, K. and KURACHI, H., 2006. Inhibition of phosphatidylinositol 3-kinase increases efficacy of cisplatin in in vivo ovarian cancer models. *Endocrinology,* **147**(4), pp. 1761-1769.

OLIVEROS, J.C.(., 2007-2015. *Venny. An interactive tool for comparing lists with Venn's diagrams. .*

OUYANG, L., SHI, Z., ZHAO, S., WANG, F.-., ZHOU, T.-., LIU, B. and BAO, J.-., 2012. Programmed cell death pathways in cancer: a review of apoptosis, autophagy and programmed necrosis. *Cell proliferation,* **45**(6), pp. 487-498.

PAPPIN, D.J., HOJRUP, P. and BLEASBY, A.J., 1993. Rapid identification of proteins by peptide-mass fingerprinting. *Current biology : CB,* **3**(6), pp. 327-332.

PAQUES, F. and HABER, J., 1999. Multiple pathways of recombination induced by double-strand breaks in Saccharomyces cerevisiae. *Microbiology and Molecular Biology Reviews,* **63**(2), pp. 349-+.

PARRALES, A. and IWAKUMA, T., 2015. Targeting Oncogenic Mutant p53 for Cancer Therapy. *Frontiers in Oncology,* **5**, pp. 288.

PARSONS, A., BROST, R., DING, H., LI, Z., ZHANG, C., SHEIKH, B., BROWN, G., KANE, P., HUGHES, T. and BOONE, C., 2004. Integration of chemical-genetic and genetic interaction data links bioactive compounds to cellular target pathways. *Nature biotechnology,* **22**(1), pp. 62-69.

PASELLO, M., MICHELACCI, F., SCIONTI, I., HATTINGER, C.M., ZUNTINI, M., CACCURI, A.M., SCOTIANDI, K., PICCI, P. and SERRA, M., 2008. Overcoming glutathione S-transferase P1-related cisplatin resistance in osteosarcoma. *Cancer research,* **68**(16), pp. 6661-6668.

PATTURAJAN, M., NOMOTO, S., SOMMER, M., FOMENKOV, A., HIBI, K., ZANGEN, R., POLIAK, N., CALIFANO, J., TRINK, B., RATOVITSKI, E. and SIDRANSKY, D., 2002. DeltaNp63 induces beta-catenin nuclear accumulation and signaling. *Cancer cell,* **1**(4), pp. 369-379.

PAUL, I., CHACKO, A., CRAWFORD, N., BARR, M., O'BYRNE, K.J., LONGLEY, D.B. and FENNELL, D.A., 2011. Cisplatin Resistant Nsclc Cells Block Acid Sphingomyelinase Dependent Caspase 8 Activation but Conserve Death Receptor Signalling. *Journal of Thoracic Oncology,* **6**(6), pp. S934-S935.

PEDERSEN, P.L., 2008. Voltage dependent anion channels (VDACs): a brief introduction with a focus on the outer mitochondrial compartment's roles together with hexokinase-2 in the "Warburg effect" in cancer. *Journal of Bioenergetics and Biomembranes,* **40**(3), pp. 123-126.

PELICANO, H., MARTIN, D.S., XU, R.-. and HUANG, P., 2006. Glycolysis inhibition for anticancer treatment. *Oncogene,* **25**(34), pp. 4633-4646.

PERFETTINI, J., KROEMER, R. and KROEMER, G., 2004. Fatal liaisons of p53 with Bax and Bak. *Nature cell biology,* **6**(5), pp. 386-388.

PERKINS, A., NELSON, K.J., PARSONAGE, D., POOLE, L.B. and KARPLUS, P.A., 2015. Peroxiredoxins: guardians against oxidative stress and modulators of peroxide signaling. *Trends in biochemical sciences,* **40**(8), pp. 435-445.

PERKINS, E., SUN, D., NGUYEN, A., TULAC, S., FRANCESCO, M., TAVANA, H., NGUYEN, H., TUGENDREICH, S., BARTHMAIER, P., COUTO, J., YEH, E., THODE, S., JARNAGIN, K., JAIN, A., MORGANS, D. and MELESE, T., 2001. Novel inhibitors of poly(ADP-ribose) polymerase/PARP1 and PARP2 identified using a cell-based screen in yeast. *Cancer research,* **61**(10), pp. 4175-4183.

PIERCE, S.E., DAVIS, R.W., NISLOW, C. and GIAEVER, G., 2007. Genome-wide analysis of barcoded Saccharomyces cerevisiae gene-deletion mutants in pooled cultures. *Nature Protocols,* **2**(11), pp. 2958-2974.

PIERCE, S.E., FUNG, E.L., JARAMILLO, D.F., CHU, A.M., DAVIS, R.W., NISLOW, C. and GIAEVER, G., 2006. A unique and universal molecular barcode array. *Nature Methods,* **3**(8), pp. 601-603.

PISKAREVA, O., HARVEY, H., NOLAN, J., CONLON, R., ALCOCK, L., BUCKLEY, P., DOWLING, P., O'SULLIVAN, F., BRAY, I. and STALLINGS, R.L., 2015. The development of cisplatin resistance in neuroblastoma is accompanied by epithelial to mesenchymal transition in vitro. *Cancer letters,* **364**(2), pp. 142-155.

POLETTO, M., LIRUSSI, L., WILSON,DAVID M.,,III and TELL, G., 2014. Nucleophosmin modulates stability, activity, and nucleolar accumulation of base excision repair proteins. *Molecular biology of the cell,* **25**(10), pp. 1641-1652.

POPOVIC, P., WONG, P.T.T., KATES, M., GREWAAL, D., GOEL, R., MOLEPO, J.M. and STEWART, D.J., 1994. Membrane fluidity and lipids in cisplatin resistant cells with low cisplatin uptake. *Proceedings of the American Association for Cancer Research Annual Meeting,* **35**(0), pp. 440-440.

PORRO, A., HABER, M., DIOLAITI, D., IRACI, N., HENDERSON, M., GHERARDI, S., VALLI, E., MUNOZ, M.A., XUE, C., FLEMMING, C., SCHWAB, M., WONG, J.H., MARSHALL, G.M., DELLA VALLE, G., NORRIS, M.D. and PERINI, G., 2010. Direct and Coordinate Regulation of ATP-binding Cassette Transporter Genes by Myc Factors Generates Specific Transcription Signatures That Significantly Affect the Chemoresistance Phenotype of Cancer Cells. *Journal of Biological Chemistry,* **285**(25), pp. 19532-19543.

PRESTON, T., ABADI, A., WILSON, L. and SINGH, C., 2001. Mitochondrial contributions to cancer cell physiology: potential for drug development. *Advanced Drug Delivery Reviews,* **49**(1-2), pp. 45-61.

PRIMIG, M., SOCKANATHAN, S., AUER, H. and NASMYTH, K., 1992. Anatomy of a Transcription Factor Important for the Start of the Cell-Cycle in Saccharomyces-Cerevisiae. *Nature,* **358**(6387), pp. 593-597.

PUGH, B. and TJIAN, R., 1991. Transcription from a Tata-Less Promoter Requires a Multisubunit Tfiid Complex. *Genes & development,* **5**(11), pp. 1935-1945.

PUISSANT, A., FRUMM, S.M., ALEXE, G., BASSII, C.F., QI, J., CHANTHERY, Y.H., NEKRITZ, E.A., ZEID, R., GUSTAFSON, W.C., GRENINGER, P., GARNETT, M.J., MCDERMOTT, U., BENES, C.H., KUNG, A.L., WEISS, W.A., BRADNER, J.E. and STEGMAIER, K., 2013. Targeting MYCN in Neuroblastoma by BET Bromodomain Inhibition. *Cancer research,* **73**(8),.

QIU, Y., MIRKIN, B. and DWIVEDI, R., 2005. Inhibition of DNA methyltransferase reverses cisplatin induced drug resistance in murine neuroblastoma cells. *Cancer detection and prevention,* **29**(5), pp. 456-463.

QUARESMA, M., COLEMAN, M.P. and RACHET, B., 2015. 40-year trends in an index of survival for all cancers combined and survival adjusted for age and sex for each cancer in England and Wales, 1971-2011: a population-based study. *Lancet (London, England),* **385**(9974), pp. 1206-1218.

RABIK, C.A. and DOLAN, M.E., 2007. Molecular mechanisms of resistance and toxicity associated with platinating agents. *Cancer treatment reviews,* **33**(1), pp. 9-23.

RAHAJENG, J., GIRIDHARAN, S.S., NASLAVSKY, N. and CAPLAN, S., 2010. Collapsin response mediator protein-2 (Crmp2) regulates trafficking by linking endocytic regulatory proteins to dynein motors. *The Journal of biological chemistry,* **285**(42), pp. 31918-31922.

RAMAGLI, L.S., 1999. Chapter 12; Quantifying protein in 2-D PAGE solubilisation buffers. In: A.J. LINK, ed, *2-D Proteome Analysis Protocols.* pp. 99-103.

RATHERT, P., ROTH, M., NEUMANN, T., MUERDTER, F., ROE, J., MUHAR, M., DESWAL, S., CERNY-REITERER, S., PETER, B., JUDE, J., HOFFMANN, T., BORYN, L.M., AXELSSON, E., SCHWEIFER, N., TONTSCH-GRUNT, U., DOW, L.E., GIANNI, D., PEARSON, M., VALENT, P., STARK, A., KRAUT, N., VAKOC, C.R. and ZUBER, J., 2015. Transcriptional plasticity promotes primary and acquired resistance to BET inhibition. *Nature,* **525**(7570), pp. 543-+.

REBILLARD, A., TEKPLI, X., MEURETTE, O., SERGENT, O., LEMOIGNE-MULLER, G., VERNHET, L., GORRIA, M., CHEVANNE, M., CHRISTMANN, M., KAINA, B., COUNILLON, L., GULBINS, E., LAGADIC-GOSSMANN, D. and DIMANCHE-BOITREL, M., 2007. Cisplatin-induced apoptosis involves membrane fluidification via inhibition of NHE1 in human colon cancer cells. *Cancer research,* **67**(16), pp. 7865-7874.

RELES, A., WEN, W., SCHMIDER, A., GEE, C., RUNNEBAUM, I., KILIAN, U., JONES, L., EL-NAGGAR, A., MINGUILLON, C., SCHONBORN, I., REICH, O., KREIENBERG, R., LICHTENEGGER, W. and PRESS, M., 2001. Correlation of p53 mutations with resistance to platinum-based chemotherapy and shortened survival in ovarian cancer. *Clinical Cancer Research,* **7**(10), pp. 2984-2997.

RENFRO, L.A., MALLICK, H., AN, M., SARGENT, D.J. and MANDREKAR, S.J., 2016. Clinical trial designs incorporating predictive biomarkers. *Cancer treatment reviews,* **43**, pp. 74-82.

RIKIISHI, H., SHINOHARA, F., SATO, T., SATO, Y., SUZUKI, M. and ECHIGO, S., 2007. Chemosensitization of oral squamous cell carcinoma cells to cisplatin by histone deacetylase inhibitor, suberoylanilide hydroxamic acid. *International journal of oncology,* **30**(5), pp. 1181-1188.

RIXE, O., ORTUZAR, W., ALVAREZ, M., PARKER, R., REED, E., PAULL, K. and FOJO, T., 1996. Oxaliplatin, tetraplatin, cisplatin, and carboplatin: Spectrum of activity in drug-resistant cell lines and in the cell lines of the National Cancer Institute's Anticancer Drug Screen panel. *Biochemical pharmacology,* **52**(12), pp. 1855-1865.

ROTTENBERG, S., JASPERS, J.E., KERSBERGEN, A., VAN DER BURG, E., NYGREN, A.O.H., ZANDER, S.A.L., DERKSEN, P.W.B., DE BRUIN, M., ZEVENHOVEN, J., LAU, A., BOULTER, R., CRANSTON, A., O'CONNOR, M.J., MARTIN, N.M.B., BORST, P. and JONKERS, J., 2008. High sensitivity of BRCA1-deficient mammary tumors to the PARP inhibitor AZD2281 alone and in combination with platinum drugs RID C-6643-2008. *Proceedings of the National Academy of Sciences of the United States of America,* **105**(44), pp. 17079-17084.

ROY, S.S., EHRLICH, A.M., CRAIGEN, W.J. and HAJNOCZKY, G., 2009. VDAC2 is required for truncated BID-induced mitochondrial apoptosis by recruiting BAK to the mitochondria. *EMBO reports,* **10**(12), pp. 1341-1347.

RUGGIERO, A., TROMBATORE, G., TRIARICO, S., ARENA, R., FERRARA, P., SCALZONE, M., PIERRI, F. and RICCARDI, R., 2013. Platinum compounds in children with cancer: toxicity and clinical management. *Anti-Cancer Drugs,* **24**(10), pp. 1007-1019.

RUTHERFORD, J. and BIRD, A., 2004. Metal-responsive transcription factors that regulate iron, zinc, and copper homeostasis in eukaryotic cells. *Eukaryotic Cell,* **3**(1), pp. 1-13.

SACCHAROMYCES GENE DATABASE (SGD) (STANFORD UNIVERSITY, STANFORD CA), . Available: http://www.yeastgenome.org.

SACCHAROMYCES GENE DELETION PROJECT (STANFORD UNIVERSITY, STANFORD CA), . Available: http://www-sequence.stanford.edu/group/yeast_deletion_project/Enter_DB.html.

SAFAEI, R., LARSON, B., CHENG, T., GIBSON, M., OTANI, S., NAERDEMANN, W. and HOWELL, S., 2005. Abnormal lysosomal trafficking and export of cisplatin in drug-resistant ovarian carcinoma cells. *Molecular Cancer Therapeutics,* **4**(10), pp. 1595-1604.

SAKAI, W., SWISHER, E.M., KARLAN, B.Y., AGARWAL, M.K., HIGGINS, J., FRIEDMAN, C., VILLEGAS, E., JACQUEMONT, C., FARRUGIA, D.J., COUCH, F.J., URBAN, N. and TANIGUCHI, T., 2008. Secondary mutations as a mechanism of cisplatin resistance in BRCA2-mutated cancers. *Nature,* **451**(7182), pp. 1116-U9.

SAMIMI, G., SAFAEI, R., KATANO, K., HOLZER, A., ROCHDI, M., TOMIOKA, M., GOODMAN, M. and HOWELL, S., 2004. Increased expression of the copper efflux transporter ATP7A mediates resistance to cisplatin, carboplatin, and oxaliplatin in ovarian cancer cells. *Clinical Cancer Research,* **10**(14), pp. 4661-4669.

SANCHEZ, R. and ZHOU, M., 2009. The role of human bromodomains in chromatin biology and gene transcription. *Current opinion in drug discovery & development,* **12**(5), pp. 659-665.

SANCHEZ-FONT, M.F., SEBASTIA, J., SANFELIU, C., CRISTOFOL, R., MARFANY, G. and GONZALEZ-DUARTE, R., 2003. Peroxiredoxin 2 (PRDX2), an antioxidant enzyme, is under-expressed in Down syndrome fetal brains. *Cellular and molecular life sciences : CMLS,* **60**(7), pp. 1513-1523.

SATO, T., JIGAMI, Y., SUZUKI, T. and UEMURA, H., 1999. A human gene, hSGT1, can substitute for GCR2, which encodes a general regulatory factor of glycolytic gene expression in Saccharomyces cerevisiae. *Molecular and General Genetics,* **260**(6), pp. 535-540.

SAWERS, L., FERGUSON, M.J., IHRIG, B.R., YOUNG, H.C., CHAKRAVARTY, P., WOLF, C.R. and SMITH, G., 2014. Glutathione S-transferase P1 (GSTP1) directly influences platinum drug chemosensitivity in ovarian tumour cell lines. *British journal of cancer,* **111**(6), pp. 1150-1158.

SCOTT, G.K., MATTIE, M.D., BERGER, C.E., BENZ, S.C. and BENZ, C.C., 2006. Rapid alteration of microRNA levels by histone deacetylase inhibition. *Cancer research,* **66**(3), pp. 1277-1281.

SCURR, L.L., GUMINSKI, A.D., CHIEW, Y., BALLEINE, R.L., SHARMA, R., LEI, Y., PRYOR, K., WAIN, G., BRAND, A., BYTH, K., KENNEDY, C., RIZOS, H., HARNETT, P.R. and DEFAZIO, A., 2008. Ankyrin Repeat Domain 1, ANKRD1, a Novel Determinant of Cisplatin Sensitivity Expressed in Ovarian Cancer. *Clinical Cancer Research,* **14**(21), pp. 6924-6932.

SEETHARAM, R.N., SOOD, A., BASU-MALLICK, A., AUGENLICHT, L.H., MARIADASON, J.M. and GOEL, S., 2010. Oxaliplatin Resistance Induced by ERCC1 Up-regulation Is Abrogated by siRNA-mediated Gene Silencing in Human Colorectal Cancer Cells. *Anticancer Research,* **30**(7), pp. 2531-2538.

SETTLEMAN, J., 2016. Bet on drug resistance. *Nature,* **529**(7586), pp. 289-290.

SHADEL, G.S., 2005. Mitochondrial DNA, aconitase 'wraps' it up. *Trends in biochemical sciences,* **30**(6), pp. 294-296.

SHAHZAD, M.M.K., LOPEZ-BERESTEIN, G. and SOOD, A.K., 2009. Novel strategies for reversing platinum resistance. *Drug Resistance Updates,* **12**(6), pp. 148-152.

SHANG, X., BURLINGAME, S.M., OKCU, M.F., GE, N., RUSSELL, H.V., EGLER, R.A., DAVID, R.D., VASUDEVAN, S.A., YANG, J. and NUCHTERN, J.G., 2009. Aurora A is a negative prognostic factor and a new therapeutic target in human neuroblastoma. *Molecular Cancer Therapeutics,* **8**(8), pp. 2461-2469.

SHARAPOV, M.G., RAVIN, V.K. and NOVOSELOV, V.I., 2014. Peroxiredoxins as multifunctional enzymes. *Molecular biology,* **48**(4), pp. 520-545.

SHARMA, R. and ABOAGYE, E., 2011. Development of radiotracers for oncology - the interface with pharmacology. *British journal of pharmacology,* **163**(8), pp. 1565-1585.

SHARMA, S., SANTISKULVONG, C., BENTOLILA, L.A., RAO, J., DORIGO, O. and GIMZEWSKI, J.K., 2012. Correlative nanomechanical profiling with super-resolution F-actin imaging reveals novel insights into mechanisms of cisplatin resistance in ovarian cancer cells. *Nanomedicine-Nanotechnology Biology and Medicine,* **8**(5), pp. 757-766.

SHARMA, S., SANTISKULVONG, C., RAO, J., GIMZEWSKI, J.K. and DORIGO, O., 2014. The role of Rho GTPase in cell stiffness and cisplatin resistance in ovarian cancer cells. *Integrative Biology,* **6**(6), pp. 611-617.

SHARMA, S.V., HABER, D.A. and SETTLEMAN, J., 2010. Cell line-based platforms to evaluate the therapeutic efficacy of candidate anticancer agents. *Nature Reviews Cancer,* **10**(4), pp. 241-253.

SHARMA, S.V. and SETTLEMAN, J., 2007. Oncogene addiction: setting the stage for molecularly targeted cancer therapy. *Genes & development,* **21**(24), pp. 3214-3231.

SHEKARIAN, T., VALSESIA-WITTMANN, S., CAUX, C. and MARABELLE, A., 2015. Paradigm shift in oncology: targeting the immune system rather than cancer cells. *Mutagenesis,* **30**(2), pp. 205-211.

SHEKHAR, M.P.V., 2011. Drug Resistance: Challenges to Effective Therapy. *Current Cancer Drug Targets,* **11**(5), pp. 613-623.

SHEN, D., POULIOT, L.M., HALL, M.D. and GOTTESMAN, M.M., 2012. Cisplatin Resistance: A Cellular Self-Defense Mechanism Resulting from Multiple Epigenetic and Genetic Changes. *Pharmacological reviews,* **64**(3), pp. 706-721.

SHEN, D., LIANG, X., GAWINOWICZ, M. and GOTTESMAN, M., 2004. Identification of cytoskeletal [C-14]carboplatin-binding proteins reveals reduced expression and disorganization of actin and filamin in cisplatin-resistant cell lines. *Molecular pharmacology,* **66**(4), pp. 789-793.

SHERBET, G. and CAJONE, F., 2005. Stathmin in cell proliferation and cancer progression. *Cancer Genomics-Proteomics,* **2**(4), pp. 227-237.

SHERMAN-BAUST, C.A., WEERARATNA, A.T., RANGEL, L.B.A., PIZER, E.S., CHO, K.R., SCHWARTZ, D.R., SHOCK, T. and MORIN, P.J., 2003. Remodeling of the extracellular matrix through overexpression of collagen VI contributes to cisplatin resistance in ovarian cancer cells. *Cancer Cell,* **3**(4), pp. 377-386.

SHEVCHENKO, A., WILM, M., VORM, O. and MANN, M., 1996. Mass spectrometric sequencing of proteins from silver stained polyacrylamide gels. *Analytical Chemistry,* **68**(5), pp. 850-858.

SHI, J. and VAKOC, C.R., 2014. The Mechanisms behind the Therapeutic Activity of BET Bromodomain Inhibition. *Molecular cell,* **54**(5), pp. 728-736.

SHINOHARA, Y., ISHIDA, T., HINO, M., YAMAZAKI, N., BABA, Y. and TERADA, H., 2000. Characterization of porin isoforms expressed in tumor cells. *European journal of biochemistry / FEBS,* **267**(19), pp. 6067-6073.

SHOEMAKER, R.H., 2006. The NCI60 human tumour cell line anticancer drug screen. *Nature Reviews Cancer,* **6**(10), pp. 813-823.

SHOSHAN-BARMATZ, V. and BEN-HAIL, D., 2012. VDAC, a multi-functional mitochondrial protein as a pharmacological target. *Mitochondrion,* **12**(1), pp. 24-34.

SHOSHAN-BARMATZ, V., DE PINTO, V., ZWECKSTETTER, M., RAVIV, Z., KEINAN, N. and ARBEL, N., 2010. VDAC, a multi-functional mitochondrial protein regulating cell life and death. *Molecular aspects of medicine,* **31**(3), pp. 227-285.

SHU, S., LIN, C.Y., HE, H.H., WITWICKI, R.M., TABASSUM, D.P., ROBERTS, J.M., JANISZEWSKA, M., HUH, S.J., LIANG, Y., RYAN, J., DOHERTY, E., MOHAMMED, H., GUO, H., STOVER, D.G., EKRAM, M.B., PELUFFO, G., BROWN, J., D'SANTOS, C., KROP, I.E., DILLON, D., MCKEOWN, M., OTT, C., QI, J., NI, M., RAO, P.K., DUARTE, M., WU, S., CHIANG, C., ANDERS, L., YOUNG, R.A., WINER, E.P., LETAI, A., BARRY, W.T., CARROLL, J.S., LONG, H.W., BROWN, M., LIU, X.S., MEYER, C.A., BRADNER, J.E. and POLYAK, K., 2016. Response and resistance to BET bromodomain inhibitors in triple-negative breast cancer. *Nature,* **529**(7586), pp. 413-+.

SIDDIK, Z., 2003. Cisplatin: mode of cytotoxic action and molecular basis of resistance. *Oncogene,* **22**(47), pp. 7265-7279.

SILBERBERG, Y., KUPIEC, M. and SHARAN, R., 2016. Utilizing yeast chemogenomic profiles for the prediction of pharmacogenomic associations in humans. *Scientific Reports,* **6**, pp. 23703.

SIMON, J. and BEDALOV, A., 2004. Opinion - Yeast as a model system for anticancer drug discovery. *Nature Reviews Cancer,* **4**(6), pp. 481-488.

SINHA, P., POLAND, J., KOHL, S., SCHNOLZER, M., HELMBACH, H., HUTTER, G., LAGE, H. and SCHADENDORF, D., 2003. Study of the development of chemoresistance in melanoma cell lines using proteome analysis. *Electrophoresis,* **24**(14), pp. 2386-2404.

SMITH, A.M., AMMAR, R., NISLOW, C. and GIAEVER, G., 2010. A survey of yeast genomic assays for drug and target discovery. *Pharmacology & therapeutics,* **127**(2), pp. 156-164.

SONG, I., SAVARAJ, N., SIDDIK, Z., LIU, P., WEI, Y., WU, C. and KUO, M., 2004. Role of human copper transporter Ctr1 in the transport of platinum-based antitumor agents in cisplatin-sensitive and cisplatin-resistant cells. *Molecular Cancer Therapeutics,* **3**(12), pp. 1543-1549.

SOS, M.L., MICHEL, K., ZANDER, T., WEISS, J., FROMMOLT, P., PEIFER, M., LI, D., ULLRICH, R., KOKER, M., FISCHER, F., SHIMAMURA, T., RAUH, D., MERMEL, C., FISCHER, S., STUECKRATH, I., HEYNCK, S., BEROUKHIM, R., LIN, W., WINCKLER, W., SHAH, K., LAFRAMBOISE, T., MORIARTY, W.F., HANNA, M., TOLOSI, L., RAHNENFUEHRER, J., VERHAAK, R., CHIANG, D., GETZ, G., HELLMICH, M., WOLF, J., GIRARD, L., PEYTON, M., WEIR, B.A., CHEN, T., GREULICH, H., BARRETINA, J., SHAPIRO, G.I., GARRAWAY, L.A., GAZDAR, A.F., MINNA, J.D., MEYERSON, M., WONG, K. and THOMAS, R.K., 2009. Predicting drug susceptibility of non-small cell lung cancers based on genetic lesions RID A-8728-2008. *Journal of Clinical Investigation,* **119**(6), pp. 1727-1740.

STEWART, D.J., 2007. Mechanisms of resistance to cisplatin and carboplatin. *Critical Reviews in Oncology Hematology,* **63**(1), pp. 12-31.

STEWART, J., WHITE, J., YAN, X., COLLINS, S., DRESCHER, C., URBAN, N., HOOD, L. and LIN, B., 2006. Proteins associated with cisplatin resistance in ovarian cancer cells identified by quantitative proteomic technology and integrated with mRNA expression levels. *Molecular & Cellular Proteomics,* **5**(3), pp. 433-443.

STORDAL, B. and DAVEY, M., 2007. Understanding cisplatin resistance using cellular models. *IUBMB life,* **59**(11), pp. 696-699.

STRICHER, F., MACRI, C., RUFF, M. and MULLER, S., 2013. HSPA8/HSC70 chaperone protein Structure, function, and chemical targeting. *Autophagy,* **9**(12), pp. 1937-1954.

SYMINGTON, L., 2002. Role of RAD52 epistasis group genes in homologous recombination and double-strand break repair. *Microbiology and Molecular Biology Reviews,* **66**(4), pp. 630-+.

TABATA, K., SAKAI, H., NAKAJIMA, R., SAYA-NISHIMURA, R., MOTANI, K., OKANO, S., SHIBATA, Y., ABIKO, Y. and SUZUKI, T., 2011. Acute application of cisplatin affects methylation status in neuroblastoma cells. *Oncology reports,* **25**(6), pp. 1655-1660.

TAJEDDINE, N., GALLUZZI, L., KEPP, O., HANGEN, E., MORSELLI, E., SENOVILLA, L., ARAUJO, N., PINNA, G., LAROCHETTE, N., ZAMZAMI, N., MODJTAHEDI, N., HAREL-BELLAN, A. and KROEMER, G., 2008. Hierarchical involvement of Bak, VDAC1 and Bax in cisplatin-induced cell death. *Oncogene,* **27**(30), pp. 4221-4232.

TAN, F., THIELE, C.J. and LI, Z., 2014. Collapsin response mediator proteins: Potential diagnostic and prognostic biomarkers in cancers. *Oncology Letters,* **7**(5), pp. 1333-1340.

TANG, C., PARHAM, C., SHOCRON, E., MCMAHON, G. and PATEL, N., 2011. Picoplatin overcomes resistance to cell toxicity in small-cell lung cancer cells previously treated with cisplatin and carboplatin. *Cancer chemotherapy and pharmacology,* **67**(6), pp. 1389-1400.

TANOSHIMA, R., YANG, M., DALVI, P., WU, A., MATSUDA, K., ZHANG, L., FUJII, H., BARUCHEL, S., HARPER, P. and ITO, S., 2014. Nrf2-Keap1 pathway does not have an important role in cisplatin resistance in neuroblastoma. *Faseb Journal,* **28**(1),.

TONINI, G., CALVIERI, A., VINCENZI, B. and SANTINI, D., 2009. First-line targeted therapies in the treatment of metastatic colorectal cancer - role of cetuximab. *OncoTargets and therapy,* **2**, pp. 73-82.

TOWNSEND, D. and TEW, K., 2003. The role of glutathione-S-transferase in anti-cancer drug resistance. *Oncogene,* **22**(47), pp. 7369-7375.

TRUDU, F., AMATO, F., VANHARA, P., PIVETTA, T., PENA-MENDEZ, E.M. and HAVEL, J., 2015. Coordination compounds in cancer: Past, present and perspectives. *Journal of Applied Biomedicine,* **13**(2), pp. 79-103.

TSAI, M., CHANG, W., HUANG, M. and KUO, P., 2014. Tumor microenvironment: a new treatment target for cancer. *ISRN biochemistry,* **2014**, pp. 351959-351959.

TUNDO, G.R., SBARDELLA, D., CIACCIO, C., DE PASCALI, S., CAMPANELLA, V., COZZA, P., TARANTINO, U., COLETTA, M., FANIZZI, F.P. and MARINI, S., 2015. Effect of cisplatin on proteasome activity. *Journal of inorganic biochemistry,* **153**, pp. 253-258.

TURSZ, T., ANDRE, F., LAZAR, V., LACROIX, L. and SORIA, J., 2011. Implications of personalized medicine-perspective from a cancer center. *Nature Reviews Clinical Oncology,* **8**(3), pp. 177-183.

UEMURA, H. and FRAENKEL, D., 1999. Glucose metabolism in gcr mutants of Saccharomyces cerevisiae. *Journal of Bacteriology,* **181**(15), pp. 4719-4723.

UEMURA, H. and FRAENKEL, D., 1990. Gcr2, a New Mutation Affecting Glycolytic Gene-Expression in Saccharomyces-Cerevisiae. *Molecular and cellular biology,* **10**(12), pp. 6389-6396.

USAMI, H., KUSANO, Y., KUMAGAI, T., OSADA, S., ITOH, K., KOBAYASHI, A., YAMAMOTO, M. and UCHIDA, K., 2005. Selective induction of the tumor marker glutathione S-transferase P1 by proteasome inhibitors. *The Journal of biological chemistry,* **280**(26), pp. 25267-25276.

VAN MAERKEN, T., FERDINANDE, L., TAILDEMAN, J., LAMBERTZ, I., YIGIT, N., VERCRUYSSE, L., RIHANI, A., MICHAELIS, M., CINATL, J.,Jr., CUVELIER, C.A., MARINE, J., DE PAEPE, A., BRACKE, M., SPELEMAN, F. and VANDESOMPELE, J., 2009. Antitumor Activity of the Selective MDM2 Antagonist Nutlin-3 Against Chemoresistant Neuroblastoma With Wild-Type p53. *Journal of the National Cancer Institute,* **101**(22), pp. 1562-1574.

VAN MALDEGEM, F., MASLEN, S., JOHNSON, C.M., CHANDRA, A., GANESH, K., SKEHEL, M. and RADA, C., 2015. CTNNBL1 facilitates the association of CWC15 with CDC5L and is required to maintain the abundance of the Prp19 spliceosomal complex. *Nucleic acids research,* **43**(14), pp. 7058-7069.

VASEVA, A.V. and MOLL, U.M., 2009. The mitochondrial p53 pathway. *Biochimica Et Biophysica Acta-Bioenergetics,* **1787**(5), pp. 414-420.

VASKO, R., MUELLER, G.A., VON JASCHKE, A., ASIF, A.R. and DIHAZI, H., 2011. Impact of cisplatin administration on protein expression levels in renal cell carcinoma: A proteomic analysis. *European journal of pharmacology,* **670**(1), pp. 50-57.

VENTERS, B.J., WACHI, S., MAVRICH, T.N., ANDERSEN, B.E., JENA, P., SINNAMON, A.J., JAIN, P., ROLLERI, N.S., JIANG, C., HEMERYCK-WALSH, C. and PUGH, B.F., 2011. A Comprehensive Genomic Binding Map of Gene and Chromatin Regulatory Proteins in Saccharomyces. *Molecular cell,* **41**(4), pp. 480-492.

WANG, C., MIRKIN, B. and DWIVEDI, R., 2001. DNA (cytosine) methyltransferase overexpression is associated with acquired drug resistance of murine neuroblastoma cells. *International journal of oncology,* **18**(2), pp. 323-329.

WANG, D. and LIPPARD, S.J., 2004. Cisplatin-induced post-translational modification of histones H3 and H4. *The Journal of biological chemistry,* **279**(20), pp. 20622-20625.

WANG, D. and LIPPARD, S., 2005. Cellular processing of platinum anticancer drugs. *Nature Reviews Drug Discovery,* **4**(4), pp. 307-320.

WANG, X., WANG, S., TANG, X., ZHANG, A., GRABINSKI, T., GUO, Z., HUDSON, E., BERGHUIS, B., WEBB, C., ZHAO, P. and CAO, B., 2010. Development and evaluation of monoclonal antibodies against phosphatidylethanolamine binding protein 1 in pancreatic cancer patients. *Journal of immunological methods,* **362**(1-2), pp. 151-160.

WANG, X. and GUO, Z., 2013. Targeting and delivery of platinum-based anticancer drugs. *Chemical Society Reviews,* **42**(1), pp. 202-224.

WANG, Y. and CHIU, J.F., 2008. Proteomic approaches in understanding action mechanisms of metal-based anticancer drugs. *Metal-based drugs,* **2008**, pp. 716329.

WANG, Y., WANG, H., LI, H. and SUN, H., 2015. Metallomic and metalloproteomic strategies in elucidating the molecular mechanisms of metallodrugs. *Dalton Transactions,* **44**(2), pp. 437-447.

WEI, M., LINDSTEN, T., MOOTHA, V., WEILER, S., GROSS, A., ASHIYA, M., THOMPSON, C. and KORSMEYER, S., 2000. tBID, a membrane-targeted death ligand, oligomerizes BAK to release cytochrome c. *Genes & development,* **14**(16), pp. 2060-2071.

WEI, M., ZONG, W., CHENG, E., LINDSTEN, T., PANOUTSAKOPOULOU, V., ROSS, A., ROTH, K., MACCREGOR, G., THOMPSON, C. and KORSMEYER, S., 2001. Proapoptotic BAX and BAK: A requisite gateway to mitochondrial dysfunction and death. *Science,* **292**(5517), pp. 727-730.

WHEATE, N.J., WALKER, S., CRAIG, G.E. and OUN, R., 2010. The status of platinum anticancer drugs in the clinic and in clinical trials RID A-9990-2008. *Dalton Transactions,* **39**(35), pp. 8113-8127.

WIEDEMEYER, W.R., BEACH, J.A. and KARLAN, B.Y., 2014. Reversing Platinum Resistance in High-Grade Serous Ovarian Carcinoma: Targeting BRCA and the Homologous Recombination System. *Frontiers in oncology,* **4**, pp. 34.

WILLIAMS, J., LUCAS, P., GRIFFITH, K., CHOI, M., FOGOROS, S., HU, Y. and LIU, J., 2005. Expression of Bcl-X-L in ovarian carcinoma is associated with chemoresistance and recurrent disease. *Gynecologic oncology,* **96**(2), pp. 287-295.

WISTUBA, I.I., GELOVANI, J.G., JACOBY, J.J., DAVIS, S.E. and HERBST, R.S., 2011. Methodological and practical challenges for personalized cancer therapies. *Nature Reviews Clinical Oncology,* **8**(3), pp. 135-141.

WITZEL, F., FRITSCHE-GUENTHER, R., LEHMANN, N., SIEBER, A. and BLUETHGEN, N., 2015. Analysis of impedance-based cellular growth assays. *Bioinformatics,* **31**(16), pp. 2705-2712.

WOLTER, K., HSU, Y., SMITH, C., NECHUSHTAN, A., XI, X. and YOULE, R., 1997. Movement of Bax from the cytosol to mitochondria during apoptosis. *Journal of Cell Biology,* **139**(5), pp. 1281-1292.

WOOD, C.G. and MULDERS, P., 2009. Vitespen: a preclinical and clinical review. *Future Oncology,* **5**(6), pp. 763-774.

WORKMAN, P. and CLARKE, P.A., 2011. Resisting Targeted Therapy: Fifty Ways to Leave Your EGFR. *Cancer Cell,* **19**(4), pp. 437-440.

WOYNAROWSKI, J., FAIVRE, S., HERZIG, M., ARNETT, B., CHAPMAN, W., TREVINO, A., RAYMOND, E., CHANEY, S., VAISMAN, A., VARCHENKO, M. and JUNIEWICZ, P., 2000. Oxaliplatin-induced damage of cellular DNA. *Molecular pharmacology,* **58**(5), pp. 920-927.

WU, B. and DAVEY, C.A., 2008. Platinum Drug Adduct Formation in the Nucleosome Core Alters Nucleosome Mobility but Not Positioning. *Chemistry & biology,* **15**(10), pp. 1023-1028.

WU, B., CHU, X., FENG, C., HOU, J., FAN, H., LIU, N., LI, C., KONG, X., YE, X. and MENG, S., 2015. Heat shock protein gp96 decreases p53 stability by regulating Mdm2 E3 ligase activity in liver cancer. *Cancer letters,* **359**(2), pp. 325-334.

WU, C., BIRD, A.J., WINGE, D.R. and EIDE, D.J., 2007. Regulation of the yeast TSA1 peroxiredoxin by ZAP1 is an adaptive response to the oxidative stress of zinc deficiency. *Journal of Biological Chemistry,* **282**(4), pp. 2184-2195.

WU, H., BROWN, J., DORIE, M., LAZZERONI, L. and BROWN, J., 2004. Genome-wide identification of genes conferring resistance to the anticancer agents cisplatin, oxaliplatin, and mitomycin C. *Cancer research,* **64**(11), pp. 3940-3948.

WU, Q., YANG, Z., NIE, Y., SHI, Y. and FAN, D., 2014. Multi-drug resistance in cancer chemotherapeutics: Mechanisms and lab approaches. *Cancer letters,* **347**(2), pp. 159-166.

WYCE, A., GANJI, G., SMITHEMAN, K.N., CHUNG, C., KORENCHUK, S., BAI, Y., BARBASH, O., LE, B., CRAGGS, P.D., MCCABE, M.T., KENNEDY-WILSON, K.M., SANCHEZ, L.V., GOSMINI, R.L., PARR, N., MCHUGH, C.F., DHANAK, D., PRINJHA, R.K., AUGER, K.R. and TUMMINO, P.J., 2013. BET Inhibition Silences Expression of MYCN and BCL2 and Induces Cytotoxicity in Neuroblastoma Tumor Models. *Plos One,* **8**(8), pp. UNSP e72967.

XU, R., PELICANO, H., ZHOU, Y., CAREW, J., FENG, L., BHALLA, K., KEATING, M. and HUANG, P., 2005. Inhibition of glycolysis in cancer cells: A novel strategy to overcome drug resistance associated with mitochondrial respiratory defect and hypoxia. *Cancer research,* **65**(2), pp. 613-621.

XU, Y., ZHENG, Q., YU, L., ZHANG, H. and SUN, C., 2013. Computational modelling of novel inhibitors targeting the human GSTP1*D homology domain. *Molecular Simulation,* **39**(7), pp. 550-562.

YADAV, R.K., CHAE, S., KIM, H. and CHAE, H.J., 2014. Endoplasmic reticulum stress and cancer. *Journal of cancer prevention,* **19**(2), pp. 75-88.

YAKES, F. and VANHOUTEN, B., 1997. Mitochondrial DNA damage is more extensive and persists longer than nuclear DNA damage in human cells following oxidative stress. *Proceedings of the National Academy of Sciences of the United States of America,* **94**(2), pp. 514-519.

YAMADA, H.Y. and RAO, C.V., 2009. BRD8 is a potential chemosensitizing target for spindle poisons in colorectal cancer therapy. *International journal of oncology,* **35**(5), pp. 1101-1109.

YAMAGUCHI, K., SAKAI, M., SHIMOKAWA, T., YAMADA, Y., NAKAMURA, Y. and FURUKAWA, Y., 2010. C20orf20 (MRG-binding protein) as a potential therapeutic target for colorectal cancer. *British journal of cancer,* **102**(2), pp. 325-331.

YAMAGUCHIIWAI, Y., DANCIS, A. and KLAUSNER, R., 1995. Aft1 - a Mediator of Iron-Regulated Transcriptional Control in Saccharomyces-Cerevisiae. *Embo Journal,* **14**(6), pp. 1231-1239.

YAMAMOTO, K., OKAMOTO, A., ISONISHI, S., OCHIAI, K. and OHTAKE, Y., 2001. Heat shock protein 27 was up-regulated in cisplatin resistant human ovarian tumor cell line and associated with the cisplatin resistance. *Cancer letters,* **168**(2), pp. 173-181.

YAMORI, T., 2003. Panel of human cancer cell lines provides valuable database for drug discovery and bioinformatics. *Cancer chemotherapy and pharmacology,* **52**, pp. S74-S79.

YAN, X., PAN, L., YUAN, Y., LANG, J. and MAO, N., 2007. Identification of platinum-resistance associated proteins through proteomic analysis of human ovarian cancer cells and their platinum-resistant sublines. *Journal of Proteome Research,* **6**(2), pp. 772-780.

YANG, W., SOARES, J., GRENINGER, P., EDELMAN, E.J., LIGHTFOOT, H., FORBES, S., BINDAL, N., BEARE, D., SMITH, J.A., THOMPSON, I.R., RAMASWAMY, S., FUTREAL, P.A., HABER, D.A., STRATTON, M.R., BENES, C., MCDERMOTT, U. and GARNETT, M.J., 2013. Genomics of Drug Sensitivity in Cancer (GDSC): a resource for therapeutic biomarker discovery in cancer cells. *Nucleic acids research,* **41**(D1), pp. D955-D961.

YANG, Y., LIU, B., DAI, J., SRIVASTAVA, P.K., ZAMMIT, D.J., LEFRANCOIS, L. and LI, Z., 2007. Heat shock protein gp96 is a master chaperone for toll-like receptors and is important in the innate function of macrophages. *Immunity,* **26**(2), pp. 215-226.

YANG, Z., SCHUMAKER, L.M., EGORIN, M.J., ZUHOWSKI, E.G., GUO, Z. and CULLEN, K.J., 2006. Cisplatin preferentially binds mitochondrial DNA and voltage-dependent anion channel protein in the mitochondrial membrane of head and neck squamous cell carcinoma: Possible role in apoptosis. *Clinical Cancer Research,* **12**(19), pp. 5817-5825.

YE, K., 2005. Nucleophosmin/B23, a multifunctional protein that can regulate apoptosis. *Cancer Biology & Therapy,* **4**(9), pp. 918-923.

YEAST FITNESS DATABASE (2008). HILLENMEYER,MAUREEN E., FUNG, E., WILDENHAIN, J., PIERCE, S.E., HOON, S., LEE, W., PROCTOR, M., ST ONGE, R.P., TYERS, M., KOLLER, D., ALTMAN, R.B., DAVIS, R.W., NISLOW, C. and GIAEVER, G., . Available: http://fitdb.stanford.edu/.

YOKOMIZO, A., KOHNO, K., WADA, M., ONO, M., MORROW, C., COWAN, K. and KUWANO, M., 1995. Markedly Decreased Expression of Glutathione-S-Transferase-Pi Gene in Human Cancer Cell-Lines Resistant to Buthionine Sulfoximine, an Inhibitor of Cellular Glutathione Synthesis. *Journal of Biological Chemistry,* **270**(33), pp. 19451-19457.

YOO, B., KU, J., HONG, S., SHIN, Y., PARK, S., KIM, H. and PARK, J., 2004. Decreased pyruvate kinase M2 activity linked to cisplatin resistance in human gastric carcinoma cell lines. *International Journal of Cancer,* **108**(4), pp. 532-539.

YOO, Y., CHUNG, Y., PARK, J., AHN, C., KIM, S. and KIM, H., 2002. Synergistic effect of peroxiredoxin II antisense on cisplatin-induced cell death. *Experimental and Molecular Medicine,* **34**(4), pp. 273-277.

YU, F., MEGYESI, J. and PRICE, P.M., 2008. Cytoplasmic initiation of cisplatin cytotoxicity. *American Journal of Physiology-Renal Physiology,* **295**(1), pp. F44-F52.

ZHANG, H., ROBERTS, D. and CAIRNS, B., 2005. Genome-wide dynamics of Htz1, a histone H2A variant that poises repressed/basal promoters for activation through histone loss. *Cell,* **123**(2), pp. 219-231.

ZHANG, J. and LIU, Y., 2007. Use of comparative proteomics to identify potential resistance mechanisms in cancer treatment. *Cancer treatment reviews,* **33**(8), pp. 741-756.

ZHANG, R., LI, Y., WANG, Z., LING, L., DONG, X. and NIE, X., 2015. Interference with HMGB1 increases the sensitivity to chemotherapy drugs by inhibiting HMGB1-mediated cell autophagy and inducing cell apoptosis. *Tumor Biology,* **36**(11), pp. 8585-8592.

ZHANG, S., LOVEJOY, K.S., SHIMA, J.E., LAGPACAN, L.L., SHU, Y., LAPUK, A., CHEN, Y., KOMORI, T., GRAY, J.W., CHEN, X., LIPPARD, S.J. and GIACOMINI, K.M., 2006. Organic cation transporters are determinants of oxaliplatin cytotoxicity. *Cancer research,* **66**(17), pp. 8847-8857.

ZHANG, Y. and SHEN, X., 2007. Heat shock protein 27 protects L929 cells from cisplatin-induced apoptosis by enhancing akt activation and abating suppression of thioredoxin reductase activity. *Clinical Cancer Research,* **13**(10), pp. 2855-2864.

ZHAO, H. and EIDE, D., 1997. Zap1p, a metalloregulatory protein involved in zinc-responsive transcriptional regulation in Saccharomyces cerevisiae. *Molecular and cellular biology,* **17**(9), pp. 5044-5052.

ZHAO, L., WANG, Z., WU, H., XI, Z. and LIU, Y., 2015. Glutathione Selectively Modulates the Binding of Platinum Drugs to Human Copper Chaperone Cox17. *The Biochemical journal,* .

ZHU, K., ZHAO, J., LUBMAN, D., MILLER, F. and BARDER, T., 2005. Protein pl shifts due to posttranslational modifications in the separation and characterization of proteins. *Analytical Chemistry,* **77**(9), pp. 2745-2755.

ZUCO, V., CASSINELLI, G., COSSA, G., GATTI, L., FAVINI, E., TORTORETO, M., COMINETTI, D., SCANZIANI, E., CASTIGLIONI, V., CINCINELLI, R., GIANNINI, G., ZUNINO, F., ZAFFARONI, N., LANZI, C. and PEREGO, P., 2015. Targeting the invasive phenotype of cisplatin-resistant Non-Small Cell Lung Cancer cells by a novel histone deacetylase inhibitor. *Biochemical pharmacology,* **94**(2), pp. 79-90.